

NUCLEAR MAGNETIC RESONANCE AND KINETIC STUDIES  
OF THE CATALYTIC MECHANISM OF THE  
SERINE PROTEASES

Thesis by  
Robert James Kaiser, Jr.

In Partial Fulfillment of the Requirements  
for the Degree of  
Doctor of Philosophy

California Institute of Technology  
Pasadena, California

1984

(Submitted December 19, 1983)

## ABSTRACT

Kinetic and nuclear magnetic resonance experiments on the catalytic mechanism of the serine proteases have been carried out using alpha lytic protease, a bacterial serine protease.  $^{13}\text{C}$  NMR measurements indicate that His 57, and not Asp 102, is the residue titrating with  $\text{pK}_a$  6.7 in the free enzyme. However, when alpha lytic protease is complexed with transition state analogs (peptide aldehydes and benzeneboronic acid), the  $\text{pK}_a$  of this residue can shift to lower values. This shift can be at least as large as 1.8 pK units, and suggests that the enzyme may behave differently in the presence of substrate, especially in its transition state or intermediate forms, than it does in its absence.

The reaction of elastase with specific peptide p-nitro-anilides is biphasic, indicating the buildup of a tetrahedral intermediate in a pre-steady state reaction, followed by linear turnover. The intermediate accumulates to about 20-25% of the total amount of substrate bound to the enzyme. The ability for the substrate to make favorable contacts along an extended portion of the enzyme binding site is important in the observation of the buildup of this intermediate.

$^{13}\text{C}$  NMR studies on model compounds for the Asp 102-His 57 dyad in water and in DMSO solution indicate that  $\text{pK}_a$  reversal of the two ionizable groups can occur under conditions of moderate dielectric and high polarity. Overall, the results indicate that the "charge relay" mechanism may be operative in cases where the substrate can make precise extended contacts with the enzyme.

"That's what makes us the unique animal, we want to know why and try to find out. We even try to find out why we want to know why, though of course we never will."

Nero Wolfe, in Please Pass the Guilt, by Rex Stout

*Robert James Kaiser, Jr.*

## ACKNOWLEDGEMENTS

I wish to thank my advisor, Dr. John H. Richards, for enabling this thesis to come to fruition. His scientific insight and creativity influenced my work tremendously, and his assistance and patience throughout my stay at Caltech are deeply appreciated.

I also wish to thank all of the members of my research group with whom I have interacted over the past years. They have all left their own indelible mark. I especially wish to thank Dr. Thomas G. Perkins and Mr. William G. Antypas for their assistance with the numerous NMR experiments in this thesis; without their help I would have been forever in the dark. I am also grateful to Neal Handly and Dr. Brian Herndier for many scientific and some not-so-scientific adventures. And yes, thanks to you too, Betty and Dwayne.

A special note of gratitude must be given to Dr. Susan Dunn of Dr. Michael Raftery's group, for the use of the stopped-flow device. Her tireless and selfless help with this project are primarily responsible for its eventual success.

My very deepest thanks and appreciation must go to my wife Michelle, who has stood by me from day one, through bad times, long hours, and much frustration; she as much as anyone is responsible for this thesis. Further thanks to my family--Dad, Mom, Bruce, Lynn, Gail, and David--and to my wife's family for their emotional support in this critical time. Thanks also to Carmen Visser for her own inimitable support.

I also wish to thank the NIH and Caltech for the financial support provided me during my graduate study.

## TABLE OF CONTENTS

	Page
CHAPTER I--INTRODUCTION.....	1
Abbreviations.....	2
References.....	21
CHAPTER II-- <sup>13</sup> C NUCLEAR MAGNETIC RESONANCE INVESTIGATION OF THE IONIZATION BEHAVIOR OF HISTIDINE 57 IN $\alpha$ -LYTIC PROTEASE.....	25
Abbreviations.....	26
Introduction.....	27
Experimental.....	31
Materials.....	31
Enzyme.....	31
Methods.....	36
NMR Samples.....	36
NMR Spectra.....	37
Results.....	38
Discussion.....	57
Ionization Behavior of the Asp-His Dyad.....	57
High Field NMR Spectra.....	58
The Previous Carbon-13 Study.....	64
The "Charge Relay" System.....	65
Conclusion.....	69
References.....	70
CHAPTER III--THE ACTIVE SITE TITRATION OF $\alpha$ -LYTIC PROTEASE.....	74
Abbreviations.....	75
Introduction.....	76
Theory.....	78
Experimental.....	83
Materials.....	83
Substrates.....	83
Enzyme.....	84
Phenylmethanesulfonyl $\alpha$ -Lytic protease.....	89
Methods.....	89
Kinetics.....	89
Results.....	92
p-Nitrophenyltrimethyl acetate.....	92
Diethyl p-nitrophenyl phosphate.....	106
N-Benzylloxycarbonyl-L-alanine p-nitro- phenyl ester.....	119
Discussion.....	120
Conclusion.....	123
References.....	124

CHAPTER IV--KINETIC AND NUCLEAR MAGNETIC RESONANCE STUDIES OF $\alpha$ -LYTIC PROTEASE AND TRANSITION STATE ANALOGS.	
I. PEPTIDE ALDEHYDES.....	126
Abbreviations.....	127
Introduction.....	128
Theory.....	142
Experimental.....	144
Materials.....	144
L-Proline methyl ester.....	144
N-Acetyl-L-alanine-L-proline.....	145
N-Acetyl-L-alanyl-L-prolyl-L-alaninol.....	146
N-Acetyl-L-alanyl-L-prolyl-D,L-alaninol.....	147
N-Acetyl-L-alanyl-L-prolyl-D-alaninol.....	147
N-Acetyl-L-alanyl-L-prolyl-D-alanine methyl ester.....	149
D-Alanine methyl ester hydrochloride.....	149
t-Butyloxycarbonyl-L-alanine N-hydroxy- succinimide ester.....	150
t-Butyloxycarbonyl-L-alanyl-L-proline.....	151
L-alanyl-L-prolyl-L-alanine methyl ester hydrochloride.....	151
N-Acetyl-L-alanyl-L-prolyl-L-alanine methyl ester.....	152
N-Acetyl-L-alanyl-L-prolyl-L-alanine benzyl ester.....	153
N-Acetyl-L-alanyl-L-prolyl-L-alanine p-nitroanilide.....	154
N-Acetyl-L-alanyl-L-prolyl-L-alanine anilide	155
N-Acetyl-L-alanyl-L-prolyl-L-alanine amide..	156
N-Acetyl-L-alanyl-L-prolyl-L-alanine benzyl amide.....	157
t-Butyloxycarbonyl-L-alanine benzyl amide...	157
L-alanine benzyl amide hydrochloride.....	157
N-Acetyl-L-alanyl-L-prolyl-L-alanine hydrazide.....	157
N-Acetyl-L-alanyl-L-prolyl-glycinol.....	158
N-Acetyl-L-alanyl-L-prolyl-glycine ethyl ester.....	158
N-Acetyl-L-alanyl-L-prolyl-glycine p-nitro- anilide.....	159
N-Benzoyl-L-alanine methyl ester.....	159
N-Acetyl-L-alanyl-L-alanyl-L-alanine.....	159
Synthesis of peptide aldehydes.....	159
5% Palladium on barium sulfate.....	161
Phthalyl-L-alanine.....	161
Phthalyl-L-alanyl chloride.....	164
Phthalyl-L-alaninal.....	164
Phthalyl-L-alaninal diethyl acetal.....	165
L-Alaninal diethyl acetal.....	166
N-Acetyl-L-alanyl-L-prolyl-L-alaninal diethyl acetal.....	167

N-Acetyl-L-alanyl-L-prolyl-L-alaninal.....	168
N-Acetyl-L-alanyl-L-prolyl-D,L-alaninal.....	170
N-Acetyl-L-alanyl-L-prolyl-glycinal.....	170
Enzyme.....	171
Methods.....	171
Kinetics.....	171
pH-Stat method.....	171
Spectrophotometric method.....	172
NMR Samples.....	173
NMR Spectra.....	174
Results.....	175
Synthesis of peptide aldehydes.....	175
Inhibition kinetics.....	181
NMR Studies.....	187
Discussion.....	199
Conclusion.....	213
Appendix I.....	216
Appendix II.....	217
Appendix III.....	219
References.....	220
CHAPTER V--KINETIC AND NUCLEAR MAGNETIC RESONANCE STUDIES OF $\alpha$ -LYTIC PROTEASE AND TRANSITION STATE ANALOGS.	
II. BENZENE BORONIC ACID.....	226
Abbreviations.....	227
Introduction.....	228
Experimental.....	233
Materials.....	233
Methods.....	233
Kinetics.....	233
NMR Samples.....	234
NMR Spectra.....	235
Results.....	236
Inhibition Kinetics.....	236
Carbon-13 NMR results.....	241
Boron-11 NMR results.....	247
Discussion.....	255
Conclusion.....	260
References.....	262
CHAPTER VI--INVESTIGATIONS OF THE TETRAHEDRAL INTERMEDIATE FORMED IN THE ELASTASE CATALYZED HYDROLYSIS OF SPECIFIC TRIPEPTIDE p-NITROANILIDES BY STOPPED- FLOW SPECTROPHOTOMETRY.....	
Abbreviations.....	266
Introduction.....	267
Theory.....	272
Experimental.....	278
Materials.....	278
Methods.....	278
Elastase purification.....	278
Stopped-flow kinetics.....	280

Spectroscopic measurements.....	281
Results.....	282
Discussion.....	303
Previous Studies.....	310
One last consideration.....	317
Conclusion.....	318
References.....	320
CHAPTER VII-- <sup>13</sup> C NUCLEAR MAGNETIC RESONANCE STUDY OF THE EFFECT OF ENVIRONMENTAL CONDITIONS ON THE IONIZATION BEHAVIOR OF IMIDAZOLE-4-ACETIC ACID AND <u>trans</u> -UROCANIC ACID.....	325
Abbreviations.....	326
Introduction.....	327
Experimental.....	332
Materials.....	332
Methods.....	332
NMR Samples.....	332
NMR Spectra.....	333
Results and Discussion.....	334
Conclusion.....	352
References.....	354
ABSTRACT.....	ii
FRONTISPIECE.....	iii
ACKNOWLEDGEMENTS.....	iv
TABLE OF CONTENTS.....	v
LIST OF FIGURES.....	ix
LIST OF TABLES.....	xiv
CHAPTER ABSTRACTS.....	xvi
NOTES.....	xxi

## LIST OF FIGURES

Chapter	Figure		Page
I	1	The generally accepted kinetic scheme for hydrolysis of a substrate by a serine protease	7
	2	Diagram of acyl-enzyme formation in the hydrolysis of an amide substrate	11
	3	Hypotheses concerning the role of the Asp-His dyad during catalysis	14
II	1	Possibilities for the one proton ionization of the catalytic triad	28
	2	Chromatography of alpha lytic protease on Amberlite CG-50	34
	3	$^{13}\text{C}$ NMR spectra of labelled and unlabelled alpha lytic protease	39
	4	25.14 MHz $^{13}\text{C}$ NMR spectra of alpha lytic protease	42
	5	Chemical shift of C-2 as a function of pH	44
	6	50.3 MHz proton decoupled $^{13}\text{C}$ NMR spectra of alpha lytic protease at pH 5.5 and 7.9	46
	7	50.3 MHz proton coupled $^{13}\text{C}$ NMR spectra of alpha lytic protease at pH 4.9 and 8.0	50
	8	125.76 MHz proton coupled $^{13}\text{C}$ NMR spectrum of alpha lytic protease at pH 5.5	52
	9	125.76 MHz proton coupled $^{13}\text{C}$ NMR spectra of alpha lytic protease at various pH	54
III	1	Chromatography of alpha lytic protease on CM-Sephadex	85
	2	Chromatography of alpha lytic protease on Sephadex G-25	87

	3	Reaction of p-nitrophenyl trimethylacetate with alpha lytic protease	93
	4	Determination of $K_m$ and $V_{max}$ for the p-nitrophenyl <sup>m</sup> trimethylacetate/alpha lytic protease system at pH 7.78	95
	5	Determination of B for the reaction of p-nitrophenyl trimethylacetate with alpha lytic protease	97
	6	The dependence of B on $S_0$ for the reaction of p-nitrophenyl <sup>o</sup> trimethylacetate with alpha lytic protease	101
	7	The titration of alpha lytic protease with p-nitrophenyl trimethylacetate	103
	8	The reaction of alpha lytic protease with diethyl p-nitrophenyl phosphate	108
	9	The dependence of $k_{obs}$ on $S_0$ for the reaction of alpha lytic protease and diethyl p-nitrophenyl phosphate	113
	10	The determination of $k_{obs}$ for the reaction of alpha lytic protease and diethyl p-nitrophenyl phosphate	115
	11	Decline in alpha lytic protease activity towards N-acetyl-L-alanyl-L-prolyl-L-alanine p-nitroanilide in the presence of diethyl p-nitrophenyl phosphate	117
IV	1	Acylation of a serine protease by an amide substrate	129
	2	The tetrahedral transition state of serine protease catalysis	133
	3	The tetrahedral complex of Ser 195 and aldehyde	136
	4	Structure of the enzyme/aldehyde adduct according to Hunkapiller et al. (1975)	139

	5	Reaction scheme for the synthesis of tripeptide aldehydes	162
	6	200 MHz $^1\text{H}$ NMR spectra of tripeptide aldehydes	177
	7	Plots of $K_I^{\text{app}}$ versus pH for the interaction of alpha lytic protease with tripeptide aldehydes	183
	8	$(k_{\text{cat}}/K_m)$ and $\log(k_{\text{cat}}/K_m)$ versus pH for the reaction of alpha lytic protease and N-acetyl-L-alanyl-L-prolyl-L-alanine p-nitroanilide	188
	9	50.3 MHz proton coupled $^{13}\text{C}$ NMR spectra of alpha lytic protease and N-acetyl-L-alanyl-L-prolyl-glycinal at pH 4.0, 6.9, and 8.6	191
	10	50.3 MHz proton decoupled $^{13}\text{C}$ NMR spectra of alpha lytic protease and N-acetyl-L-alanyl-L-prolyl-glycinal at pH 5.2, 6.7 and 8.3	193
	11	Chemical shift of C-2 versus pH for the alpha lytic protease/N-acetyl-L-alanyl-L-prolyl-L-alaninal complex	195
	12	Chemical shift of C-2 versus pH for the alpha lytic protease/N-acetyl-L-alanyl-L-prolyl-glycinal complex	197
	13	$K_I^{\text{obs}}$ versus pH for the inhibition of alpha lytic protease by N-acetyl-L-alanyl-L-prolyl-L-alaninal according to the mechanism of Hunkapiller et al. (1975)	202
V	1	Proposed structures for the interaction of boronic acids with the serine proteases	230
	2	$K_I^{\text{app}}$ as a function of pH for the benzenboronic acid inhibition of alpha lytic protease	238
	3	50.3 MHz proton decoupled $^{13}\text{C}$ NMR spectra of the alpha lytic protease/BBA complex at pH 8.0 and 6.0	243

	4	50.3 MHz proton coupled $^{13}\text{C}$ NMR spectrum of the alpha lytic protease/BBA complex at pH 8.1	245
	5	64.17 MHz $^{11}\text{B}$ NMR spectra of the alpha lytic protease/BBA complex at pH 8.1	249
VI	1	Raw transmittance versus time data for the reaction of elastase and STAPNA at pH 8.25	283
	2	Hand-drawn curve for the data in Figure 1	285
	3	$A_{410}$ versus time for the reaction of elastase and APAPNA	287
	4	$A_{410}$ versus time for the reaction of elastase and APAPNA for various enzyme concentrations	289
	5	$A_{410}$ versus time for the reaction of elastase and STAPNA for various enzyme concentrations	291
	6	First-order analysis of the pre-steady state reaction of elastase and APAPNA	294
	7	Dependence of the burst on enzyme concentration	298
	8	Raw data of Hunkapiller et al. (1976)	311
	9	Determination of $\pi$ and B for the data of Hunkapiller et al. (1976)	315
VII	1	$^{13}\text{C}$ chemical shift of C-2 versus pH for imidazole-4-acetic acid	335
	2	50.3 MHz proton coupled $^{13}\text{C}$ NMR spectra of imidazole-4-acetic acid in aqueous solution	340
	3	50.3 MHz proton coupled $^{13}\text{C}$ NMR spectra of imidazole-4-acetic acid in dry dimethyl sulfoxide	343
	4	Comparison of the chemical shift and coupling constant of C-2 of imidazole-4-acetic acid in water and dimethyl sulfoxide	345

5	50.3 MHz proton coupled $^{13}\text{C}$ NMR spectra of imidazole-4-acetic acid in water/dimethyl sulfoxide mixtures	348
---	---	-----

## LIST OF TABLES

Chapter	Table		Page
II	I	$^{13}\text{C}$ NMR parameters for the C-2 carbon of Histidine 57 in alpha lytic protease	49
III	I	The effect of substrate concentration of the reaction of alpha lytic protease and p-nitrophenyl trimethylacetate	100
	II	The effect of enzyme concentration on the reaction of alpha lytic protease and p-nitrophenyl trimethylacetate	105
	III	Determination of $k_2/K_S$ from the initial rate of the pre-steady state reaction of alpha lytic protease and p-nitrophenyl trimethylacetate	107
	IV	The effect of substrate concentration on the reaction of alpha lytic protease and diethyl p-nitrophenyl phosphate	111
	V	The effect of enzyme concentration on the reaction of alpha lytic protease and diethyl p-nitrophenyl phosphate	112
IV	I	Kinetic constants for the interaction of alpha lytic protease and various peptide derivatives	185
	II	NMR parameters for the C-2 carbon of His 57 in the alpha lytic protease/peptide aldehyde complexes	190
V	I	Kinetic constants for the inhibition of alpha lytic protease activity by various aromatic compounds	237
	II	$^{13}\text{C}$ NMR parameters for C-2 of His 57 of the alpha lytic protease/BBA complex	242

	III	$^{13}\text{C}$ NMR parameters for C-2 of imidazole in the presence and absence of BBA	248
	IV	$^{11}\text{B}$ NMR parameters of some boron-containing acids	251
	V	$^{11}\text{B}$ NMR parameters for BBA in the presence and absence of alpha lytic protease at pH 8.1	253
VI	I	Kinetic parameters for the reaction of elastase and APAPNA	296
	II	Kinetic parameters for the reaction of elastase and STAPNA	297
	III	Calculation of accumulated intermediate in the reaction of elastase and specific tripeptide p-nitro-anilides	304
	IV	Comparison of the results in Table II with the hypothesis $k_{\text{cat}} = k_3$ .	308
VII	I	$^{13}\text{C}$ NMR parameters for C-2 of imidazole-4-acetic acid and <u>trans</u> -urocanic acid derivatives in water and dimethyl sulfoxide	337
	II	$^{13}\text{C}$ NMR parameters of C-2 of imidazole-4-acetic acid in water/dimethyl sulfoxide mixtures	347

## CHAPTER ABSTRACTS

CHAPTER I.

This chapter presents background information on the important aspects of the mechanism of action of the serine proteases. It discusses the various general aspects of enzyme catalysis in terms of this family of enzymes. The various structures of the catalytic pathway of these enzymes are discussed in light of the current level of understanding of the roles of the residues of the catalytic triad. Some general information about alpha lytic protease, a bacterial serine protease used extensively in this research, is also given.

CHAPTER II.

This chapter presents the results of a  $^{13}\text{C}$  NMR study at 50.3 MHz and 125.76 MHz designed to determine the ionization behavior of His 57 of  $^{13}\text{C}$ -labelled alpha lytic protease. The NMR data indicate that His 57 titrates with a normal  $\text{pK}_a$  (6.7) in the free enzyme, contrary to previously published reports using this technique (Hunkapiller et al., 1973), and in accord with the results of a  $^{15}\text{N}$  NMR investigation of this residue (Bachovchin and Roberts, 1978). Spectra acquired at high field (125.76 MHz) also indicate the existence of two conformational forms of the protein below pH 6; however, it could not be determined if multiple forms also exist at higher pH. The source of error in the results of the previously published  $^{13}\text{C}$  NMR study (Hunkapiller et al., 1973) are discussed in terms of the multiple low pH forms of alpha lytic protease

and their effect on the appearance of the decoupled versus coupled spectra obtained in that study, as well as the low sensitivity of the spectrometer and the use of spectral subtraction to measure coupling constants. The "charge relay" mechanism is re-examined in light of these results; due caution is advised in extending the results of any study on the behavior of the catalytic triad in the free enzyme to a discussion of its behavior during the catalytic process.

### CHAPTER III.

This chapter presents the results of an investigation of the reaction of alpha lytic protease with p-nitrophenyl trimethylacetate and diethyl p-nitrophenyl phosphate. The latter reagent can be used to determine the molar concentration of active alpha lytic protease by active site titration.

### CHAPTER IV.

This chapter presents the results of an investigation of the structure of the complex of alpha lytic protease with specific tripeptide aldehydes. The results indicate that these aldehydes are bound as neutral hemiacetals to Ser 195 of the active site; however, the role of the Asp 102-His 57 dyad in forming these covalent adducts is not yet resolved. Interestingly, the  $pK_a$  of the His 57 residue in these complexes as determined by  $^{13}\text{C}$  NMR and the pH dependence of the binding constant of these

aldehydes is lowered by as much as 0.5  $pK_a$  unit relative to its value in the free enzyme. A speculative mechanistic explanation featuring increased acidity of His 57 in the transition state over the ground state to facilitate proton abstraction and donation is presented. The results also suggest that movement of the His 57 side-chain during formation of the tetrahedral intermediate may be important to catalysis. A new procedure for the synthesis of peptide aldehydes is presented.

#### CHAPTER V.

This chapter presents the results of a study concerning the structure of the alpha lytic protease/benzeneboronic acid complex.  $^{11}\text{B}$  NMR data reveal that the complex is a tetrahedral adduct of Ser 195 and the boron atom of the inhibitor; this is further confirmed by  $^{13}\text{C}$  NMR studies of C-2 of His 57 in the complex, and by a measurement of the pH dependence of the dissociation constant of the complex. As was observed for the alpha lytic protease/peptide aldehyde system, the  $pK_a$  of His 57 is lowered in this complex from its normal value by about 1.8  $pK_a$  units. These results suggest that the presence of a negative charge on the tetrahedral adduct is important in determining the magnitude of the shift. Thus it appears that, during catalysis, the formation of a negatively charged transition state or intermediate may allow the enzyme to manifest behavior not observed in the free enzyme.

CHAPTER VI.

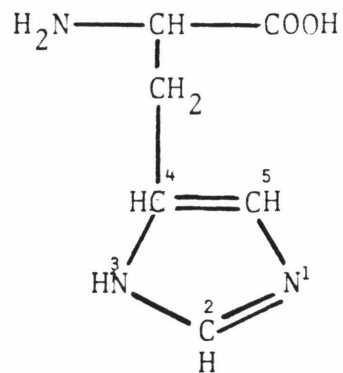
This chapter presents the results of a stopped-flow kinetic study of the hydrolysis of two specific tripeptide p-nitroanilides, N-acetyl-L-alanyl-L-prolyl-L-alanine p-nitroanilide and N-succinyl-L-alanyl-L-alanyl-L-alanine p-nitroanilide, by porcine elastase. Biphasic kinetics are observed for both substrates; in both cases, the initial absorbance burst is linearly proportional to the enzyme concentration. Thus, the biphasic kinetics are consistent with a mechanism in which a tetrahedral intermediate builds up to a steady state concentration prior to turnover. The intermediates accumulate to about 20-25% of the total amount of substrate bound to enzyme at steady state. These results are then discussed in light of a report by Markley et al. (1981) that challenges the existence of these intermediates. The ability to detect intermediate will depend on the relative rates of its formation and its breakdown, as well as its thermodynamic stability in relation to the ES-complex and the acyl-enzyme. Since we have specifically engineered these substrates to provide stable tetrahedral intermediates, it is probable that the observed accumulation is near the upper limit for intermediate concentration. For less specific substrates, or those having less stable intermediates, observation of an accumulated intermediate may not be possible. The importance of extended enzyme-substrate contacts for efficient catalysis is also discussed.

CHAPTER VII.

This chapter presents a  $^{13}\text{C}$  NMR investigation of the ionization of two model compounds for the Asp 102-His 57 dyad, imidazole-4-acetic acid and trans-urocanic acid, in water, in dimethyl sulfoxide, and in water dimethyl sulfoxide mixtures. In water both molecules ionize normally, with the imidazole being a stronger base than the carboxylate. However, in dimethyl sulfoxide solution, the situation is reversed, the imidazole now being a weaker base than the carboxylate. Thirty to fifty mole percent of water can be added to dimethyl sulfoxide before substantial protonation of the imidazole by the carboxylate is observed. The results therefore indicate that the "charge relay" mechanism of serine protease catalysis could be a viable explanation of the catalytic process; if, in the presence of substrate, at some point along the reaction pathway the dielectric of the active site can be lowered, probably through exclusion of water from the active site by active site residues and the substrate,  $\text{pK}_a$  reversal could occur even in a highly polar environment. The results further indicate that only moderate, and not gross, changes in the conformation of the protein might be required to elicit the "charge relay" behavior.

## NOTES

1. The sequence numbering system used throughout this thesis for residues of the serine proteases is that determined for chymotrypsinogen. For example, the serine residue at position 188 in porcine elastase is analogous to the serine residue at position 195 in chymotrypsinogen, etc.
2. The following numbering system for the imidazole ring of histidine has been used in this thesis:



CHAPTER I

INTRODUCTION

## ABBREVIATIONS

NMR	Nuclear Magnetic Resonance
Gly	Glycine
Asp	L-Aspartic acid
Ser	L-Serine
His	L-Histidine
Arg	L-Arginine
Thr	L-Threonine
Met	L-Methionine
Ala	L-Alanine
Asn	L-Asparagine
Ile	L-Isoleucine

## CHAPTER I--INTRODUCTION

The study of enzyme mechanisms and the understanding of the relationship between protein structure and function is one of the most interesting and exciting areas of biochemical research. These polypeptide molecules have evolved to catalyze a wide variety of basic chemical reactions which in vitro are too slow to be biologically feasible to sustain a living organism. At the same time, nature has managed to exert control over the actions of enzymes by including in the tertiary structure of the protein the means to discern among a plethora of possible natural substrates through the incorporation of a specificity binding pocket, as well as by providing the means to monitor their activity through the presence of natural enzyme inhibitors, allostery, and zymogen activation.

The study of the mechanism of action of enzymes, that is, the microscopic pathway along which the enzymatic reaction progresses from substrate(s) to product(s), has been prompted by the curiosity about how nature has managed to accomplish what man has so far failed to imitate. This thesis will present some experimental attempts to further elucidate the mechanism of catalysis of a well-studied family of enzymes, the serine proteases.

The Serine Proteases. The serine proteases are a family of enzymes that catalyze the hydrolysis of peptide bonds at

neutral or slightly basic pH. These enzymes are characterized by the presence of a uniquely reactive serine residue in the active site region of the protein molecule. They are of extremely widespread occurrence and diverse function, and include the mammalian digestive enzymes chymotrypsin, trypsin, and elastase, the bacterial enzymes such as the subtilisins, several proteases of Streptomyces griseus, and the  $\alpha$ -lytic protease of Lysobacter enzymogenes (for reviews concerning these enzymes, see Stroud, 1974 and Kraut, 1977, and the references cited therein), as well as enzymes connected with cellular chemotaxis (Hatcher et al., 1977), fertilization (acrosomal protease), blood clot formation (thrombin) and dissolution (plasmin), the complement cascade (Stroud, 1974; Neurath and Walsh, 1976; Davie et al., 1979), hormone activation (bradykinin and kallikrein; Schacter, 1980), and other cellular functions (Woodbury and Neurath, 1980). The term "family" is used in connection with these proteins to signify the high degree of primary sequence homology among these proteins, especially in the region of the active site, as well as the high degree of topological equivalence of their tertiary structures (Dayhoff, 1972; Kraut, 1977; James et al., 1978).

Two sub-families of the serine proteases have been especially well-studied to date, the trypsin sub-family and the subtilisin sub-family. All serine proteases so far characterized contain a precisely arranged triad of catalytically important residues--the carboxylate side-chain of aspartic acid, the imidazole side-chain of histidine, and the hydroxyl side-chain of serine. The trypsin sub-family is further

characterized by the primary sequence Gly-Asp-Ser-Gly-Gly around the catalytically important serine residue, and a catalytic triad of Asp 102, His 57, and Ser 195. The Asp 194 residue is conserved in this sub-family as it is an integral feature of the tertiary structure of active enzyme. In the mammalian enzymes, this residue forms a salt bridge to the amino terminus of Ile 16 on zymogen activation, resulting in catalytically competent enzyme; in the bacterial proteases of this sub-family, no zymogens have yet been isolated, and the salt bridge is internal in these proteins between Asp 194 and the guanidinium group of Arg 138 (Stryer, 1975; Brayer et al., 1979). By comparison, the subtilisin sub-family is characterized by the primary sequence Thr-Ser-Met-Ala around the catalytically important serine residue, and a catalytic triad of Asp 32, His 64, and Ser 221. Thus, these two sub-families are an example of convergent evolution, in that two classes of protein that are quite different in their overall tertiary structures have evolved to utilize the same triad of amino acid side-chains as a unique catalytic entity.

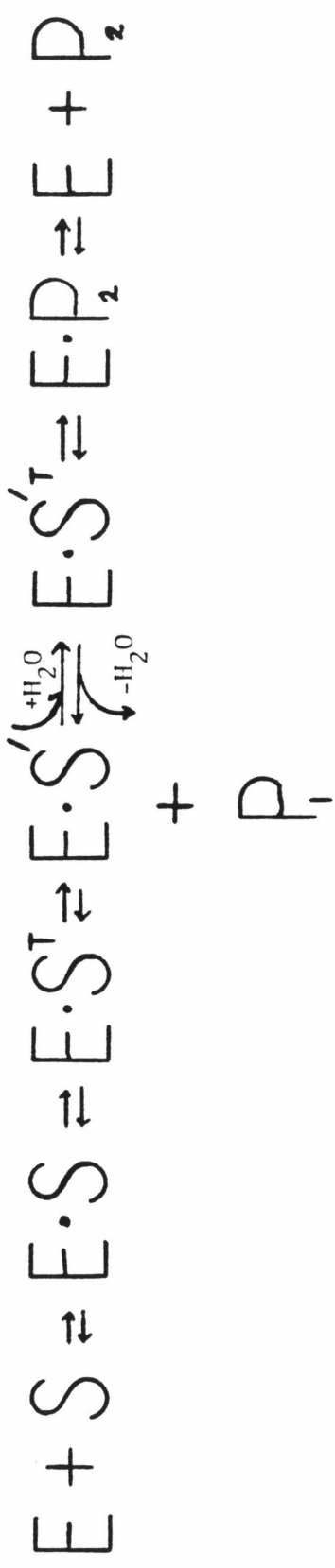
Another key structural feature of the serine protease enzymes is the "oxyanion hole", which consists of the amide backbone NH groups of Ser 195 and Gly 193 in the trypsin sub-family (Kraut, 1977; Steitz et al., 1969; Henderson, 1970), and the amide backbone NH group of Ser 221 and the side-chain NH<sub>2</sub> group of Asn 155 in the subtilisin sub-family (Robertus et al., 1972). This region of the active site is proposed to

be crucial for the stabilization of the negatively charged tetrahedral intermediate formed during the catalytic process through strong hydrogen bonding to the oxyanion portion of the intermediate.

Lastly, it must be mentioned that the numerous, extended, non-covalent contacts made between the substrate and the enzyme surface, including the specificity pocket, seem to be critical for the precise orientation and alignment of the residues of the active site and the scissile bond of the substrate with respect to each other, so as to allow the enzyme to manifest its total catalytic potential.

The Catalytic Mechanism of the Serine Proteases. The generally accepted overall kinetic scheme for catalysis by the serine proteases is diagrammed in Figure 1. As in all enzyme processes on natural substrates, the initial step in the reaction sequence is the formation of an enzyme-substrate (Michaelis) complex, usually a diffusion controlled process. This complex is held together by non-covalent forces--hydrogen bonds, charge-transfer interactions, ionic attractions, and Van der Waal's interactions. In the formation of the Michaelis complex the specificity pocket of the enzyme plays its part in determining which bond of the substrate will be cleaved and by setting the stereochemical preference of the enzyme; the known serine proteases rapidly catalyze the hydrolysis of L-amino acid derivatives, while only sluggishly catalyzing the hydrolysis of their D-configuration counterparts, if at all (Walsh and Wilcox, 1970; Whitaker, 1970; Shotton, 1970).

Figure 1. The accepted kinetic scheme for hydrolysis of a substrate (S) by a serine protease (E) to products ( $P_1$ ,  $P_2$ ). ES is the Michaelis complex;  $ES^T$  is a tetrahedral adduct between Ser 195 and the carbonyl of the scissile bond of the substrate;  $ES'$  is an acyl enzyme intermediate;  $ES'^T$  is the tetrahedral adduct formed between the acyl enzyme and a molecule of solvent water;  $EP_2$  is a complex between the enzyme and the product of acyl enzyme hydrolysis, prior to expulsion of the product from the enzyme.



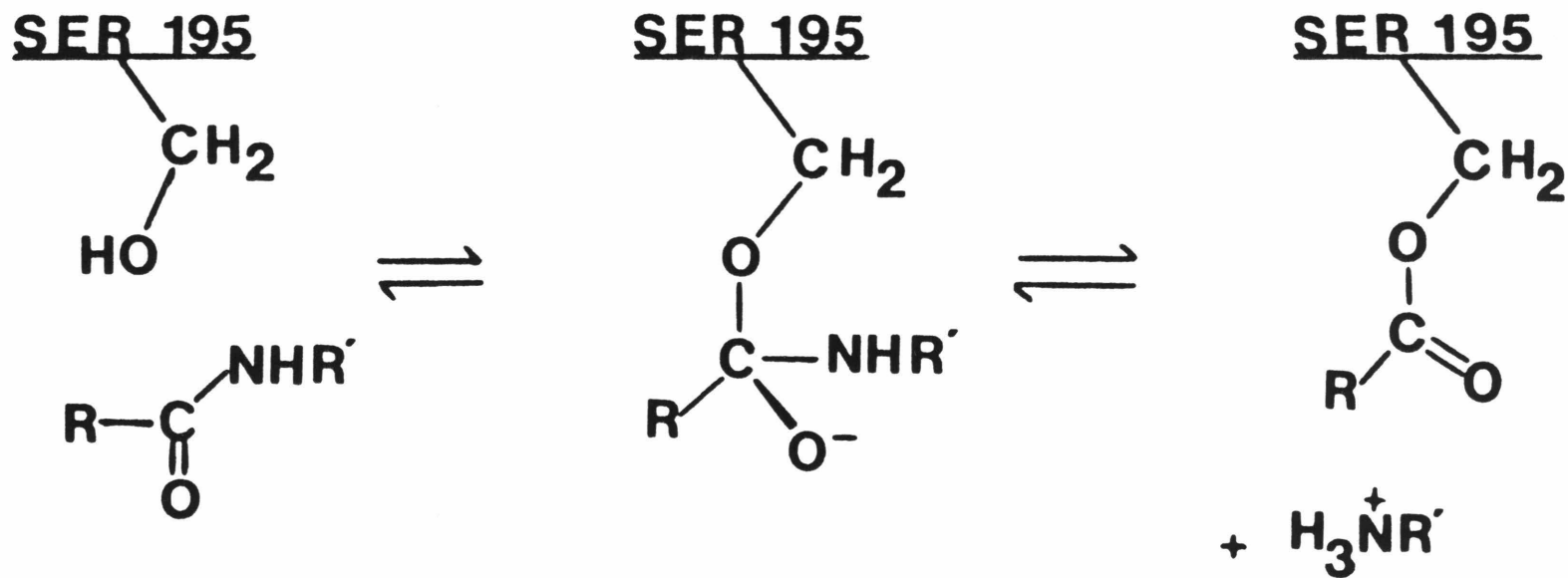
The formation of the enzyme-substrate complex is fundamentally important to the catalytic event, as it serves two vital functions: it allows for selectivity among substrates, as has been previously mentioned, and it allows for proper alignment of the scissile bond with respect to the active site residues that participate in catalysis, thereby reducing the collisional randomness generally involved in a non-enzymatic reaction, since rapid reaction necessitates a precise orientation between reacting species (Bender and Brubacher, 1973)

The next well-documented step in the catalytic reaction is the formation of an acyl-enzyme intermediate (Bender and Kezdy, 1964; Stroud, 1974; Blow, 1976; Kraut, 1977; and references cited therein). The acyl-enzyme is formed through nucleophilic attack of the hydroxyl of Ser 195 on the carbonyl carbon of the scissile bond of the substrate, accompanied by cleavage of the substrate carbon-nitrogen amide or carbon-oxygen ester bond. It is therefore a covalent enzyme-substrate intermediate. Acyl-enzyme formation is considered to proceed through a postulated tetrahedrally oriented, oxyanionic intermediate (see Figure 2), although the existence of this intermediate is still the subject of considerable debate. Chapters IV, V, and VI will discuss this subject.

The role of Ser 195 is thus fairly well understood. However, much controversy exists about the role of the remaining two residues of the catalytic triad. Specifically, one needs an adequate account of how a normally poor nucleophile, the hydroxyl  $\gamma\text{O}$  of Ser 195, has become such a potent nucleophile in the case of the serine proteases. The answer to this problem must be inextricably linked with the special properties of the Asp 102-His 57 dyad in these enzymes.

The overall role of the Asp-His couple is generally agreed upon. This pair of basic residues acts to accept, store, and donate the proton originally on  $\gamma\text{O}$  of Ser 195 during its attack on the substrate, formation of the tetrahedral intermediate, and breakdown to acyl-enzyme; as such, the dyad functions as a general base catalyst with an apparent  $\text{pK}_a$  of about 7 affecting most hydrolyses (Blow, 1976; Kraut, 1977; and references cited therein). However, the microscopic events involved in this process have yet to be clearly demonstrated. Initially, the discovery of the negatively charged Asp 102 side-chain in the crystallographic structure of chymotrypsin led Blow and coworkers (Blow et al., 1969) to postulate a "charge relay" mechanism for the triad, whereby the proton on  $\gamma\text{O}$  of Ser 195 could be transferred to N-1 of His 57 while the proton on N-3 of His 57 was transferred to, or involved in a very strong hydrogen bond with, the carboxylate of Asp 102, with the result that the negative charge originally

Figure 2. Diagram of acyl-enzyme formation in the hydrolysis of an amide substrate by a serine protease. The proton originally on Ser 195 in the ES-complex has been transferred to the Asp 102-His 57 dyad during formation of the tetrahedral intermediate, and subsequently transferred to the leaving group of the substrate (the amine product) on breakdown of the intermediate to acyl-enzyme.



**E-S COMPLEX**

**TETRAHEDRAL  
INTERMEDIATE**

**ACYL ENZYME**

residing on Asp 102 at catalytic pH had been relayed to Ser 195, thus creating a more nucleophilic oxyanion at Ser 195 instead of the less nucleophilic hydroxyl group (see Figure 3A). This hypothesis was subsequently modified by Hunkapiller et al. (1973) to remove the difficulty of explaining how a dyad of  $pK_a \sim 7$  could generate a sufficient amount of an oxyanion of  $pK_a$  12-14 under conditions of nearly neutral pH to be catalytically useful. These researchers instead postulated that, if two sufficiently strong hydrogen bonds were formed between the residues of the catalytic triad (Figure 3B), a concerted two-proton transfer from His 57 to Asp 102 and from Ser 195 to His 57 could occur as the Ser 195-substrate bond was forming. The system of tight hydrogen bonds would allow for polarization of the Ser 195 hydroxyl by partial transfer of the negative charge on Asp 102 to Ser 195, thereby enhancing the nucleophilic character of this residue. This mechanism further allows for the alleviation of unfavorable charge separation in a predominantly hydrophobic region of the active site of these enzymes. However, critical to this mechanism is the necessity that, at some appropriate point in the catalytic reaction, the carboxylate of Asp 102 must be a stronger base than His 57, contrary to the normal ionization behavior of these two residues in aqueous solution. This mechanism, more properly termed a "proton shuttle" mechanism, seemed to be supported by a  $^{13}\text{C}$  NMR study carried out by these researchers which indicated that Asp 102 was indeed a stronger base than His 57 in the bacterial serine protease,  $\alpha$ -lytic protease (Hunkapiller et al., 1973).

Figure 3. Hypotheses concerning the role of the Asp-His dyad during catalysis by the serine proteases.

A) The original "charge relay" mechanism of Blow et al. (1969). This mechanism postulates that the negative charge on the carboxylate of Asp 102 is relayed to Ser 195 through the imidazole ring of His 57, yielding a Ser 195 oxyanion which subsequently attacks the substrate to form the tetrahedral intermediate.

B) The modified "charge relay", or "proton shuttle", mechanism of Hunkapiller et al. (1973). This mechanism postulates the polarization of Ser 195 by Asp 102 through a tightly hydrogen bonded system of Asp-His-Ser, followed by concerted two-proton transfer from Ser to His and from His to Asp as the tetrahedral intermediate is formed.

C) The "carboxylate assisted" mechanism of Bachovchin and Roberts (1978). This mechanism postulates that His is the ultimate base accepting the Ser proton, and that the role of Asp is to properly orient the imidazole ring of His to facilitate acceptance of this proton, and to stabilize the positive charge thus formed on His through ion-pairing.



More recent NMR experiments (Markley, 1979; Bachovchin and Roberts, 1978; Bachovchin et al., 1981) have led Roberts and coworkers to postulate a different mechanism (Figure 3C), as it now clear that His 57 is a stronger base than Asp 102 in the variety of free serine proteases thus far examined. Labelled the "carboxylate-assisted" mechanism (Bachovchin and Roberts, 1978; Kanamori and Roberts, 1983), it postulates that the residues of the catalytic triad retain their normal aqueous ionization behaviors in the enzyme during catalysis, and that as such His 57 is the ultimate residue offering general base assistance during catalysis. The role of Asp 102 is then two-fold: first, to ensure that the imidazole ring of His 57 is in the proper tautomeric form (the proton residing on N-3) for facile transfer of the hydroxyl proton of Ser 195 to N-1 during intermediate formation; this tautomeric form is not the normally predominant form for 4-substituted imidazoles, but is favored by hydrogen bonding between Asp 102 and His 57 (Roberts et al., 1982); and second, it acts to stabilize the positive charge developed on His 57 in the intermediate. Although this mechanism accords with the known ionization behavior of the catalytic triad in the free enzymes, it remains to be proven that the same behavior is manifested during catalysis. Chapters II, IV, V, and VII relate to this topic.

A mechanism seeking to explain the high degree of nucleophilicity of Ser 195 based primarily on crystallographic data has also been proposed (Henderson, 1970; Kraut, 1977; Robertus et al., 1972). It appears that, due to the relative positions of the side-chains of His 57 and Ser 195, any

hydrogen bond between these two residues in the free enzyme is at best extremely weak, if present at all. Hence, the serine hydroxyl cannot be polarized by this weak hydrogen bonding, and as such the serine  $\gamma$ O is not intrinsically nucleophilic. However, crystallographic evidence on acyl-enzymes (Birktoft and Blow, 1972; Henderson, 1970; Steitz et al., 1969) and on trypsin/protein trypsin inhibitor complexes (Sweet et al., 1974; Blow et al., 1974; Ruhlmann et al., 1973; Huber et al., 1974; Huber et al., 1975) has indicated that the side-chain of Ser 195 has rotated in forming these complexes relative to its position in the free enzyme to a new position near where the substrate carbonyl would be in an enzyme-substrate complex. This rotation allows for the formation of a strong His-Ser hydrogen bond, as well as the steric destabilization of the substrate when it is bound in the active site. These two factors lead to covalent bond formation, with a concomittant relief of strain in the substrate, as the tetrahedral intermediate is formed; the Asp-His dyad therefore acts in some unspecified way to store the serine proton during this process. It must thus be realized that while the enzyme is held in a generally rigid conformation by the forces determining its gross tertiary structure, considerable local flexibility, especially in the active site region, is available, and side-chain mobility may indeed be an important part of any complete explanation of the catalytic process.

Acyl-enzyme formation is accompanied by the release of the first product of hydrolysis, an amine (from an amide

substrate) or an alcohol (from an ester substrate). Subsequent hydrolysis of the acyl-enzyme by solvent water regenerates free enzyme and the acid portion of the substrate, presumably again through a tetrahedral intermediate in a process similar to acyl-enzyme formation. However, this segment of the catalytic cycle is relatively unstudied.

The driving force for catalysis is primarily provided by the structure of the enzyme itself. It should be understood that enzymatic catalysis is inseparable from preferential stabilization of the transition states of the reaction sequence over the ground states of enzyme, substrate, and products, including the ES-complex (Pauling, 1946; Wolfenden, 1972; Fersht, 1974; Wolfenden, 1976); this provides for a reduction in the activation energies of the elementary processes involved. The primary means for the stabilization of high energy species available to the enzyme are the strength and number of covalent and non-covalent interactions gained by the substrate in the transition state over those available to the substrate in its ground state(s) (Lienhard, 1973). This, then, is the crucial role of the "oxyanion hole", to afford the substrate in its transition state structure stabilizing forces not present in its ground state appearance, namely, strong hydrogen bonding of the oxyanion to the NH amide backbone of Ser 195 and Gly 193.  $\alpha$ -Lytic protease. Much of the research presented in this thesis is concerned with kinetic and NMR structure-function probes performed on a bacterial homolog of the trypsin sub-family,  $\alpha$ -lytic protease. This serine protease is an extra-

cellular protein, secreted by Lysobacter enzymogenes (formerly Myxobacter 495). This enzyme was isolated and characterized largely through the work of Whitaker and coworkers (Whitaker, 1965; Whitaker et al., 1965 a,b; Whitaker et al., 1966;

Whitaker and Roy, 1967; Tsai et al., 1965; Whitaker, 1970). It is specific for derivatives of L-alanine, L-valine, and glycine, similar to the pancreatic serine protease elastase (Shaw and Whitaker, 1973; Kaplan et al., 1970). Its primary amino acid sequence is known (Olson et al., 1970) and its crystal structure has been determined (Brayer et al., 1979). It possesses only 18% primary sequence homology with elastase, but the tertiary structure shows 55% topological equivalence with this enzyme, mostly in the active site and substrate binding regions. Like elastase (Thompson and Blout, 1973 a,b), it possesses an extended but shallow substrate binding locus for amino acid residues on both sides of the scissile peptide bond (Bauer et al., 1981). Its molecular weight is 19,778 daltons (Smillie and Whitaker, 1967), and it has no known zymogen.

$\alpha$ -Lytic protease is particularly well-suited for NMR studies of the catalytic triad. The enzyme possesses but a single histidine residue, present in the active site (Smillie and Whitaker, 1967). Furthermore, being of bacterial origin, the enzyme can be biosynthesized and isolated containing labelled amino acids in large quantities and in excellent purity by a relatively facile procedure. Thus we are afforded the unique opportunity to study the catalytic histidine without

substantial interference from other parts of the protein. The enzyme is readily available in the amounts required to effectively employ current NMR techniques, is soluble in 0.1 to 0.2 M salt solution to several millimolar in concentration, and is sufficiently stable toward autolysis and denaturation at room temperature to allow for its use for the extended periods of time necessary for NMR signal accumulation (Hunkapiller et al., 1973; Hunkapiller et al., 1975). As such, it is the current enzyme of choice for mechanistic NMR studies of the serine proteases.

## REFERENCES

- Bachovchin, W.W, and Roberts, J.D. (1978), J. Am. Chem. Soc. 100, 8041-8047.
- Bachovchin, W.W., Kaiser, R., Richards, J.H., and Roberts, J.D. (1981), Proc. Natl. Acad. Sci. USA 78, 7323-7326.
- Bauer, C.-A., Brayer, G.D., Sielecki, A.R., and James, M.N.G. (1981), Eur. J. Biochem. 120, 289-294.
- Bender, M.L., and Kezdy, F.J. (1964), J. Am. Chem. Soc. 86, 3704-3714.
- Bender, M.L., and Brubacher, L.J. (1973), "Catalysis and Enzyme Action", McGraw-Hill , New York.
- Birktoft, J.J. and Blow, D.M. (1972), J. Mol. Biol. 68, 652-656.
- Blow, D.M., Birktoft, J.J., and Hartley, B.S. (1969), Nature (London) 221, 337-339.
- Blow, D.M., Janin, J., and Sweet, R.M. (1974), Nature (London) 249, 54-57.
- Blow, D.M. (1976), Acc. Chem. Res. 9, 145-152.
- Brayer, G.D., Delbaere, L.T.J., and James, M.N.G. (1979), J. Mol. Biol. 131, 743-775.
- Davie, G.W., Fujikawa, K., Kurachi, K., and Kisiel, W. (1979), Adv. Enzymol. 48, 277-318.
- Dayhoff, M.O. (1972), "Atlas of Protein Sequence and Structure", vol. 5, National Biomedical Research Foundation, Washington, D.C.
- Fersht, A.R. (1974), Proc. R. Soc. Lond. B 187, 397-407.
- Hatcher, V.B., Lazarus, G.S., Levine, N., Burk, P.G., and Yost, F.J. Jr. (1977), Biochim. Biophys. Acta 483, 160-171.

- Henderson, R. (1970), J. Mol. Biol. 54, 341-354.
- Huber, R., Kukla, D., Bode, W., Schwager, P., Bartels, K.,  
Deisenhofer, J., and Steigemann, W. (1974), J. Mol. Biol.  
89, 73-101.
- Huber, R., Bode, W., Kukla, D., Kohl, U., and Ryan, C.A. (1975),  
Biophys. Struct. Mechanism 1, 189-201.
- Hunkapiller, M.W., Smallcombe, S.H., Whitaker, D.R., and Richards,  
J.H. (1973), Biochemistry 12, 4732-4743.
- Hunkapiller, M.W., Smallcombe, S.H., and Richards, J.H. (1975),  
Org. Magn. Reson. 7, 262-265.
- James, M.N.G., Delbaere, L.T.J., and Brayer, G.D. (1978), Can.  
J. Biochem. 56, 396-402.
- Kanamori, K., and Roberts, J.D. (1983), Acc. Chem. Res. 16, 35-41.
- Kaplan, H., Symonds, V.B., Dugas, H., and Whitaker, D.R. (1970),  
Can. J. Biochem. 48, 649-658.
- Kraut, J. (1977), Ann. Rev. Biochem. 46, 331-358.
- Lienhard, G.E. (1973), Science 180, 149-154.
- Markley, J.L. (1979), in "Biological Applications of Magnetic  
Resonance", R.G. Shulman, ed., Academic Press, New York,  
397-461.
- Neurath, H., and Walsh, K.A. (1976), Proc. Natl. Acad. Sci. USA  
73, 3825-3832.
- Olson, M.O.J., Nagabhushan, M., Dzwiniel, M., Smillie, L.B.,  
and Whitaker, D.R. (1970), Nature (London) 228, 438-442.
- Pauling, L. (1946), Chem. Eng. News 24, 1375-1377.
- Roberts, J.D., Yu, C., Flanagan, C., and Birdseye, T.R. (1982),  
J. Am. Chem. Soc. 104, 3945-3949.

- Robertus, J.D., Kraut, J., Alden, R.A., and Birktoft, J.J. (1972), Biochemistry 11, 4293-4303.
- Ruhlmann, A., Kukla, D., Schwager, P., Bartels, K., and Huber, R. (1973), J. Mol. Biol. 77, 417-436.
- Schachter, M. (1980), Pharm. Rev. 31, 1-17.
- Shaw, M.C., and Whitaker, D.R. (1973), Can. J. Biochem. 51, 112-114.
- Shotton, D.M. (1970), in "Methods in Enzymology", vol. XIX, G.E. Perlmann and L. Lorand, eds., Academic Press, New York, 113-139.
- Smillie, L.B., and Whitaker, D.R. (1967), J. Am. Chem. Soc. 89, 3350-3352.
- Steitz, T.A., Henderson, R., and Blow, D.M. (1969), J. Mol. Biol. 46, 337-348.
- Stroud, R.M. (1974), Sci. Amer. 231, 74-88.
- Stryer, L. (1975), "Biochemistry", 2nd ed., W.H. Freeman and Co., San Francisco.
- Sweet, R.M., Wright, H.T., Janin, J., Chothia, C.H., and Blow, D.M., Biochemistry 13, 4212-4228.
- Thompson, R.C., and Blout, E.R. (1973a), Biochemistry 12, 57-65.
- Thompson, R.C., and Blout, E.R. (1973b), Biochemistry 12, 66-71.
- Tsai, C.S., Whitaker, D.R., Jurasek, L., and Gillispie, D.C., Can. J. Biochem. 43, 1971-1983.
- Walsh, K.A., and Wilcox, P.E. (1970), in "Methods in Enzymology", vol XIX, G.E. Perlmann and L. Lorand, eds., Academic Press, New York, 31-40.

- Whitaker, D.R. (1965), Can. J. Biochem. 43, 1935-1954.
- Whitaker, D.R., Gillespie, D.C., and Cook, F.D. (1965a), Can. J. Biochem. 43, 1927-1934.
- Whitaker, D.R., Roy, C., Tsai, C.S., and Jurasek, L. (1965b), Can. J. Biochem. 43, 1961-1970.
- Whitaker, D.R., Jurasek, L., and Roy, C. (1966), Biochem. Biophys. Res. Commun. 24, 173-178.
- Whitaker, D.R., and Roy, C. (1967), Can. J. Biochem. 45, 911-916.
- Whitaker, D.R. (1970), in "Methods in Enzymology", vol. XIX, G.E. Perlmann and L. Lorand, eds., Academic Press, New York, 599-612.
- Wolfenden, R. (1972), Acc. Chem. Res. 5, 10-18.
- Wolfenden, R. (1976), Ann. Rev. Biophys. Bioeng. 5, 271-306.
- Woodbury, R.G., and Neurath, H. (1980), FEBS Letters 114, 189-196.

## CHAPTER II

$^{13}\text{C}$  NUCLEAR MAGNETIC RESONANCE INVESTIGATIONS  
OF THE IONIZATION BEHAVIOR OF HISTIDINE 57  
IN  $\alpha$ -LYTIC PROTEASE

## ABBREVIATIONS

NMR	Nuclear magnetic resonance
Asp	L-Aspartic acid
His	L-Histidine
Ser	L-Serine
$K^{13}CN$	$^{13}C$ -labelled potassium cyanide
Ala	L-Alanine
Arg	L-Arginine
Asn	L-Asparagine
Gln	L-Glutamine
Gly	Glycine
Ile	L-Isoleucine
Lys	L-Lysine
Leu	L-Leucine
Met	L-Methionine
Phe	L-Phenylalanine
Pro	L-Proline
Thr	L-Threonine
Tyr	L-Tyrosine
Val	L-Valine
TRIS	Tris(hydroxymethyl)aminomethane
FID	Free induction decay

## CHAPTER II--INTRODUCTION

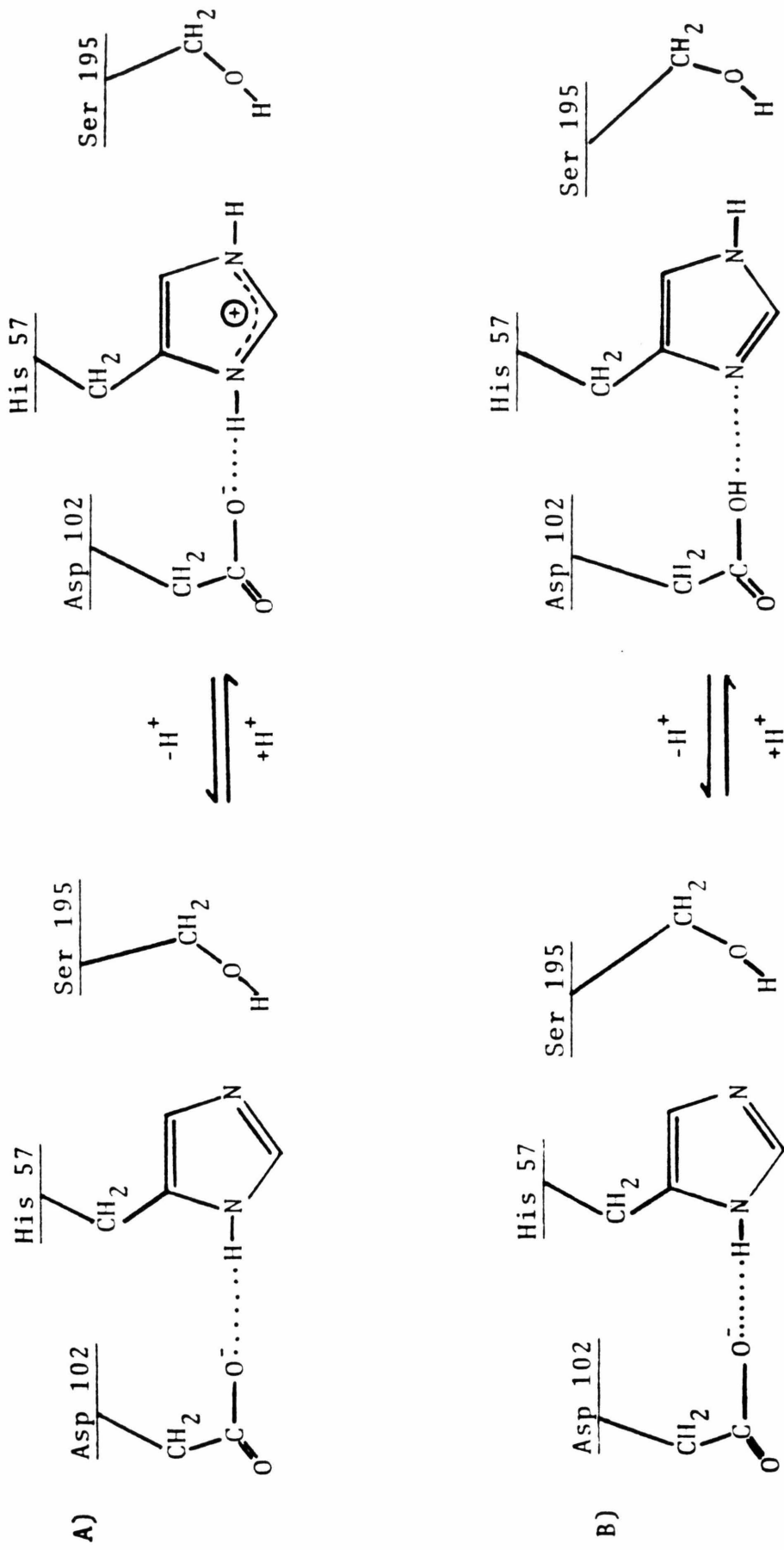
In catalysis by the serine proteases, the side chains of three residues--aspartic acid, histidine, and serine--form a catalytic triad in which the hydroxyl group of serine acts as a nucleophile to attack the carbonyl carbon of the scissile ester or amide bond while the aspartic acid-histidine dyad stores the proton thus released (Blow, 1976; Stroud et al., 1975; Kraut, 1977). As an aid in understanding the molecular details of catalysis, it is helpful to know the microscopic ionization behavior of the Asp-His dyad, since formally two possibilities exist (see Figure 1).

With the advent of highly sophisticated technology, nuclear magnetic resonance (NMR) has become a powerful tool in the study of this problem, due to the sensitivity of proton, carbon-13, and nitrogen-15 chemical shifts and coupling constants to pH. An early carbon-13 study (Hunkapiller et al., 1973) of  $\alpha$ -lytic protease suggested that proton transfer was complete (Figure 1B), resulting in a neutral imidazole ring and neutral carboxylic acid; infrared observations (Koeppel and Stroud, 1976); pulseradiolysis measurements (Faraggi et al., 1978); and theoretical calculations (Amidon, 1974; Beppu and Yomosa, 1977; Kitayama and Fukutome, 1976; Scheiner et al., 1975) supported this suggestion. In contrast, proton (Robillard and Shulman, 1972; Robillard and Shulman, 1974; Markley and Porubcan, 1976; Westler and Markley, 1979; Markley, 1978; Markley, 1975; Westler et al., 1982) and

Figure 1. Two possibilities for the one proton ionization of the catalytic triad of the serine protease enzymes.

A) Ionization behavior assuming normal  $pK_a$  values for the Asp 102 and His 57 side-chains.

B) Ionization behavior assuming that the enzyme tertiary structure is such that the normal  $pK_a$  values for Asp 102 and His 57 are reversed.



nitrogen-15 (Bachovchin and Roberts, 1978) studies on a variety of serine proteases, and the results of a neutron diffraction study (Kossiakoff and Spencer, 1980) have supported normal ionizations for the dyad (see Figure 1A), so that by analogy the imidazole ring is the ultimate proton acceptor during catalysis, the aspartic acid carboxylate aiding this process by providing structural alignment and transition state stabilization.

To resolve the apparent discrepancy between the carbon-13 results and others, we have reexamined the NMR behavior of  $\alpha$ -lytic protease enriched with  $^{13}\text{C}$  at C-2 of the imidazole ring of its single histidine residue at higher magnetic field than the previous experiment (Hunkapiller et al., 1973).

## EXPERIMENTAL

Materials.

L-(2-<sup>13</sup>C)-histidine was synthesized by the method of Hunkapiller et al. (1973), and Ashley and Harington (1930), starting from L-2, 5-diamino-4-ketovaleric acid dihydrochloride and K<sup>13</sup>CN (purchased from Prochem, 90.6% <sup>13</sup>C, lot 43x80). Yield from 5.0 g of K<sup>13</sup>CN was 4.2 g of L-(2-<sup>13</sup>C)-histidine. The <sup>1</sup>H and <sup>13</sup>C NMR spectra in <sup>2</sup>H<sub>2</sub>O were consistent with L-histidine enriched 90.6% with <sup>13</sup>C at C-2.

Deuterium oxide (99.8%) was purchased from Aldrich and used as received.

The water used was deionized and glass-distilled.

The casamino acids, tryptone, and agar used in the bacterial culture were purchased from Difco. The amino acids were from Sigma. All salts were reagent grade from various manufacturers. Sucrose was purchased from Mallinkrodt. Amberlite IR-45 (20-50 mesh), IR-120 (20-50 mesh), and CG-50 (50-100 mesh) ion exchange resins were purchased from Mallinkrodt. Bio-Rad AG11A8 ion retardation resin was purchased from Bio-Rad.

Enzyme. Lysobacter enzymogenes (ATC92847, formerly Myxobacter 495) cultures were procured from Dr. E. A. Peterson of Agriculture Canada, Research Branch. The basic growth procedure was that of Hunkapiller et al. (1973), using a modified culture medium designed to reduce both incorporation of unlabelled histidine into the protein and dilution of the <sup>13</sup>C label into non-specific protein sites.

The bacteria were grown initially on slopes<sup>1</sup> (1% agar, 0.2% tryptone) for 36-48 hours prior to transfer to shake cultures.<sup>2</sup> The shake cultures (first 100 ml in 300 ml Erlenmeyer flasks, then 1 liter in 2.8 l Fernbach flasks) consisted of the following synthetic medium:

L-Amino acids (mg/l): Ala, 120; Asp, 200; Arg, 120; Asn, 120; Gln, 200; Gly, 100; Ile, 150; Lys, 200; Leu, 250; Met, 100; Phe, 75; Pro, 250; Ser, 150; Thr, 100; Tyr, 50; Val, 130; Inorganic Salts (mg/l):  $K_2HPO_4 \cdot 3H_2O$ , 2000; NaCl, 2000;  $MgSO_4 \cdot 7H_2O$ , 1000;  $KNO_3$ , 500;  $Fe_2(SO_4)_3$ , 15;  $ZnSO_4 \cdot 7H_2O$ , 15;  $MnSO_4 \cdot H_2O$ , 2; Monosodium Glutamate (20 g/l) was added as the primary nitrogen source. The above substances were dissolved in distilled water and autoclaved from 20 minutes at 121°C. Sucrose (10 g/l, autoclaved separately) was used as the major carbon source. The above amino acid mixture is designed to simulate the composition of histidine-free commercial casamino acids (casein acid-hydrolysate). Hence, no unlabelled histidine was introduced into the medium. The medium was adjusted to pH 7.1-7.2, and the growth temperature was maintained at 27-29°C.

L-(2-<sup>13</sup>C)-histidine (100 mg/l) was added to each 100 ml culture initially. These cultures were grown for three days and then transferred to the 1 liter cultures of the same synthetic

---

<sup>1</sup>The cultures can be maintained on slopes in the cold (2-4°C) for several weeks; for longer storage, the bacteria should be suspended in 15% sterile glycerol, quick frozen in dry-ice/acetone, and stored at -80°C, or stored freeze-dried at -20°C.

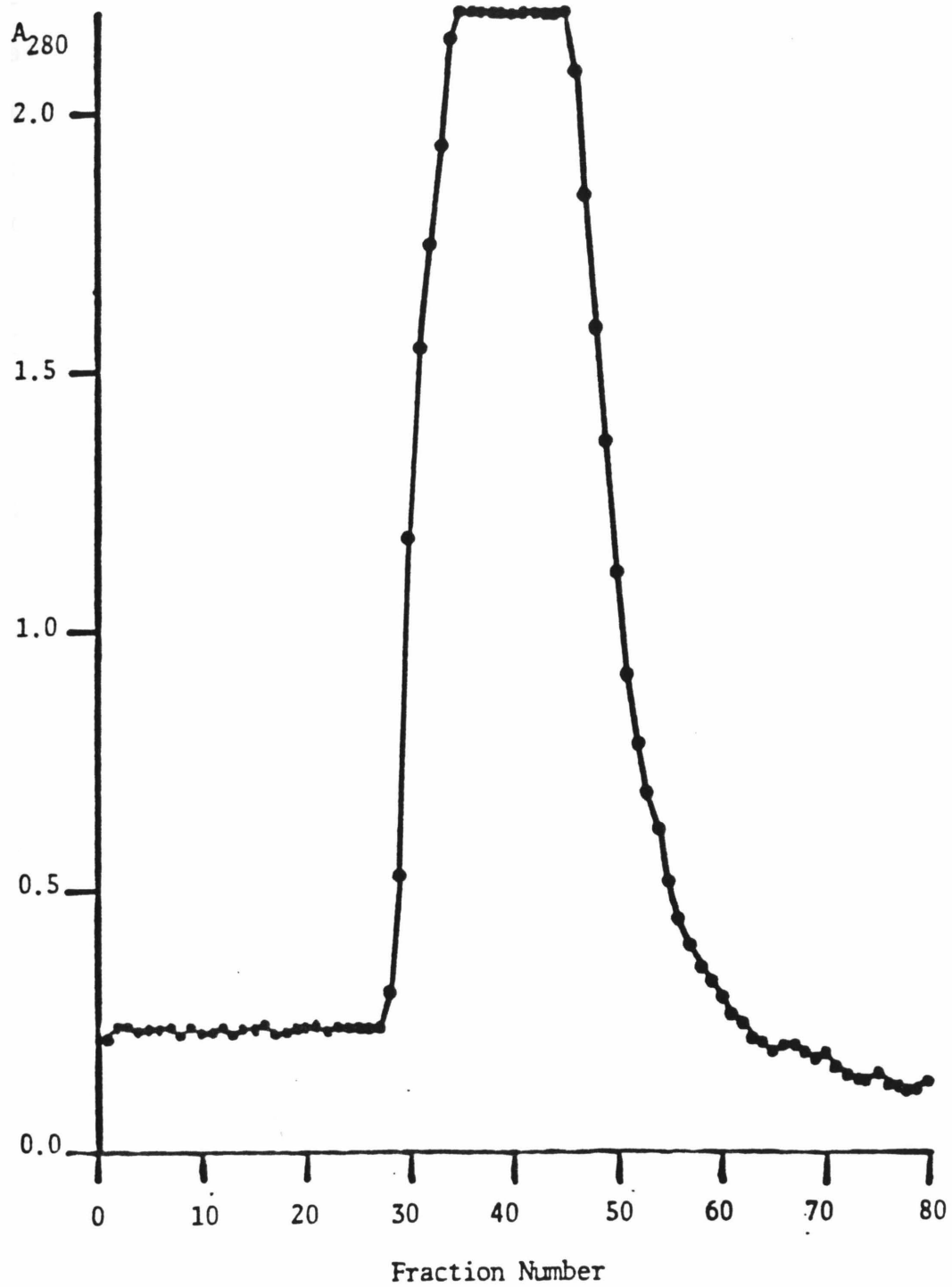
<sup>2</sup>Adequate aeration of the cultures is critical for good enzyme production.

medium containing 50 mg/l of labelled histidine. One ml of a 2.5% (w/v) sterile solution of labelled histidine in distilled water was added at 24-hour intervals to the 1 liter cultures for four to five days. After this time, the bacteria were harvested;  $\alpha$ -lytic protease activity in the medium at this point was  $\sim 150$  mg/l. Activity was assayed versus the synthetic substrate N-ac-L-alanyl-L-prolyl-L-alanine p-nitro-anilide in 0.1 M KCl, 0.05 M Tris(hydroxymethyl)aminomethane/HCl, pH 8.75, 25°C,  $4 \times 10^{-4}$  M substrate;  $k_{cat}/K_m$  under these conditions (pseudo-first order kinetics,  $S_0 \approx 3\%$  of  $K_m$ ) is  $1700 \pm 150 \text{ M}^{-1} \text{ s}^{-1}$ .

Unlabelled enzyme was produced from bacteria grown in the same medium as labelled enzyme, except that the synthetic amino acid mixture was replaced by 2.5 g/l of casamino acids, and the amount of added NaCl was reduced to 1.35 g/l, to account for the NaCl present in the casamino acid mixture.

Isolation and purification of the enzyme was performed as per the method of Hunkapiller et al. (1973), with three minor modifications. Two-hundred ml (settled bed volume) of Amberlite CG-50 cation exchange resin, pH 4.95, 0.1 M NaOH/acetic acid, was added to the combined bacteria-free media, instead of 100 ml. Adsorption of the protein onto this resin was continued for two days, rather than one. Also, the final elution step required 0.50 M NaOH/citric acid buffer, pH 6.40, rather than 0.27 M NaOH/citric acid, pH 6.20. These changes were necessary due to some modification in the properties of the presently available CG-50 resin over that

Figure 2. Chromatography of  $\alpha$ -lytic protease adsorbed onto Amberlite CG-50 (200 ml). The resin was poured into a 2.5 cm diameter column. The eluting buffer in the chromatogram was 0.50 M NaOH/citric acid, pH 6.40. Chromatography was done at 4°C. Fractions were 8.0 ml in volume.



used in the previous isolation procedure. The enzyme was chromatographed on CG-50 twice; a typical chromatogram is shown in Figure 2. Fractions containing enzyme were dialyzed versus three changes of 6 l of 0.1 M KCl and versus three changes of distilled water, and lyophilized. The lyophilized enzyme can be stored at -20°C for extended periods without substantial loss of activity. Yield was 400-500 mg of  $\alpha$ -lytic protease from six liters of culture.

#### Methods.

NMR Samples. NMR samples were made by dissolving the desired amount of protein in 0.2 M KCl, 90% double-distilled water--10%  $^2\text{H}_2\text{O}$  (v/v). In order to adjust the pH of the samples, they were first cooled in an ice bath. The pH of the cold solution was then adjusted by slowly and carefully adding 1 N HCl or 1 N KOH while stirring the sample on a vortexer; this procedure was used to prevent as much as possible any local denaturation of the protein on addition of concentrated acid or base to the concentrated enzyme solution. The solution was allowed to warm to room temperature prior to recording the final pH. The pH of the sample was checked on a Radiometer PHM26 pH meter equipped with a Radiometer GK2322C combination electrode that could be inserted into the NMR tube; pH measurements were taken prior to and following each spectrum, with an agreement of  $\pm 0.05$  pH units between readings. The electrode was standardized versus pH 7 and pH 4 aqueous buffers, and the reported pH values are uncorrected for the  $^2\text{H}_2\text{O}$  present in the NMR samples.

The concentration of (active) protein in each sample was checked by determining both the absorbance at 280 nm ( $[E] = 5.16 \times 10^{-5} \times A_{280}^{1\text{cm}}$  (Whitaker, 1970)) and by monitoring the hydrolysis of N-acetyl-L-alanyl-L-prolyl-L-alanine p-nitroanilide at 410 nm ( $4 \times 10^{-4}$  M in 0.1 M KCl, 0.05 TRIS/HCl, pH 8.75, 25°C). These two methods agreed to within  $\pm 2\%$  and were  $\pm 5\%$  with respect to added mass of protein. Comparison of these NMR spectra with representative spectra done by Hunkapiller et al. (1973) showed a  $^{13}\text{C}$ -histidine enrichment of 65-75% and little non-specific enrichment.

NMR Spectra.  $^{13}\text{C}$  NMR spectra were taken on four different spectrometers. Low field measurements were done on a Varian XL-100-15 spectrometer operating at 25.14 MHz. 50.3 MHz data were performed on a Nicolet NT-200 or a Varian XL-200. The high field spectra were obtained on a Bruker WM-500 spectrometer. Sample tubes were 10, 12 and 20 mm in diameter, depending on the instrument used. The linewidths were determined by subtracting the line broadening applied to the free induction decay (FID) from the resulting transformed spectra. Chemical shifts are reported relative to the arginine guanidinium carbons which resonate at 157.25 ppm downfield from the methyl carbons of external tetramethylsilane and whose position did not change over the pH range investigated.

## RESULTS

Figure 3 compares the natural abundance 50.3 MHz carbon-13 spectrum of  $\alpha$ -lytic protease with the spectrum of  $^{13}\text{C}$ -histidyl- $\alpha$ -lytic protease. The selective enrichment of the C-2 carbon of the lone histidine side-chain is seen quite clearly.

Figure 4 shows the coupled and decoupled 25.14 MHz carbon-13 spectra for  $\alpha$ -lytic protease at pH 5.1. Even at this field strength, the resonances corresponding to the C-2 carbon of the histidine ring are clearly discernible above the unenriched protein carbon resonances. The observed coupling constant at this pH is 214 Hz, not 205 as previously reported (Hunkapiller et al., 1973). However, if the coupling constant is measured using the method of Hunkapiller et al. (1973), by taking twice the difference between the downfield resonance of the proton-coupled C-2 doublet and the decoupled C-2 resonance, a value of 206 Hz is obtained. This discrepancy between the observed coupling constant (from the coupled spectrum) and the calculated coupling constant (from the measurement of  $1/2 \ ^1J_{\text{CH}}$ ) will be discussed later.

The titration of  $^{13}\text{C}$ -histidyl- $\alpha$ -lytic protease is shown in Figure 5, and representative spectra are shown in Figure 6. As the two forms (protonated and neutral) of the imidazole ring are fast exchange, the data can be fitted by the following equation (as described by Hunkapiller et al., 1973):

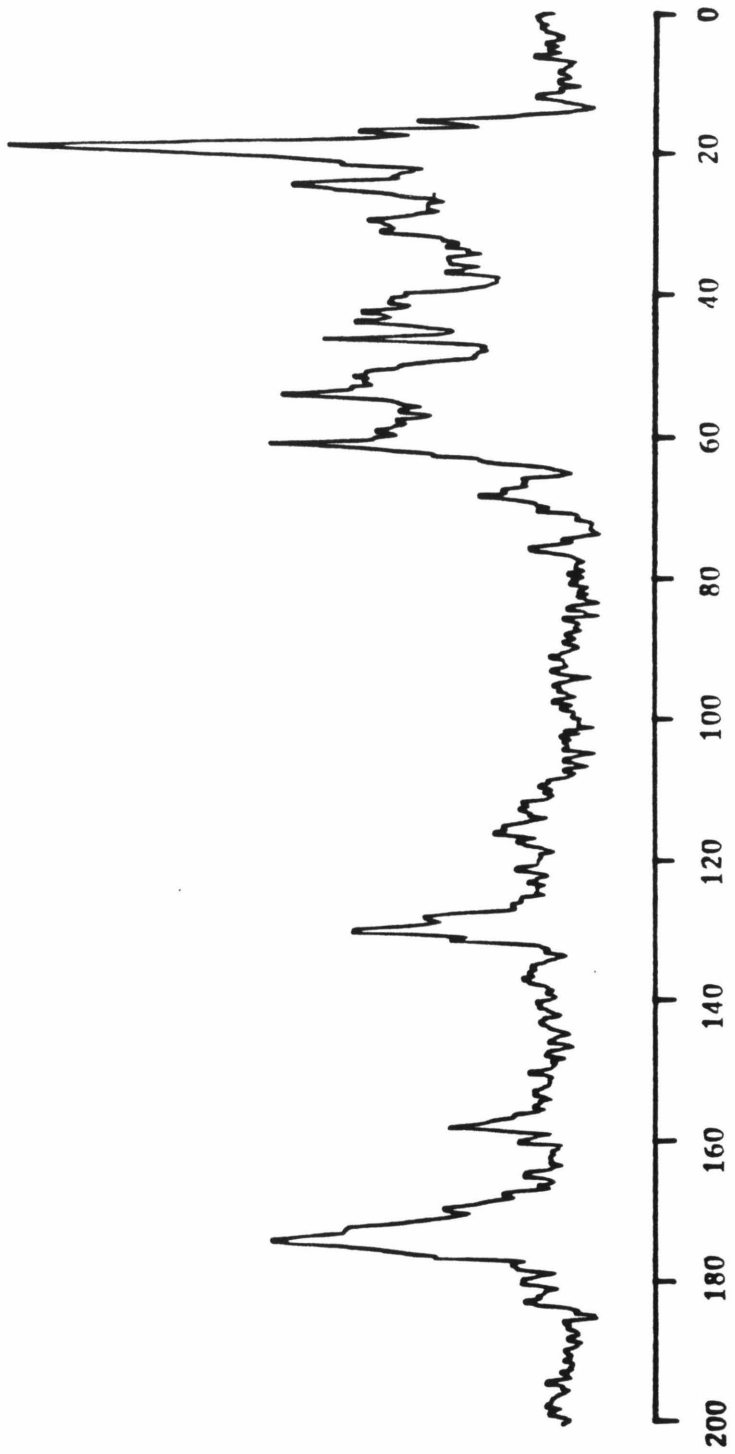
$$(\delta_{\text{obs}} - \delta_{\text{A}})/(\delta_{\text{A}} - \delta_{\text{B}}) = K_{\text{a}}/[\text{H}^+] + K_{\text{a}}]$$

where  $\delta_{\text{obs}}$   $\equiv$  the observed chemical shift,  $\delta_{\text{A}}$   $\equiv$  the limiting

Figure 3. A) 50.3 MHz (XL-200) broadband decoupled  $^{13}\text{C}$  nmr spectrum of unlabelled  $\alpha$ -lytic protease. The sample was 7.5 mM enzyme in 0.1 M KCl, 10% (v/v)  $^2\text{H}_2\text{O}$ , pH 8.1. The spectrum represents 3288 transients taken with an acquisition time of 0.25 sec, a 12 KHz spectral width, and a  $90^\circ$  pulse of 14.0  $\mu\text{sec}$ . A 0.25 sec delay was used between pulses. The decoupler was turned off during this delay. 6002 FID points were zero-filled to a Fourier number of 8192 and transformed with 20 Hz line broadening.

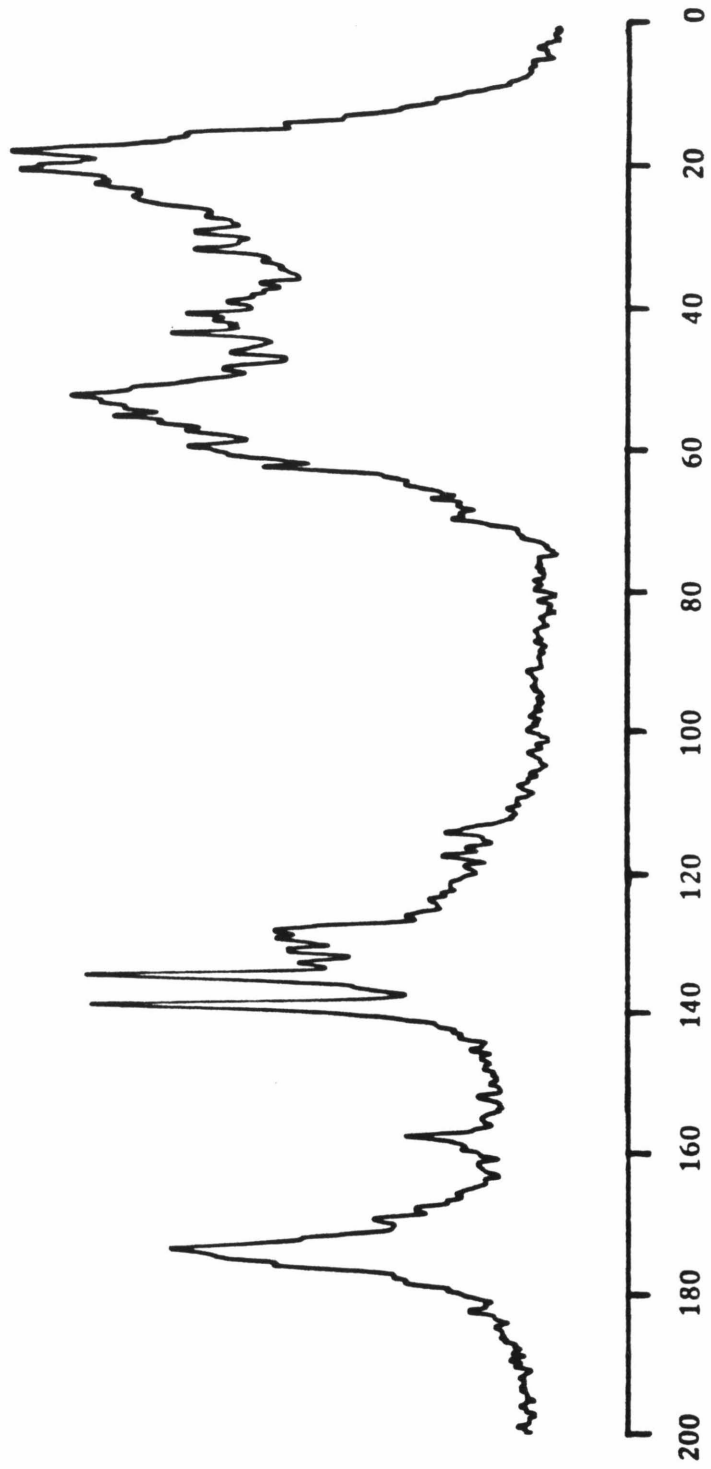
B) 50.3 MHz (XL-200) proton-coupled  $^{13}\text{C}$  nmr spectrum of (2- $^{13}\text{C}$ )-histidyl- $\alpha$ -lytic protease. The sample was 3.8 mM enzyme in 0.1 M KCl, 10% (v/v)  $^2\text{H}_2\text{O}$ , pH 8.0. The spectrum represents 110,783 transients taken with an acquisition time of 0.25 sec, a 12 KHz spectral width, and a  $90^\circ$  pulse of 14.0  $\mu\text{sec}$ . 6002 FID points were zero-filled to a Fourier number of 8192 and transformed with 20 Hz line broadening.

A



Chemical Shift  
(ppm downfield from Me<sub>4</sub>Si)

B



Chemical Shift  
(ppm downfield from Me<sub>4</sub>Si)

Figure 4. A) 25.14 MHz proton-decoupled  $^{13}\text{C}$  nmr spectrum of  $\alpha$ -lytic protease in 10%  $^2\text{H}_2\text{O}$ . The sample was 0.2 M KCl, 7.5 mM enzyme,  $32^\circ\text{C}$ , pH 5.1. 144,000 transients were taken with an acquisition time of 0.15 sec, 5 KHz spectral width, and a  $90^\circ$  pulse of 90  $\mu\text{sec}$ . The FID was zero-filled to 8192 data points and transformed with a line broadening of 3 Hz.

B) 25.14 MHz proton-coupled spectrum of the sample in (A) above. The probe temperature was  $26^\circ\text{C}$ . 169,000 transients were taken under the same conditions as in (A).

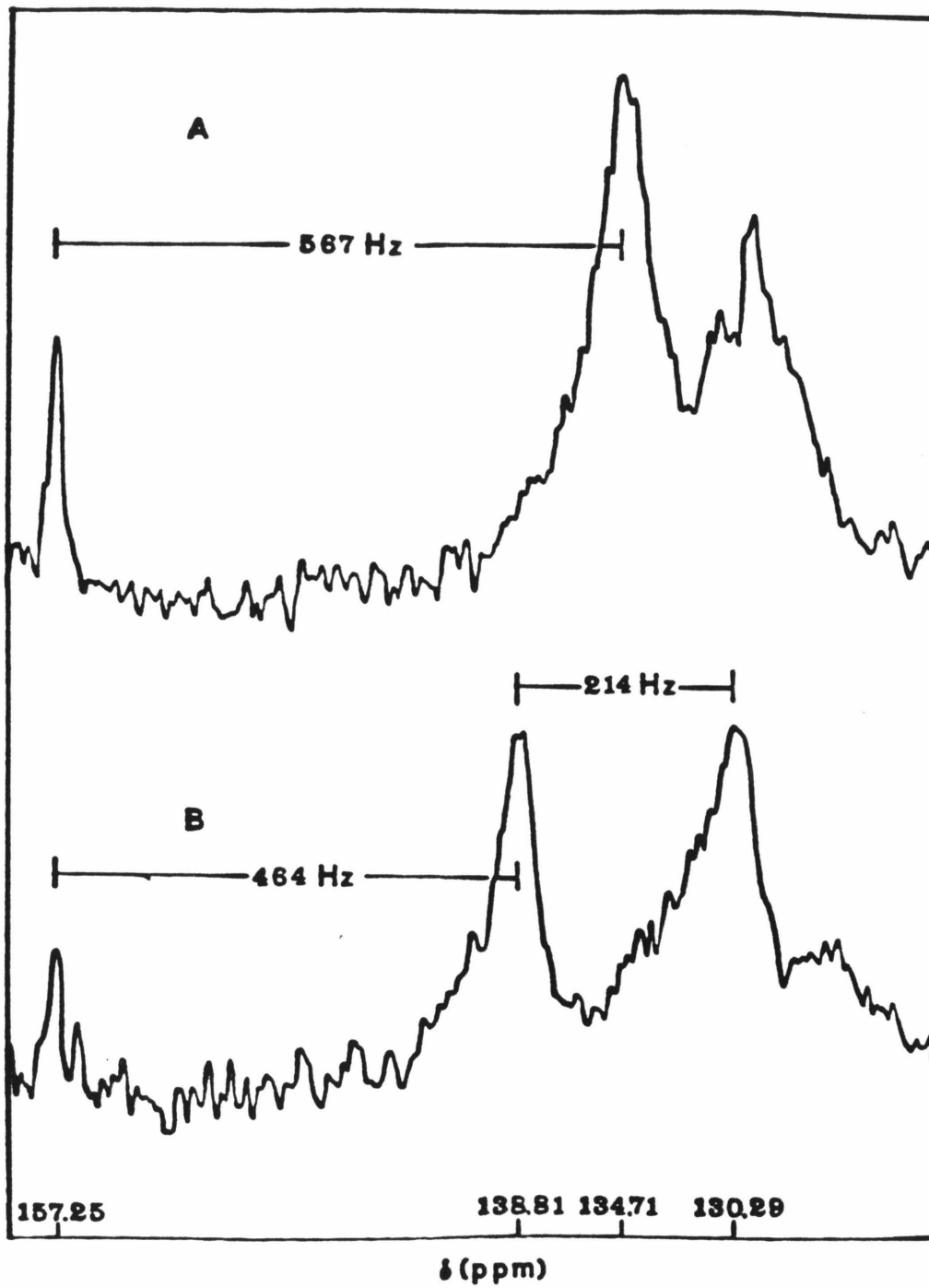


Figure 5. Chemical shift of the Histidine 57 C-2 carbon resonance of  $\alpha$ -lytic protease as a function of pH. The solid line is the theoretical titration curve calculated using a  $pK_a$  of 6.7 and a value of  $\delta_A - \delta_B$  of 2.66 ppm.

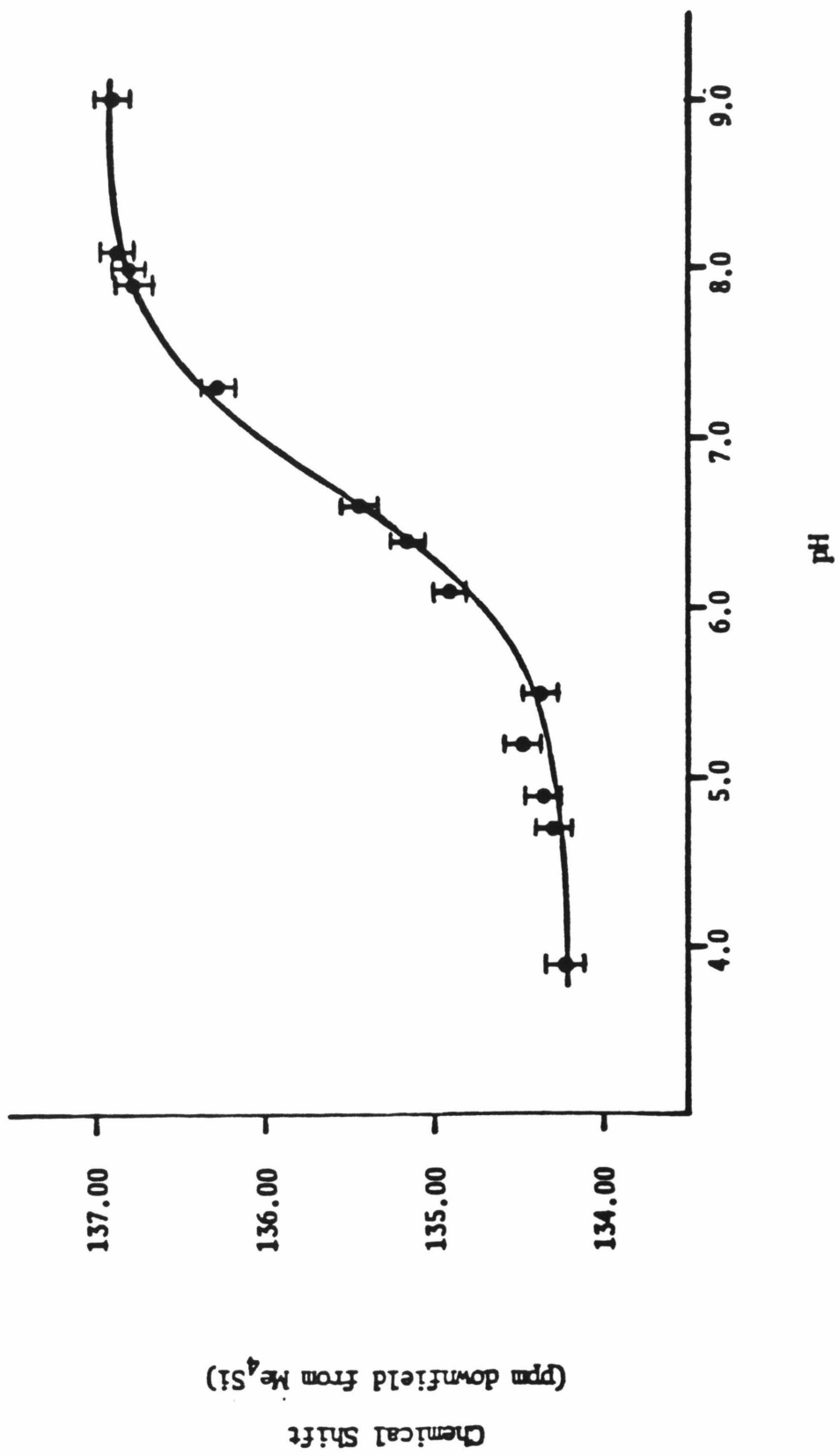
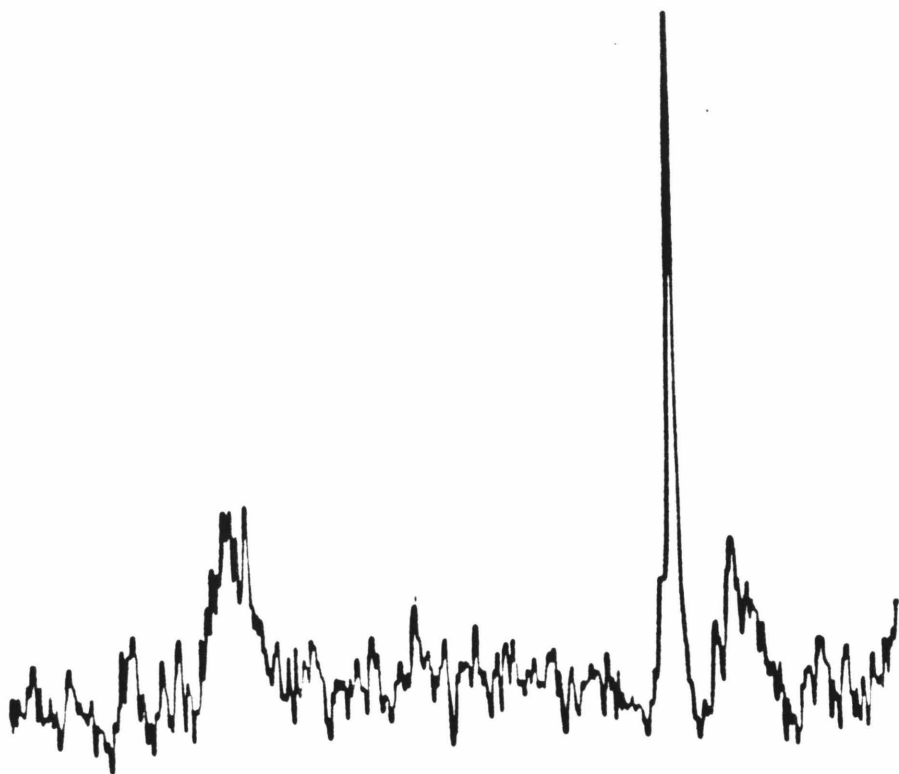
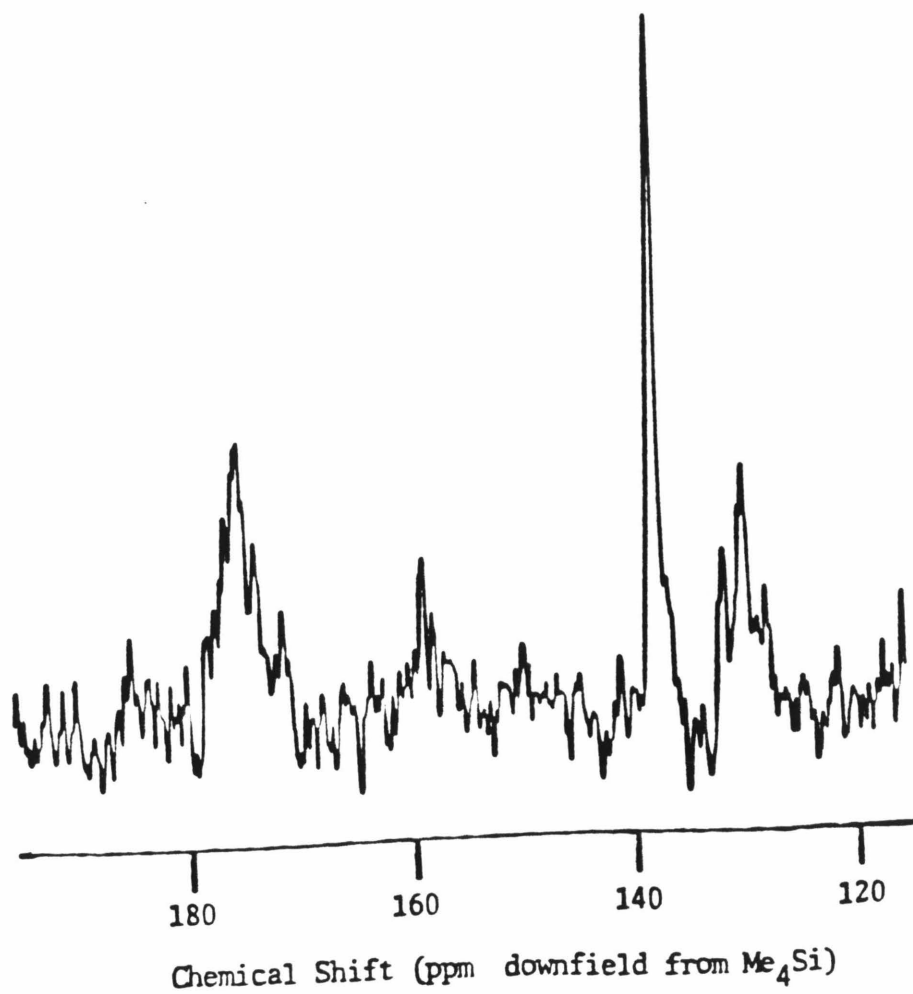


Figure 6. A) 50.3 MHz (XL-200) broadband proton-decoupled  $^{13}\text{C}$  nmr spectrum of  $\alpha$ -lytic protease at pH 5.5. The sample was 2.0 mM protein in 0.2 M KCl, 10% (v/v)  $^2\text{H}_2\text{O}$ . The spectrum represents 7764 transients taken with an acquisition time of 0.20 sec, a 12 KHz spectral width, and a  $75^\circ$  pulse of 15.6  $\mu\text{sec}$ . Gated decoupling was used to reduce dielectric heating of the sample. The decoupler was turned off during a 0.50 sec delay between pulses and turned on during acquisition. 4800 FID points were zero-filled to a Fourier number of 8192 and transformed with 10 Hz line broadening.

B) 50.3 MHz (XL-200) broadband proton-decoupled  $^{13}\text{C}$  nmr spectrum of  $\alpha$ -lytic protease at pH 7.9. The sample was the same as in (A) above, and was taken under identical conditions (10,000 transients). 4800 FID points were zero-filled to a Fourier number of 8192 and transformed with a line broadening of 10 Hz.

AB

chemical shift of the acidic (protonated) species,  $\delta_B \equiv$  the limiting chemical shift of the basic (neutral) species, and  $K_a$  is the equilibrium (dissociation) constant for the reaction  $A \rightleftharpoons H^+ + B$ . The solid line in the figure is calculated for  $pK_a = 6.7$  using the above equation. The chemical shift titration data therefore indicate that the C-2 carbon is affected by an ionization of  $pK_a 6.7 \pm 0.1$ , as determined previously.

To determine unambiguously the identity of the group titrating with the above  $pK_a$ , the determination of the coupling constant  $^1J_{CH}$  between the C-2 carbon and its attached proton was examined as a function of pH at various magnetic field strengths. Table I collects these data; Figures 7 and 8 show representative spectra. It is seen that at pH 5.5 the histidine residue has acquired a proton, as  $^1J_{CH} \approx 220$  Hz is the characteristic value of an imidazolium cation (Hunkapiller et al., 1973; Wasylishen and Tomlinson, 1975).

The 125.76 MHz spectrum of  $\alpha$ -lytic protease at pH 5.5 shows other interesting features (see Figure 8) that are not apparent at 25.14 or 50.3 MHz. First, a new doublet is seen centered at 135.54 ppm which has a coupling constant  $^1J_{CH} = 225$  Hz. Also, the intensities of the two peaks of the major doublet assigned to the C-2 resonance are noticeably different. A similar difference is observed in the intensities of the two peaks of the doublet in the 125.76 MHz spectrum at pH 8.1. A smaller difference of the same type characterizes the 50.3 MHz spectrum at pH 4.9; however, both peaks of the doublet appear

TABLE I. NMR parameters for the C-2 carbon in the Histidine 57 residue of  $\alpha$ -lytic protease.

Field(MHz)	pH	$\delta$ (ppm) <sup>a</sup>	$^1J_{CH}$ (Hz) <sup>b</sup>	$\nu_{1/2}$ (Hz) <sup>c</sup>
25.14	5.1	134.71 <sup>d</sup>	---	40
		134.55 <sup>e</sup>	214	40
50.3 <sup>f</sup>	5.2	134.52	218	40
50.3 <sup>g</sup>	5.2	134.48	222	--
	6.6	135.44	---	--
	8.0	136.80	209	--
	8.1	136.86	204	--
125.76	8.1	136.68	204	50
	5.5	135.54	225	40
		134.47	221	40
	4.8	135.21	217	35
		134.55	214	35
		134.34	216	35

<sup>a</sup>Chemical shift values are  $\pm$  0.10 ppm at 25.14 and 50.3 MHz, and  $\pm$  0.05 ppm at 125.76 MHz. The shifts are relative to external tetramethylsilane = 0.00 ppm.

<sup>b</sup> $^1J_{CH}$  values are  $\pm$  3 Hz.

<sup>c</sup> $\nu_{1/2}$  values are  $\pm$  10%.

<sup>d</sup>Proton-decoupled.

<sup>e</sup>Proton-coupled.

<sup>f</sup>Bruker NT-200 spectrometer (20 mm sample tube).

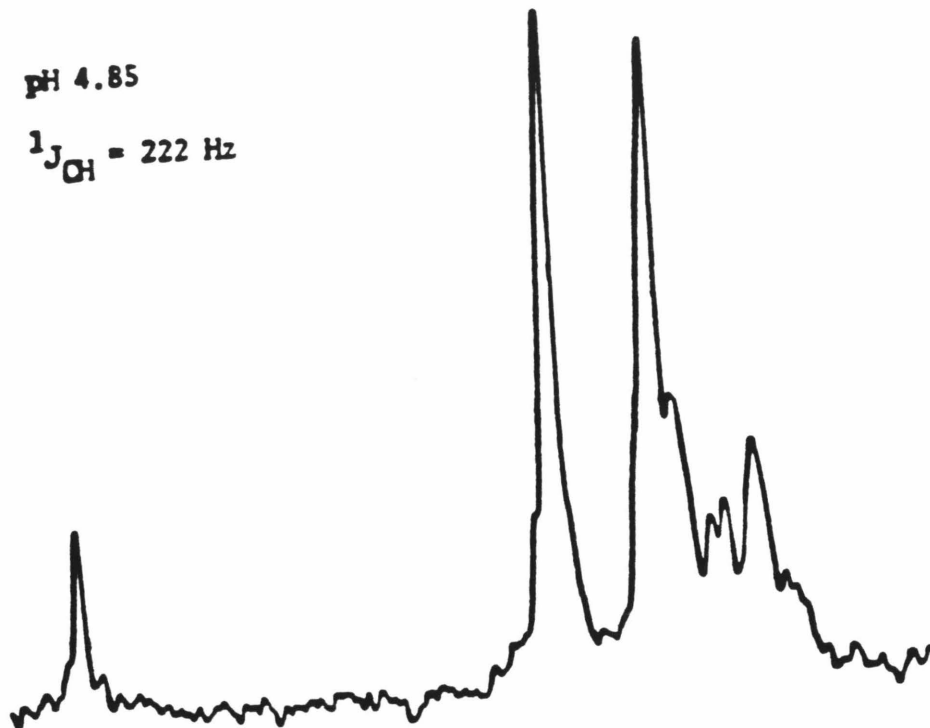
<sup>g</sup>Varian XL-200 spectrometer (10 mm sample tube).

Figure 7. 50.3 MHz (XL-200) proton-coupled  $^{13}\text{C}$  nmr spectrum of  $\alpha$ -lytic protease at pH 4.9. The sample is the same as that described in Figure 6. NOE-enhancement was used to reduce the accumulation time needed to obtain good signal-to-noise; the decoupler was turned on during a 0.3 sec delay between pulses, and turned off during acquisition. The spectrum represents 50,000 transients taken with an acquisition time of 0.20 sec, a 12 KHz spectral width, and a  $75^\circ$  pulse of 15.6  $\mu\text{sec}$ . 4800 FID points were zero-filled to a Fourier number of 8192 and transformed with a line broadening of 10 Hz.

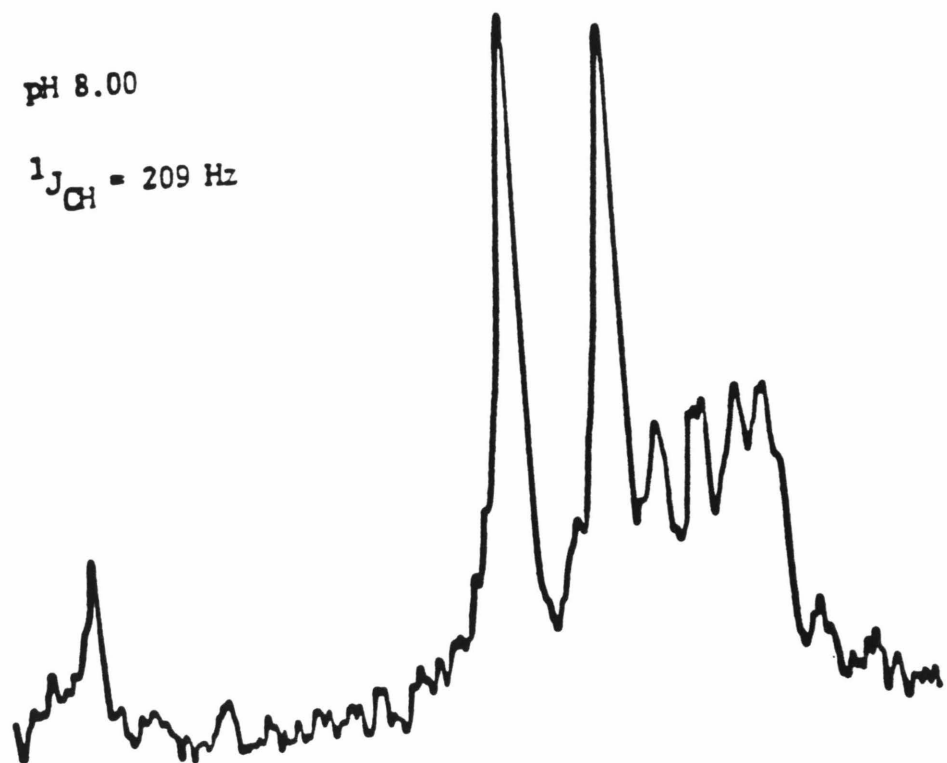
B) 50.3 MHz (XL-200) proton-coupled  $^{13}\text{C}$  nmr spectrum of  $\alpha$ -lytic protease at pH 8.0. The sample is the same as in Figure 6. The spectrum was taken (60,000 transients) and processed using the same parameters as in (A) above.

A

pH 4.85

 $^1J_{\text{CH}} = 222 \text{ Hz}$ B

pH 8.00

 $^1J_{\text{CH}} = 209 \text{ Hz}$ 

160

150

140

130

Chemical Shift (ppm from Me<sub>4</sub>Si)

Figure 8. 125.76 MHz proton coupled  $^{13}\text{C}$  nmr spectrum of  $\alpha$ -lytic protease at pH 5.5. The sample was 3.2 mM protein in 0.2 M KCl, 10% (v/v)  $^2\text{H}_2\text{O}$ , 25°C. The spectrum represents 37,660 transients taken with an acquisition time of 0.52 sec, a 31.25 KHz spectral width, and a  $23^\circ$  pulse of 30 sec. The FID was transformed using a line broadening of 5 Hz.

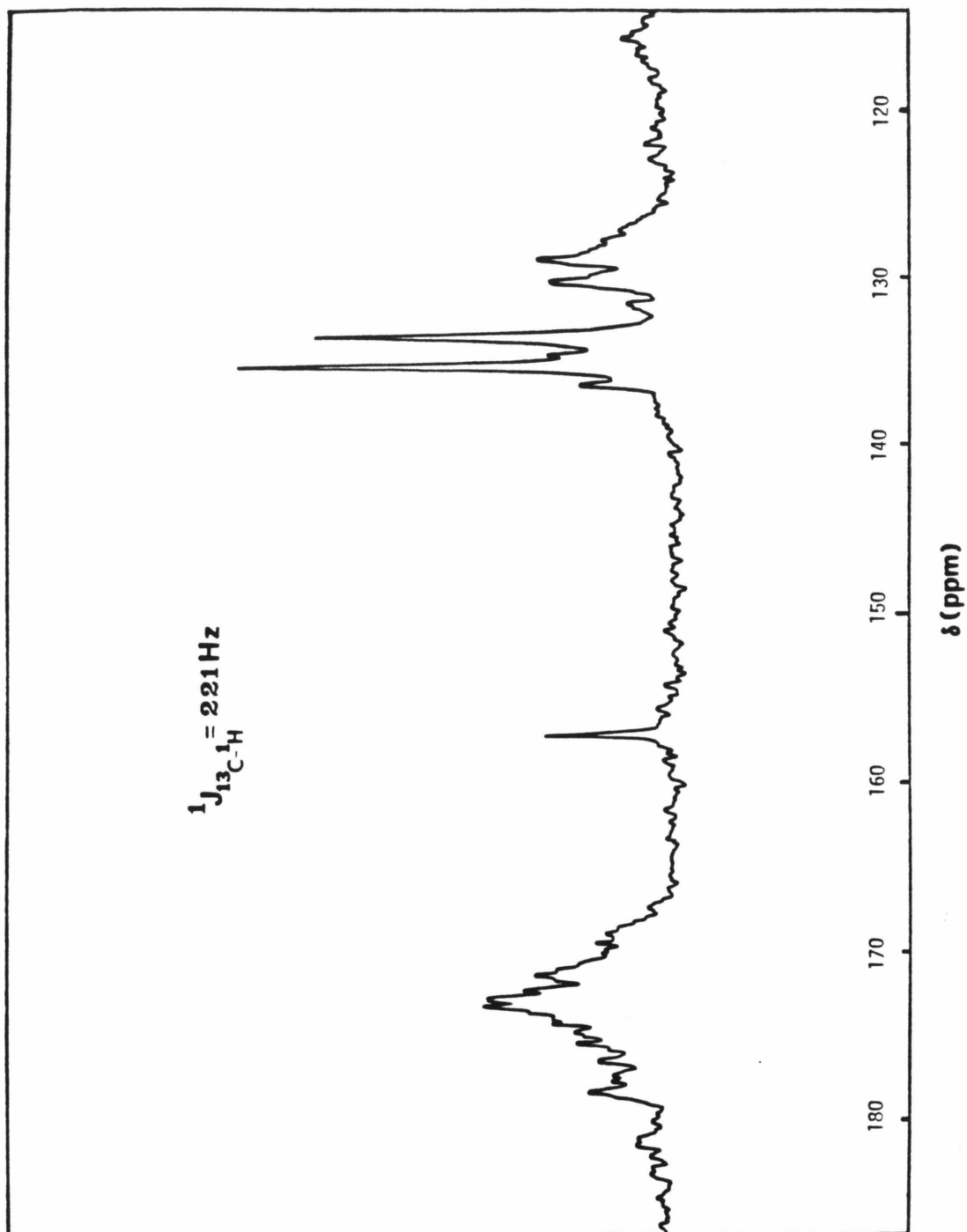


Figure 9. 125.76 MHz proton-coupled  $^{13}\text{C}$  nmr spectra of  $\alpha$ -lytic protease in 0.2 M KCl, 10%  $^2\text{H}_2\text{O}$ , at 25°C.

A) Same sample as in Figure 8. pH 5.5, 37,660 transients, 20 Hz line broadening.

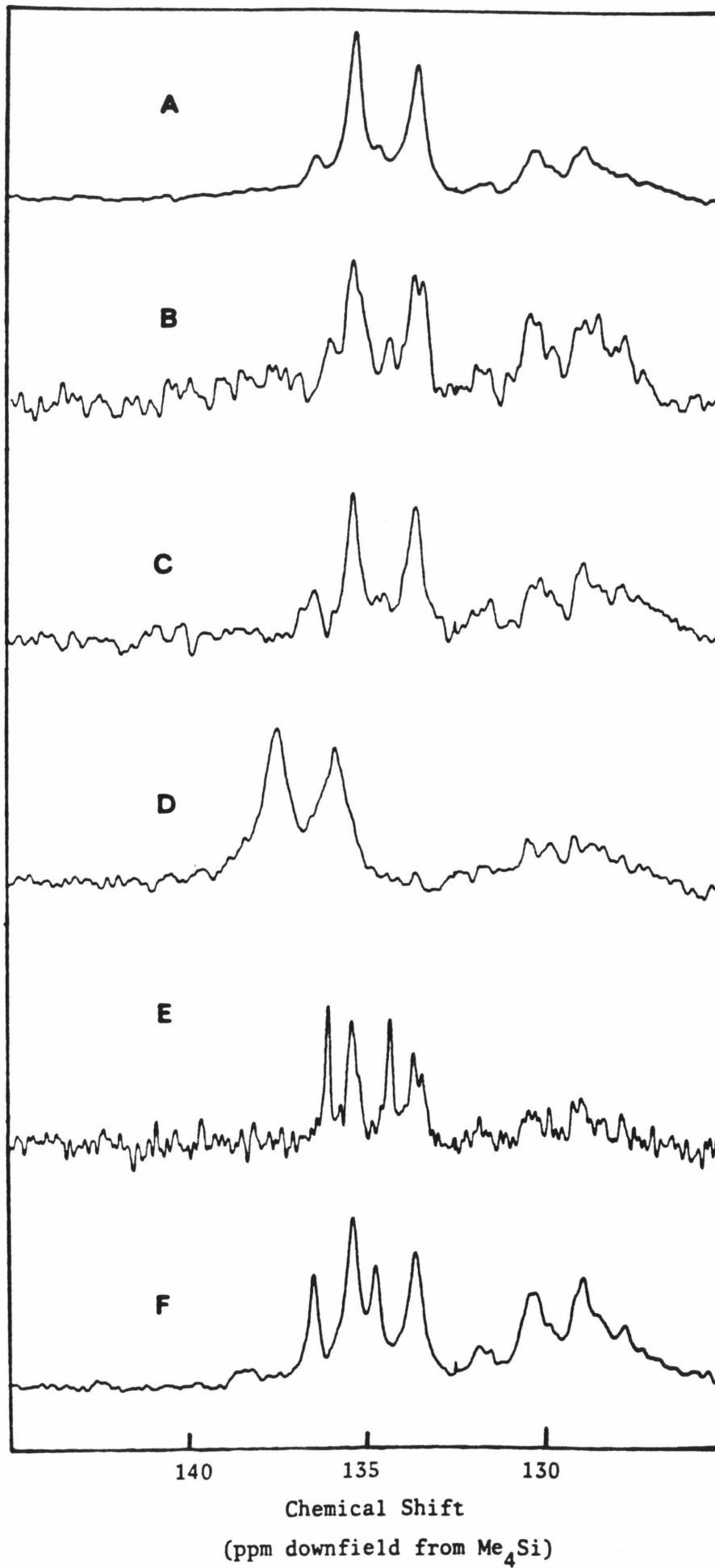
B) 2.0 mM protein in 0.2 M KCl, 10%  $^2\text{H}_2\text{O}$ . The pH was adjusted to 4.8 after initially having been at 5.5 during a prior spectrum. 7,600 transients, 20 Hz line broadening. Other parameters are the same as in Figure 8.

C) Same sample as in (B) above. The pH was adjusted to 5.5 after having been at 4.8. 12,080 transients, 20 Hz line broadening.

D) Same sample as in (A) above. pH 8.1, 8630 transients, 20 Hz line broadening.

E) Same sample as in (D) above, pH 4.8, 6140 transients, 20 Hz line broadening. The lower trace is resolution enhanced.

F) Same sample as in (B) above. The pH was adjusted to 5.5 after having been at 8.1 during a prior spectrum. 63,008 transients, 20 Hz line broadening.



to have nearly the same intensity in the 50.3 MHz spectrum at pH 8.0 (see Figure 7).

As the pH is lowered from 5.5 to 4.8, a third doublet, slightly upfield of the other two doublets and centered at  $\delta = 134.34$  ppm appears (Figure 9B). This doublet disappears as the pH is once again raised to 5.5 (Figure 9C). The changes in the spectra in going from pH 5.5 to pH 4.8 and back to pH 5.5 again are reversible and reproducible as long as the sample has not been at pH  $\geq 7$  at any time. When the sample is titrated to pH 8.1 (Figure 9D) and subsequently returned to pH 4.8, the spectrum in Figure 9E is obtained. Raising the pH of this sample to pH 5.5 yields a spectrum similar to the previous pH 5.5 spectra, except that the intensity of the downfield doublet is greater (Figure 9F).

## DISCUSSION

Ionization Behavior of the Asp-His dyad. For  $\alpha$ -lytic protease at pH 5.5, the coupling constant  $^1J_{CH}$  observed for C-2 of the imidazole ring of the catalytic histidine (His 57 using the amino acid sequence numbering of chymotrypsinogen; His 36 in the actual protein sequence) and its attached protein are 218-22 Hz at 50.3 MHz and 221 Hz at 125.76 MHz; these values indicate a protonated imidazole (Wasylishen and Tomlinson, 1975; Hunkapiller et al., 1973), and agree with the  $^{15}N$  and  $^1H$  NMR observations (Bachovchin and Roberts, 1978; Robillard and Shulman, 1972, 1974; Markley and Porubcan, 1976; Westler and Markley, 1979; Markley et al., 1980; Porubcan et al., 1979; Markley, 1978; Markley, 1975; Westler et al., 1982) on  $\alpha$ -lytic protease and other serine proteases.

The titration curve for the catalytic histidine shows a  $pK_a$  of 6.7 as seen previously (Hunkapiller et al., 1973). This value agrees well with values obtained kinetically from  $\log(k_{cat}/K_m)$  versus pH plots for benzoyl-L-alanine methyl ester (6.55) and acetyl-L-valine methyl ester (6.70, Kaplan and Whitaker, 1969), and for N-acetyl-L-alanyl-L-prolyl-L-alanine p-nitroanilide (6.70) (Chapter IV of this thesis). It is known that these plots generate  $pK_a$  values for catalytic groups in the free enzyme ( $k_{cat}/K_m = k_2/K_s$ , Bender et al., 1964). Furthermore, it coincides (within experimental error) with the value determined by  $^1H$  NMR (6.6, Markley et al., 1980) and  $^{15}N$  NMR (7.0, Bachovchin and Roberts, 1978).

High Field NMR Spectra. The  $^{13}\text{C}$  spectra of  $\alpha$ -lytic protease at 125.76 MHz at pH 5.5 show two signals from the single histidine residue, indicating the existence of two structural forms of the enzyme which are in slow exchange relative to the NMR time scale at this field strength. At lower fields these forms appear to be in fast to intermediate exchange. For both signals,  $^1J_{\text{CH}}$  is that characteristic of an imidazolium cation (at  $\delta = 134.37$  ppm  $^1J_{\text{CH}} = 221$  Hz; at  $\delta = 135.54$  ppm,  $^1J_{\text{CH}} = 225$  Hz). Both signals appear to have about equal linewidths (30-40 Hz) which suggests that in neither case does the imidazole ring rotate freely in solution, as such as residue has a much narrower linewidths ( $\sim 12$  Hz, Hunkapiller et al., 1973). A reservation in this conclusion is that, if the exchange process is on the borderline between slow and intermediate, the observed linewidth could reflect not only the mobility of the residue but could also be broadened by virtue of the exchange process itself. The relative contributions of these two processes cannot presently be dissected.

At pH 4.8, a third pair of resonances occurs at 134.34 ppm which likewise has a  $^1J_{\text{CH}}$  characteristic of a protonated imidazole. The overlap of these resonances with the resonances centered at  $\delta = 134.55$  ppm causes the differences in intensities observed for the upfield doublet at pH 5.5 and pH 8.1.

Initially we were concerned that the multiplicity of low pH forms was due to denaturation of the protein. Two observations

mitigate against this proposal. First, after this series of NMR observations ( $\sim 12$  hours), and being returned to pH 8.0, the enzyme preparation retained  $96 \pm 5\%$  of its original activity. Second, the linewidths of all of the low pH forms are essentially the same at 35-40 Hz; denatured protein is expected to display a much narrower linewidths ( $\sim 12$  Hz). Hence, the multiple forms likely represent different conformations of potentially active protein.

Markley and coworkers (Markley et al., 1980; Westler et al., 1982) have observed two discrete resonances in the 360 MHz  $^1\text{H}$  NMR spectrum of  $\alpha$ -lytic protease throughout the pH range 3 to 9 which they have assigned to H-2 of the imidazole ring of His 57. The existence and relative intensities of these two signals depends on the history of the NMR sample. Conformer a is seen in freshly dialyzed and lyophilized enzyme; conformer b is seen after incubation of the sample for several hours at pH 8.0. The chemical shift difference between the two resonances is about 0.1 ppm, or about 36 Hz at this frequency; this separation remains essentially constant throughout the pH range 3 to 9. Since these two conformers are in slow exchange, as judged by the observation of two discrete signals, the lifetime of either conformer,  $\tau$ , must be greater than  $1/36 \text{ Hz}^{-1}$ , or about 0.03 sec.

The multiple high field  $^{13}\text{C}$  resonances observed at low pH may also be due to the presence of these two conformers of  $\alpha$ -lytic protease. If this is the case, the two resonances

at 135.5 ppm and 134.5 ppm observed at pH 5.5 could be assigned to conformer b and conformer a, respectively, since the b to a ratio changes in favor of the b conformer on incubation of the protein at pH 8 in the  $^1\text{H}$  NMR spectrum, and the intensity of the  $^{13}\text{C}$  resonance at 135.5 ppm increases relative to the intensity of the resonance at 134.5 ppm following incubation of the sample at pH 8.1 (see Figures 9A, 9C, and 9F). The  $^{13}\text{C}$  chemical shift difference at pH 5.5 is about 1.0 ppm, or about 125 Hz at 125.76 MHz, so that the observation of separate signals at this pH implies that the two conformers are in slow exchange with  $\tau > 0.008$  sec. This is consistent with the  $^1\text{H}$  results.

The inability to observe two discrete signals at pH 8.1 in the  $^{13}\text{C}$  spectrum is potentially disconcerting. However, due to the linewidths of the resonances involved (40-50 Hz), we would be unable to resolve a chemical shift difference between two discrete signals of less than about 0.1 ppm, or 10-12 Hz. Thus, two separate signals could exist in the pH 8.1 spectrum, albeit unresolved, if  $\tau > 0.2$  sec. Since we have no evidence bearing on what the environment of His 57 in the two putative high pH species would be, we unfortunately cannot predict what the  $^{13}\text{C}$  chemical shift difference between these two forms might be. It is interesting to note that, in contrast to the  $^1\text{H}$  NMR spectra in which the separation between the resonances assigned to the two conformers remains constant at about 36 Hz (0.1 ppm) throughout the pH range 3

to 9, the approximately 125 Hz (1 ppm) separation between the resonances assigned to the two conformational species at pH 5.5 must decrease to 12 Hz (0.1 ppm) or less at pH 8.1 in order for two species to be present at high pH.

Markley has reported that the half-life of the transition between conformers a and b is about 2.5 hours at pH 8 (Markley et al., 1980). We can also estimate the rate of this equilibration from the  $^{13}\text{C}$  data presented in Figure 9. Figure 9A is the spectrum observed for a sample of  $\alpha$ -lytic protease, lyophilized from distilled water, dissolved in 0.2 M KCl, 10% (v/v)  $^2\text{H}_2\text{O}$ , and adjusted to pH 5.5. The sample had never been above pH 6.0. The spectrum in Figure 9C represents a sample that had been at low pH for at least 8 to 8.5 hours (the time necessary to acquire one 4.5 and two 1.5 hour spectra), had never been above 6.0, and had been readjusted to pH 5.5. By comparing Figures 9A and 9C, one can observe no major differences in the relative intensities of the two doublets, indicating that at pH < 6.0 the rate of interconversion between the two species giving rise to the two NMR signals is very slow. At pH 5.5, the ratio of protein with a neutral His 57 to protein with a protonated His 57 is about 1:16, since the  $\text{pK}_a$  of this residue is 6.7. The rate of interconversion may be represented by  $R = k_o(\text{Im}) + k_H(\text{HIm}^+)$ , where (Im) is the concentration of protein with neutral His 57, ( $\text{HIm}^+$ ) is the concentration of protein with protonated His 57, and  $k_o$  and  $k_H$  are the respective rate

constants for the interconversion process. Since at pH 5.5 little or no interconversion occurs, even in the presence of a small but significant amount of protein with neutral His 57, both  $k_O$  and  $k_H$  must be reasonably small, and the half-life of the process must therefore be reasonably large. This conclusion is further supported by comparing the spectra in Figures 9D and 9F. Figure 9D represents the spectrum obtained after 1.5 hours of acquisition at pH 8.1 on a sample that had previously been several (5-6) hours at low pH (pH<6.0), and was then adjusted to pH 8.1. Figure 9F represents the spectrum obtained after 9 hours of acquisition at pH 5.5 on the sample used to generate the spectrum in Figure 9D after this sample had been readjusted to pH 5.5. It is apparent that some interconversion had occurred over the 1.5-2 hours that the sample had been at pH 9.1; however, the mixture still favored the major species observed in Figures 9A and 9C after this time. If we assume that the species giving rise to the  $^{13}\text{C}$  doublet centered at 134.5 ppm at pH 5.5 can be essentially completely converted to the species giving rise to the  $^{13}\text{C}$  doublet at 135.5 ppm at pH 5.5 after an appropriately long equilibration period at pH 8, as is the case for the conversion of conformer a to conformer b in the  $^1\text{H}$  study (Markley et al., 1980), then an estimate of the half-life of the interconversion of the two species observed in the low pH  $^{13}\text{C}$  spectra would be several hours at least at pH 8.1, and considerably longer below pH 6.

Therefore, it is possible that the two species observed in the low pH  $^{13}\text{C}$  spectra are identical with the conformers a and b reported by Markley and coworkers (Markley et al., 1980; Westler et al., 1982); furthermore, the lifetimes of the two  $^{13}\text{C}$  species at pH 8.1 are sufficiently long that two separate signals might exist in the  $^{13}\text{C}$  spectrum at this pH but be so close together as to be unresolvable. Of course, the above assumption is experimentally verifiable by conducting a time-course investigation of the interconversion process at pH 8 over a sufficiently long period of time, say, two to three days, in order to determine if indeed the species giving rise to the 134.5 ppm  $^{13}\text{C}$  doublet at pH 5.5 can be completely converted to the species giving rise to the 135.5 ppm low pH doublet at equilibrium. Such an experiment remains to be performed, and would require alternating incubation of the protein at pH 8 for appropriate periods of time, followed by assay for the relative amounts of the two conformational species at pH 5.5, a pH where the relative high pH concentrations present at any given time can essentially be frozen by the extremely slow rate of the interconversion process below pH 6.

Any sort of analysis of the potential structures of the two conformations of  $\alpha$ -lytic protease would be purely speculative and will not be attempted here. The observation of more than one conformation of the protein at low pH is not particularly bothersome, however, since this enzyme is

designed to be catalytically effective only above pH 7. For this reason, no detailed  $^{13}\text{C}$  NMR study of the dynamics of the interconversion process was performed, since we were primarily concerned with the measurement of the  $\text{pK}_a$  of His 57 in the free enzyme, and not the multiplicity of conformations at non-catalytic pH. However, the presence of more than one conformation at catalytic pH is troublesome, especially if both metastable forms of the enzyme are assumed to be catalytically competent, unless binding of substrate can cause one or both conformers of the free enzyme to assume a unique, stable, catalytically active structure. It is more pleasing that there exist one stable structure for the free enzyme at catalytic pH, as initially suggested by the  $^{13}\text{C}$  NMR data, as opposed to the indications of the  $^1\text{H}$  NMR reports.

#### The Previous $^{13}\text{C}$ NMR Study.

It is now known that there are multiple conformers of this 57 at low pH whose C-2 resonances are in slow exchange at 125.76 MHz. However, at 25.14 MHz, this multiplicity of resonances is unresolvable due to their being in fast to intermediate exchange. Furthermore, the exchange rate will be a sensitive function of temperature. In the Hunkapiller et al. (1973) experiment, the sample temperature was likely to be higher during the acquisition of decoupled spectra, a result of dielectric heating, than during the acquisition of coupled spectra, even though cooling air was used in an

attempt to maintain a nearly constant sample temperature. The result of this situation is depicted in Figure 4. Due to the higher temperature during decoupling, the decoupled resonance corresponding to C-2 has been shifted slightly downfield from the coupled chemical shift position because of the increase in exchange rate. Thus, the measured difference between the coupled downfield peak and the decoupled resonance is less than the actual difference; this measurement of  $J/2$  results in the calculation of an artifactually small coupling constant.

The low specific enrichment of the protein used in the previous work (Hunkapiller et al., 1973) precluded accurate measurement of the coupling constant. Use of a difference program to subtract out native, unenriched carbon resonances also led to substantial errors in measuring the coupling constant due to difficulties in the phasing of the resonances in the histidine region of the spectrum.

#### The "Charge Relay" Hypothesis

The current body of information concerning the ionization behavior of the catalytic triad (Asp 102, His 57, Ser 195) of  $\alpha$ -lytic protease indicates that the imidazole side-chain of the histidine residue is the initial active-site locus for acceptance of proton during titration of the free enzyme (see Figure 1a). Thus, the ionization behavior of the active site residues of the free enzyme cannot be that proposed by Hunkapiller et al. (1973).

Such a result should not be unexpected, however, based on the recent refined X-ray structures of several serine proteases, including  $\alpha$ -lytic protease. In the case of  $\alpha$ -lytic protease (Brayer et al., 1979), chymotrypsin and Streptomyces griseus protein A (Brayer et al., 1978), trypsin and subtilisin (Matthews et al., 1977), and elastase (Sawyer et al., 1978; Shotton and Watson, 1970) it is observed that the hydroxyl oxygen of Ser 195 is  $\sim 2.5$  Å away from the expected location for efficient hydrogen bonding to N-1, so that if a hydrogen bond exists between Ser 195 and His 57, it is exceedingly distorted. The presence of such a (supposedly strong) hydrogen bond is one of the keystones of the "charge relay" hypothesis as originally propounded by Blow et al. (1969), and as subsequently modified by Hunkapiller et al. (1973). The lack of such a hydrogen bond apparently undermines the plausibility of the above hypothesis, and supports the normal ionization behavior that has been observed in the native enzymes. Furthermore, another important premise of the "charge relay" hypothesis is that the histidine side-chain acts as a solvent shield to maintain a hydrophobic environment for the aspartic carboxylate, thereby promoting the transfer of a proton from His to Asp and alleviating unfavorable charge separation. Once again, none of the crystallographically determined serine protease structures are consistent with this idea (Brayer et al., 1978; Delbaere et al., 1979; Bode and Schwager, 1975; Sawyer et al., 1978). In the specific case

of  $\alpha$ -lytic protease Asp 102 is the recipient of four hydrogen bonds, from the amide NH of His 57, N-3 of His 57, the hydroxyl of Ser 195, and the amide NH of Gly 56. Thus, Asp 102 in the free enzyme is found in a strongly polar environment, albeit shielded from solvent water (Brayer et al., 1979).

The results of studies on the free enzyme must be extended to the description of the behavior of the enzyme in the presence of substrate with due care and caution. Although it is now clear that the residues of the catalytic triad are not involved in a tightly hydrogen bonded array in the free enzyme, due to the lack of a strong His 57 N-1 - Ser 195  $\gamma$ O hydrogen bond, recent crystal structures of trypsin/protein trypsin inhibitor complexes (Sweet et al., 1974; Blow et al., 1974; Ruhlmann et al., 1973; Huber et al., 1974; Huber et al., 1975) indicate that a strong hydrogen bond can be formed between these two residues in these complexes. Furthermore, the crystal structure of the covalent complex formed between serine protease A of Streptomyces griseus and a specific aldehyde transition state analog (see Chapter IV for a discussion of transition state analogs) indicates that the imidazolyl ring of His 57 has moved relative to its position in the free enzyme, and is hydrogen bonded through a water molecule to  $\gamma$ O of Ser 195 (Brayer et al., 1979). Crystal structures of tosyl-chymotrypsin (Birktoft and Blow, 1972) and indoleacryloyl-chymotrypsin (Henderson, 1970) have been interpreted as showing N-3 of His 57 hydrogen bonded,

again through a tightly bound water molecule, to the carbonyl oxygen of the substrate portion of the acyl-enzyme. Besides these crystallographic indications, kinetic studies also offer evidence that the catalytic triad may manifest different properties during catalysis than are observed in the free enzyme. Proton inventory experiments (Hunkapiller et al., 1976; Elrod et al., 1979; Quinn et al., 1980) have demonstrated the concerted movement of two protons during the hydrolysis of highly specific oligopeptide substrates, while less specific substrates may be cleaved in a process characterized by uncoupled single proton transfer (Quinn et al., 1980; Elrod et al., 1975; Pollock et al., 1973). Thus, only when both the enzyme and the substrate can interact in a highly precise manner is the true catalytic mechanism with all of its potential features observed. Hence, it should be recognized that the properties of the catalytic triad of the serine proteases in the free enzymes need not, and probably are not, identical with those of the triad in the presence of natural substrates.

## CONCLUSION

The present carbon-13 nuclear magnetic resonance study indicates that His 57 is the residue of the catalytic triad of  $\alpha$ -lytic protease that becomes protonated with a  $pK_a$  of 6.7. Furthermore, it reveals the presence of multiple forms of the enzyme at acidic pH; the chemical exchange behavior of these forms explains the previous erroneous assignment of this  $pK_a$  to Asp 102. The carbon-13 results now agree with other NMR determinations for  $\alpha$ -lytic protease (Bachovchin and Roberts, 1978; Westler and Markley, 1979; Westler et al., 1982) and other serine proteases (Robillard and Shulman, 1972, 1974; Markley and Porubcan, 1976; Markley, 1975; Markley, 1978).

Lastly, recent findings, particularly using proton inventory techniques (Elrod et al., 1975; Gandour et al., 1974; Schowen, 1972; Albery, 1975; Pollock et al., 1973) reveal differences in catalytic behavior of serine proteases as a function of the substrate; structurally more physiological substrates (e.g., those that interact with the enzyme in a more precise manner over an extended portion of the substrate binding site) manifest aspects of catalysis not observed with smaller substrates (Hunkapiller et al., 1976; Elrod et al., 1980, Quinn et al., 1980). Accordingly, these NMR results on the ionization behavior of the catalytic residues of the free enzyme should be extended to the behavior of these residues during the catalytic event only with appropriate caution.

## REFERENCES

- Albery, J. (1975), in "Proton Transfer Reactions", E. Caldin and V. Gold, eds., Chapman and Hall, London, 263-315.
- Amidon, G.L. (1974), J. Theor. Biol. 47, 101-109.
- Ashley, J.N., and Harington, C.R. (1930), J. Chem. Soc., 2586-2591.
- Bachovchin, W.W., and Roberts, J.D. (1978), J. Am. Chem. Soc. 100, 8041-8047.
- Bender, M.L., Clement, G.E., Kezdy, F.J., and Heck, H.d'A. (1964), J. Am. Chem. Soc. 86, 3680-3690.
- Beppu, Y., and Yomosa, S. (1977), J. Phys. Soc. Japan 42, 1694-1700.
- Birktoft, J.J., and Blow, D.M. (1972), J. Mol. Biol. 68, 187-240.
- Blow, D.M., Birktoft, J.J., and Hartley, B.S. (1969), Nature (London) 221, 337-339.
- Blow, D.M., Janin, J., and Sweet, R.M. (1974), Nature (London) 249, 54-57.
- Blow, D.M. (1976), Acc. Chem. Res. 9, 145-152.
- Bode, W., and Schwager, P. (1975), J. Mol. Biol. 98, 693-717.
- Brayer, G.D., Delbaere, L.T.J., and James, M.N.G. (1978), J. Mol. Biol. 124, 261-283.
- Brayer, G.D., Delbaere, L.T.J., and James, M.N.G. (1979), J. Mol. Biol. 131, 743-775.
- Delbaere, L.T.J., Brayer, G.D., and James, M.N.G. (1979) Can. J. Biochem. 57, 135-144.

- Elrod, J.P., Gandour, R.D., Hogg, J.L., Kise, M., Maggiora, G.M., Schowen, R.L., and Venkatasubban, K.S. (1975) Faraday Symp. Chem. Soc. 10, 145-153.
- Elrod, J.P., Hogg, J.L., Quinn, D.M., Venkatasubban, K.S., and Schowen, R.L. (1980) J. Am. Chem. Soc. 102, 3917-3922.
- Farragi, M., Klapper, M.H., and Dorfman, L.M. (1978) J. Phys. Chem. 82, 508-512.
- Gandour, R.D., Maggiora, G.M., and Schowen, R.L. (1974) J. Am. Chem. Soc. 96, 6967-6979.
- Henderson, R. (1970), J. Mol. Biol. 54, 341-354.
- Huber, R., Kukla, D., Bode, W., Schwager, P., Bartels, K., and Deisenhofer, J. (1974), J. Mol. Biol. 89, 73-101.
- Huber, R., Bode, W., Kukla, D., Kohl, U., and Ryan C.A. (1975), Biophys. Struct. Mechanism 1, 189-201.
- Hunkapiller, M.W., Smallcombe, S.H., Whitaker, D.R., and Richards, J.H. (1973), Biochemistry 12, 4732-4743.
- Hunkapiller, M.W., Forgac, M.D., and Richards, J.H. (1976), Biochemistry 15, 5581-5588.
- Kaplan, H., and Whitaker, D.R. (1969), Can. J. Biochem. 47, 307-315.
- Kitayama, H.P., and Fukutome, H. (1976), J. Theor. Biol. 60, 1-18.
- Koepe, R.E. II, and Stroud, R.M. (1976), Biochemistry 15, 3450-3458.
- Kossiakoff, A.A., and Spencer, S.A. (1980) Nature (London) 288, 414-416.

- Kraut, J. (1977), Ann. Rev. Biochem. 46, 331-358.
- Markley, J.L. (1975) Acc. Chem. Res. 8, 70-80.
- Markley, J.L., and Porubcan, M.A. (1976), J. Mol. Biol. 102,  
487-509.
- Markley, J.L. (1978), Biochemistry 17, 4648-4656.
- Markley, J.L., Neves, D.E., Westler, W.M., Ibanez, I.B., Porubcan,  
M.A., and Baillargeon, M.W. (1980) Dev. Biochem. 10, 31-61.
- Matthews, D.A., Alden, R.A., Birktoft, J.J., Freer, S.T., and  
Kraut, J. (1977), J. Biol. Chem. 252, 8875-8883.
- Pollock, E., Hogg, J.L., and Schowen, R.L. (1973), J. Am. Chem.  
Soc. 95, 968-969.
- Porubcan, M.A., Westler, W.M., Ibanez, I.B., and Markley, J.L.  
(1979), Biochemistry 18, 4108-4116.
- Quinn, D.M., Elrod, J.P., Ardis, R., Friesen, P., and Schowen,  
R.L. (1980) J. Am. Chem. Soc. 102, 5358-5365.
- Robillard, G., and Shulman, R.G. (1972), J. Mol. Biol. 71, 507-  
511.
- Robillard, G., and Shulman, R.G. (1974), J. Mol. Biol. 86, 519-  
540.
- Ruhlmann, A., Kukla, D., Schwager, P., Bartels, K., and Huber,  
R. (1973), J. Mol. Biol. 77, 417-436.
- Sawyer, L., Shotton, D.M., Campbell, J.W., Wendell, P.L., Muirhead,  
H., Watson, H.C., Diamond, R., and Ladner, R.C. (1978),  
J. Mol. Biol. 118, 137-208.
- Scheiner, S., Kleier, D.A., and Lipscomb, W.N. (1975), Proc.  
Natl. Acad. Sci. USA 72, 2606-2610.
- Schowen, R.L. (1972), Prog. Phys. Org. Chem. 9, 275-332.

- Shotton, D.M., and Watson, H.C. (1970), Nature (London) 225, 811-816.
- Stroud, R.M., Krieger, M., Koeppe, R.E. II, Kossiakoff, A.A., and Chambers, J.L. (1975), in "Proteases and Biological Control", E. Reich, D.M. Rifkin, and E. Shaw, eds., Cold Spring Harbor Laboratory, Cold Spring Harbor, N.Y., 13-32.
- Sweet, R.M., Wright, H.T., Janin, J., Chothia, C.H., and Blow, D.M. (1974) Biochemistry 13, 4212-4228.
- Wasylishen, R.E., and Tomlinson, G. (1975), Biochem. J. 147, 605-607.
- Westler, W.M., and Markley, J.L. (1979), Fed. Proc. FASEB 3. 1795.
- Westler, W.M., Markley, J.L., and Bachovchin, W.W. (1982), FEBS Letters 138, 233-235.

## CHAPTER III

THE ACTIVE SITE TITRATION OF  $\alpha$ -LYTIC PROTEASE

## ABBREVIATIONS

APAPNA	N-acetyl-L-alanyl-L-prolyl-L-alanine p-nitroanilide
TRIS	Tris(hydroxymethyl)aminomethane
CH <sub>3</sub> CN	Acetonitrile
Cbz-L-alaONp	N-carbobenzoxy-L-alanine p-nitrophenyl ester

CHAPTER III--INTRODUCTION

The use of active site titrants for the determination of the molar concentration of catalytically able enzyme molecules is well documented (Bender et al., 1966). Specific and non-specific substrates of the pancreatic serine proteinases chymotrypsin (Bender et al., 1966; Kezdy and Kaiser, 1970), trypsin (Chase and Shaw, 1970; Bender et al., 1966; Chase and Shaw, 1967; Tanizawa et al., 1968) and elastase (Bender et al., 1966; Bender and Marshall, 1968), as well as of other enzymes, have been used as such titrants. Such titrations, if designed correctly, are inherently more accurate than standard rate assays of enzymatic activity, and can be used to determine the absolute concentration of catalytically competent enzyme, rather than a concentration that is relative to an assumed standard of purity.

The design of proper titrants is not always a simple procedure. Such titrants should take advantage of the differences between active and inactive protein, and hence should generally be directed toward reaction with the active site of the enzyme. Specific substrates are to be preferred over non-specific substrates, as this will allow for discrimination between proteins in preparations containing more than one enzyme. Furthermore, the titrant should interact with the enzyme on a one-to-one basis, yield catalytically inactive enzyme, and be unreactive toward the enzyme under conditions that render the enzyme catalytically inept. Of course, such molecules may be difficult to find, and one may therefore be forced to compromise with the above conditions.

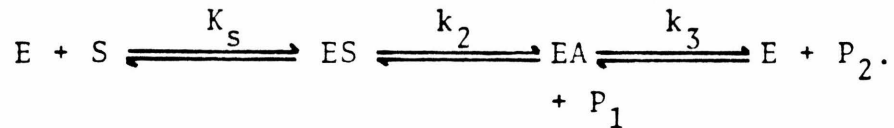
In the case of  $\alpha$ -lytic protease, no suitable titrant has yet been defined. Kaplan and Whitaker (1969) describe the use of p-nitrophenyl trimethylacetate, a non-specific substrate of the enzyme that has been

used for elastase as well; however, the low solubility of this substrate in aqueous solution renders it less than an ideal choice.

It is the purpose of this chapter to describe the use of the non-specific substrate Paraoxon (diethyl p-nitrophenyl phosphate) for the determination of active  $\alpha$ -lytic protease. Although this titrant represents a substantial compromise with the desired qualifications, it appears to be adequate; it is also the titrant of choice for elastase (Bender et al., 1966), the closest mammalian homolog of  $\alpha$ -lytic protease (McLachlan and Shotton, 1971; Shaw and Whitaker, 1972; Kaplan, et al., 1970).

## THEORY

The hydrolysis of p-nitrophenyl ester substrates by the serine proteases in general (and  $\alpha$ -lytic protease in specific) can be described by the following kinetic sequence<sup>1</sup>:



In this formulation, E represents free enzyme; S, substrate (p-nitrophenyl ester); ES, non-covalent Michaelis complex; EA, covalent acyl-enzyme intermediate;  $P_1$ , p-nitrophenol;  $P_2$ , acid component of the ester substrate.  $K_S$  is assumed to be a true equilibrium constant;  $k_2$  and  $k_3$  are both first-order rate constants.

The kinetic analysis of the above mechanism can be broken down into two phases: the steady-state (Michaelis-Menten) phase, and the pre-steady-state phase. In all cases in the following derivation,  $E_0$  (the initial enzyme concentration) is assumed to be much less than  $S_0$  (the initial substrate concentration), so that the steady-state assumption can be made for appropriate species.

Steady-state phase. The steady-state assumption for this system is

$$\frac{d(EA)}{dt} = 0. \quad (1)$$

$$d(EA)/dt = k_2(ES) - k_3(EA) = 0 \quad (2)$$

<sup>1</sup>This section is taken in large part from Bender and Marshall, 1968.

$$(ES) = (E)(S)/K_s \quad (3)$$

so  $(k_2/K_s)(E)(S) = k_3(EA) \quad (4)$

Now,  $E_0 = (E) + (ES) + (EA) \quad (5)$

Combining (4) and (5) and rearranging,

$$(k_2/K_s)(E)(S) = k_3E_0 - k_3(E)\{(1 + (S))/K_s\} \quad (6)$$

and

$$(E) = \frac{k_3E_0}{\frac{(k_2 + k_3)(S) + k_3}{K_s}} \quad (7)$$

Now, the steady-state velocity  $v_{ss} = (dP_1/dt)$ .

$$dP_1/dt = k_2(ES) = (k_2/K_s)(E)(S) \quad (8)$$

so that

$$v_{ss} = \frac{(k_2k_3/K_s)E_0(S)}{\frac{(k_2 + k_3)(S) + k_3}{K_s}} \quad (9)$$

$$= \frac{\{k_2k_3/(k_2 + k_3)\} E_0(S)}{(S) + \{k_3K_s/(k_2 + k_3)\}} \quad (10)$$

For the case of initial rates (less than 10% of  $S_0$  converted to products),  $(S) = S_0$ , and standard Michaelis-Menten kinetics are observed:

$$v_{ss} = \frac{k_{cat} E_0 S_0}{K_m + S_0} \quad (11)$$

where  $k_{cat} \equiv k_2k_3/(k_2 + k_3)$  and  $K_m \equiv k_3K_s/(k_2 + k_3)$ . (12)

Pre-steady-state phase.

$$d(EA)/dt = k_2(ES) - k_3(EA) \quad (13)$$

From (3) and (5),

$$d(EA)/dt = \frac{(k_2/K_s) E_0(S)}{1 + \{(S)/K_s\}} - \left[ \frac{(k_2/K_s)(S)}{1 + \{(S)/K_s\}} + k_3 \right] (EA). \quad (14)$$

Rearranging and assuming  $(S) = S_0$ ,

$$d(EA)/dt = \{k_2 E_0 S_0 / (K_s + S_0)\} - \{(k_2 S_0 / (K_s + S_0)) + k_3\} (EA). \quad (15)$$

$$\text{Defining } A \equiv k_2 E_0 S_0 / (K_s + S_0) \text{ and } B \equiv (k_2 S_0 / (K_s + S_0)) + k_3, \quad (16)$$

$$d(EA)/dt = A - B(EA). \quad (17)$$

Integrating this expression from  $t=0$  to  $t=t$ ,

$$(EA) = (A/B)(1 - \exp(-Bt)). \quad (18)$$

Therefore,  $B$  is the first-order rate constant for the attainment of a steady-state concentration of  $EA$ .

Combination of steady-state and pre-steady-state. The combination of the rate expressions for the two phases gives the overall kinetic description for this mechanism:

$$\begin{aligned} v &= (dP_1/dt)_{\text{pre-steady}} + (dP_1/dt)_{\text{steady}} \\ &= (A/B)(1 - \exp(-Bt)) + v_{ss}. \end{aligned} \quad (19)$$

This equation describes a biphasic reaction velocity profile: an initial first-order "burst" of product followed by a zero-order steady-state velocity (typically termed "turnover"). The magnitude of the "burst" will depend on the relative magnitudes of  $k_2$  and  $k_3$ .

Burst analysis.

$$d(P_1/dt) = k_2(ES) = (k_2/K_s)(E)S_0. \quad (20)$$

From (3) and (5),

so that

$$(E) = \frac{E_0 - (EA)}{1 + (S_0/K_s)} \quad (21)$$

$$\begin{aligned} (dP_1/dt) &= \{k_2 E_0 S_0 / (K_s + S_0)\} - \{k_2 S_0 / (K_s + S_0)\} (EA) \\ &= \{k_2 E_0 S_0 / (K_s + S_0)\} - \\ &\quad \{k_2 S_0 / (K_s + S_0)\} (A/B) (1 - \exp(-Bt)). \quad (22) \end{aligned}$$

Integrating this expression,

$$P_1 = \left[ \frac{k_2 E_0 S_0}{K_s + S_0} - \frac{k_2 (A/B) S_0}{K_s + S_0} \right] t - \left[ \frac{k_2 (A/B^2) S_0}{K_s + S_0} \right] (\exp(-Bt) - 1). \quad (23)$$

When  $t$  is large, that is, steady-state is attained,  $\exp(-Bt)$  is small relative to 1 and

$$\begin{aligned} P_1 &= \frac{k_2 (A/B^2) S_0}{K_s + S_0} + \left[ \frac{k_2 E_0 S_0}{K_s + S_0} - \frac{k_2 (A/B) S_0}{K_s + S_0} \right] t \\ &= \pi + Ct. \quad (24) \end{aligned}$$

Hence, the burst

$$\begin{aligned} \pi &= k_2 A S_0 / B^2 (K_s + S_0) \\ &= k_2^2 S_0^2 E_0 / \{(k_2 + k_3) S_0 + k_3 K_s\} \\ &= \{k_2 / (k_2 + k_3)\}^2 \{S_0 / (S_0 + K_m)\}^2 E_0, \quad (25) \end{aligned}$$

and

$$\begin{aligned} C &= \frac{k_2 E_0 S_0}{K_s + S_0} - \frac{k_2^2 S_0^2 E_0}{K_s + S_0} \left[ \frac{1}{(k_2 + k_3) S_0 + k_3 K_s} \right] \\ &= k_2 k_3 E_0 S_0 / \{(k_2 + k_3) S_0 + k_3 K_s\} \quad (26) \end{aligned}$$

$\neq v_{ss}$ , as expected.

Therefore,

$$(E_0/\pi)^{1/2} = \{(k_2 + k_3)(K_m + S_0)\}/k_2 S_0. \quad (27)$$

If  $S_0 \gg K_m$  and  $k_2 \gg k_3$ , then  $E_0 = \pi$ .

EXPERIMENTALMaterials.

Substrates. p-Nitrophenol was purchased from MCB. It was dissolved in ethanol and precipitated as the sodium salt by adding a concentrated ethanolic solution of sodium hydroxide (Baker). The yellow solid was redissolved in a minimum of water and precipitated as p-nitrophenol by the addition of concentrated hydrochloric acid (Mallinkrodt). It was recrystallized twice from water, and dried in vacuo over NaOH pellets. The crystals were almost white and melted at 113-114°C (uncorrected) (lit. 113-4°C).

p-Nitrophenyl trimethylacetate was synthesized from the above p-nitrophenol and trimethylacetyl chloride (purchased from Aldrich) in dry pyridine (MCB, distilled from KOH pellets). It was recrystallized three times from ethanol, and liberated 99.1% of the theoretical amount of p-nitrophenol upon hydrolysis in 0.1 N NaOH. It contained <0.2% free p-nitrophenol, and the white crystals melted at 94-95°C(uncorrected) (lit. 94-95°C).

Paraoxon (diethyl p-nitrophenyl phosphate) was purchased from Sigma and was used as received.

The synthesis of the specific substrate N-acetyl-L-alanyl-L-prolyl-L-alanine p-nitroanilide (APAPNA) will be described in Chapter IV.

Acetonitrile was reagent grade, purchased from Eastman. It was distilled from phosphorous pentoxide prior to use. Stock substrate solutions were made up in this solvent.

The water used was deionized and glass-distilled. The tris(hydroxymethyl)aminomethan (TRIS) used to make up the buffers was purchased from Sigma.

N-benzyloxycarbonyl-L-alanine p-nitrophenolate was purchased from Sigma. It was recrystallized from ether/hexane, and the white crystals melted at 78-79°C (uncorrected) (lit. 78-80°C).

Phenylmethanesulfonyl fluoride (PMSF) was purchased from Sigma.

Enzyme. The  $\alpha$ -lytic protease used in this experiment was produced and isolated as described in Chapter II of this thesis. It was further purified in the following manner. The lyophilized enzyme from the CG-50 chromatography (400 mg) was dissolved in 100 ml of a cold buffer that was 10 mM in NaOH and adjusted to pH 5.3 (measured at 4°C) with 2 M citric acid. The solution was centrifuged 15 minutes at 10,000 rpm in a GSA rotor to remove any suspended insoluble material. The pH of the solution was then checked, and readjusted to 6.3 with citric acid or NaOH if necessary. The solution was then applied to a 35 cm x 2.5 cm column of CM-Sephadex C-50-120 (Sigma) that had been previously equilibrated with 2 l of the same buffer. The chromatography was done at 4°C in the cold room.

After all of the protein solution had been loaded onto the column, another 500 ml of pH 6.3 buffer was run through. Following this, a linear chloride gradient was applied to the column, and 7.5 ml fractions were collected. The initial gradient conditions were 400 ml of 10 mM Na-citrate, pH 6.3; the final conditions were 400 ml of 10 mM Na-citrate, 0.6 M NaCl, pH 6.3. The protein was eluted between 0.2 and 0.3 M NaCl in about 175 ml; fractions were read at 280 nm and those fractions having  $A_{280} > 0,1$  were combined. The enzyme was dialyzed once against 6 l of 0.1 M KCl and three times against distilled water, and lyophilized. The CM-Sephadex chromatogram is shown in Figure 1.

The enzyme was further purified by gel permeation chromatography

Figure 1. Chromatography of 400 mg of  $\alpha$ -lytic protease on CM-Sephadex C-50-120. Loading buffer was 10 mM NaOH/Citric acid, pH 6.3. A linear salt (NaCl) gradient (0.0 to 0.6 M) in the above buffer was used to elute the protein from the column. Column dimensions: 35 cm x 2.5 cm. Chromatography was done at 4°C. Fractions were 7.5 ml in volume.

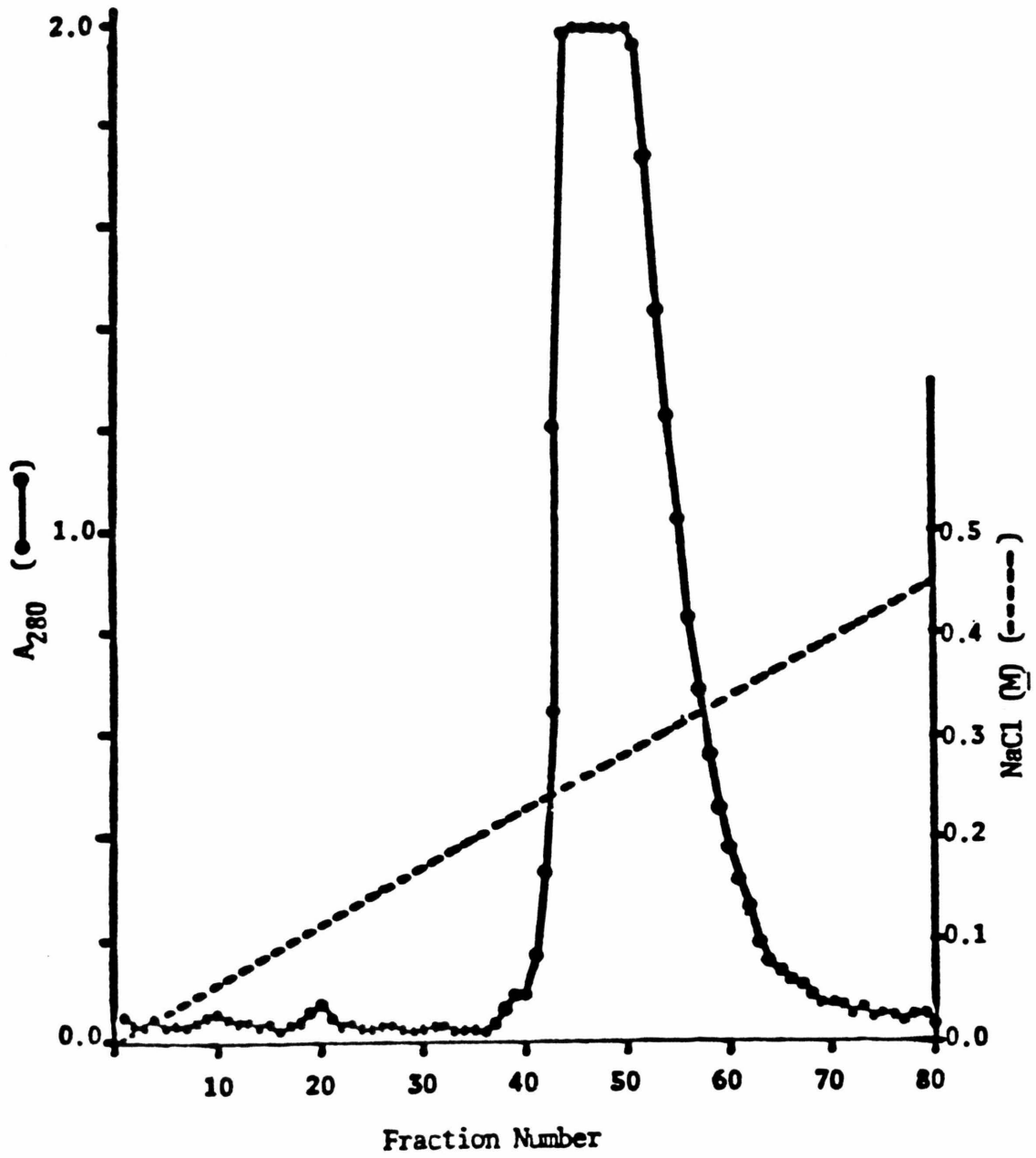
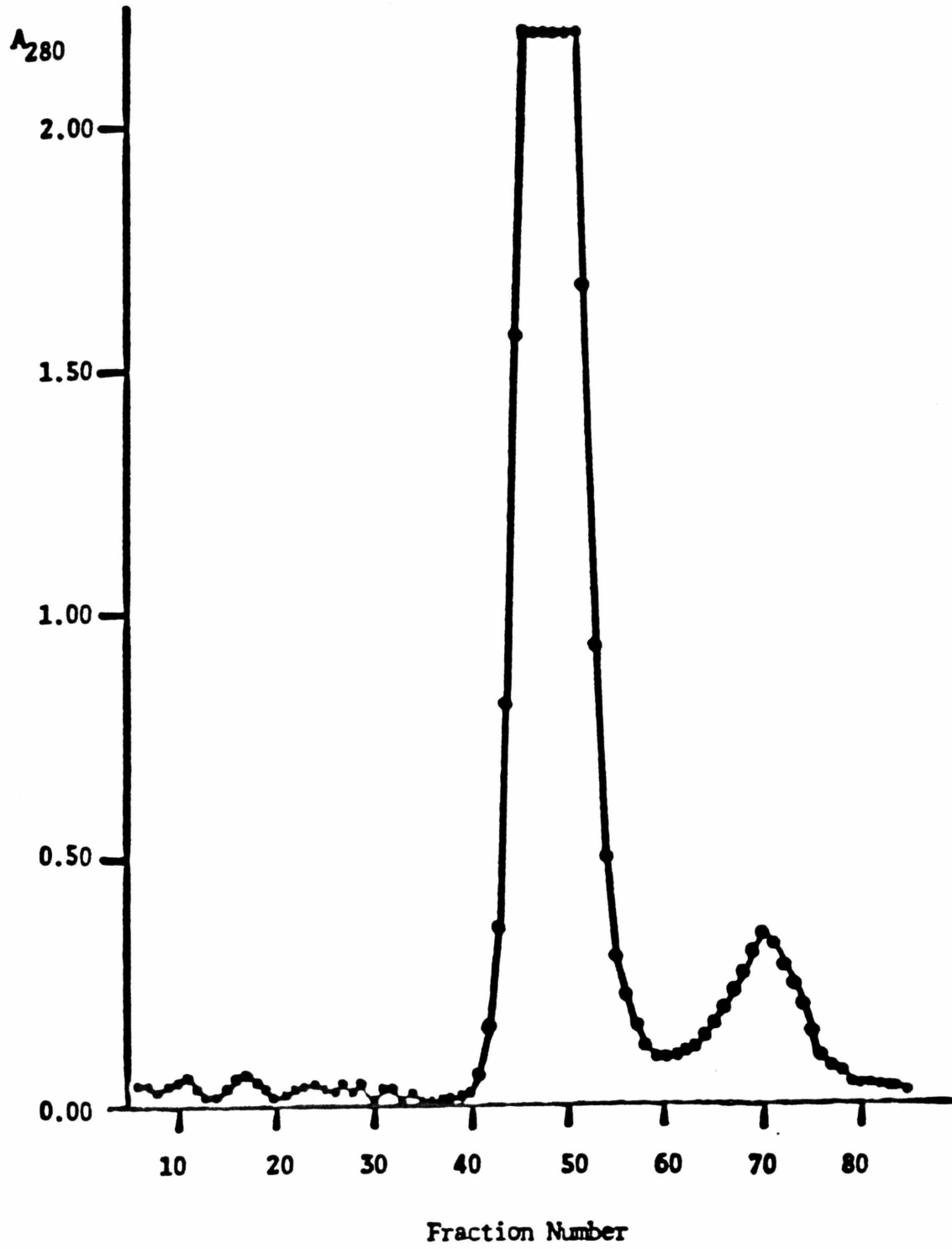


Figure 2. Chromatography of  $\alpha$ -lytic protease (about 250 mg) on Sephadex G-75 (fine). 0.1 M KCl was used as the eluting solvent. The larger peak is active toward the specific substrate N-acetyl-L-alanyl-L-prolyl-L-alanine p-nitroanilide; the smaller peak is not. Column dimensions: 120 cm x 4 cm. Chromatography was done at 4°C. Fractions were 8.0 ml in volume.



on Sephadex G-75 (Sigma) at 4°C with 0.1 M KCl as the eluting solvent. Eight ml fractions were collected; the major peak (see Figure 2) is active protein, as determined from rate assays using the specific substrate, from N-acetyl-L-alanyl-L-prolyl-L-alanine p-nitoranilide (as described in Chapter II). The smaller peak is inactive toward this substrate. The enzyme-containing fractions were pooled, dialyzed thrice versus 6 l of distilled water at 4°C, and lyophilized. The yield following these additional two chromatographic steps, starting from ~400 mg enzyme, is ~340 mg. The purified, lyophilized enzyme, is soluble up to at least 100 mg/ml in 0.1 M KCl with no insoluble material. The enzyme is stored, lyophilized, at -20°C. Enzyme solutions were made up fresh daily in distilled water and stored at 2° until needed. Enzyme from the same isolation was used for this entire set of experiments.

Phenylmethanesulfonyl  $\alpha$ -lytic protease. 28.8 mg of  $\alpha$ -lytic protease (1.45 mole) is dissolved in 5 ml of 0.2 M TRIS/HCl, pH 7.5, and the solution is cooled to 4°C. Phenylmethanesulfonyl fluoride (0.250 g) (PMSF) in 500  $\mu$ l of acetonitrile is added to 9 ml of the enzyme solution; the other 1 ml is saved to determine the initial activity of the enzyme preparation. The solution containing PMSF is shaken at 4° for 48 hours, after which time it was centrifuged for 15 minutes at 10,000 rpm. The resulting enzyme solution showed less than 1% of its original activity toward N-acetyl-L-alanyl-L-prolyl-L-alanine p-nitroanilide. It was stored frozen until needed.

### Methods.

Kinetics. Kinetics were measured on a Beckman ACTA CIII double-beam, recording ultraviolet-visible spectrophotometer in 1 cm quartz cells. The cell holder was thermostatted by a Lauda K-2/R (Brinkmann)

circulating water bath; the temperature could be maintained to  $\pm 0.2^\circ\text{C}$  for the times encountered in the kinetic runs. The cell compartment was also equipped with a magnetic stirring apparatus for stirring the cuvette solutions during recording.

A critical aspect of these titrations is the accurate knowledge of  $\Delta\epsilon$ , the difference between the molar absorptivities of the product, p-nitrophenol, and the substrate esters. For maximum sensitivity to be obtained in the titration,  $\Delta\epsilon$  should be as large as possible; for this reason, a wavelength of 400 nm was used to observe the production of p-nitrophenol on ester hydrolysis. This wavelength is near the  $\lambda_{\text{max}}$  for p-nitrophenol ( $\lambda_{\text{max}} = 402 \text{ nm}$ , Kezdy and Bender, 1962), and the ester substrates are virtually transparent at this wavelength. The determination of  $\Delta\epsilon$  under the conditions of the titrations ( $25.0^\circ\text{C}$ ,  $0.05 \text{ M}$  TRIS/HCl buffer, pH 7.78, containing 10% (v/v) acetonitrile) gave a value of  $14,750 \pm 200$  as the average of five determinations (compared to 14,600 at pH 7.66; Fife and Milstein, 1969). To check this value, a determination of  $\epsilon_{400}$  for completely hydrolyzed p-nitrophenyl trimethyl acetate in  $0.1 \text{ M}$  KOH gave a value of  $18,120 \pm 390$ , corresponding well to the value of 18,300 determined by Bender and Marshall (1968). Furthermore, a value for the pKa of p-nitrophenol of  $7.15 \pm 0.03$  can be calculated from the above two  $\Delta\epsilon$  values ( $\text{pK}_a$  7.11, Bender and Marshall, 1968).

The pH of each run was checked following the run in order to determine the pH fidelity during reaction, since  $\Delta\epsilon$  is a sensitive function of pH. In all cases, the pH fidelity was  $\pm 0.03$  pH units. The pH meter used was a Radiometer PHM26 equipped with a Radiometer MY-1 or GK2322C combination electrode that could be inserted into the reaction cuvette.

The protocol for running the titrations is as follows: 2.80 ml of buffer (0.05 M TRIS, titrated to pH 7.78 with HCl, containing 10% (v/v) CH<sub>3</sub>CN) is pipetted into both the reference and the sample cuvette. The spectrophotometer is set at 600 nm and recording allowed to proceed for several minutes to determine the zero baseline, and to allow for temperature equilibration. When a good baseline is obtained, an aliquot of substrate in acetonitrile is then added to the sample cuvette, and recording re-started at 600 nm. When the A<sub>600</sub> had returned to the baseline reading (indicating complete dissolution of the substrate as the substrate and product are transparent at 600 nm), the wavelength was changed to 400 nm and the spontaneous hydrolysis of the substrate was monitored for an appropriate length of time. At time zero an aliquot of enzyme solution was added to the cuvette without turning off the recorder, and the reaction was monitored at 400 nm. The large increase in absorbance due to opening the cover of the cell compartment on addition of enzyme served to describe t=0, and recording was recommenced typically within 5 s using the fast response mode of the spectrophotometer.

The determination of slopes and intercepts for the linear analysis was carried out using a standard linear regression (least squares).

## RESULTS

The choice of a viable active site titrant for  $\alpha$ -lytic protease is predicated on the titrants described for elastase (Bender, et al., 1966; Bender and Marshall, 1968), and the structural homology and similar substrate specificities of these two enzymes (Kaplan et al., 1970; McLachlan and Shotton, 1971; Shaw and Whitaker, 1972). Thus, the relative merits of p-nitrophenyl trimethyl acetate and diethyl p-nitrophenyl phosphate (Paraoxon) were investigated; a specific substrate, N-benzyl-oxy-carbonyl-L-alanine p-nitrophenolate (Cbz-L-alaONp), was also considered as a possible titrant.

p-Nitrophenyl trimethyl acetate. Figure 3 shows a typical recorder trace of the reaction of  $\alpha$ -lytic protease with p-nitrophenyl trimethylacetate. As expected from the theoretical considerations, the reaction consists of a fast initial first-order production of p-nitrophenol followed by a slower linear (zero-order) hydrolysis.

The steady-state (zero-order) portion of the reaction was analyzed by standard procedures. Michaelis-Menten kinetics were observed over the range  $1.99 \times 10^{-5} \text{ M} \leq S_0 \leq 14.97 \times 10^{-5} \text{ M}$ . Figure 4 shows a standard Lineweaver-Burk plot (Lineweaver and Burk, 1934) for this system at pH 7.78;  $K_m = 3.8 \times 10^{-5} \text{ M}$  and  $V_{\max} = 8.5 \times 10^{-8} \text{ M s}^{-1}$  under the assay conditions.

The pre-steady state portion of the reaction was analyzed using standard procedures, on the assumption that it is a first-order process. A typical first-order plot of  $\ln(A_{ss} - A_{obs})$  versus time, where  $A_{ss} \equiv$  the extrapolated steady state (linear) absorbance and  $A_{obs} \equiv$  to observed absorbance, is shown in Figure 5. The slope of such a plot gives B,

Figure 3. A) Typical recorder trace of the reaction of p-nitrophenyl trimethylacetate ( $3.94 \times 10^{-5}$  M) and  $\alpha$ -lytic protease ( $6.56 \times 10^{-6}$  M, as determined by titration) in 0.05 M TRIS/HCl, pH 7.78, 10% (v/v) acetonitrile-water,  $25.0 \pm 0.2^\circ\text{C}$ . The waviness of the trace is due to an oscillation of the recorder pen present whenever the stirring apparatus of the instrument is in use. The rapid increase in absorbance due to the addition of the enzyme to the cuvette is seen around  $t=0$  and is attenuated in the figure for aesthetic purposes.  $\pi$  is the observed burst as described in the text.

B) Replot of the raw data of Figure 3A. Replots of this type were used to calculate the various kinetic parameters described in the text, due to the noisiness of the raw data.

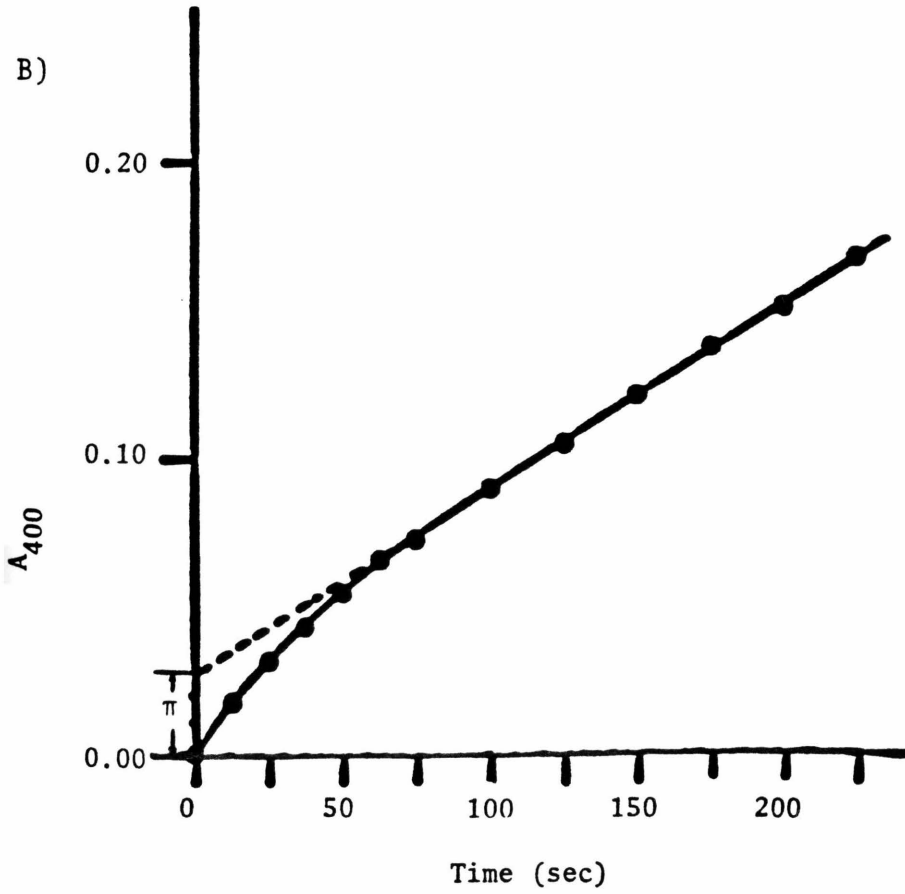
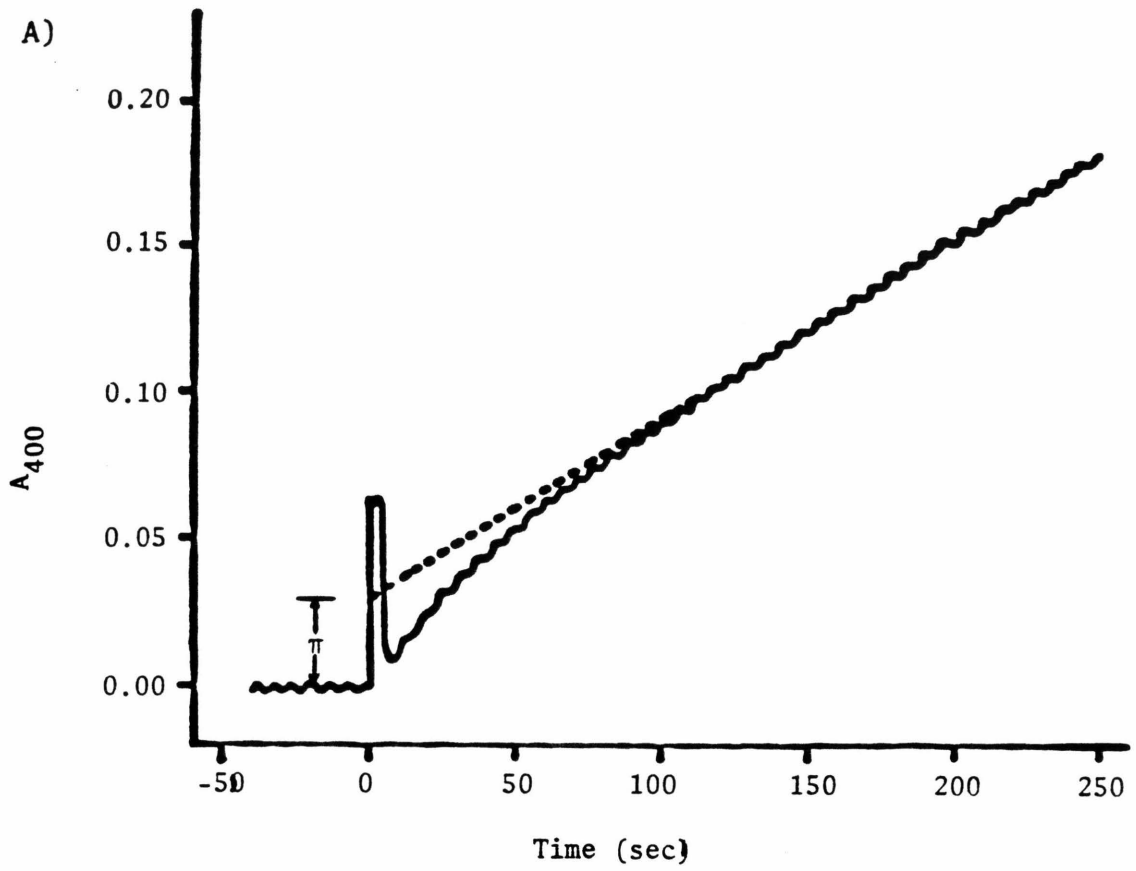


Figure 4. Lineweaver-Burk plot of the reaction of p-nitro-phenyl trimethylacetate and  $\alpha$ -lytic protease.  $r$ , the correlation coefficient of the linear least-squares regression use to fit the data, is 0.9945.

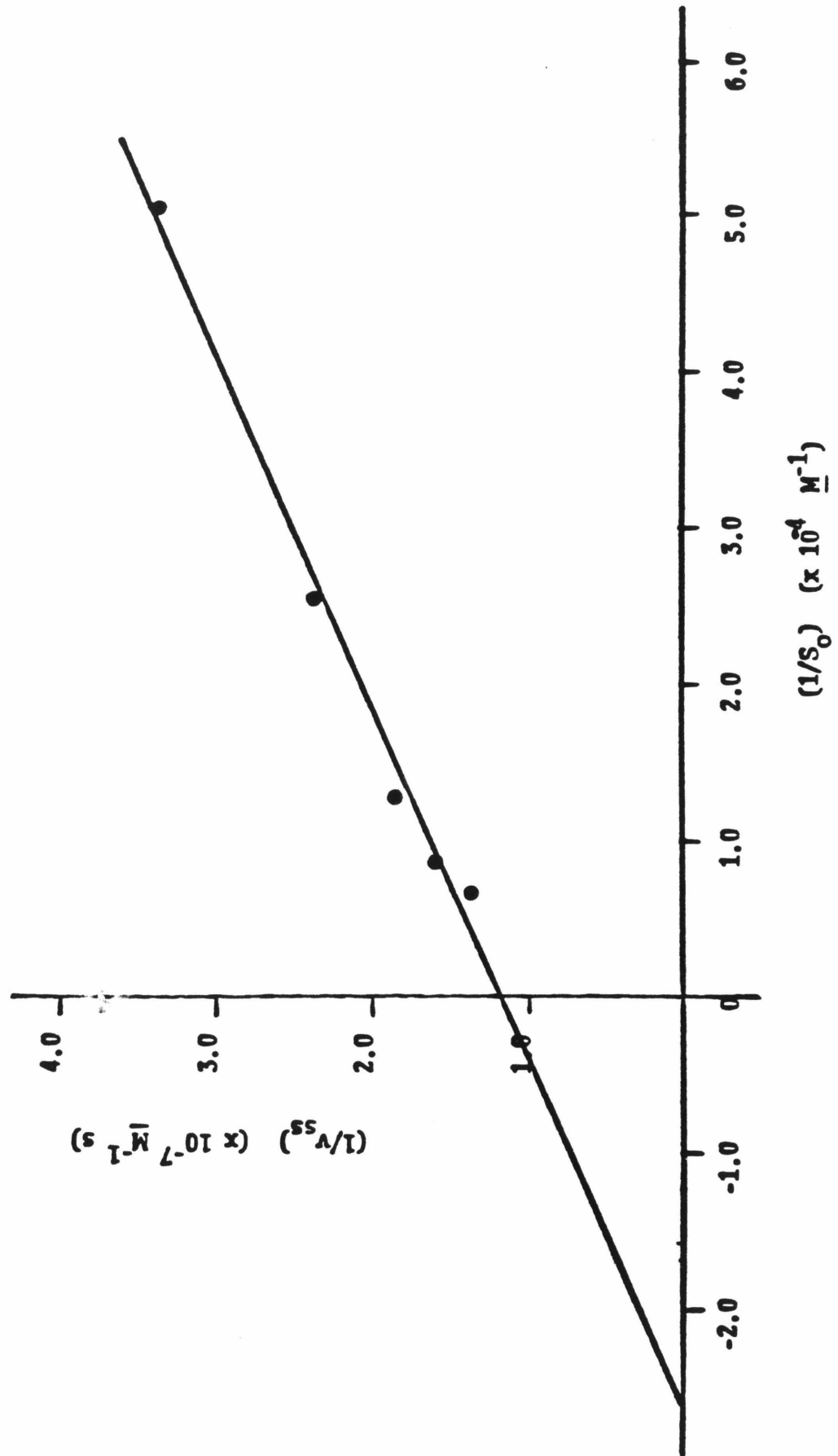
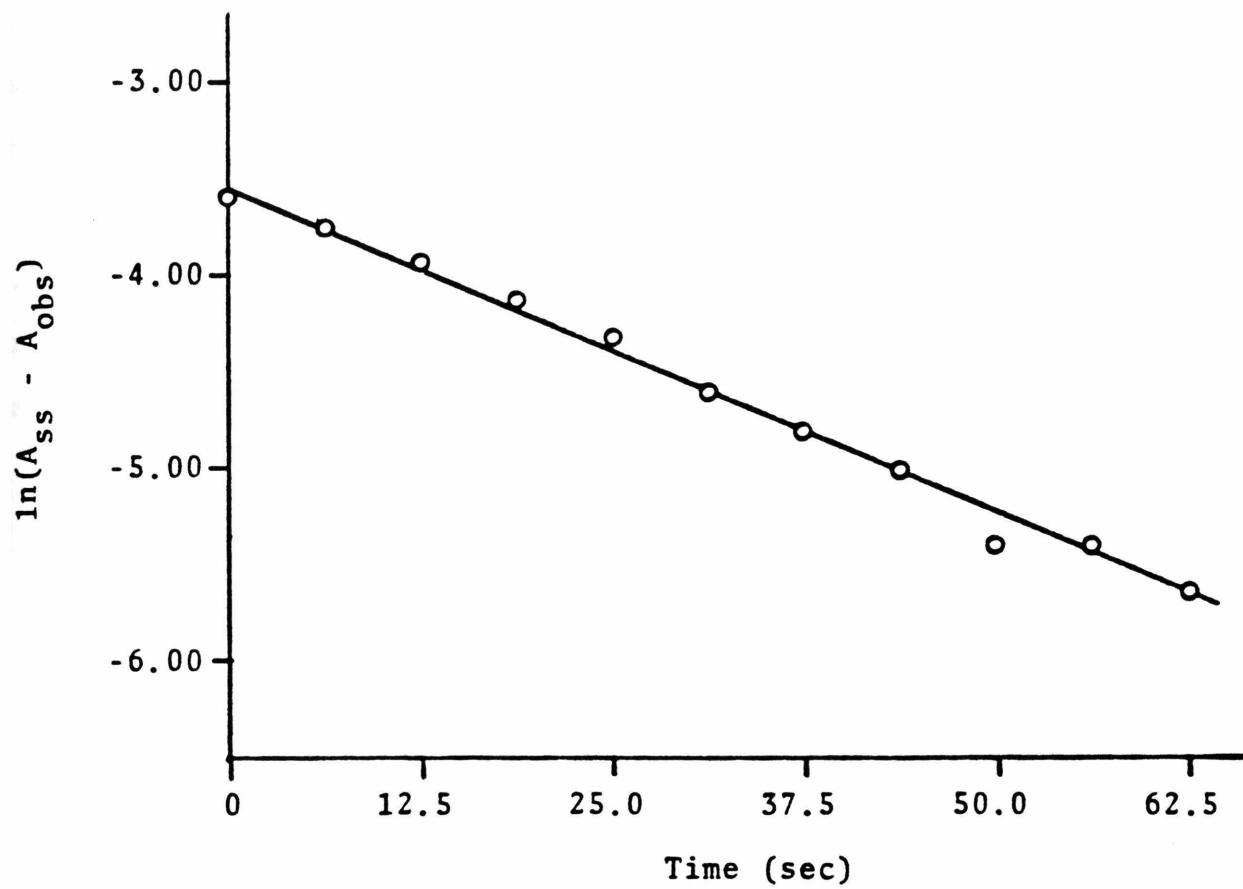


Figure 5. Typical analysis of the first-order pre-steady-state reaction of p-nitrophenyl trimethylacetate and  $\alpha$ -lytic protease.  $S_0 = 3.94 \times 10^{-5} \text{ M}$ ;  $E_0 = 6.56 \times 10^{-6} \text{ M}$  (as determined by titration); 10% (v/v) acetonitrile-water, 0.05 M TRIS/HCl, pH 7.78,  $25.0 \pm 0.2^\circ\text{C}$ .  $r$ , the correlation coefficient of the linear least-squares regression used to fit the data, is -0.9980 for this plot. This is the analysis for the data of Figure 3.



the first order rate constant; the intercept gives the logarithm of the calculated burst,  $\pi$ . Table I gives the dependence of B,  $v_{SS}$ , and  $\pi$  on  $S_0$ . Figure 6 shows the dependence of B on  $S_0$ ; Figure 7, the dependence of  $(1/\sqrt{\pi})$  on  $(1/S_0)$ . Two observations can be made from these data: first, over the range of substrate concentrations studied, the pre-steady state rate constant, B, is linear with respect to substrate concentration; and second,  $1/\sqrt{\pi}$  is linear with  $1/S_0$ . These observations accord well with the proposed mechanism. From equation (16),  $B = k_2(S_0/[K_S + S_0]) + k_3$ . If B is linear with  $S_0$ , then  $S_0 \ll K_S$  so that  $B = (k_2/K_S)S + k_3$ . From the slope and intercept of Figure 6,  $k_3 = 0.022 \text{ s}^{-1}$  and  $k_2/K_S = 294 \text{ M}^{-1}\text{s}^{-1}$ . In order for  $S_0 \ll K_S$ ,  $K_S$  must be at least ten times larger than the largest substrate concentration used; a lower limit on  $K_S$  is thus  $1.5 \times 10^{-3} \text{ M}$ . This puts a lower limit on  $k_2$  of  $0.44 \text{ s}^{-1}$ .

The plot of  $1/S_0$  versus  $1/\sqrt{\pi}$  can be used to determine the concentration of active enzyme. From equation (27),  $1/\sqrt{\pi} = ([k_2 + k_3]/k_2) ([S_0 + K_m]/S_0)(1/E_0)$ . Thus, the y-intercept of Figure 7 gives  $E_0$ :  
 y-intercept =  $([k_2 + k_3]/k_2)(1/E_0)$ . This analysis, using the predetermined values of  $k_2$  and  $k_3$ , gives  $E_0 = 6.56 \times 10^{-6} \text{ M}$ . This means that the stock solution is at least 98% active enzyme, using its  $A_{280}$  as a measure of protein concentration (see Table I). Of course, this number depends on the accuracy of the value of  $k_2$ . Using the same values of  $k_2$  and  $k_3$  and the slope of Figure 7, a value of  $K_m = 3.0 \times 10^{-5}$  can be calculated which accords well with the value calculated from the steady state data.

Another prediction of the theory is that  $\pi$  should be directly proportional to  $E_0$ , and B independent of  $E_0$ . The relevant data are presented in Table II. Within experimental error, B is independent of  $E_0$ .

**TABLE I.** The effect of substrate concentration on the reaction of  $\alpha$ -lytic protease with p-nitrophenyl trimethylacetate.<sup>a</sup>

$S_0$ ( $\times 10^5$ <u>M</u> )	$v_{SS}$ ( $\times 10^8$ <u>M</u> s <sup>-1</sup> ) <sup>b</sup>	B (sec <sup>-1</sup> ) <sup>c</sup>	$\pi$ ( $\times 10^6$ <u>M</u> ) <sup>d</sup>
1.99	2.97	0.0270	0.95
3.94	4.24	0.0337	1.85
7.74	5.44	0.0436	3.36
11.41	6.34	0.0607	3.69
14.97	7.42	0.0626	3.93

<sup>a</sup> $E_0 = 6.68 \times 10^{-6}$  M, as determined from an  $A_{280}$  measurement ((E) =  $5.16 \times 10^{-5}$   $\times A_{280}$ , Whitaker, 1970); pH 7.78, 0.05 M TRIS/HCl, 10% (v/v) acetonitrile-water,  $25.0 \pm 0.2^\circ\text{C}$ .

<sup>b</sup> $v_{SS} \equiv$  steady-state (linear) velocity.

<sup>c</sup>B  $\equiv$  first-order rate constant of the pre-steady state.

<sup>d</sup> $\pi \equiv$  value of burst in M, using  $\Delta\epsilon = 14,750$  M<sup>-1</sup>cm<sup>-1</sup>.

Figure 6. The dependence of  $B$ , the first-order rate constant of the pre-steady-state, on  $S_0$ , for the reaction of p-nitrophenyl trimethyl acetate and  $\alpha$ -lytic protease. Data of Table I.  $r$ , the correlation coefficient of the linear least-squares regression used to fit the data, is 0.9800.

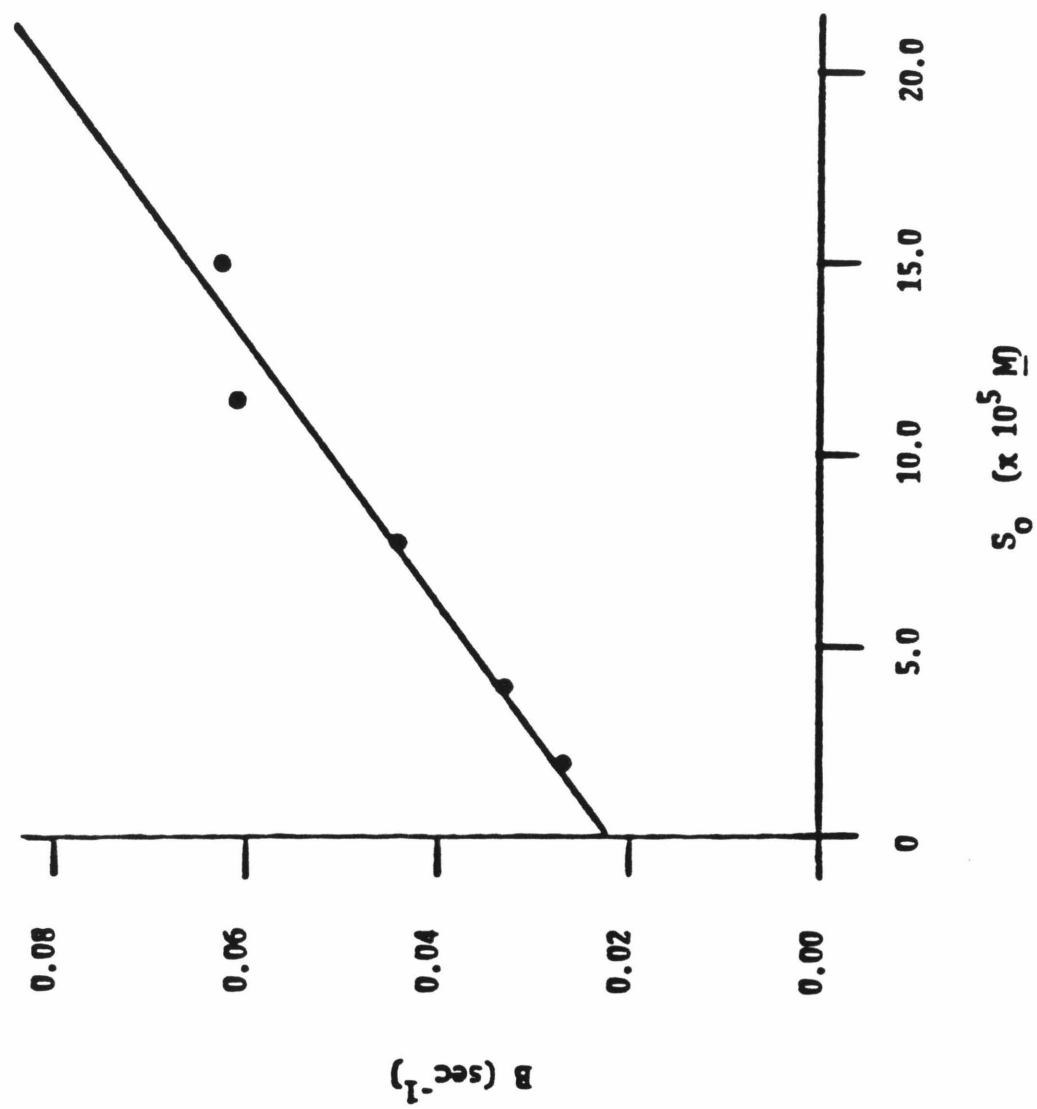
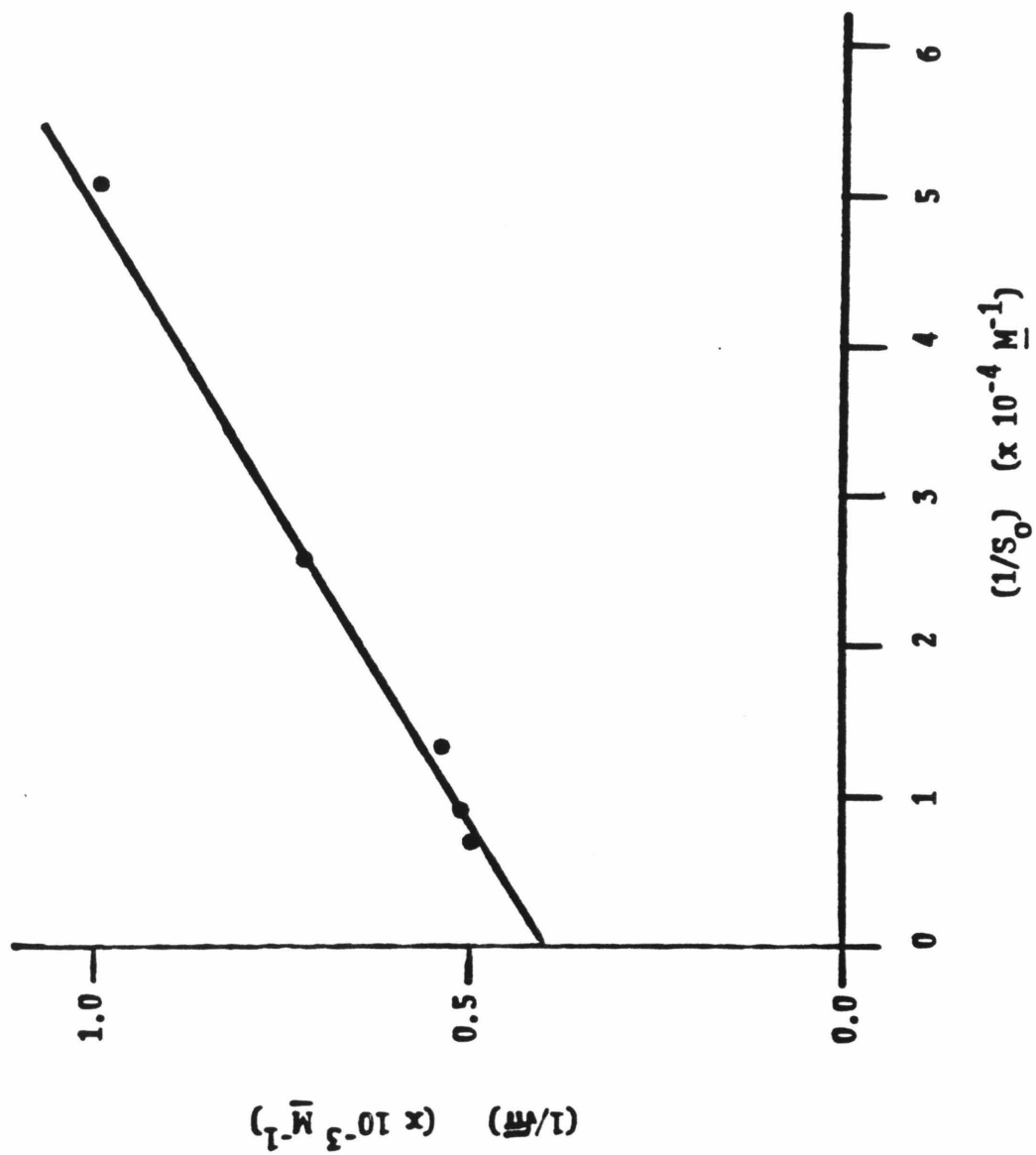


Figure 7. The titration of  $\alpha$ -lytic protease with p-nitro-phenyl trimethylacetate. Data of Table I.  $r$ , the correlation coefficient of the linear least-squares regression used to fit the data, is 0.9981.  $E_0$  can be determined from the  $1/\sqrt{\pi}$ -intercept of the plot.



**TABLE II.** The effect of enzyme concentration on the reaction of  $\alpha$ -lytic protease with p-nitrophenyl trimethylacetate.<sup>a</sup>

$E_o$ ( $\times 10^6$ <u>M</u> ) <sup>b</sup>	$\pi$ ( $\times 10^6$ <u>M</u> ) <sup>c</sup>	B ( $\text{sec}^{-1}$ ) <sup>d</sup>
6.56	3.36	0.0436
4.92	2.44	0.0398
3.28	1.73	0.0434

<sup>a</sup> $S_o = 7.74 \times 10^{-5}$  M; 0.05 M TRIS/HCl, pH 7.78, 10% (v/v) acetonitrile-water,  $25.0 \pm 0.2^\circ\text{C}$ .

<sup>b</sup>As determined from the titration of Figure 7 and Table I.

<sup>c</sup>See Table I, note d.

<sup>d</sup>See Table I, note e.

Furthermore, the slope of a plot of  $E_0$  versus  $\pi$  gives a value for  $(k_2/[k_2 + k_3])^2(S_0/[K_m + S_0])^2$  of 0.487 ( $r = 0.9972$ ); the value calculated from the previous data with  $S_0 = 11.48 \times 10^{-5} \text{ M}$  is 0.512. The correlation between these two numbers indicates that the estimates of  $k_s$  and  $k_2$  are eminently reasonable.

The last piece of information that can be gleaned from this data concerns the initial rate of the pre-steady state. This rate, designated  $v_2$ , is given by  $(k_2/K_s)E_0S_0$ , and is a second order rate. From these  $v_2$  values, a value of  $k_2/K_s$  can be estimated (see Table III). This value is  $301 \pm 45 \text{ M s}^{-1}$ .

Diethyl p-nitrophenyl phosphate. A typical recorder trace of the reaction between  $\alpha$ -lytic protease and diethyl p-nitrophenyl phosphate (paraoxon) is shown in Figure 8. In contrast to the reaction with p-nitrophenyl trimethylacetate, the reaction with Paraoxon is characterized by a slow first-order release of p-nitrophenol, and within experimental error, no detectable turnover. The rate of spontaneous hydrolysis of the substrate before and after reaction are within 5% of each other. Further proof of the lack of substrate turnover is evidenced by the observation that enzyme that had been treated with excess Paraoxon had no detectable activity versus the specific substrate N-acetyl-L-alanyl-L-prolyl-L-alanine p-nitroanilide (APAPNA) after 16 hours and 30 hours of standing at room temperature. Thus, operationally,  $k_3 = 0$  in the proposed kinetic scheme. The observed reaction will be strictly second order, with  $v = dP_1/dt = (k_2/K_2)[E][S]$ . If  $S_0 \gg E_0$  so that  $S_0$  changes only marginally over the course of the titration, then pseudo-first-order kinetics will be observed:  $v = (k_2S_0/K_s)[E] = k_{obs}[E]$ . Furthermore, the observed burst  $\pi$  will correspond to all  $E_0$  converted to  $E'$ ,

**TABLE III.** Determination of  $k_2/K_s$  from the initial rates of the pre-steady-state phase of the reaction of  $\alpha$ -lytic protease with p-nitrophenyl trimethylacetate.<sup>a</sup>

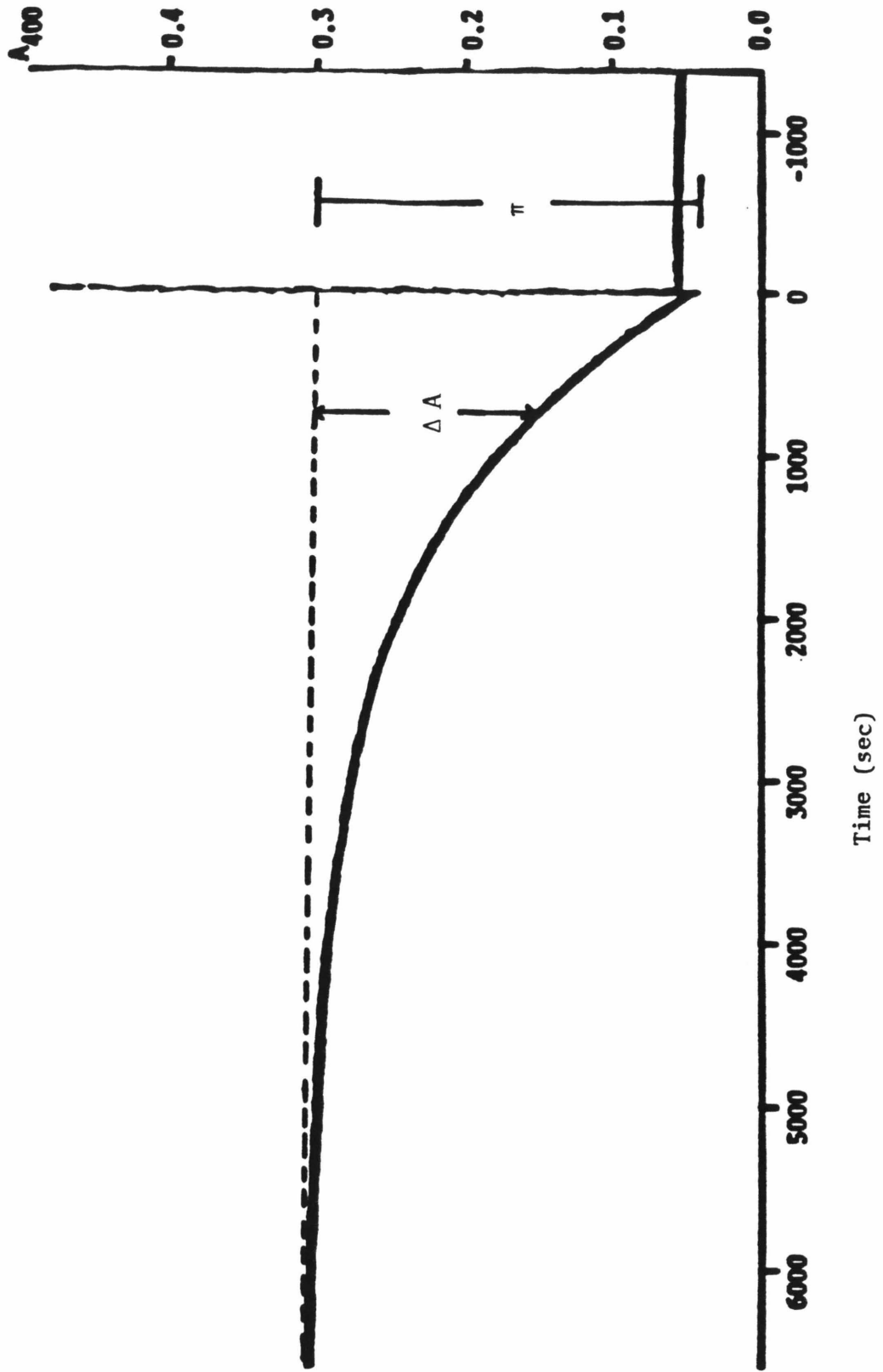
$S_0$ ( $\times 10^5$ <u>M</u> )	$E_0$ ( $\times 10^6$ <u>M</u> )	$v_2$ ( $\times 10^7$ <u>M s</u> <sup>-1</sup> )	$k_2/K_s$ <sup>c</sup>
1.99	6.56	0.48	368
3.94	6.56	0.93	360
7.74	6.56	1.50	295
11.41	6.56	2.00	267
14.97	6.56	2.90	295
7.74	4.92	1.00	263
7.74	3.28	0.66	260

<sup>a</sup>0.05 M TRIS/HCl, pH 7.78, 10% (v/v) acetonitrile-water, 25.0  $\pm$  0.2°C.

<sup>b</sup>Calculated by approximating the initial (linear) rate of the pre-steady-state reaction.

<sup>c</sup>Calculated from  $v_2 = (k_2/K_s)E_0S_0$ ; units are M<sup>-1</sup>s<sup>-1</sup>.

Figure 8. Typical reaction profile of the reaction of  $\alpha$ -lytic protease and diethyl p-nitrophenyl phosphate.  $E_0 = 1.75 \times 10^{-5} \text{ M}$ ;  $S_0 = 5.17 \text{ mM}$ ; 10% (v/v) acetonitrile-water, 0.05 M TRIS/HCl, pH 7.78,  $25.0 \pm 0.2^\circ\text{C}$ . The dotted line represents the extrapolation of the spontaneous hydrolysis of the substrate (also seen at negative times) after more than ten half-lives of the reaction. The rapid increase in absorbance due to addition of the enzyme to the cuvette is seen at  $t=0$ .  $\Delta A$  and  $\pi$  are as described in the text.



so that  $\pi = E_0$  (see Figure 8).

The reaction of  $\alpha$ -lytic protease with Paraoxon was analyzed by the method used to determine B for the case of p-nitrophenyl trimethylacetate. In this case,  $A_{SS}$  is the extrapolated rate of spontaneous hydrolysis. Tables IV and V present the effect of substrate and enzyme concentration on the reaction, respectively. A plot of the data in Table IV is given in Figure 9; a typical determination of  $k_{obs}$  is shown in Figure 10. From the data in Tables IV and V a value of  $0.140 \text{ M}^{-1}\text{s}^{-1}$  can be calculated for  $k_2/K_S$ . Furthermore, it can be seen that  $\pi$  is dependent on  $E_0$  and independent of  $S_0$ ; the reverse is true of  $S_0$ , as predicted.

The titration of  $\alpha$ -lytic protease with Paraoxon can therefore be used to directly measure the concentration of active protein, if it can be shown that the titrant interacts only with the active site of the enzyme, so that there is no spurious production of p-nitrophenol. Two experiments were performed to answer this question. First, a solution of  $\alpha$ -lytic protease which had been inactivated with phenylmethane sulfonyl fluoride, which inactivates the enzyme by esterifying the critical active site serine side-chain, was treated with Paraoxon for five hours under the standard assay conditions. During this time, only the zero-order spontaneous hydrolysis of the substrate was observed; no first-order reaction was apparent, even under the maximum sensitivity (0-0.1A) of the spectrophotometer. Hence, catalytically incapacitated enzyme does not react with Paraoxon.

The second experiment involved the determination of the rate of loss of enzymatic activity toward APAPNA. The results of this experiment are shown in Figure 11. The calculated value of  $(k_2/K_S)$  (= slope of Figure 11B/ $S_0$ ) is  $0.150 \text{ M}^{-1}\text{s}^{-1}$  in reasonable agreement with the value

**TABLE IV.** The effect of substrate concentration on the reaction of  $\alpha$ -lytic protease with diethyl p-nitrophenyl phosphate.<sup>a</sup>

$S_0$ (mM)	$k_{obs}$ ( $\times 10^4$ sec <sup>-1</sup> ) <sup>b</sup>	$\pi$ ( $\times 10^5$ M) <sup>c</sup>	$E_s$ (mM) <sup>d</sup>
2.67	4.64	1.74	1.01
2.67	3.20	1.87	1.08
3.97	5.11	1.83	1.06
5.17	6.83	1.86	1.08
5.17	6.99	1.79	1.04
6.51	9.37	1.77	1.03
6.51	9.08	1.84	1.07
6.51	8.81	<u>1.90</u>	<u>1.10</u>
		ave. 1.83	ave. 1.06

<sup>a</sup> $E_0$  = 50  $\mu$ l of  $E_s$  added to the cuvette, total volume 2.90 ml; 0.05 M TRIS/HCl, pH 7.78, 10% (v/v) acetonitrile-water, 25.0  $\pm$  0.2<sup>o</sup>C.

<sup>b</sup> $k_{obs}$   $\equiv$  pseudo-first-order rate constant =  $(k_2/K_s)S_0$ .

<sup>c</sup> $\pi$   $\equiv$  size of the burst (=  $E_0$ ) in M, using  $\Delta\epsilon = 14750$  M<sup>-1</sup> cm<sup>-1</sup>.

<sup>d</sup> $E_s$   $\equiv$  concentration of enzyme in stock solution, made up from 109 mg of purified, lyophilized  $\alpha$ -lytic protease in 5.00 ml of distilled water. The average value represents 96.4% purity by weight.

**TABLE V.** The effect of enzyme concentration on the reaction of  $\alpha$ -lytic protease with diethyl p-nitrophenyl phosphate.<sup>a</sup>

$E_o$ ( $\mu$ l) <sup>b</sup>	$k_{obs}$ ( $\times 10^4 \text{ sec}^{-1}$ ) <sup>c</sup>	$\pi$ ( $\times 10^5 \text{ M}$ ) <sup>d</sup>	$E_s$ (mM) <sup>e</sup>
50	7.44	1.76	1.06
60	7.64	1.81	0.91
75	7.06	2.30	0.92
80	7.08	2.58	0.97
100	7.01	3.55	1.07
50	6.99	1.86	1.12
100	<u>7.76</u>	3.64	<u>1.09</u>
	ave. 7.28		ave. 1.02

<sup>a</sup> $S_o = 5.17 \text{ mM}$ ; total volume 3.00 ml, 0.05 M TRIS/HCl, pH 7.78, 10% (v/v) acetonitrile-water,  $25.0 \pm 0.2^\circ\text{C}$ .

<sup>b</sup>Volume of  $E_s$  added to the cuvette.

<sup>c</sup>See Table III, note b.

<sup>d</sup>See Table III, note c.

<sup>e</sup>Same solution as Table III, note d.

Figure 9. Dependence of  $k_{obs}$  on  $S_0$  for the reaction of  $\alpha$ -lytic protease and diethyl p-nitrophenyl phosphate. Data of Table IV.  $r$ , the correlation coefficient of the linear least-squares regression used to fit the data, is 0.9780.

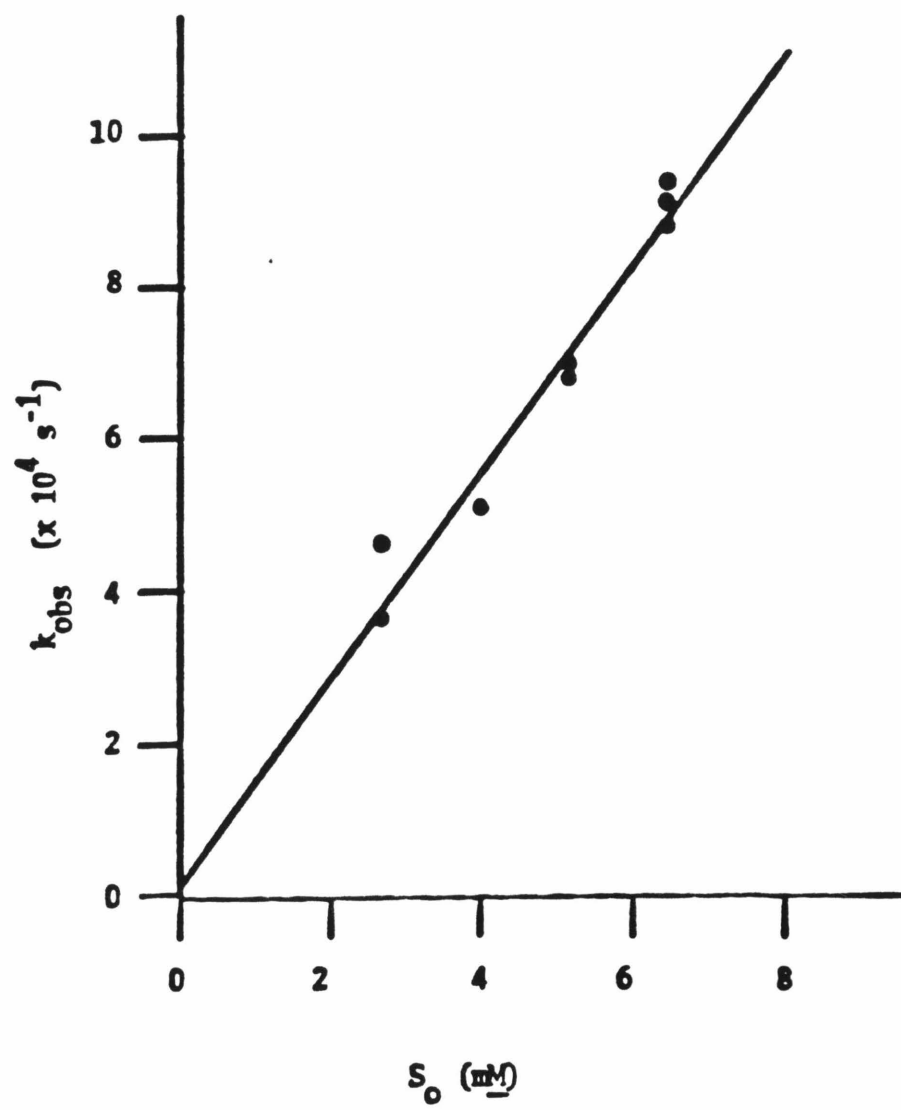


Figure 10. Typical determination of  $k_{\text{obs}}$  for the reaction of  $\alpha$ -lytic protease ( $1.75 \times 10^{-5}$  M) and diethyl p-nitrophenyl phosphate (5.17 mM). Data of Table V.  $r$ , the correlation coefficient of the linear least-squares regression used to fit the data, is 0.9998.

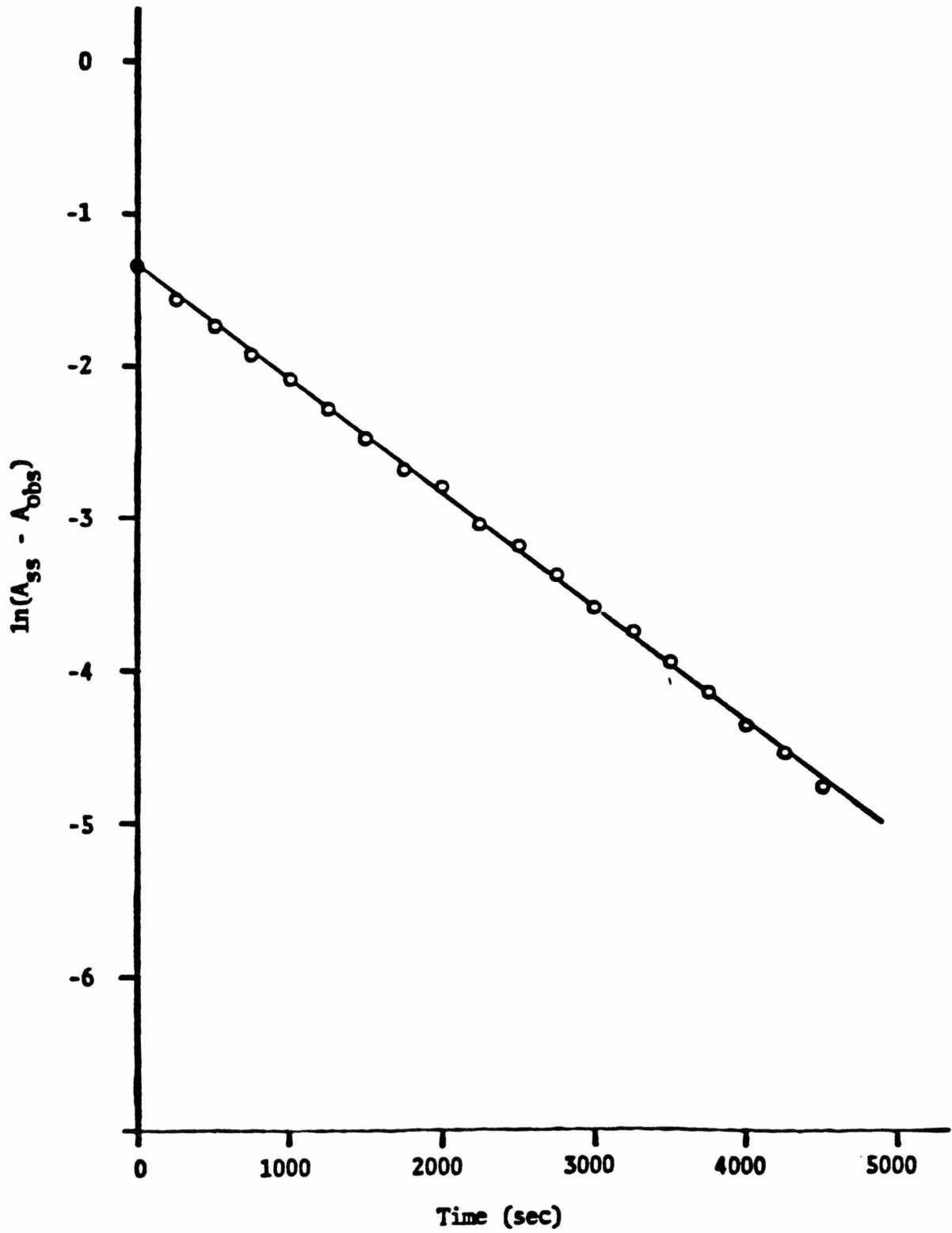
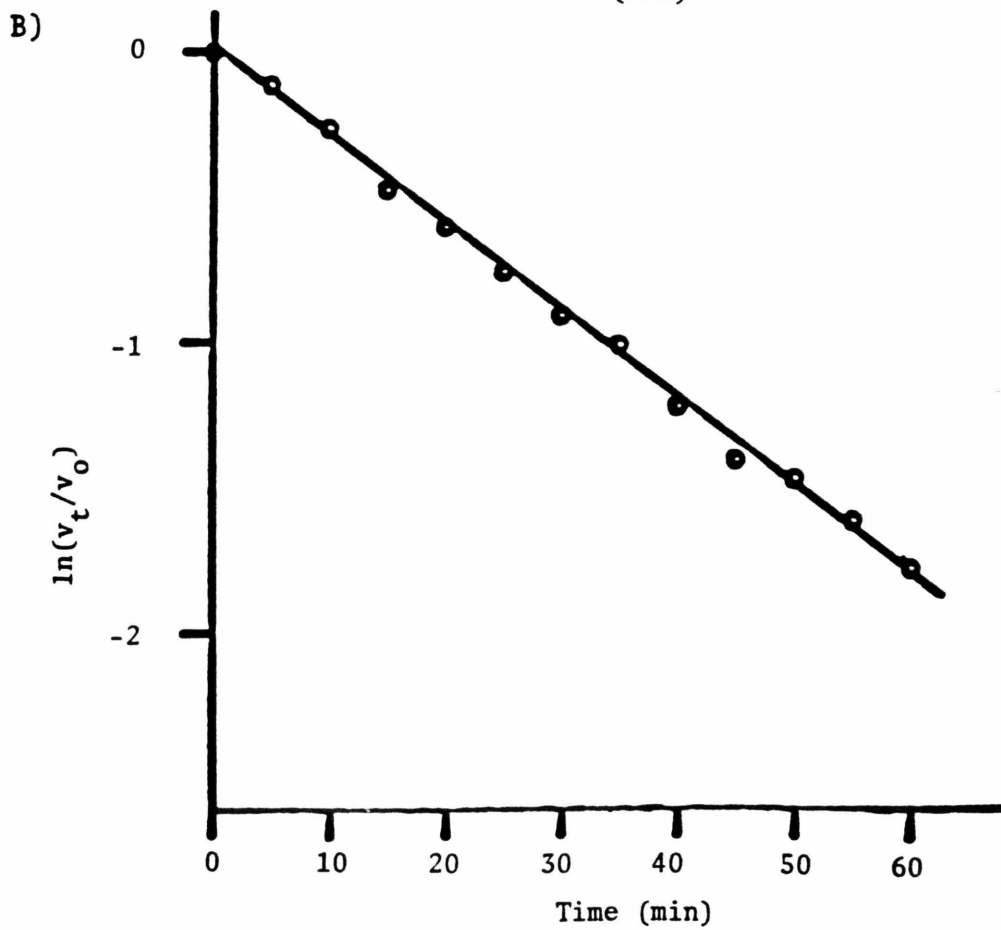
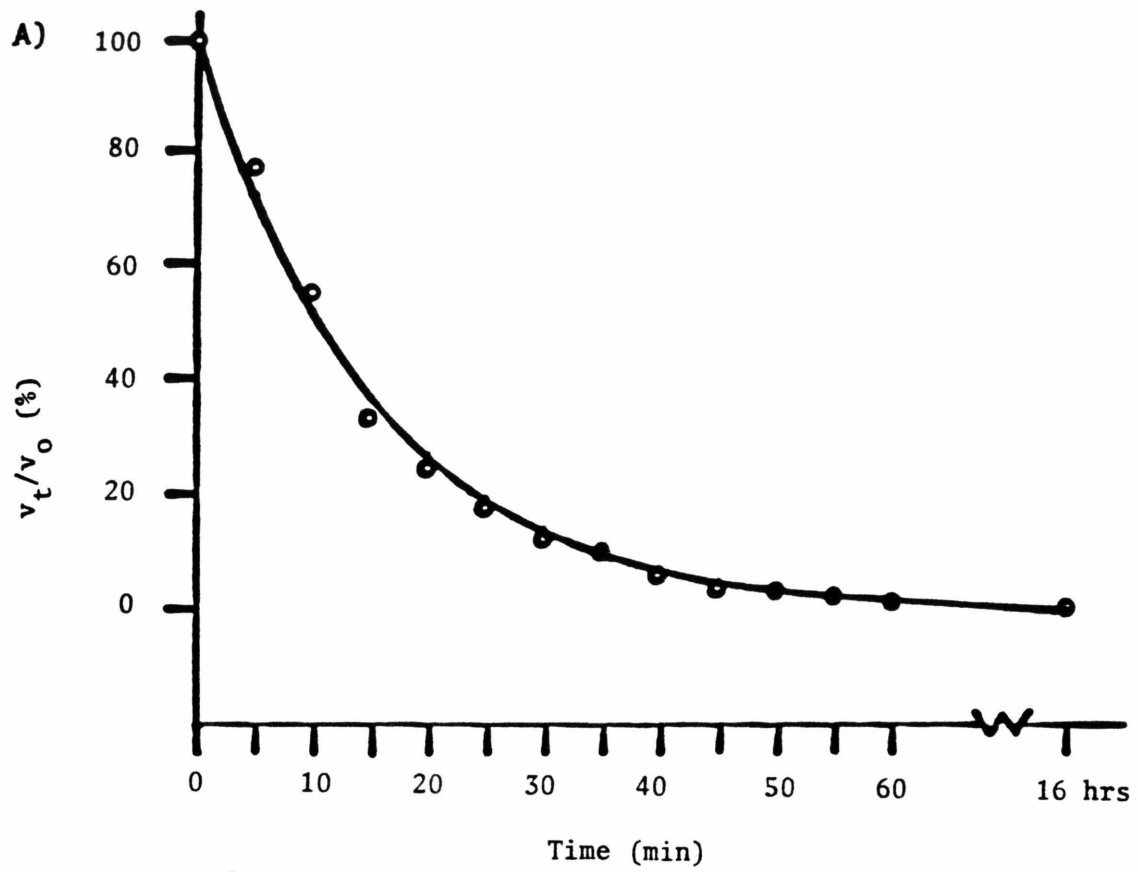


Figure 11. A) Decline in  $\alpha$ -lytic protease activity toward N-acetyl-L-alanyl-L-prolyl-L-alanine p-nitroanilide in the presence of diethyl p-nitrophenyl phosphate. The enzyme was dissolved in 10% (v/v) acetonitrile-water, 0.05 M TRIS/HCl, pH 7.78, and a 100  $\mu$ l aliquot was used to determine 100% activity under these conditions against  $2.5 \times 10^{-4}$  M APAPNA ( $v_0$ ). An aliquot of a stock solution of diethyl p-nitrophenyl phosphate was then added to the stock enzyme solution, so that  $S_0 = 7.38 \times 10^{-3}$  M. 100  $\mu$ l aliquots were taken at five minute intervals and assayed for APAPNA activity ( $v_t$ ) as a percentage of  $v_0$ .

B) First-order analysis of the data of Figure 11A.  $r$ , the correlation coefficient of the linear least-squares regression used to fit the data, is -0.9873.



calculated above.

N-Benzoyloxycarbonyl-L-alanine p-nitrophenolate. Cbz-L-alaONp was initially tested as a possible titrant, as it is a semi-specific substrate for the enzyme, unlike the previous two candidates. Unfortunately, only the steady state turnover reaction was observed. Furthermore, the reaction is too fast to determine burst kinetics effectively, and therefore use of this substrate as a titrant is not feasible. However, it represents one of the most effective substrates for the enzyme.

Michaelis-Menten kinetics were observed for the hydrolysis of the substrate at pH 8.00 in 0.05 M potassium phosphate, 0.1 M potassium chloride, 25°C; Lineweaver-Burk analysis gives  $K_m = 2.50 \times 10^{-3} \text{ M}$ ,  $k_{cat} = 707 \text{ s}^{-1}$ , and  $k_{cat}/K_m = 2.80 \times 10^5 \text{ M}^{-1} \text{ s}^{-1}$ . These values rank this substrate with good specific ester substrates of the enzyme such as N-acetyl-L-alanyl-L-prolyl-L-alanine methyl ester (at pH 8.0, 25°C,  $k_{cat} = 300 \text{ s}^{-1}$ ,  $K_m = 1.0 \times 10^{-3} \text{ M}$ ,  $k_{cat}/K_m = 3.0 \times 10^5 \text{ M}^{-1} \text{ s}^{-1}$ ; Hunkapiller, et al., 1976). However, use of this substrate is much more convenient and accurate as the hydrolysis can be followed spectrophotometrically, rather than in the more cumbersome pH-stat.

DISCUSSION

The use of p-nitrophenyl ester substrates as titrants for proteolytic enzymes depends on the exhibition of biphasic (fast acylation/slow deacylation) kinetics with these substrates. This kinetic behavior manifests itself in a "burst" of p-nitrophenol due to rapid acylation of the active enzyme that is directly proportional to its concentration, the proportionality factor being a function of rate constants and the degree of substrate saturation of the enzyme.

The reaction of  $\alpha$ -lytic protease and p-nitrophenyl trimethylacetate is typical of the above behavior. The rate of acylation is approximately twenty times that of deacylation ( $k_2 = 0.44\text{s}^{-1}$ ,  $k_3 = 0.022\text{s}^{-1}$ ). However, the fact that deacylation does proceed at a reasonable rate (relative to acylation) coupled with the low solubility of this substrate (relative to  $K_m$ ) means that the observed "burst" will be less than the actual enzyme concentration. Thus, accurate determination of active enzyme concentrations will depend either on accurate determination of  $k_2$ ,  $k_3$ ,  $\frac{E_o}{\pi} = \frac{(k_2 + k_3)}{k_2} \cdot \frac{(S_o + K_m)^2}{S_o^2}$ , or on the measurement of  $\pi^{1/2}$  as a function of  $S_o$  for several values of  $S_o$ . The former procedure will generally be less exact, due to the difficulties inherent in accurately measuring  $k_2$  (and to some extent,  $K_m$ ), while the latter will require the performance of a large number of hydrolyses for each enzyme concentration to be determined. In short, the use of p-nitrophenyl trimethylacetate as a titrant for  $\alpha$ -lytic protease, although possible, is somewhat impractical as a routine procedure.

Kaplan and Whitaker (1969) have briefly reported the reaction of p-nitrophenyl trimethylacetate with  $\alpha$ -lytic protease. They determined

a value of  $5.1 \times 10^{-5} \text{ M}$  for  $K_m$  in 5.9% acetonitrile, 0.01 M TRIS/HCl, pH 8.5 buffer, in reasonable agreement with the value of  $3.8 \times 10^{-5} \text{ M}$  determined in this study. This disparity reflects the difficulty in reproducibly determining an accurate value for and the subsequent determination of  $E_0$  using this substrate. Their value of  $0.0135 \text{ s}^{-1}$  for  $k_{\text{cat}}$  also agrees well with the value of  $0.0130 \text{ s}^{-1}$  determined here ( $V_{\text{max}} = 8.5 \times 10^{-8} \text{ M s}^{-1}$  for  $E_0 = 6.56 \times 10^{-6} \text{ M}$ ), especially considering the difference in pH used in the two studies (8.5 as opposed to 7.78). Unfortunately, they did not carry their analysis too much further than to show that the reaction was consistent qualitatively with  $k_2 \gg k_3$ , and  $K_m \ll S_0 \ll K_S$ . These features are, of course, what has been described here in a more quantitative manner.

The reaction of  $\alpha$ -lytic protease with diethyl p-nitrophenyl phosphate exhibits more of the features desirable in a successful titrant. The rate of deacylation is virtually zero, and substrate solubility is such that  $S_0 \gg E_0$  is easily attainable, so that the observed burst is equal to the concentration of active enzyme. This means that the measurement of  $E_0$  is solely dependent on the accuracy of the spectrophotometric data and the care with which the experiment is done, and not on the more difficult measurement of kinetic constants. Unfortunately, two other considerations render this substrate a less than perfect titrant. First, for a reasonable substrate concentration ( $\sim 5 \text{ mM}$ ), the half-time for the reaction is  $\sim 1000 \text{ sec}$ . To get an accurate determination of  $\pi (= E_0)$ , the reaction should be carried out for eight to ten half-lives or 2-2½ hours. This is sometimes an inconvenient length of time for a single concentration determination. Second, and more important, although it has been shown that Paraoxon reacts only at the

active site of  $\alpha$ -lytic protease, it is not a specific substrate of the enzyme and hence will not show much specificity in contaminated preparations of the protein. Third, this method requires the use of somewhat large concentrations of enzyme, in order to obtain a reasonable absorbance burst. However, if these three considerations are not limitations in a particular application, Paraoxon is an acceptable titrant for  $\alpha$ -lytic protease.

It should be noted that the behavior of  $\alpha$ -lytic protease with the substrates studied here mimics the behavior of elastase with these substrates (Bender, et al., 1966; Bender and Marshall, 1968), thereby reinforcing the similarity of this microbial enzyme and a (related) pancreatic one (Kaplan and Whitaker, 1969; Kaplan et al., 1970; McLachlan and Shotton, 1971; Shaw and Whitaker, 1972).

CONCLUSION

Both p-nitrophenyl trimethylacetate and diethyl p-nitrophenyl phosphate exhibit the biphasic kinetics that are consistent with the acyl-enzyme mechanism of serine protease hydrolysis. This behavior can be used to determine the concentration of active enzyme in a protein preparation, and as such these substrates can be termed "active site titrants" (Bender et al., 1966).

Diethyl p-nitrophenylphosphate is a better titrant for  $\alpha$ -lytic protease than is p-nitrophenyl trimethylacetate, since enzyme concentrations determined using this substrate do not depend on the accurate determination of kinetic constants. However, diethyl p-nitrophenyl phosphate does not resemble a specific substrate for the enzyme, and as such is not a perfect titrant, since it will lack specificity for  $\alpha$ -lytic protease.

Finally, it should be noted that the procedure for isolation and purification of  $\alpha$ -lytic protease yields several hundred milligrams of a product that is at least 95% (by weight) active enzyme, a not insignificant achievement.

## REFERENCES

- Bender, M.L., Begue-Canton, M.L., Blakely, R.L., Brubacher, L.J., Feder, J., Gunter, C.R., Kezdy, F.J., Killheffer, J.V. Jr., Marshall, T.H., Miller, C.G., Roeske, R.W., and Stoops, J.K. (1966), J. Am. Chem. Soc. 88, 5890-5913.
- Bender, M.L., and Marshall, T.H. (1968), J. Am. Chem. Soc. 90, 201-207.
- Chase, T. Jr., and Shaw, E. (1967), Biochem. Biophys. Res. Commun. 29, 508-514.
- Chase, T. Jr., and Shaw, E. (1970), in "Methods in Enzymology", vol. XIX, G.E. Perlmann and L. Lorand, eds., Academic Press, New York, 3-20.
- Fife, T.H., and Milstein, J.B. (1967), Biochemistry 6, 2901-2907.
- Hunkapiller, M.W., Forgac, M.D., and Richards, J.H. (1976), Biochemistry 15, 5581-5588.
- Kaplan, H., and Whitaker, D.R. (1969), Can. J. Biochem. 47, 305-315.
- Kaplan, H., Symonds, V.B., Dugas, H., and Whitaker, D.R. (1970), Can. J. Biochem. 48, 649-658.
- Kezdy, F.J., and Bender, M.L. (1962), Biochemistry 1, 1097-1106.
- Kezdy, F.J., and Kaiser, E.T. (1970), in "Methods in Enzymology", vol. XIX, G.E. Perlmann and L. Lorand, eds., Academic Press, New York, 21-40.
- Lineweaver, H., and Burk, D. (1934), J. Am. Chem. Soc. 56, 658-666.
- McLachlan, A.D., and Shotton, D.M. (1971), Nature (London) 229, 202-205.

Shaw, M.C., and Whitaker, D.R. (1973), Can. J. Biochem. 51,  
112-114.

Tanizawa, K., Ishii, S., and Kanaoka, Y. (1968), Biochem. Biophys.  
Res. Commun. 32, 893-897.

## CHAPTER IV

KINETIC AND NUCLEAR MAGNETIC RESONANCE STUDIES  
OF  $\alpha$ -LYTIC PROTEASE AND TRANSITION STATE ANALOGS

## I. PEPTIDE ALDEHYDES

## ABBREVIATIONS

Ser	L-Serine
His	L-Histidine
Asp	L-Aspartic Acid
NMR	Nuclear magnetic resonance
TLC	Thin layer chromatography
TMS	Tetramethylsilane
DSS	Sodium 2,2-dimethyl-2-silapentane-5-sulfonate
IR	Infrared
Pro	L-Proline
Ala	L-alanine
DCC	Dicyclohexylcarbodiimide
$\text{CDCl}_3$	Deuteriochloroform
$\text{D}_2\text{O}$	Deuterium oxide, $^2\text{H}_2\text{O}$
Boc	tert-Butyloxycarbonyl
Ac	Acetyl
Gly	Glycine
$\text{d}_6$ -Acetone	Perdeuterated acetone
Pht	Phthalyl
dec.	Decomposed

The abbreviations for the substrates and inhibitors used in this chapter are given in the Experimental section with their respective syntheses.

FID	Free induction decay
ppm	Parts per million

## CHAPTER IV--INTRODUCTION

The serine proteases are enzymes that have evolved to catalyze the hydrolysis of peptide bonds using a triad of amino acid side-chains: the hydroxyl of Ser 195, the imidazole of His 57, and the carboxylate of Asp 102. Catalysis occurs through general acid-base assisted alcoholysis of the scissile (amide) bond of the substrate, a process supposed to proceed through a tetrahedrally-oriented intermediate or transition state. This process is diagrammed in Figure 1; the actual location of the proton originally on  $\gamma\text{O}$  of Ser 195 during the intermediate portions of the reaction has yet to be determined. Hydrolysis of the acyl-enzyme proceeds by a similar mechanism, substituting water for the serin hydroxyl as the nucleophile.

Direct observation of the high-energy intermediates, and especially the transition states, of these enzymatic reactions using modern techniques (crystallographic and spectroscopic, generally) is difficult at best. Although the existence of the acyl-enzyme intermediate in the catalytic sequence has been well documented (Stroud, 1974; Kraut, 1977; Bender et al., 1964; Bender and Kezdy, 1964; Blow, 1976; Stroud et al., 1975), the presence of other intermediate structures is less well established (Caplow, 1969; Lucas et al., 1973; O'Leary and Kluetz, 1972; Fersht, 1972; Fastrez and Fersht, 1973; Fink, 1979; Hunkapiller et al., 1976). Much of this latter evidence is indirect in nature, based on kinetic observations. In any case, the majority of the experimental attention has been

Figure 1. The first half of the catalytic hydrolysis of an amide substrate by a serine protease enzyme. The upper diagram represents the formation of the tetrahedral adduct of Ser 195 and the substrate; the lower diagram depicts the breakdown of this structure to acyl enzyme and the first product of hydrolysis. It should be noted that the charges on the catalytic His and Asp residues have been depicted in accord with their relative  $pK_a$  values in the free enzyme, as the true catalytic ionization behavior of these residues is at present unknown.



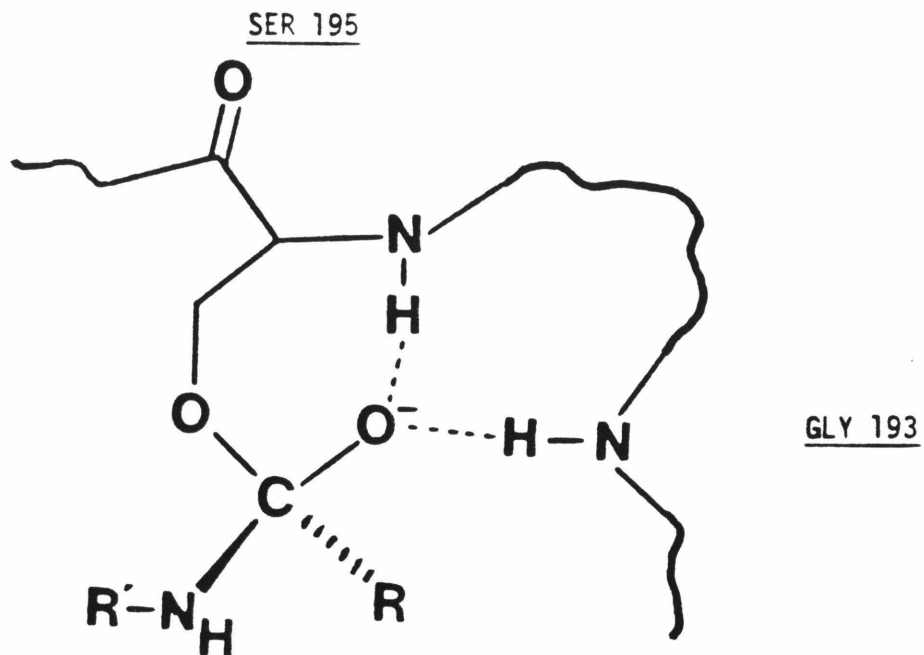
focussed on the events concerning the interaction of Ser 195 and the substrate; little direct attention has been paid to the role of the Asp 102-His 57 dyad.

Since it is difficult to study the dynamic high-energy enzyme-substrate interactions directly, other techniques have been devised. One of the most promising is the use of "transition state analogs". This approach takes advantage of the fact that enzymes are designed to specifically stabilize the transition states of the reactions they catalyze over the ground states (Pauling, 1948; Fersht, 1974; Wolfenden, 1976). Thus, if one can design suitable stable molecules that are able to exploit the special interactions that distinguish the enzyme-substrate complex in the transition state from that in the ground state, some information relevant to the identity of the forces and structures existing in the transition state might be uncovered. It should be realized that a "perfect" analog, that is, one containing the partial-bond characteristics of the actual transition state, can never be designed, so that indicative, rather than absolute, structural information will be the best one could obtain from this technique. A corollary of this enzyme-transition state complementarity is that these transition state analogs will be potent reversible inhibitors of the enzymes for which they are designed (Wolfenden, 1972; Lienhard et al., 1972; Lienhard, 1973; Wolfenden, 1976).

The use of aldehydes as transition state analogs of

specific and non-specific substrates of the serine proteases has become common practice (Lowe and Nurse, 1977; Kennedy and Schultz, 1979; Thompson, 1973; Hunkapiller et al., 1975; Gorenstein et al., 1976). Similar aldehydes have also proven to be potent inhibitors of cysteine proteases such as papain (Westerik and Wolfenden, 1972; Lewis and Wolfenden, 1977b; Mattis et al., 1977) and leucine aminopeptidase (Andersson et al., 1982). Furthermore, natural peptide aldehydes have been discovered and isolated (Aoyagi et al., 1969; Kawamura et al., 1969; Umezawa et al., 1970; Suda et al., 1972; Umezawa et al., 1973; Kondo et al., 1969); these are also potent serine protease inhibitors. The inhibitory power of these aldehydes is proposed to be due to their ability to form stable tetrahedral addition complexes with the active site nucleophile (serine hydroxyl or cysteine thiol) that resemble the putative tetrahedral transition states of the catalytic reaction. These tetrahedral transition state structures bear a formal negative charge at catalytic pH, localized on the carbonyl oxygen of the substrate (see Figure 2). The serine proteases have evolved to stabilize this charge through hydrogen bonding to the backbone amide nitrogens of Ser 195 and Gly 193. The role of this "oxyanion hole" for transition state stabilization was first suggested by Henderson (1970), and was elaborated by Robertus et al. (1972). Crystallographic determinations have shown that the "oxyanion hole" is a common feature of all mammalian and bacterial serine proteases studied thus far (Birktoft and Blow, 1972; Bode and Schwager,

Figure 2. Diagram of the interactions stabilizing the tetrahedrally oriented transition state depicted in Figure 1. The NH groups of Ser 195 and Gly 193 have been called the "oxyanion hole"; stabilization of the transition state comes from the formation of tight hydrogen bonds between the oxyanion and the amide groups depicted.



TETRAHEDRAL INTERMEDIATE STABILIZED  
BY STRONG HYDROGEN BONDING TO THE  
OXYANION HOLE

1975; Kraut, 1977; Sawyer et al., 1978; Brayer et al., 1978; Brayer et al., 1979a; Delbaere et al., 1979). Refinements of these structures have indicated the presence of a bound (tetrahedral) sulfate anion in the oxyanion hole in crystals formed in the presence of sulfate (Matthews et al., 1977; Brayer et al., 1979a; Bode and Schwager, 1975), reinforcing the claim of the ability of this site to support tetrahedrally oriented species.

A recent X-ray determination of the crystal structure of Streptomyces griseus protease A complexed with a specific tetrapeptide aldehyde has been interpreted as covalent hemiacetal formation between Ser 195 and the aldehydic carbonyl (Brayer et al., 1979b). The resolution of the crystallographic data unfortunately cannot allow the unambiguous assignment of a charge to this adduct, since it would be highly informative to know if this complex can take full advantage of the "oxyanion hole" by existing as a negatively charged species, as an ideal transition state analog would be expected to do; this would be contrary to the normal solution behavior, which should be a neutral hemiacetal under the conditions of crystallization of the complex (see Figure 3).

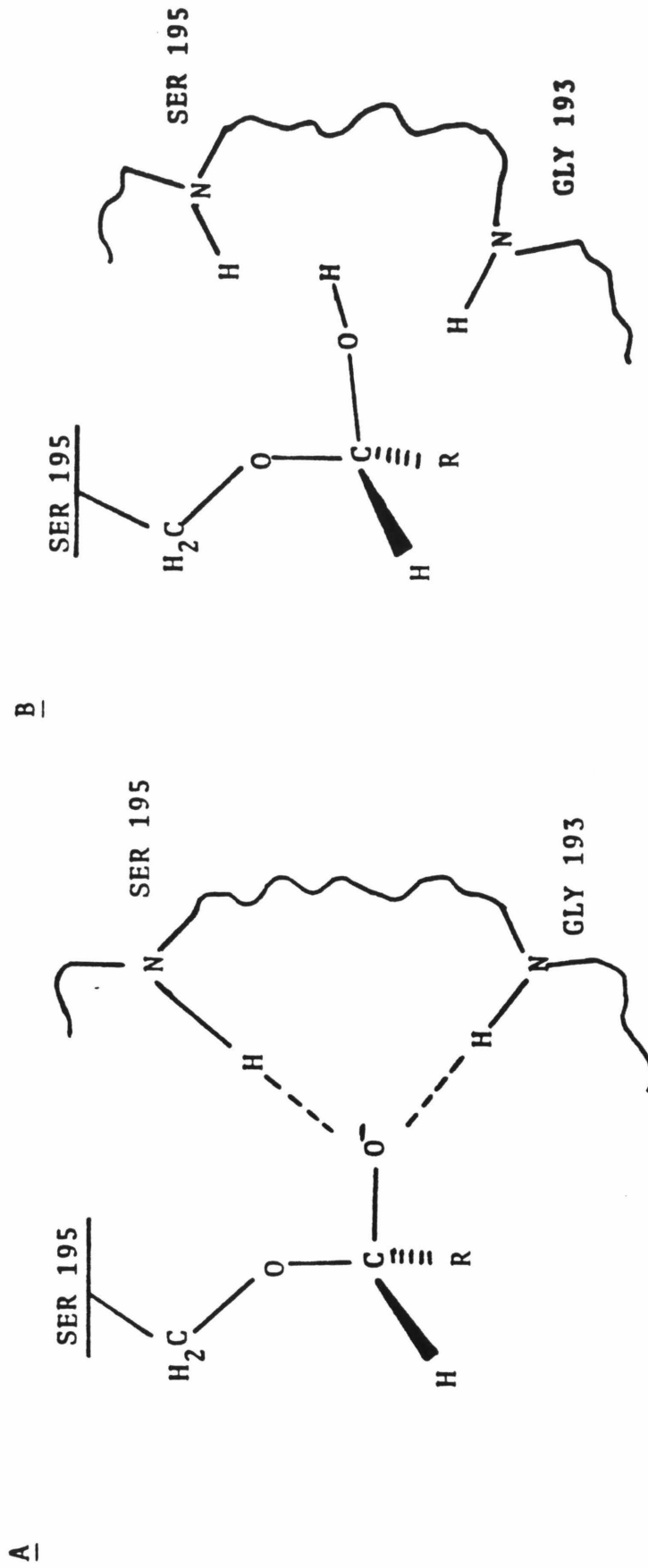
In order to gain insight into the nature of the structures and charge distributions during the catalytic process,  $^{13}\text{C}$  NMR techniques have been used to investigate the complex between  $\alpha$ -lytic protease and a tripeptide aldehyde analog of a specific substrate, N-acetyl-L-alanyl-L-prolyl-L-alaninal (Hunkapiller et al. 1975). The titration behavior of the chemical shift

Figure 3. Tetrahedral complex of aldehyde and Ser 195.

A) Complex depicted assuming it mimics the tetrahedral transition state of the catalytic reaction to a high degree of accuracy, in that it exists in its oxyanion form and is stabilized by hydrogen bonds to the oxyanion hole. At catalytic pH, this would imply that the normal  $pK_a$  of the oxyanion (12 to 14) has been lowered substantially due to the stabilizing influence of the enzyme.

B) Complex depicted assuming that the hemiacetal has its normal  $pK_a$ . No hydrogen bonds have been drawn in the diagram; this is not to say that hydrogen bonding does not exist in the tetrahedral adduct, but is meant to suggest that the special tight interactions with the oxyanion hole are probably not available in the neutral adduct.

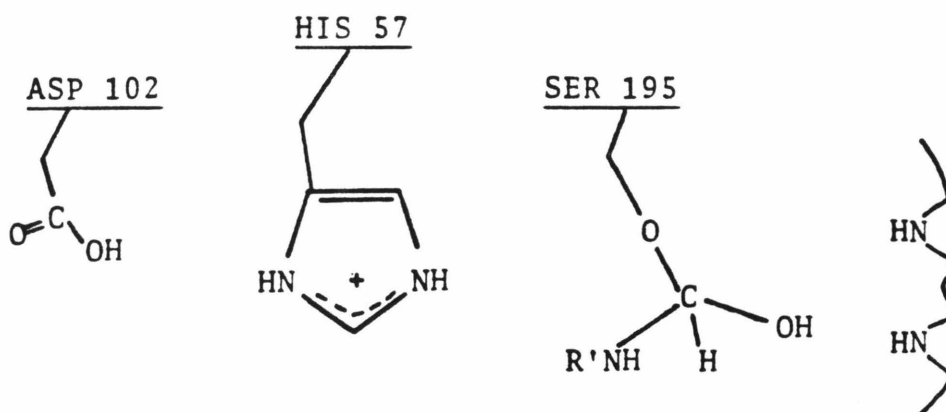
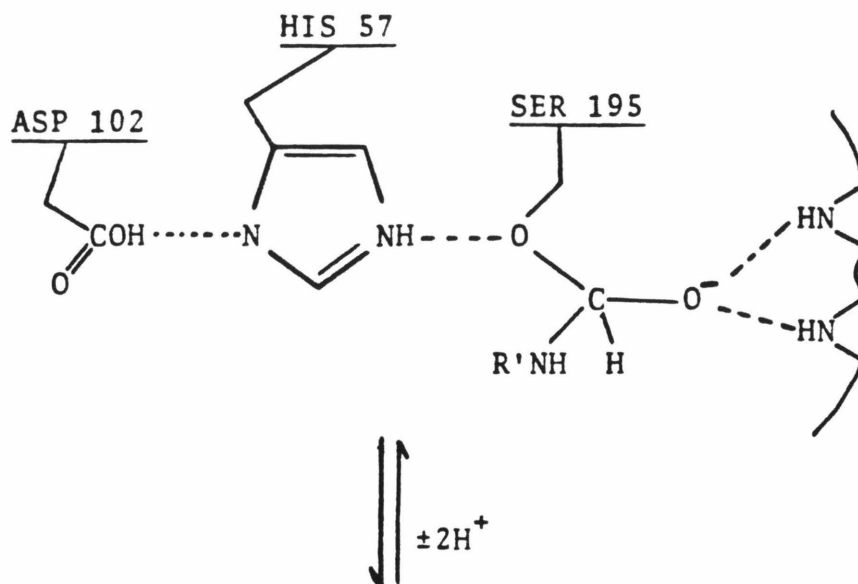
Note that in both cases, the leaving group of the substrate (see Figure 2) has been replaced with -H, a poor leaving group.



and coupling constant of the C-2 carbon of the lone histidine side-chain in this complex indicated a neutral imidazole above pH 7. More important, on lowering the pH to 5.5, two protons appeared to be added cooperatively to the complex (see Figure 4). These researchers interpreted this behavior as suggesting a well ordered, tightly hydrogen bonded network of neutral Asp 102-neutral His 57-hemiacetal oxyanion at high (catalytic) pH; addition of a single proton to the system would completely disrupt the precise orientation of these groups and result in the cooperative addition of another proton (Figure 4). Thus, the enhanced binding of aldehyde to the enzyme was postulated to be due to covalent attachment of the aldehydic carbonyl to the active site serine, generating a negatively charged adduct stabilized by the "oxyanion hole", and utilizing the Asp 102-His 57 dyad to store the Ser 195 hydroxyl proton. The high pH behavior of the enzyme/aldehyde complex was therefore supposed to mimic catalysis with a high degree of accuracy, in that it required active participation of the "charge relay" system for its formation and generated a structure highly analogous, in terms of charge and stabilizing interactions with the enzyme, to the tetrahedral transition states of the catalytic process.

The cooperativity of the ionization of this enzyme/aldehyde complex predicts a unique kinetic behavior for  $K_I$ , the dissociation constant of this complex, as a function of pH (see Figure 13 and the Discussion). We therefore undertook to measure  $K_I$  versus pH for three tripeptide aldehydes, N-acetyl-L-alanyl-L-prolyl-L-alaninal, N-acetyl-L-alanyl-L-prolyl-D,L-

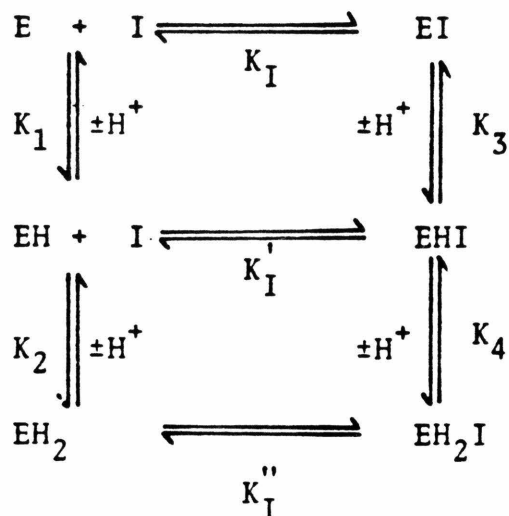
Figure 4. Structure of the enzyme/aldehyde adduct and catalytic triad proposed by Hunkapiller et al.(1975). The high pH structure (upper diagram) consists of a tightly hydrogen bonded array of neutral Asp - neutral His - hemiacetal oxyanion, in accord with their assignments of the  $pK_a$  values of the residues in the free enzyme. The enzyme/aldehyde complex is supposed to mimic the tetrahedral transition state to a high degree of accuracy. Addition of two protons to this system in a cooperative manner results in disruption of this precise array (lower diagram).



alaninal, and N-acetyl-L-alanyl-L-prolyl-glycinal with  $\alpha$ -lytic protease. We also re-examined the  $^{13}\text{C}$  NMR titration behavior of these enzyme/aldehyde complexes, using improved NMR instrumentation.

## THEORY

The results of Hunkapiller et al. (1975) suggest that the pH behavior of the enzyme/aldehyde interaction can be described by the following set of equilibria:



In this formulation, E represents free enzyme (in its high pH, catalytically active form); I, free inhibitor; EI, enzyme/inhibitor complex; EH and  $EH_2$ , free enzyme to which one and two protons have been added to catalytically important residues, respectively; EHI and  $EH_2I$ , enzyme/inhibitor complex to which one and two protons have been added to catalytically important structures, respectively.  $K_1$ ,  $K_2$ ,  $K_3$ , and  $K_4$  are acid dissociation constants;  $K_I$ ,  $K_I'$ , and  $K_I''$  are dissociation constants of the enzyme/inhibitor complexes. Hence, we can define

$$\begin{aligned}
 K_I^{\text{obs}} &= \frac{(\text{all forms of E})(\text{all forms of I})}{(\text{all forms of EI})} \\
 &= \frac{\{(E) + (EH) + (EH_2)\}(I)}{\{(EI) + (EHI) + (EH_2I)\}}
 \end{aligned}$$

where  $K_I^{\text{obs}}$  is the observed value of the inhibition constant at a given pH.

Therefore,

$$\begin{aligned}
 K_I^{\text{obs}} &= \frac{(E)\{1 + ((H^+)/K_1) + ((H^+)^2/K_1K_2)\}(I)}{(EI)\{1 + ((H^+)/K_3) + ((H^+)^2/K_3K_4)\}} \\
 &= K_I \frac{\{1 + ((H^+)/K_1) + ((H^+)^2/K_1K_2)\}}{\{1 + ((H^+)/K_3) + ((H^+)^2/K_3K_4)\}} . \quad (1)
 \end{aligned}$$

If  $K_1 = K_3$  and  $K_2 = K_4$  (that is, the binding of the inhibitor does not perturb the ionizations of the free enzyme),  $K_I^{\text{obs}}$  will appear to be independent of pH. Otherwise,  $K_I^{\text{obs}}$  will show a dependence on pH.

## EXPERIMENTAL

Materials.

All peptides were synthesized by standard procedures known to reduce racemization. All solvents were reagent grade and were used as received unless otherwise indicated. Thin layer chromatography (TLC) was performed on silica gel-coated glass plates obtained from Merck. Proton NMR spectra were recorded on either a Varian EM-390 or XL-200 spectrometer. Proton chemical shifts are reported relative to internal tetramethylsilane (TMS) or sodium 2,2-dimethyl-2-silapentane-5-sulfonate (DSS). Infrared spectra were taken on a Beckman IR-4240 spectrophotometer. All melting points are uncorrected. All reported yields are isolated quantities.

L-Proline methyl ester. L-Proline (25.00 g, 0.217 mole, purchased from Aldrich) was suspended in 250 ml of absolute methanol and the mixture was magnetically stirred in an ice bath. Thionyl chloride (28.40 g, 0.239 mole, redistilled prior to use, purchased from Aldrich) was then carefully added dropwise to the suspension over thirty minutes. During this time, all solid material dissolved. The solution was then warmed to room temperature and stirred for one hour. The solvent was then evaporated in vacuo to yield a clear resinous material which was dried overnight in vacuo over sodium hydroxide pellets to give the ester hydrochloride.

The free base of the ester was liberated by shaking the above material with 500 ml of cold 50% (w/v) aqueous  $K_2CO_3$ . The ester separated as a pale yellow liquid (some KCl precip-

itated in the aqueous phase) and was extracted into 200 ml of diethyl ether. The aqueous phase was extracted twice more with 100 ml portions of ether; the ether extracts were then combined and dried over anhydrous sodium sulfate. The ether was removed in vacuo at 25-30°C, and the resulting liquid was distilled in vacuo at 0.25 torr. The yield was 21.85 g (78%) of a clear liquid that was stored dessicated at 4°C. The ester is easily hydrolyzed and should be used as soon as possible. TLC (9:1 chloroform/methanol): one spot (iodine stained),  $R_f$  0.54, ninhydrin positive. 90 MHz  $^1\text{H}$  NMR ( $\text{CDCl}_3$ , TMS): multiplets, 1.8 and 3.0 ppm, prolyl  $-\text{CH}_2$  and  $\alpha\text{-CH}$ ; singlet, 2.3 ppm, 1 H,  $-\text{NH}$ ; singlet, 3.7 ppm, 3 H, ester  $-\text{CH}_3$ .

N-Acetyl-L-alanyl-L-proline (Ac-ala-pro). N-Acetyl-L-alanine (20.00 g, 0.153 mole, purchased from Sigma or Bachem) and L-proline methyl ester (19.74 g, 0.153 mole) were suspended in 500 ml of chloroform, and the mixture was magnetically stirred in an ice bath. Dicyclohexylcarbodiimide (DCC) (34.61 g, 0.168 mole, purchased from Aldrich or Sigma) was slowly added to the cold solution, and the mixture was stirred at 4°C overnight. The precipitated urea was filtered from the solution and was washed with a little cold chloroform. The combined filtrates were evaporated in vacuo and the resulting clear oil was dried in vacuo overnight. Occasionally the dipeptide ester would solidify during this time.

The ester was saponified by dissolving the above material in 500 ml of absolute ethanol and 50 ml of 6 N aqueous NaOH, and stirring the mixture 2-3 hours at room temperature. The solution was titrated to pH 1 with 6 N aqueous HCl (some

solid NaCl separated) and evaporated to dryness in vacuo. The residual material was extracted with 500 ml of warm chloroform; the chloroform solution was filtered, dried over anhydrous sodium sulfate, and evaporated to dryness in vacuo. The resulting gummy residue was crystallized from hot chloroform/*n*-hexane, and recrystallized from 95% acetone-5% water/diethyl ether in the cold. The yield was 22.65 g (66%) of a white crystalline solid, mp 173-175°C (lit. 173-175°C). 200 MHz <sup>1</sup>H NMR (D<sub>2</sub>O, DSS): doublet, 1.3 ppm, 3 H, J = 8 Hz, alanyl α-CH<sub>3</sub>; singlet, 2.0 ppm, 3 H, acetyl -CH<sub>3</sub>; multiplet, 2.0 ppm, prolyl -CH<sub>2</sub>; multiplet, 3.7 ppm, prolyl -CH<sub>2</sub>; multiplet, 4.4 ppm, alanyl α-CH; multiplet, 4.5 ppm, prolyl α-CH. The <sup>1</sup>H NMR spectrum also indicated 5-8% racemization of the N-terminal alanine residue. TLC (4:1:1 *n*-butanol/acetic acid/water): one spot (iodine stained), R<sub>f</sub> 0.44.

N-Acetyl-L-alanyl-L-prolyl-L-alaninol (Ac-ala-pro-L-ala-CH<sub>2</sub>OH).

Ac-ala-pro (2.90 g, 0.0127 mole) and triethylamine (1.28 g, 0.0127 mole, distilled from *p*-toluenesulfonyl chloride, redistilled from KOH pellets, purchased from Eastman) were dissolved in 70 ml of acetonitrile (distilled from P<sub>2</sub>O<sub>5</sub>, purchased from Eastman). The solution was cooled to -15°C in an ice/methanol bath, and isobutylchloroformate (1.74 g, 0.0127 mole, purchased from Sigma) was added. The solution was stirred an additional ten minutes and then a cold solution of L-alaninol (L-2-amino-1-propanol, 1.90 g, 0.253 mole, purchased from Aldrich) in 10 ml of acetonitrile was added. The solution was then warmed to room temperature and stirred

for five hours. The solvent was then removed under reduced pressure and the residue was dissolved in 50 ml of water. This solution was treated with excess Rexyn I-300 indicating mixed-bed ion-exchange resin (purchased from Fisher) for one hour, and the resin was removed by filtration. The aqueous solution was evaporated in vacuo to give a clear, glassy material, which was crystallized twice from ethyl acetate. The yield was 2.82 g (78%) of a white crystalline solid, mp. 175-176°C (lit. 174-176°C). 200 MHz <sup>1</sup>H NMR (D<sub>2</sub>O, DSS): doublet, 1.1 ppm, 3 H, J = 8 Hz, C-terminal alanyl α-CH<sub>3</sub>; doublet, 1.3 ppm, 3 H, J = 8 Hz, N-terminal alanyl α-CH<sub>3</sub>; singlet, 2.0 ppm, 3 H, acetyl -CH<sub>3</sub>; multiplets, 2.0, 2.2, 3.7 ppm, prolyl -CH<sub>2</sub>; doublet, 3.5 ppm, 2 H, J = 6 Hz, alaninol -CH<sub>2</sub>; multiplet, 3.9 ppm, 1 H, C-terminal alanyl α-CH; triplet, 4.3 ppm, 1 H, prolyl α-CH; quartet, 4.5 ppm, 1 H, J = 8 Hz, N-terminal alanyl α-CH. TLC (9:1 chloroform/methanol): one spot (iodine stained), R<sub>f</sub> 0.20; (4:1:1 n-butanol/acetic acid/water): one spot (iodine stained), R<sub>f</sub> 0.39. N-Acetyl-L-alanyl-L-prolyl-D,L-alaninol (Ac-ala-pro-D,L-ala-CH<sub>2</sub>OH).

This mixture of peptides was synthesized in exactly the same way as Ac-ala-pro-L-ala-CH<sub>2</sub>OH. From 2.28 g of Ac-ala-pro and 1.50 g of D,L-alaninol (purchased from Aldrich), the yield was 1.13 g (40%) of white crystalline solid (ethyl acetate/n-hexane), mp. 125-135°C. 200 MHz <sup>1</sup>H NMR (D<sub>2</sub>O, DSS) was consistent with the desired product. TLC (4:1:1 n-butanol/acetic acid/water): one spot (iodine stained), R<sub>f</sub> 0.40.

N-Acetyl-L-alanyl-L-prolyl-D-alaninol (Ac-ala-pro-D-ala-CH<sub>2</sub>OH).

The D-amino alcohol precursor is not a commercially available

product, so the tripeptide alcohol was synthesized by reduction of the corresponding tripeptide methyl ester. The procedure is a modification of the procedure of Bailey (1955).

N-acetyl-L-alanyl-L-prolyl-D-alanine methyl ester (1.61 g, 5.14 mmole) was dissolved in 35 ml of anhydrous tetrahydrofuran (distilled from lithium aluminum hydride under dry nitrogen, stored under nitrogen over 4A molecular sieves). This solution was stirred under nitrogen at room temperature while 5.0 ml (1.75 equivalents) of a 1.8 M solution of lithium borohydride (recrystallized from anhydrous diethyl ether, purchased from Ventron) in the same solvent was added. A small amount of foaming was observed during the addition. The solution was stirred eighteen hours at room temperature, during which time a gelatinous precipitate had formed. A saturated solution of dry HCl in absolute methanol (about 5 ml) was added slowly to the stirred suspension to decompose the excess borohydride, and the mixture was stirred an additional hour. During this time the precipitate dissolved to give a clear solution. Further addition of a small amount of saturated methanolic HCl solution produced no further visible reaction, so 20 ml of water was added and the solution was titrated to pH 8 with 1 N aqueous LiOH. The solution was stirred for 15 minutes and then concentrated to about 15 ml under reduced pressure. Another 20 ml of water was added, and the solution was stirred with excess Rexyn I-300 resin until the resin was no longer neutralized by the solution. The solution was filtered, evaporated to dryness, and the resulting clear, glassy material was crystallized from ethyl

acetate/n-hexane. The yield was 1.35 g (90%) of a white crystalline solid. TLC and 90 MHz  $^1\text{H}$  NMR were both consistent with that for the alcohols synthesized by the previous procedure. N-Acetyl-L-alanyl-L-prolyl-D-alanine methyl ester (Ac-ala-pro-D-ala-OMe). The synthesis of this peptide ester was a modification of the procedure employed by Hunkapiller et al. (1976) for the corresponding L-isomer.

D-Alanine methyl ester hydrochloride was synthesized by the thionyl chloride procedure used to synthesize L-proline methyl ester. It was crystallized from absolute methanol/diethyl ether in the cold, and was then dried in vacuo over NaOH pellets.

Ac-ala-pro (4.56 g, 0.020 mole), D-alanine methyl ester hydrochloride (2.78 g, 0.020 mole), and triethylamine (2.02 g, 0.020 mole, distilled from p-toluenesulfonyl chloride, redistilled from KOH pellets) were suspended in 100 ml of chloroform, and the suspension was stirred at  $0^\circ\text{C}$  in an ice bath. DCC (4.53 g, 0.022 mole) was added, and the solution was stirred overnight at  $4^\circ\text{C}$ . The mixture was filtered, and the solvent was removed under reduced pressure. The residue was dissolved in absolute methanol, and excess Rexyn I-300 resin (which had been previously freed of water by washing with a large volume of absolute methanol) was added to the solution. The mixture was shaken several hours (shaking is important, since magnetic stirring of the resin in methanol fractures the beads and releases colored material into the solution), filtered from the resin, and the methanol evaporated. The tripeptide ester

was crystallized from chloroform/ether at  $-20^{\circ}\text{C}$ ; the yield was 3.20 g (51%) of a white crystalline solid, mp.  $129-131^{\circ}\text{C}$ .

200 MHz  $^1\text{H}$  NMR ( $\text{D}_2\text{O}$ , DSS): doublet, 1.3 ppm, 3 H,  $J = 8$  Hz, C-terminal alanyl  $\alpha$ - $\text{CH}_3$ ; doublet, 1.4 ppm, 3 H,  $J = 8$  Hz, N-terminal alanyl  $\alpha$ - $\text{CH}_3$ ; singlet, 2.0 ppm, 3 H, acetyl  $-\text{CH}_3$ ; multiplets, 2.0, 2.2, 3.7 ppm, prolyl  $-\text{CH}_2$  and C-terminal alanyl  $\alpha$ -CH; multiplet, 4.4 ppm, 1 H, prolyl  $\alpha$ -CH; quartet, 4.5 ppm, 1 H,  $J = 7$  Hz, N-terminal alanyl  $\alpha$ -CH; singlet, 3.7 ppm, 3 H, ester  $-\text{OCH}_3$ . TLC (9:1 chloroform/methanol):

one spot (iodine stained),  $R_f$  0.33; (4:1:1 n-butanol/acetic acid/water): one spot (iodine stained),  $R_f$  0.48; (9:1 acetonitrile/water): one spot (iodine stained),  $R_f$  0.39.

t-Butyloxycarbonyl-L-alanine N-hydroxysuccinimide ester (Boc-

ala-OSu). t-Boc-L-alanine (25.00 g, 0.132 mole, purchased from Bachem) and N-hydroxysuccinimide (15.20 g, 0.132 mole, purchased from Sigma, recrystallized from ethyl acetate) were dissolved in tetrahydrofuran and the solution was cooled in an ice bath. DCC (27.80 g, 0.135 mole) was added slowly, and the solution was stirred overnight at  $4^{\circ}\text{C}$ . The mixture was filtered and the solid urea was washed with about 100 ml of ethyl acetate. The combined filtrates were evaporated to dryness and the residue was dissolved in 250 ml of warm toluene. On cooling in ice crystals formed; crystallization was completed by adding ligroin (bp.  $60-70^{\circ}\text{C}$ ). The fluffy white crystals were filtered and dried in vacuo. The yield was 37.21 g (98%), mp.  $159-160^{\circ}\text{C}$ . TLC (4:1:1 n-butanol/acetic acid/water): one spot (iodine stained),  $R_f$  0.51.

t-Butyloxycarbonyl-L-alanine-L-proline (Boc-ala-pro). L-Proline (14.00 g, 0.122 mole) was suspended in 200 ml of dimethylformamide and triethylamine (12.32 g, 0.122 mole) was added. This mixture was stirred for two hours at room temperature, and then Boc-ala-OSu (35.00 g, 0.122 mole) was added. The suspension was stirred 48 hours at room temperature, during which time all of the solid material had dissolved. The solvent was then removed under reduced pressure (vacuum pump,  $T \leq 50^{\circ}\text{C}$ ). The resulting resinous material was then slowly and carefully dissolved in 50 ml of saturated aqueous  $\text{NaHCO}_3$ , and the solution was filtered. The filtrate was extracted once with 100 ml of ethyl acetate, and the aqueous layer was titrated to pH 1.2 with saturated aqueous  $\text{NaHSO}_4$ . The precipitated solid is filtered and dried overnight in vacuo. It was recrystallized from ethyl acetate/n-hexane. The yield was 33.20 g (95%) of a white crystalline solid, mp.  $153\text{-}156^{\circ}\text{C}$  (lit.  $156\text{-}158^{\circ}\text{C}$ ). 200 MHz  $^1\text{H}$  NMR ( $\text{CDCl}_3$ , TMS): doublet, 1.3 ppm, 3 H,  $J = 8$  Hz, alanyl  $\alpha\text{-CH}_3$ ; singlet, 1.4 ppm, 9 H, Boc  $\text{-CH}_3$ ; multiplets, 2.1, 3.7 ppm, 6 H, prolyl  $\text{-CH}_2$ ; quintet, 4.5 ppm, 1 H,  $J = 8$  Hz, alanyl  $\alpha\text{-CH}$ ; triplet, 4.6 ppm, 1 H,  $J = 7$  Hz, prolyl  $\alpha\text{-CH}$ ; doublet, 5.4 ppm, 1 H,  $J = 9$  Hz, amide  $\text{-NH}$ . TLC (4:1:1 n-butanol/acetic acid/water): one spot (iodine stained),  $R_f$  0.69.

L-Alanyl-L-prolyl-L-alanine methyl ester hydrochloride (Ala-pro-ala-OMe $\cdot$ HCl). L-Alanine methyl ester hydrochloride (7.00 g, 0.0504 mole, purchased from Bachem) was dissolved in 500 ml of chloroform, and di-isopropylethylamine (6.50 g, 0.0504 mole, purchased from Aldrich, distilled from p-toluenesulfonyl chloride,

redistilled from KOH pellets) was added. When all of the solid material had dissolved, Boc-ala-pro (14.40 g, 0.0504 mole) was added, followed by DCC (10.40 g, 0.0505 mole). The solution was stirred overnight at room temperature. The solid was removed by filtration, and the chloroform solution was extracted with several 100 ml portions of water, and finally with one 100 ml volume of saturated aqueous NaCl. It was then dried with anhydrous sodium sulfate, filtered, and evaporated to dryness.

The residue was then dissolved in 200 ml of ethyl acetate, and dry HCl gas was bubbled through the solution for 15 minutes. The solution was stirred overnight at room temperature; a white solid precipitated during this time. Anhydrous ether (200 ml) was then added, and the white solid was filtered and dried in vacuo over NaOH pellets overnight. The yield was 14.60 g (94%) of a white, hygroscopic powder, not recrystallized. TLC (4:1:1 n-butanol/acetic acid/water): one spot (iodine stained),  $R_f$  0.25, ninhydrin positive.

N-Acetyl-L-alanyl-L-prolyl-L-alanine methyl ester (Ac-ala-pro-L-ala-OMe). Ala-pro-ala-OMe·HCl (13.40 g, 0.0436 mole), di-isopropylethylamine (6.00 g, 0.0465 mole, distilled from p-toluene-sulfonyl chloride, redistilled from KOH pellets), and pyridine (1.0 ml, distilled from KOH pellets) were dissolved in 150 ml of chloroform and the solution was cooled in an ice bath. Redistilled acetic anhydride (20 ml) was added, and the solution was stirred overnight at room temperature. Absolute methanol (20 ml) was then added to destroy excess anhydride, and the

solution was stirred one hour. The solvent was removed under reduced pressure, and the residue was dissolved in absolute methanol and treated (shaken) with excess methanol-washed Rexyn I-300 resin. The resin was filtered, washed well with methanol, and the combined methanol solutions were evaporated under reduced pressure. The residue was crystallized for 2 days at  $-20^{\circ}\text{C}$  from ethyl acetate/n-hexane. The yield was 10.00 g (73%) of a white crystalline solid, mp.  $153-155^{\circ}\text{C}$  (lit.  $156-157^{\circ}\text{C}$ ). 200 MHz  $^1\text{H}$  NMR ( $\text{D}_2\text{O}$ , DSS): doublet, 1.3 ppm, 3 H,  $J = 8$  Hz, C-terminal alanyl  $\alpha\text{-CH}_3$ ; doublet, 1.4 ppm, 3 H,  $J = 8$  Hz, N-terminal alanyl  $\alpha\text{-CH}_3$ ; singlet, 2.0 ppm, 3 H, acetyl  $\text{-CH}_3$ ; multiplets, 1.9, 2.3, 3.6 ppm, prolyl  $\text{-CH}_2$ ; singlet, 3.7 ppm, 3 H, ester  $\text{-OCH}_3$ ; multiplet, 4.4 ppm, 2 H, C-terminal alanyl and prolyl  $\alpha\text{-CH}$ ; quartet, 4.5 ppm, 1 H,  $J = 7$  Hz, N-terminal alanyl  $\alpha\text{-CH}$ . TLC (9:1 chloroform/methanol): one spot (iodine stained),  $R_f$  0.33; (4:1:1 n-butanol/acetic acid/water): one spot (iodine stained),  $R_f$  0.48; (9:1 acetonitrile/water): one spot (iodine stained),  $R_f$  0.38.

N-Acetyl-L-alanyl-L-prolyl-L-alanine benzyl ester (Ac-ala-pro-ala-OBzl). This tripeptide ester was synthesized using the same reaction sequence as that for Ac-ala-pro-L-ala-OMe. L-Alanine benzyl ester p-toluensulfonate (purchased from Bachem) was converted to the hydrochloride on a 25 cm x 2.5 cm column of Dowex 1X8 ( $\text{Cl}^-$  form) anion exchange resin using water as the eluting solvent. The hydrochloride was crystallized from ethanol/ether. It was coupled to Boc-ala-pro with DCC in chloroform in the presence of 1 equivalent of triethylamine.

The Boc protecting group was removed with dry HCl in ethyl acetate; the yield of tripeptide benzyl ester hydrochloride was 93%. This material was acetylated with acetic anhydride in chloroform; crystallized from ethyl acetate/n-hexane, the yield of Ac-ala-pro-ala-OBzl was 78% of a white crystalline solid, mp. 78-80°C. 200 MHz  $^1\text{H}$  NMR ( $\text{CDCl}_3$ , TMS): overlapping pair of doublets, 1.35 ppm, 6 H,  $J = 8$  Hz, alanyl  $\alpha$ - $\text{CH}_3$ ; singlet, 2.0 ppm, 3 H, acetyl  $-\text{CH}_3$ ; multiplets, 2.0, 2.3, 3.6 ppm, prolyl  $-\text{CH}_2$ ; multiplet, 4.6 ppm, 2 H, prolyl and C-terminal alanyl  $\alpha$ -CH; quintet, 4.7 ppm, 1 H,  $J = 7$  Hz, N-terminal alanyl  $\alpha$ -CH; singlet, 5.2 ppm, 2 H, ester  $-\text{OCH}_2$ ; doublet, 6.5 ppm, 1 H,  $J = 9$  Hz, amide  $-\text{NH}$ ; doublet, 7.1 ppm, 1 H,  $J = 9$  Hz, amide  $-\text{NH}$ ; singlet, 7.3 ppm, 5 H, phenyl ring  $-\text{CH}$ .

N-Acetyl-L-alanyl-L-prolyl-L-alanine p-nitroanilide (Ac-ala-pro-ala-PNA). Ac-ala-pro (4.60 g, 0.0202 mole), triethylamine (2.04 g, 0.0202 mole, distilled from p-toluenesulfonyl chloride, redistilled from KOH pellets), and L-alanine p-nitroanilide hydrochloride (5.00 g, 0.0202 mole, purchased from Sigma) were dissolved in 500 ml of chloroform and the solution was cooled in an ice bath. DCC (4.60 g, 0.0223 mole) was added, and the solution was stirred at 4°C for two days. The mixture was then filtered, and the chloroform was removed under reduced pressure. The residue was dissolved in 300 ml of 50% aqueous methanol with gentle warming. The cooled yellow solution was shaken with excess Rexyn I-300 resin for one hour; the resin was then removed by filtration and the solvent was removed gently ( $T \leq 35^\circ\text{C}$ ) in vacuo and the pale yellow residue was

crystallized from ethyl acetate/n-hexane. It was recrystallized by dissolving the solid in hot ethyl acetate, treating this hot solution with decolorizing carbon (Norit), filtering the hot suspension through a Celite pad, and adding n-hexane. The yield was 5.50 g (66%) of an off-white crystalline solid, mp. 196-197°C (lit. 198-199°C). 200 MHz  $^1\text{H}$  NMR ( $\text{CDCl}_3$ , TMS): doublet, 1.4 ppm, 3 H,  $J = 8$  Hz, C-terminal alanyl  $\alpha$ - $\text{CH}_3$ ; doublet, 1.5 ppm, 3 H,  $J = 8$  Hz, N-terminal alanyl  $\alpha$ - $\text{CH}_3$ ; singlet, 2.0 ppm, 3 H, acetyl - $\text{CH}_3$ ; multiplets, 2.1 and 3.7 ppm, prolyl - $\text{CH}_2$ ; multiplet, 4.6 ppm, 2 H, C-terminal alanyl and prolyl  $\alpha$ -CH; quintet, 4.7 ppm, 1 H,  $J = 7$  Hz, N-terminal alanyl  $\alpha$ -CH; doublet, 6.3 ppm, 1 H,  $J = 8$  Hz, amide -NH; doublet, 7.3 ppm, 1 H,  $J = 8$  Hz, amide -NH; doublet, 7.8 ppm, 2 H,  $J = 10$  Hz, phenyl ring -CH; doublet, 8.2 ppm, 2 H,  $J = 10$  Hz, phenyl ring -CH; singlet, 9.3 ppm, anilide -NH. TLC (4:1:1 n-butanol/acetic acid/water): one spot (iodine stain or UV light),  $R_f$  0.53; (9:1 acetonitrile/water): one spot (iodine stain or UV light),  $R_f$  0.51.

N-Acetyl-L-alanyl-L-prolyl-L-alanine anilide (Ac-ala-pro-ala-An).

t-Butyloxycarbonyl-L-alanine anilide (Boc-ala-An) was synthesized by the same procedure used to make Boc-ala-OSu. t-Butyloxycarbonyl-L-alanine and aniline (distilled from zinc dust just prior to use) were coupled using DCC; the yield was 85% of a white crystalline solid (ethyl acetate/n-hexane), mp. 155-156°C. TLC (acetone): one spot (UV light),  $R_f$  0.75; (4:1:1 n-butanol/acetic acid/water): one spot (UV light),  $R_f$  0.93; (9:1 chloroform/methanol): one spot (UV light),  $R_f$  0.82.

The protecting group was removed using dry HCl in ethyl acetate for one hour. On evaporation of the solvent, a gummy

residue was obtained. It was crystallized from methanol/ether. The yield was 86%. TLC (4:1:1 n-butanol/acetic acid/water): one spot (iodine stained),  $R_f$  0.56, ninhydrin positive. This material was coupled with Ac-ala-pro with DCC in chloroform containing one equivalent of triethylamine. On evaporation of the solvent, the residue was dissolved in 50% aqueous methanol and was shaken with excess Rexyn I-300 resin. Filtration and evaporation gave a clear resinous product, which was crystallized from ethyl acetate/n-hexane. The yield was 50% of a white crystalline solid, mp. 160-162°C. 200 MHz  $^1\text{H}$  NMR ( $\text{CDCl}_3$ , TMS): overlapping pair of doublets, 1.4 ppm, 6 H,  $J = 8$  Hz, alanyl  $\alpha$ - $\text{CH}_3$ ; singlet, 2.0 ppm, 3 H, acetyl  $-\text{CH}_3$ ; multiplets, 2.1, 3.7 ppm, prolyl  $-\text{CH}_2$ ; multiplet, 4.5 ppm, 2 H, C-terminal alanyl and prolyl  $\alpha$ -CH; quintet, 4.7 ppm, 1 H,  $J = 7$  Hz, N-terminal alanyl  $\alpha$ -CH; doublet, 6.5 ppm, 1 H,  $J = 7$  Hz, amide  $-\text{NH}$ ; doublet, 6.9 ppm, 1 H,  $J = 7$  Hz, amide  $-\text{NH}$ ; doublet, 7.3 ppm, 3 H,  $J = 10$  Hz, phenyl ring  $-\text{CH}$ ; doublet, 7.5 ppm, 2 H,  $J = 10$  Hz, phenyl ring  $-\text{CH}$ ; singlet, 8.7 ppm, 1 H, anilide  $-\text{NH}$ . TLC (4:1:1 n-butanol/acetic acid/water): one spot (iodine stained or UV light),  $R_f$  0.53.

N-Acetyl-L-alanyl-L-prolyl-L-alanyl amide (Ac-ala-pro-ala-NH<sub>2</sub>).

This peptide was synthesized by the DCC method used for Ac-ala-pro-ala-An starting with Ac-ala-pro and L-alanine amide hydrochloride (purchased from Bachem). The yield was 64% of a white crystalline solid, mp. 198-200°C (lit. 207-208°C). 200 MHz  $^1\text{H}$  NMR in both  $\text{D}_2\text{O}$  and  $\text{CDCl}_3$  were consistent with the desired product. TLC (4:1:1 n-butanol/acetic acid/water): one spot (iodine stained),  $R_f$  0.28.

N-Acetyl-L-alanyl-L-prolyl-L-alanine benzyl amide (Ac-ala-pro-ala-NHBz). This peptide was synthesized using the same procedure as that for Ac-ala-pro-ala-An, starting with Ac-ala-pro and Ala-NHBz·HCl. t-Butyloxycarbonyl-L-alanine benzylamide was synthesized from Boc-ala and benzylamine (distilled prior to use) using the DCC method of coupling. The yield was 85% (ethyl acetate/n-hexane), mp. 106-107°C. TLC (4:1:1 n-butanol/acetic acid/water): one spot (UV light),  $R_f$  0.89. L-Alanine benzyl amide hydrochloride was obtained by removal of the protecting group from Boc-ala-NHBz with dry HCl in ethyl acetate. The yield was 92%, mp. 143-144°C. TLC (4:1:1 n-butanol/acetic acid/water): one spot (UV light),  $R_f$  0.51. Ac-ala-pro-ala-NHBz was obtained from the DCC coupling of Ac-ala-pro and Ala-NHBz·HCl in chloroform and triethylamine in 68% yield. The 200 MHz  $^1\text{H}$  NMR in  $\text{CDCl}_3$  and TMS was consistent with the desired product.

N-Acetyl-L-alanyl-L-prolyl-L-alanine hydrazide (Ac-ala-pro-ala-NHNH<sub>2</sub>). Ac-ala-pro-L-ala-OMe (2.00 g, 6.39 mmoles) was dissolved in 10 ml of absolute ethanol and 1.0 ml of hydrazine hydrate (purchased from MCB) was added. The solution was shaken 24 hours at room temperature and the solvent was removed under reduced pressure to give a white solid. This was recrystallized from ethyl acetate/ether to yield 1.80 g (99%) of a white crystalline solid, mp. 197-199°C. 200 MHz  $^1\text{H}$  NMR ( $\text{D}_2\text{O}$ , DSS) was consistent with the desired peptide hydrazide; no signal at 3.7 ppm corresponding to the starting ester could be observed. TLC (4:1:1 n-butanol/acetic acid/water):

one spot (iodine stained),  $R_f$  0.25, trinitrobenzenesulfonate positive.

N-Acetyl-L-alanyl-L-prolyl-glycinol (Ac-ala-pro-gly-CH<sub>2</sub>OH).

This peptide alcohol was synthesized by the mixed-anhydride method used to produce Ac-ala-pro-L-ala-CH<sub>2</sub>OH. The yield was 68% of a white crystalline solid (ethyl acetate), mp. 138-141°C, starting from Ac-ala-pro and glycinol (2-aminoethanol, redistilled prior to use). 200 MHz <sup>1</sup>H NMR (D<sub>2</sub>O, DSS): doublet, 1.4 ppm, 3 H, J = 8 Hz, alanyl α-CH<sub>3</sub>; singlet, 2.0 ppm, 3 H, acetyl -CH<sub>3</sub>; multiplets, 2.0, 2.3, 3.8 ppm, prolyl -CH<sub>2</sub>; triplet, 3.4 ppm, 2 H, J = 7 Hz, glycyll α-CH<sub>2</sub>; triplet, 3.7 ppm, 2 H, J = 7 Hz, alcohol -OCH<sub>2</sub>; triplet, 4.4 ppm, 1 H, J = 7 Hz, prolyl α-CH; quartet, 4.6 ppm, 1 H, J = 7 Hz, alanyl α-CH. TLC (4:1:1 n-butanol/acetic acid/water): one spot (iodine stained),  $R_f$  0.35; (9:1 acetonitrile/water): one spot (iodine stained),  $R_f$  0.20.

N-Acetyl-L-alanyl-L-prolyl-glycine ethyl ester (Ac-ala-pro-gly-OEt).

This tripeptide ester was synthesized by the DCC coupling method used for Ac-ala-pro-D-ala-OMe, starting with Ac-ala-pro and glycine ethyl ester hydrochloride (purchased from Sigma). The yield was 51% of a white crystalline solid (chloroform/n-hexane), mp. 135-137°C. 200 MHz <sup>1</sup>H NMR (D<sub>2</sub>O, DSS): triplet, 1.3 ppm, 3 H, J = 8 Hz, ester -CH<sub>3</sub>; doublet, 1.4 ppm, 3 H, J = 8 Hz, alanyl α-CH<sub>3</sub>; singlet, 2.0 ppm, acetyl -CH<sub>3</sub>; multiplets, 2.0, 2.3, 3.7 ppm, prolyl -CH<sub>2</sub>; pair of singlets, 4.0 ppm, 2 H, glycyll α-CH<sub>2</sub>; quartet, 4.2 ppm, 2 H, J = 8 Hz, ester -CH<sub>2</sub>; multiplet, 4.5 ppm, 1 H, prolyl α-CH; quartet, 4.6 ppm, 1 H, J = 8 Hz, alanyl α-CH.

TLC (4:1:1 n-butanol/acetic acid/water): one spot (iodine stained),  $R_f$  0.44; (9:1 acetonitrile/water): one spot (iodine stained),  $R_f$  0.36.

N-Acetyl-L-alanyl-L-prolyl-glycine p-nitroanilide (Ac-ala-pro-gly-PNA). This peptide was synthesized by the mixed anhydride method used to synthesize the peptide alcohols, starting with Ac-ala-pro and glycine p-nitroanilide (purchased from Bachem). The solvent used was dimethylformamide, for solubility reasons. The yield was 28% of an off-white crystalline solid (95% acetone-5% water/diethyl ether), mp. 237-239°C. TLC (4:1:1 n-butanol/acetic acid/water): one spot (UV light),  $R_f$  0.44.

Benzoyl-L-alanine methyl ester (Bz-ala-OMe). This compound was synthesized essentially according to the method of Whitaker (1970). It was crystallized from ether/n-hexane as long, water-white prisms, mp. 58.5-59.5°C (lit. 58-59°C). 200 MHz  $^1\text{H}$  NMR ( $\text{D}_6$ -acetone, TMS): doublet, 1.5 ppm, 3 H,  $J = 8$  Hz, alanyl  $\alpha$ - $\text{CH}_3$ ; singlet, 3.7 ppm, 3 H, ester  $-\text{CH}_3$ ; quintet, 4.7 ppm, 1 H,  $J = 8$  Hz, alanyl  $\alpha$ -CH; multiplets, 7.5, 7.9 ppm, 5 H, phenyl ring  $-\text{CH}$ .

N-Acetyl-L-alanyl-L-alanyl-L-alanine (Ac-ala-ala-ala). This peptide was purchased from Bachem and was used as received.

Synthesis of peptide aldehydes. The purity of the aldehydes need for this study is critical. Previous syntheses (Thompson, 1973; Hunkapiller et al., 1975) based on the dicyclohexylcarbodiimide/dimethyl sulfoxide procedure of Pfitzner and Moffatt (1963, 1965) produced low yields, and the purification of the peptide aldehydes from unreacted starting materials

and other reaction products proved difficult at best. Substantial racemization of the C-terminal alanine residue also occurred during the synthesis. For these reasons, a new synthetic method was desired.

Since the synthesis of the required peptide alcohols is facile and yields crystalline, highly pure products, new methods of oxidation were attempted. Oxidation of Ac-ala-pro-L-ala-CH<sub>2</sub>OH with chromium trioxide/pyridine complex in ethanol-free chloroform (Collins et al., 1968; Ratcliffe and Rodehorst, 1970) gave a reasonable yield (40-50% of peptide aldehyde); however, this method was unsuccessful when applied to Ac-ala-pro-gly-CH<sub>2</sub>OH. Furthermore, the aldehyde was severely contaminated with starting alcohol, which was difficult to separate from the product. Column chromatography on silica gel in chloroform/methanol (9:1, 4:1, and 1:1) resulted in substantial product loss on the column, even when the silica gel had been pretreated for an extended period of time with either acetaldehyde or propionaldehyde in an attempt to destroy the aldehyde reactivity of the silica gel. Oxalyl chloride/dimethyl sulfoxide complex (Mancuso et al., 1978) also proved fruitless, as did barium manganate in dichloromethane (Firouzabadi and Ghaderi, 1978).

As standard oxidation methods seemed to be unsuccessful, a new procedure was required. The use of  $\alpha$ -amino acetals as intermediates in the synthesis of peptide aldehydes had been reported (Thompson, 1977). The dimethyl and diethyl acetals of glycinal ( $\alpha$ -amino acetaldehyde) are commercially

available. Hence, a reaction sequence for the production of alaninal acetals was needed.

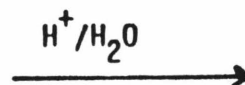
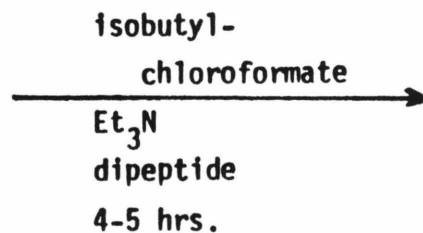
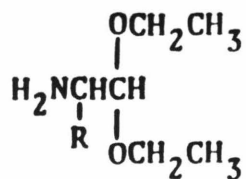
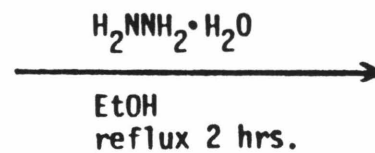
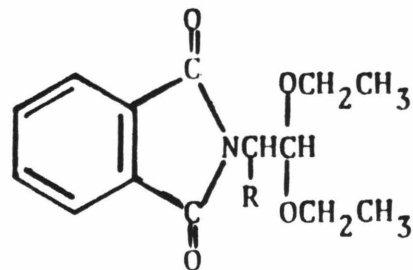
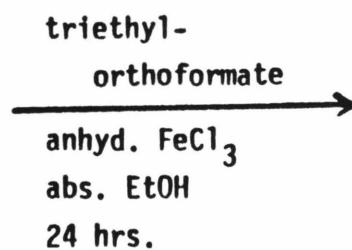
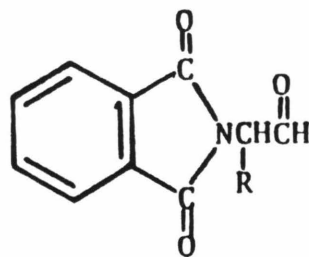
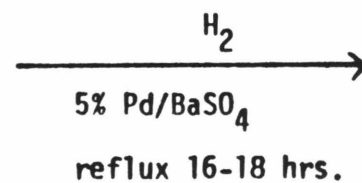
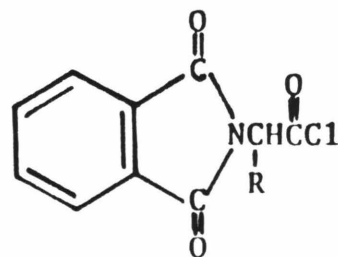
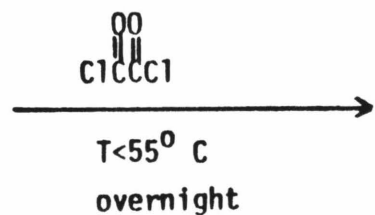
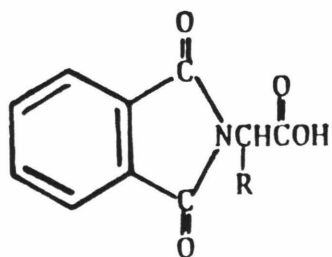
The synthesis of the diethyl acetal of alaninal (2-amino-propionaldehyde) is outlined in Figure 5. The products of each step are easily purified, and the yields are good. The key to the reaction sequence is the Rosenmund reduction (Rosenmund, 1918; Rosenmund and Zetsche, 1921) of phthalyl-alanyl chloride to phthalyl-alaninal.

5% palladium on barium sulfate. The catalyst for the reduction was synthesized by standard procedures (Mozingo, 1955), as a commercial product (Aldrich) was unsatisfactory.

Xylene was dried by distillation from sodium metal and was stored over 4A molecular sieves under dry nitrogen.

Phthalyl-L-alanine. L-Alanine (17.82 g, 0.20 mole), phthalic anhydride (29.62 g, 0.20 mole), and triethylamine (2.6 ml) were suspended in 300 ml of toluene and the suspension was refluxed five hours under a Dean-Stark water separator. The solvent was evaporated in vacuo and the gummy residue was triturated with water (400 ml) containing concentrated hydrochloric acid (5 ml). The product solidified and was chilled in an ice bath and filtered. The solid was crystallized from ethanol/water, air-dried, and recrystallized from chloroform/n-hexane. The yield was 38.48 g (88%) of a white crystalline solid, mp. 144.5-147°C (lit. 146°C). 90 MHz <sup>1</sup>H NMR (CDCl<sub>3</sub>, TMS): doublet, 1.7 ppm, 3 H, J = 7 Hz, alanyl α-CH<sub>3</sub>; quartet, 5.0 ppm, 1 H, J = 7 Hz, alanyl α-CH; multiplet, 7.8 ppm, 4 H, phenyl ring -CH; broad singlet, 11.0 ppm, 1 H, acid -COOH. IR (CHCl<sub>3</sub>): 1790 cm<sup>-1</sup> (acid C=O), 1725 cm<sup>-1</sup>

Figure 5. Synthetic scheme used for the production of  $\alpha$ -amino aldehyde acetals and peptide aldehydes, beginning from the appropriate phthalyl-protected amino acids.



tripeptide aldehyde (hydrate)

(imide C=O). TLC (1:1 ethyl acetate/toluene): one spot (UV light),  $R_f$  0.31.

Phthalyl-L-alanyl chloride (Pht-ala-Cl). Phthalyl-L-alanine (21.92 g, 0.10 mole), toluene (200 ml), and oxalyl chloride (25 ml, purchased from Aldrich) were warmed to 55°C for three hours in the absence of moisture (CaSO<sub>4</sub> drying tube), then stirred at room temperature for 12 hours. After this time gas evolution had ceased, and the pale yellow solution was treated with decolorising charcoal (Norit) and filtered. The solvent was removed in vacuo (vacuum pump, 0.25 torr,  $T \leq 55^\circ\text{C}$ ) to give a pale yellow syrup, which was dried in vacuo over NaOH pellets. During this time the syrup solidified. The material was then crystallized from chloroform/ligroin (bp. 60-70°C) in a dry ice/acetone bath. The yield was 21.45 g (90%) of a white crystalline solid, mp. 50-52°C (lit. 48°C). 90 MHz <sup>1</sup>H NMR (CDCl<sub>3</sub>, TMS): doublet, 1.8 ppm, 3 H,  $J = 7$  Hz, alanyl  $\alpha$ -CH<sub>3</sub>; quartet, 5.2 ppm, 1 H,  $J = 7$  Hz, alanyl  $\alpha$ -CH; multiplet, 7.9 ppm, 4 H, phenyl ring -CH. No resonance corresponding to the carboxyl proton of the starting acid was observed. IR (CHCl<sub>3</sub>): 1790 cm<sup>-1</sup> (acid chloride C=O), 1725 cm<sup>-1</sup> (imide C=O). TLC (1:1 ethyl acetate/toluene): smear (UV light),  $R_f$  0.40. The material was stored dessicated.

Phthalyl-L-alaninal (Pht-ala-CHO). Pht-ala-Cl (29.30 g, 0.123 mole), (1,1,3,3)-tetramethyl-2-thiourea (12 mg, purchased from Aldrich), and 5% palladium on barium sulfate catalyst (6.0 g) were mixed under 250 ml of dry xylene in a one liter three-neck round-bottom flask fitted with a condenser, a

thermometer, and a gas inlet tube reaching almost to the bottom of the reaction flask. The system was purged with dry hydrogen for thirty minutes in a fume hood, and the suspension was stirred well magnetically. The mixture was then heated to reflux (135-140°C) for 16-18 hours while hydrogen was vigorously bubbled through the suspension. The gas effluent was bubbled into a concentrated NaOH solution to trap the hydrogen chloride produced by the reaction. The solution was then cooled, treated with decolorising charcoal (Norit), filtered, and the solvent was removed in vacuo (vacuum pump, 0.25 torr,  $T \leq 50^\circ\text{C}$ ). The resinous product was crystallized twice from benzene/ligroin (bp. 60-70°C). The yield was 22.12 g (88%) of an off-white crystalline solid, mp. 108-110°C. This material gave a crystalline 2,4-dinitrophenylhydrazone (mp. 205°C, dec.) and a crystalline semicarbazone (mp. 234-237°C). 90 MHz  $^1\text{H}$  NMR ( $\text{CDCl}_3$ , TMS): doublet, 1.7 ppm, 3 H,  $J = 7$  Hz, alanyl  $\alpha$ - $\text{CH}_3$ ; quartet, 4.8 ppm, 1 H,  $J = 7$  Hz, alanyl  $\alpha$ -CH; multiplet, 7.9 ppm, 4 H, phenyl ring -CH; singlet, 9.8 ppm, 1 H, aldehydic CHO. IR ( $\text{CHCl}_3$ ): 1777  $\text{cm}^{-1}$  (aldehyde C=O), 1720  $\text{cm}^{-1}$  (imide C=O). TLC (1:1 ethyl acetate/toluene): one spot (UV light),  $R_f$  0.74, 2,4-dinitrophenylhydrazine positive.

Phthalyl-L-alaninal diethyl acetal (Pht-ala-DEA). Pht-ala-CHO (25.00 g, 0.123 mole) was suspended in 200 ml of triethylorthoformate (purchased from Aldrich) and 50 ml of absolute ethanol. A warm solution of anhydrous iron(III) chloride in 100 ml of absolute ethanol was added, and the solution was stirred for 48 hours at room temperature. Diethyl ether

(300 ml) was then added, followed by 300 ml of 1 N aqueous NaOH. The suspension was stirred 30 minutes, filtered from ferric hydroxide, the layers separated, and the aqueous layer washed with a further 100 ml of ether. The combined ether extracts were dried over anhydrous sodium sulfate, filtered, and the ether removed in vacuo to give a clear oil, which solidified on prolonged drying in vacuo. The solid was recrystallized from n-hexane. The yield was 24.30 g (89%) of an off-white crystalline solid, mp. 53-55°C. 90 MHz <sup>1</sup>H NMR (CDCl<sub>3</sub>, TMS): two triplets, 1.0 and 1.2 ppm, 3 H each, J = 8 Hz, two non-equivalent acetal -CH<sub>3</sub>; doublet, 1.5 ppm, 3 H, J = 7 Hz, alanyl α-CH<sub>3</sub>; two overlapping quartets, 3.5 and 3.7 ppm, 4 H, J = 8 Hz, two non-equivalent acetal -CH<sub>2</sub>; quintet, 4.4 ppm, 1 H, J = 7 Hz, alanyl α-CH; doublet, 5.1 ppm, 1 H, J = 8 Hz, acetal -CH; multiplet, 7.8 ppm, 4 H, phenyl ring -CH. IR (CHCl<sub>3</sub>): 1715 cm<sup>-1</sup> (imide C=O). TLC (1:1 ethyl acetate/toluene): one spot (UV light), R<sub>f</sub> 0.89, 2,4-dinitrophenylhydrazine positive on heating to 105°C.

L-Alaninal diethyl acetal (Ala-DEA). Pht-ala-DEA (20.00 g, 0.072 mole) was suspended in 150 ml of absolute ethanol and hydrazine hydrate (4.00 g, 0.080 mole, 10% excess) was added. The mixture was refluxed gently for two hours, during which time the solution initially cleared, and then a flocculent white precipitate formed (phthalylhydrazide). The solution was cooled, filtered, and the yellowish filtrate was treated with decolorising charcoal (Norit) to little avail. The ethanol was distilled from the solution until the temperature of the

boiling vapors reached 80°C. The residue was then dissolved in 150 ml of diethyl ether and the ether solution was extracted twice with saturated aqueous NaCl. The ether layer was then dried over anhydrous sodium sulfate, filtered, and evaporated in vacuo at room temperature to give a pale yellow liquid. This liquid was then fractionally distilled under water aspirator pressure; the product boiled at 125-130°C. The yield was 6.90 g (65%) of a clear liquid; it was stored desiccated. 90 MHz <sup>1</sup>H NMR (CDCl<sub>3</sub>, TMS): doublet, 1.2 ppm, 3 H, J = 8 Hz, alanyl α-CH<sub>3</sub>; triplet, 1.3 ppm, 6 H, J = 8 Hz, acetal -CH<sub>3</sub>; broad singlet, 2.0 ppm, 2 H, amino -NH<sub>2</sub>; quintet, 3.1 ppm, 1 H, J = 8 Hz, alanyl α-CH; two quartets, 3.7 and 3.9 ppm, 4 H, J = 7 Hz, acetal -CH<sub>2</sub>; doublet, 4.3 ppm, 1 H, J = 7 Hz, acetal -CH. TLC (9:1 chloroform/methanol): one spot (iodine stained), R<sub>f</sub> 0.33, ninhydrin positive, 2,4-dinitrophenylhydrazine positive on heating at 105°C.

N-Acetyl-L-alanyl-L-prolyl-L-alaninal diethyl acetal (Ac-ala-pro-L-ala-DEA). Ac-ala-pro (4.65 g, 0.0204 mole) and triethylamine (2.06 g, 0.0204 mole) were dissolved in 100 ml of acetonitrile and the resulting solution was cooled to -15°C in a dry ice/carbon tetrachloride bath. Isobutylchloroformate (2.79 g, 0.0204 mole) was then added, and the solution was stirred for fifteen minutes. After this time, a solution of Ala-DEA (3.00 g, 0.0204 mole) in 10 ml of cold acetonitrile was added. The solution was allowed to warm to room temperature and was stirred for five hours. The solution was then evaporated to dryness in vacuo to produce a gummy residue.

This residue was dissolved in 100 ml of absolute ethanol and was shaken for several hours with excess Rexyn I-300 resin (previously exhaustively washed with absolute methanol), filtered, and evaporated to give a clear oil that solidified on standing overnight. The solid was recrystallized from ethyl acetate/n-hexane. The yield was 5.57 g (77%) of a white crystalline solid, mp. 128-131°C. 90 MHz  $^1\text{H}$  NMR ( $\text{CDCl}_3$ , TMS): two overlapping triplets, 1.2 ppm, 6 H, acetal  $-\text{CH}_3$ ; doublet, 1.3 ppm, 3 H,  $J = 8$  Hz, C-terminal alanyl  $\alpha$ - $\text{CH}_3$ ; doublet, 1.4 ppm, 3 H,  $J = 8$  Hz, N-terminal alanyl  $\alpha$ - $\text{CH}_3$ ; singlet, 2.0 ppm, 3 H, acetyl  $-\text{CH}_3$ , multiplets, 2.0, 2.2 ppm, prolyl  $-\text{CH}_2$ ; multiplet, 3.7 ppm, prolyl  $-\text{CH}_2$  and acetal  $-\text{CH}_2$ ; multiplet, 4.3 ppm, C-terminal alanyl and prolyl  $\alpha$ -CH; doublet, 4.5 ppm, 1 H,  $J = 8$  Hz, acetal  $-\text{CH}$ ; quintet, 4.7 ppm, 1 H,  $J = 8$  Hz, N-terminal alanyl  $\alpha$ -CH; multiple resonances, 6.7-6.8 ppm, 3 H, amide  $-\text{NH}$ . IR ( $\text{CHCl}_3$ ):  $1640\text{ cm}^{-1}$ ,  $1670\text{ cm}^{-1}$  (amide  $\text{C}=\text{O}$ ). TLC (9:1 chloroform/methanol): one spot (iodine stained),  $R_f$  0.38, 2,4-dinitrophenylhydrazine positive on heating to 105°C.

N-Acetyl-L-alanyl-L-prolyl-L-alaninal (Ac-ala-pro-L-ala-CHO).

Ac-ala-pro-ala-DEA (5.00 g, 0.0140 mole) was dissolved in 25 ml of water and Dowex 50WX8 resin ( $\text{H}^+$  form, 10.0 g dry weight, purchased from Bio-rad) was added. The mixture was shaken for 4-5 hours at room temperature until TLC showed the absence of any starting acetal. The solution was then filtered and the resin washed with a little water. The combined aqueous solutions were then lyophilized to give a glassy, hygroscopic solid.

This material was dissolved in a minimum amount of water and

chromatographed on a 100 cm x 2.5 cm column of Bio-gel P-2 (-400 mesh) (purchased from Bio-rad) using water as the eluting solvent. Fractions were assayed for absorbance at 245 nm; those containing 2,4-dinitrophenylhydrazine positive material were combined and lyophilized. Generally, the aldehyde was pure enough after this treatment. In the event that it was not, it could be further purified on silica gel in 95% acetone/5% water. This solvent system seemed to minimize the irreversible loss of aldehyde on the column. The glassy solid was triturated for two days under several changes of anhydrous diethyl ether to give a hygroscopic white powder which could not be crystallized. The yield was variable, depending on the chromatography necessary, from 60-85%. The material was stored dessicated over phosphorous pentoxide in the freezer. 200 MHz  $^1\text{H}$  NMR in  $\text{D}_2\text{O}$  showed that some racemization had taken place at the aldehyde terminus. 200 MHz  $^1\text{H}$  NMR ( $\text{D}_2\text{O}$ , DSS): pair of doublets, 1.1 ppm, 3 H,  $J = 8$  Hz, C-terminal alanyl  $\alpha\text{-CH}_3$  (partially racemized); doublet, 1.3 ppm, 3 H,  $J = 8$  Hz, N-terminal alanyl  $\alpha\text{-CH}_3$ ; singlet, 1.9 ppm, 3 H, acetyl  $\text{-CH}_3$ ; multiplets, 1.9, 2.2, 3.7 ppm, prolyl  $\text{-CH}_2$ ; multiplet, 3.8 ppm, C-terminal alanyl  $\alpha\text{-CH}$ ; triplet, 4.3 ppm, 1 H, prolyl  $\alpha\text{-CH}$ ; quartet, 4.5 ppm, 1 H, N-terminal alanyl  $\alpha\text{-CH}$ ; pair of doublets, 4.9 ppm,  $\sim 1$  H,  $J = 8$  Hz, hydrate  $\text{-CH(OD)}_2$ ; broad singlet, 9.4 ppm, small amount of aldehyde  $\text{-CHO}$ . TLC (9:1 chloroform/methanol): one spot (iodine stained),  $R_f$  0.24, 2,4-dinitrophenylhydrazine positive; (4:1:1 n-butanol/acetic acid/water): one spot (iodine stained),  $R_f$  0.49. IR ( $\text{CHCl}_3$ ):  $1730\text{ cm}^{-1}$  (weak, aldehyde  $\text{C=O}$ ),  $1670\text{ cm}^{-1}$ ,  $1630\text{ cm}^{-1}$  (amide  $\text{C=O}$ ).

N-Acetyl-L-alanyl-L-prolyl-D,L-alaninal (Ac-ala-pro-D,L-ala-CHO).

This peptide aldehyde was synthesized by the same procedure as Ac-ala-pro-L-ala-CHO, starting with D,L-alanine. Pht-D,L-ala: mp. 163-165°C (lit. 166°C). Pht-D,L-ala-Cl: mp. 70-71°C (lit. 73°C). Pht-D,L-ala-CHO: mp. 112-114°C. Pht-D,L-ala-DEA: mp. 57-59°C. D,L-alaninal DEA: bp. 133-137°C under water aspirator pressure. The tripeptide acetal was not isolated in this case; the crude acetal was subjected to hydrolysis immediately after Rexyn I-300 treatment.

N-Acetyl-L-alanyl-L-prolyl-glycinal (Ac-ala-pro-gly-CHO).

This peptide aldehyde was synthesized from Ac-ala-pro and  $\alpha$ -aminoacetaldehyde dimethyl acetal (purchased from Aldrich) by the mixed anhydride method used for the alaninals. The yield of tripeptide dimethyl acetal (Ac-ala-pro-gly-DMA) was 68% of a white solid (not crystallized, triturated under anhydrous ether), mp. 111-114°C. The 200 MHz  $^1\text{H}$  NMR in  $\text{D}_2\text{O}$  was consistent with this tripeptide sequence, with a singlet at 3.4 ppm, 6 H, acetal  $-\text{CH}_3$ , and a triplet at 4.6 ppm, acetal  $-\text{CH}$ . TLC (8:1 chloroform/methanol): one spot (iodine stained),  $R_f$  0.48, 2,4-dinitrophenylhydrazine positive on heating to 105°C; (4:1:1 n-butanol/acetic acid/water): one spot (iodine stained),  $R_f$  0.48.

The acetal was removed using Dowex 50WX8 ( $\text{H}^+$  form); the yield was 82% after Bio-gel P-2 chromatography and lyophilization. The glassy solid obtained after lyophilization was triturated under anhydrous diethyl ether to give a white hygroscopic powder, which was stored dessicated in the freezer. 200 MHz

$^1\text{H}$  NMR in  $\text{D}_2\text{O}$  was consistent with the desired tripeptide sequence, with a triplet at 5.1 ppm,  $\sim 1$  H, hydrate  $-\text{CH}(\text{OD})_2$ , and a small broad singlet, 9.5 ppm, aldehyde  $-\text{CHO}$ . No resonance corresponding to starting acetal was observed (at 3.4 ppm). TLC (8:1 chloroform/methanol): one spot (iodine stained),  $R_f$  0.30, 2,4-dinitrophenylhydrazine positive; (4:1:1 n-butanol/acetic acid/water): one spot (iodine stained),  $R_f$  0.36. IR ( $\text{CHCl}_3$ ):  $1720\text{ cm}^{-1}$  (weak, aldehyde  $\text{C}=\text{O}$ ),  $1630\text{ cm}^{-1}$ ,  $1660\text{ cm}^{-1}$  (amide  $\text{C}=\text{O}$ ).

Enzyme.  $\alpha$ -lytic protease (labelled and unlabelled) was isolated and purified as described in Chapters II and III of this thesis. Enzyme stock solutions for kinetics were made up in  $0.1\text{ M}$   $\text{KCl}$  and stored frozen until needed. All stock solutions were titrated with diethyl p-nitrophenylphosphate to determine the concentration of active enzyme as described in Chapter III. Enzyme solutions stored longer than one week were discarded.

#### Methods.

Kinetics. Inhibition kinetics were performed either in a Radiometer pH-Stat (consisting of a Radiometer model PHM26 pH meter fitted with a Radiometer MY-1 combination electrode, a Radiometer TTT11b autotitrator, a Radiometer ABU12 autoburette, a Radiometer model SBR3 Titrigraph recorder, and a mechanical overhead stirring device) using the substrates Bz-ala-OMe and Ac-ala-pro-L-ala-OMe, or in a Beckman Acta CIII UV-visible spectrophotometer using the substrate Ac-ala-pro-ala-PNA.

pH-Stat method. The following procedure is typical of that used in following the  $\alpha$ -lytic protease-catalyzed hydrolysis of

methyl esters. KCl solution (0.1 M, 5.0 ml) is pipetted into the reaction vessel, followed by 25  $\mu$ l of 1 M stock buffer solution (NaOH/acetic acid for pH 4-6, NaOH/NaH<sub>2</sub>PO<sub>4</sub> · 3 H<sub>2</sub>O for pH 6-8.5); the buffer concentration in the reaction mixture is 5 mM. The vessel is placed in the thermostating water jacket of the pH-Stat (set at 25.0  $\pm$  0.5°C), the stirrer started, and the pH is adjusted to the desired value using the automatic titrator. The proportional band of the titrator is set at zero. An aliquot of inhibitor stock solution (in water) or, in the case of zero inhibitor, 0.1 M KCl, is then added, and the solution is allowed to reach thermal equilibrium. An aliquot of the substrate stock solution in methanol (to prevent spontaneous hydrolysis) is added, and the spontaneous hydrolysis of the substrate is observed for an appropriate period of time. This rate is later subtracted from the observed enzymatic rate to give the true enzymatic rate. The maximum concentration of methanol in any experiment was 4% (v/v). The titrant is 0.0336 N KOH (standardized versus primary standard grade potassium hydrogen phthalate, phenolphthalein indicator). Finally, an aliquot of enzyme solution is added, and the enzymatic hydrolysis is recorded. All reactions are done under a moist nitrogen atmosphere.

Spectrophotometric method. Substrate stock solutions were made up in 0.1 M KCl, 2% (v/v) acetonitrile; in all cases,  $S_0 \leq 0.05 K_m$ . Substrate solution (2.60 ml) is pipetted into a 1.0 cm cuvette, followed by 100  $\mu$ l of 1 M buffer stock solution (NaOH/acetic acid for pH 4-6, NaOH/NaH<sub>2</sub>PO<sub>4</sub> · 3 H<sub>2</sub>O for pH 6-8.5). An aliquot

of inhibitor stock solution (or, in the case of zero inhibitor, 0.1 M KCl) is then added, plus enough 0.1 M KCl so that the total volume of added inhibitor plus KCl solution is 200  $\mu$ l. The cuvette is placed in the thermostatted cell compartment of the spectrophotometer (set at  $25.0 \pm 0.2^{\circ}\text{C}$ ) and is allowed to equilibrate thermally for several minutes. No significant non-enzymatic hydrolysis of the anilide substrate was observed over the pH range of the experiment. After an appropriate length of time, 100  $\mu$ l of enzyme stock solution is added, and the enzymatic reaction is observed at 410 nm. The pH of each solution was checked before and after each run; in no case was the difference greater than 0.05 pH unit. The same enzyme solution was used for the kinetic runs necessary to determine  $K_I$  for a given inhibitor at a given pH.

NMR samples. Samples were made by dissolving the desired amount of protein in 0.1 M KCl, 10% (v/v)  $^2\text{H}_2\text{O}$ . The desired amount of solid inhibitor was then added, and the pH of the solution adjusted to the desired value by the procedure outlined in Chapter II. Any insoluble material was removed by centrifugation at 10,000 rpm for 15 minutes at  $4^{\circ}\text{C}$ . The pH of each sample was checked prior to and following each spectral acquisition using a combination electrode that could be inserted into the 10 mm diameter NMR tube (Radiometer GK2322C electrode attached to a Radiometer PHM26 pH meter); in all cases, the initial and final pH readings were  $\pm 0.05$  pH unit.

It was assumed that the concentration of active protein in these samples was the same as its added mass. Furthermore,

it was assumed that little degradation of the protein occurred during a given experiment (especially in the presence of saturating concentrations of inhibitor), since activity assays were not reliable under these conditions. These two assumptions are in accord with the observations of Chapters II and III, however.

NMR spectra.  $^{13}\text{C}$  NMR spectra were taken on a Varian XL-200 spectrometer operating at 50.3 MHz for  $^{13}\text{C}$  using standard pulsed Fourier transform technology. All spectra were taken with the constant temperature device of the spectrometer operating at  $25.0 \pm 0.2^\circ\text{C}$ . Proton decoupled spectra were obtained with an appropriate delay between pulses (usually 0.10-0.25 sec) to minimize the dielectric heating of the sample. All samples were 2.5-3.0 ml in 10 mm diameter NMR tubes, containing 10% (v/v)  $^2\text{H}_2\text{O}$  to provide an internal field-frequency lock. Chemical shifts are reported relative to the arginine guanidinium carbon resonance which appears at 157.25 ppm downfield from the methyl carbons of external tetramethylsilane, and whose position did not change ( $\pm 0.05$  ppm) over the pH range investigated.

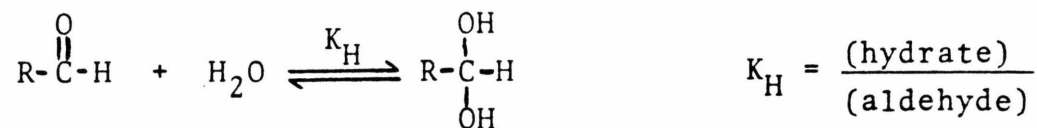
## RESULTS

Synthesis of peptide aldehydes. The method for the synthesis of peptide aldehydes reported in this chapter allows for the production of highly pure materials in reasonable overall yield. The sequence is characterized by generally mild reaction conditions and should be applicable to a variety of amino acetals, starting from the parent amino acids. Purification of the intermediate products is generally straightforward, since all are crystalline except the final amino acetal.

The synthesis, at least for alaninals, does have one unfortunate aspect: a moderate degree of racemization is seen at the aldehyde terminus. The origin of this racemization was not determined, but probably occurs during the acid-catalyzed hydrolysis of the tripeptide acetals. However, all other methods attempted to synthesize these aldehydes also resulted in about the same degree of racemization. The degree of racemization can be observed in the  $^1\text{H}$  NMR spectra of the aldehydes, as this racemization leads to a mixture of diastereomers, and is manifested by the presence of two resolved resonances (doublets) for both the C-terminal alanyl  $\alpha$ -methyl protons and the hydrate  $-\text{CH}(\text{OD})_2$ . A less well resolved pair of resonances for the aldehyde ( $-\text{CHO}$ ) protons can also be observed. The ratio of peak areas (integrals) for these resonances can be used to estimate the relative amounts of the L- and D-configurations of the aldehyde terminus. Representative 200 MHz  $^1\text{H}$  NMR spectra used to make this estimate are shown

in Figure 6. As can be seen, the aldehyde labelled Ac-ala-pro-L-ala-CHO is actually a 70:30 mixture of (L-L-L)<sup>1</sup> and (L-L-D)<sup>1</sup> diastereomers. Likewise, Ac-ala-pro-D,L-ala-CHO is a 50:50 mixture of (L-L-L) and (L-L-D) isomers as expected. Furthermore, aldehyde synthesized by the Pfitzner-Moffatt procedure (as described in Thompson, 1973, and Hunkapiller et al., 1975) starting from Ac-ala-pro-L-ala-CH<sub>2</sub>OH shows an isomeric composition of about 60:40 (L-L-L):(L-L-D). This aldehyde had identical <sup>1</sup>H NMR, TLC, and IR properties as the alaninals produced by the hydrolysis of the corresponding diethyl acetals.

Another important feature of the <sup>1</sup>H NMR spectra is the observation that, in aqueous solution, these peptide aldehydes prefer to exist as hydrates rather than free aldehydes, as shown in Scheme I.



#### Scheme I

The ratios of the integrals of the hydrate resonance (appearing near 5.1 ppm) to the aldehyde resonance (appearing near 9.4 ppm) can be used to estimate the values of  $K_{\text{H}}$  for the alaninals and the glycinal. These values are about 21 for the alaninals, and

<sup>1</sup> The nomenclature (L-L-L) signifies a peptide in which all three amino acid residues have the L-configuration; likewise, (L-L-D) represents a peptide in which the C-terminal residue has the D-configuration instead of L.

**Figure 6.** 200 MHz proton nmr of the tripeptide aldehydes used in this study. In each spectrum, the upper trace is the chemical shift region for the aldehyde hydrate proton ( $\text{CH}(\text{OH})_2$ ), and the lower trace is the region for the free aldehyde proton ( $\text{CHO}$ ). All spectra were taken in  $^2\text{H}_2\text{O}$  in 5 mm diameter nmr tubes, using a 3000 Hz sweep width, a 2.0 sec acquisition time, and a  $90^\circ$  pulse of 4.5  $\mu\text{sec}$ . 12000 FID points were zero-filled to a Fourier number of 16384 and transformed without line broadening. Each spectrum is the result of 256 scans on about 20 mg of product dissolved in 0.6 ml of  $^2\text{H}_2\text{O}$ .

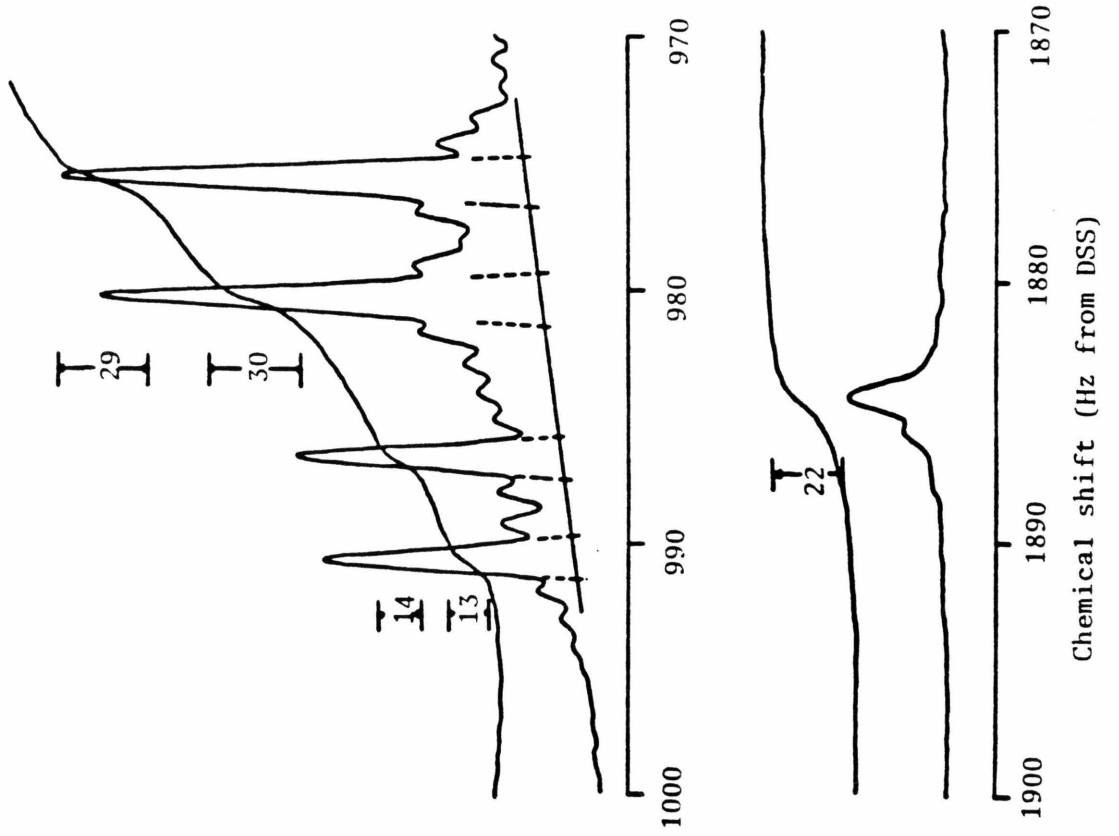
A) N-ac-ala-pro-L-alaCHO synthesized by the method depicted in Figure 5. The dotted lines are the result of the triangulation procedure used to estimate the integrals of the overlapping resonances. The upper trace has a vertical scaling (VS) of 200 and an integral scaling (IS) of 500. The lower trace has VS = 2000 and IS = 2500. The more downfield doublet in the upper trace is assigned to the (L,L,D) diastereomer of the mixture. The integrals shown were used to calculate the (L,L,L):(L,L,D) and (hydrate):(free aldehyde) ratios.

B) N-ac-ala-pro-L-alaCHO synthesized by the method of Thompson (1973) and Hunkapiller et al. (1975).

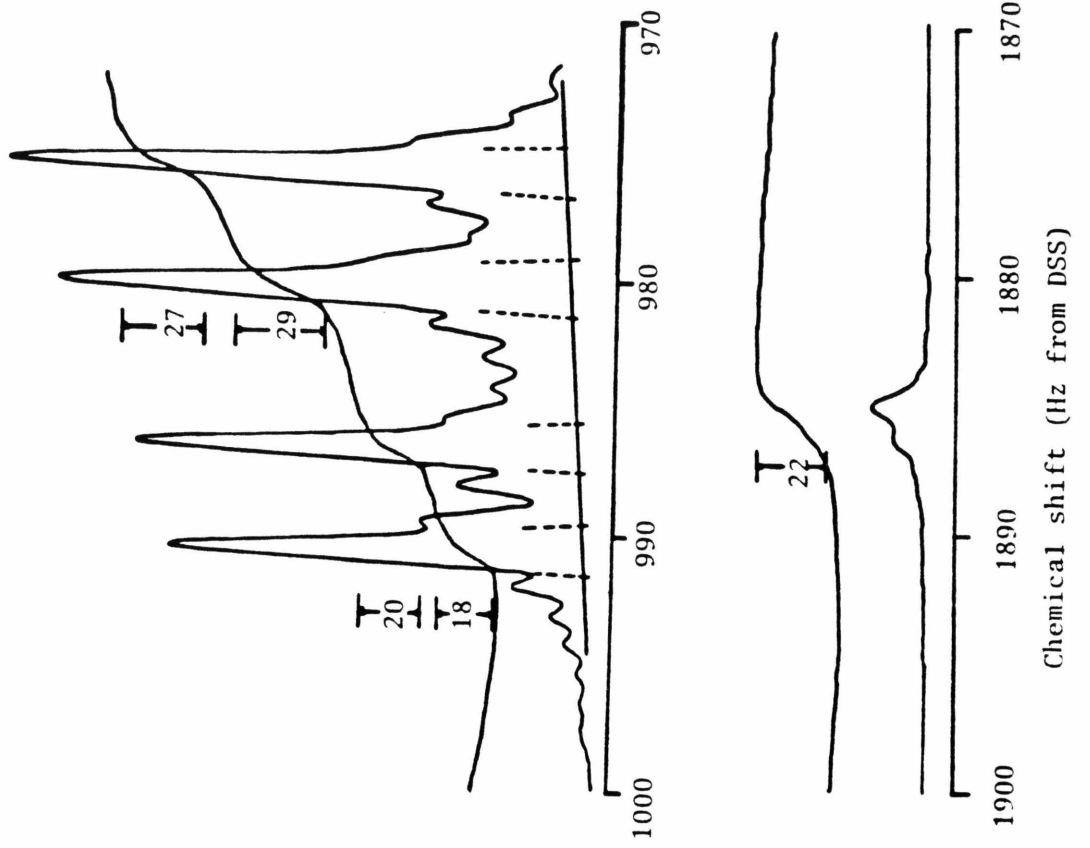
C) N-ac-ala-pro-D,L-alaCHO.

D) N-ac-ala-pro-glyCHO.

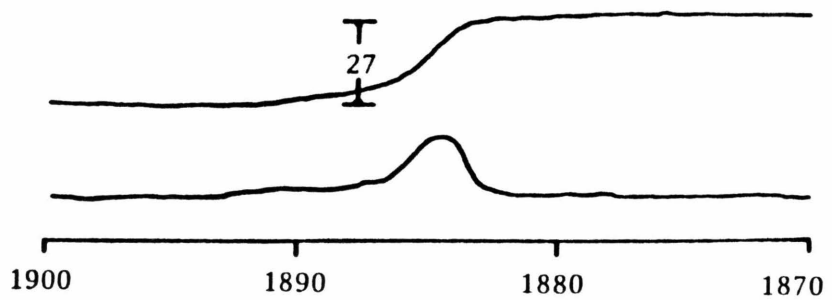
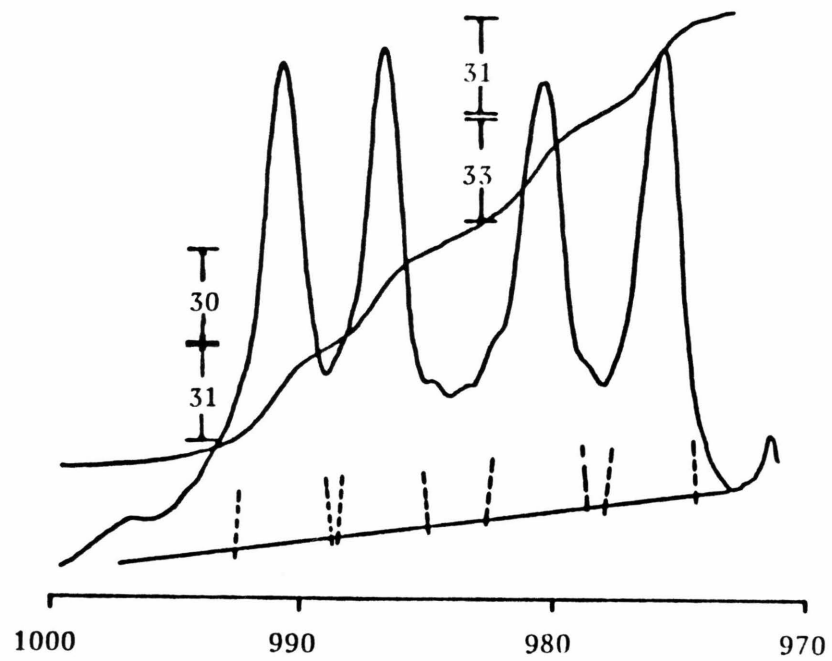
A)



B)

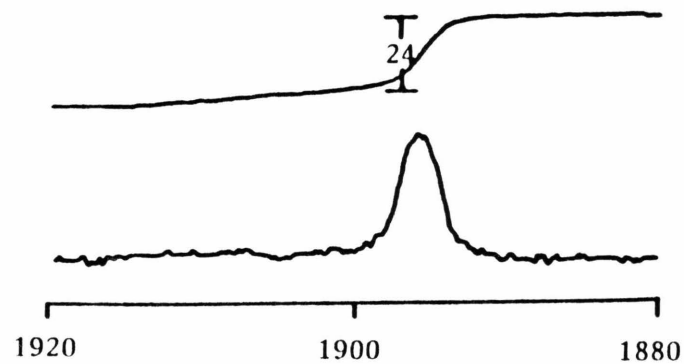
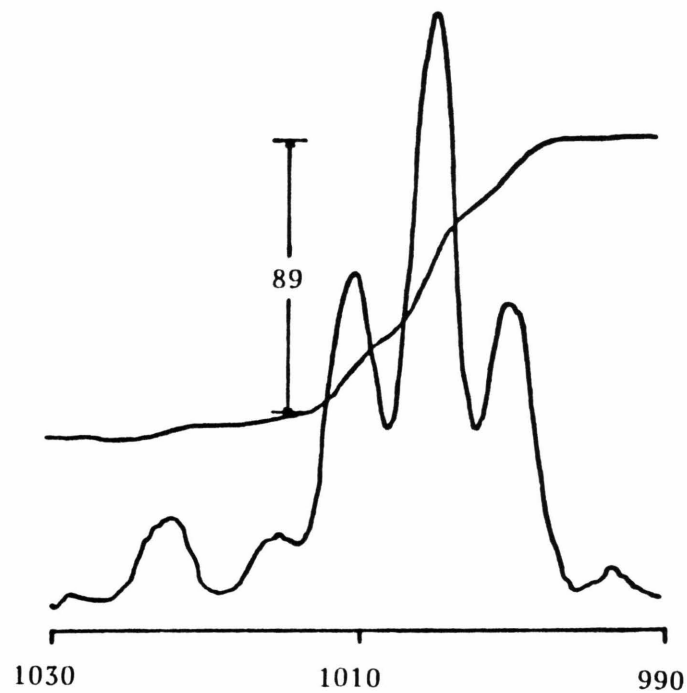


C)



Chemical shift (Hz from DSS)

D)



Chemical shift (Hz from DSS)

18 for the glycinal. Thus, the values of  $K_I^{\text{obs}}$  reported in this section have been adjusted to reflect this (assuming only the free aldehyde binds appreciably to the enzyme):

$$K_I^{\text{obs}} = K_I^{\text{app}} / (1 + K_H)$$

where  $K_I^{\text{app}}$  is the measured value of the inhibition constant (Thompson, 1973; Kennedy and Schultz, 1979). These values have been determined for the hydration of aldehydes in  $^2\text{H}_2\text{O}$ ; actual  $K_H$  values for  $^1\text{H}_2\text{O}$  may be slightly different, depending on the isotope effect. These values can be compared to values of  $K_H$  of about 11-12 for acyl-aminoacetaldehyde derivatives (Lewis and Wolfenden, 1977a). The high degree of hydration of these aldehydes also explains the weak IR absorption corresponding to the aldehydic carbonyl, if the materials isolated from aqueous solution are isolated primarily as the hydrates rather than the free aldehydes; this is probably the case.

One final note about these peptide aldehydes. On prolonged storage of the dry powders the products develop a distinctive odor and give a decidedly acidic aqueous solution on dissolution, even if these materials have been stored dessicated at low temperature ( $-20^\circ\text{C}$ ). These changes result in a concomitant partial loss of inhibitory activity; a sample stored over six months showed a three-fold increase in the value of  $K_I^{\text{app}}$  at pH 8, from  $3.2 \times 10^{-4} \text{ M}$  to  $1.0 \times 10^{-3} \text{ M}$ . Also, a new, slower moving spot appears in the TLC of these materials, as well as the original aldehyde spot. This new spot is 2,4-dinitrophenylhydrazine negative. Although no effort was made to

characterize this new product, the above evidence seems to support an auto-oxidation of the aldehyde to the corresponding acid on storage. Thus, the powdered aldehydes should be used soon after their synthesis; if prolonged storage is necessary, it should be as a frozen aqueous solution to retard deterioration.

Inhibition kinetics. Initial experiments with the aldehyde and alcohol inhibitors were performed in the pH-Stat, using the method of Dixon (1953). Inhibition was found to be purely competitive in all cases. Since the spectrophotometric method is simpler and more accurate, it was the primary method used. Substrate (Ac-ala-pro-ala-PNA) concentrations were always less than  $0.05 K_m$  ( $K_m = 15 \text{ mM}$ , Hunkapiller et al., 1976) so that good pseudo-first-order kinetics were observed. Pseudo-first-order rate constants ( $k_1 = V_{\max}/K_m^{\text{app}}$ ) were calculated from plots of  $\ln(A_\infty - A_t)$  versus time, where  $A_\infty$  is the absorbance at 410 nm at  $t = \infty$  and  $A_t$  is the absorbance at time  $t = t$  at this wavelength. In all kinetic runs,  $A_\infty$  represented better than 98% of the starting substrate converted to p-nitroaniline and tripeptide, as calculated using  $\Delta\epsilon_{410} = 8800$  (Hunkapiller et al., 1976; Chapter VI of this thesis).

Table I presents the inhibition constants for a variety of peptide inhibitors of  $\alpha$ -lytic protease, and  $K_m$  values for a few peptide substrates.  $K_m$  values were calculated from Lineweaver-Burk plots (Lineweaver and Burk, 1934) using at least five substrate concentrations from about  $0.2 K_m$  to about  $2 K_m$  whenever possible.  $K_I^{\text{app}}$  values were calculated from

$$K_I^{\text{app}} = \frac{I_0}{(k_0/k_i) - 1}$$

where  $I_0$  is the total concentration of added inhibitor; this amount was always such that  $I_0 \gg E_0$ , so that  $(I) \approx I_0$ ;  $k_0$  is the pseudo-first-order rate constant of the reaction in the absence of inhibitor; and  $k_i$  is the pseudo-first-order rate constant of the reaction in the presence of inhibitor of concentration  $I_0$  (see Appendix I). This equation was used for all values of  $\text{pH} > 5.0$ ; below this  $\text{pH}$ , the reactions were sufficiently slow to allow accurate calculation of zero-order initial rates, and  $v_0$  and  $v_i$  (the zero-order velocities in the absence and presence of inhibitor, respectively), were substituted for  $k_0$  and  $k_i$ . At least five inhibitor concentrations from about  $0.5 K_I^{\text{app}}$  to about  $5 K_I^{\text{app}}$  were used to determine  $K_I^{\text{app}}$ , except in cases where  $K_I^{\text{app}}$  values were too large to allow  $I_0 > K_I^{\text{app}}$  ( $K_I^{\text{app}} > 0.1 \text{ M}$ ).

The  $\text{pH}$  dependence of  $K_I^{\text{app}}$  for Ac-ala-pro-L-ala-CHO, Ac-ala-pro-D,L-ala-CHO, and Ac-ala-pro-gly-CHO is shown in Figure 7. From this figure and Table I, it is clear that the peptide aldehydes have a markedly greater affinity for  $\alpha$ -lytic protease than the other peptide derivatives tested (amides, esters, alcohols, and acetals), in agreement with the theory of transition state analogs.

An additional piece of information is available due to the technique used to measure  $K_I^{\text{app}}$ . Plots of  $k_{\text{cat}}/K_m$  and  $\log(k_{\text{cat}}/K_m)$  for Ac-ala-pro-ala-PNA with  $\alpha$ -lytic protease

Figure 7. Plots of  $K_I^{\text{app}}$  versus pH for three peptide aldehydes with  $\alpha$ -lytic protease.  $E_0$  ranged from 1.0 - 2.5  $\mu\text{M}$ ;  $S_0$  was always less than  $0.05 K_m$  ( $K_m = 15 \text{ mM}$ ). All kinetic runs were done in 0.1  $\text{M}$  KCl, 0.04  $\text{M}$  buffer (acetate or phosphate), at  $25.0 \pm 0.2^\circ\text{C}$ . The closed circles represent Ac-ala-pro-L-alaCHO, the open circles represent Ac-ala-pro-D,L-alaCHO, and the closed squares represent Ac-ala-pro-glyCHO. The curve for the Ac-ala-pro-L-alaCHO data was fit to equation (1) using  $\text{p}K_1 = 6.7$ ,  $\text{p}K_3 = 6.25$ ,  $\text{p}K_2 = 5.0$ ,  $\text{p}K_4 = 4.0$ , and  $K_I = 0.34 \text{ mM}$ . The curve for the Ac-ala-pro-glyCHO data was fit to equation (1) using  $\text{p}K_1 = 6.7$ ,  $\text{p}K_3 = 6.5$ ,  $\text{p}K_2 = 5.0$ ,  $\text{p}K_4 = 4.5$ , and  $K_I = 13.7 \text{ mM}$ . The error bars in all cases represent  $\pm$ (one standard deviation of the average of at least five values of  $K_I^{\text{app}}$ ). The values shown are uncorrected for the effect of hydration of the aldehydes in aqueous solution.

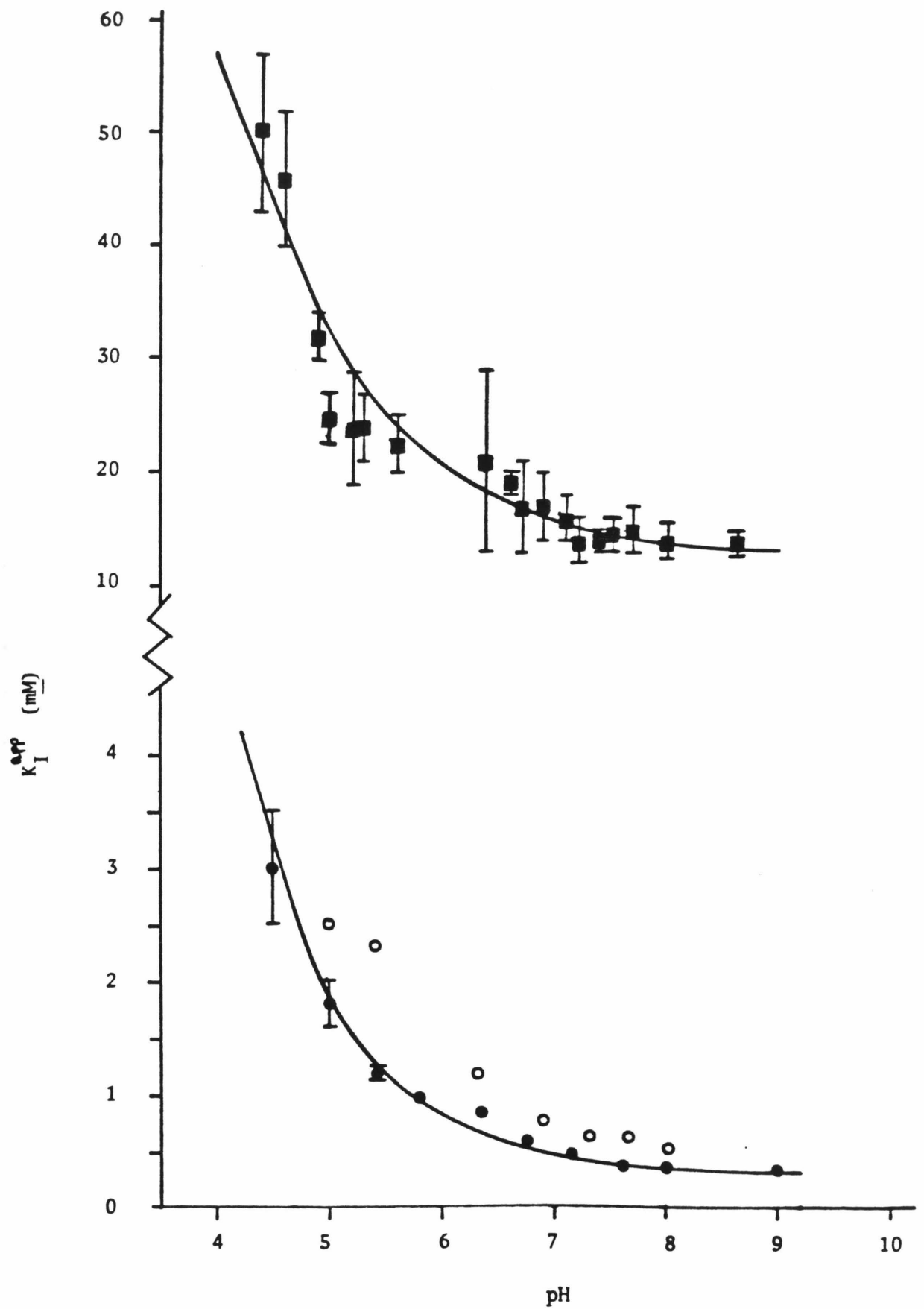


TABLE I. Kinetic constants for the interaction of  $\alpha$ -lytic protease with a variety of peptide derivatives.<sup>a,j,k</sup>

Peptide	pH	$K_I^{\text{obs}}$ (mM)	$K_m$ (mM)
Ac-ala-ala-ala	8.0	$67.7 \pm 6.8^e$	
	5.0	$127 \pm 8$	
Ac-ala-pro-alaPNA	8.0		$16.1 \pm 4.8^{b,f}$
	8.0		11
Ac-ala-pro-alaNHBz	8.0		$17 \pm 4^{b,f}$
Ac-ala-pro-alaNH <sub>2</sub>	8.0	$113 \pm 8^{c,d}$	
	5.0	$362 \pm 23^c$	
Ac-ala-pro-alaNHNH <sub>2</sub>	8.0	$105 \pm 15^c$	
	5.0	$113 \pm 5^c$	
Ac-ala-pro-alaAn	8.0		$12.2 \pm 3.0^{b,f}$
Ac-ala-pro-L-alaOMe	8.0		$1.1 \pm 0.1^{f,i}$
Ac-ala-pro-D-alaOMe	8.0	$21.2 \pm 4.9^f$	
	5.0	$55.5 \pm 8.3^f$	
Ac-ala-pro-L-alaCH <sub>2</sub> OH	8.0	$17.7 \pm 1.7$	
	5.0	$374 \pm 32$	
Ac-ala-pro-D,L-alaCH <sub>2</sub> OH	8.0	$23.8 \pm 1.1$	
	5.0	$343 \pm 22$	
Ac-ala-pro-D-alaCH <sub>2</sub> OH	8.0	$40 \pm 5^f$	
Ac-ala-pro-L-alaCHO	8.0	$0.016 \pm 0.001^g$	
	5.0	$0.086 \pm 0.007^g$	
Ac-ala-pro-D,L-alaCHO	8.0	$0.025 \pm 0.002^g$	
	5.0	$0.120 \pm 0.010^g$	
Ac-ala-pro-glyCH <sub>2</sub> OH	8.1	$109 \pm 4$	
	5.0	> 1000	
Ac-ala-pro-glyDMA	8.0	$149 \pm 37$	
	5.0	> 1000	

TABLE I. (continued)

Peptide	pH	$K_I^{\text{obs}}$ (mM)	$K_m$ (mM)
Ac-ala-pro-glyOEt	8.0		$3.5 \pm 0.5^f$
Ac-ala-pro-glyPNA	8.0		$24.3 \pm 3.2$
Ac-ala-pro-glyCHO	8.0	$0.67 \pm 0.08^g$	
	5.0	$1.2 \pm 0.1^g$	
Ac-ala-pro-alaCHO <sup>h</sup>	8.1	$0.022 \pm 0.002^g$	

<sup>a</sup>All constants were determined by the spectrophotometric method outlined in the Experimental section unless otherwise noted.

<sup>b</sup>The reaction solution contained 10% dimethyl sulfoxide in order to improve the solubility of the peptide.

<sup>c</sup>The hydrolysis of this substrate was slow enough under the conditions used to allow for determination of  $K_I^{\text{obs}}$  without a substantial decrease in its concentration.

<sup>d</sup> $K_m = 110 \pm 25$  mM at pH 9.00 (Bauer et al. 1981).

<sup>e</sup> $K_I = 70 \pm 3$  mM at pH 8.0 (Shaw and Whitaker 1973).

<sup>f</sup>As determined in the pH-Stat. Values of  $K_I^{\text{obs}}$  were obtained using Ac-ala-pro-L-alaOMe as the substrate.

<sup>g</sup>These values have been corrected for the effect of hydration of the aldehyde in aqueous solution (see text).

<sup>h</sup>This aldehyde was synthesized using the method of Thompson(1973) and Hunkapiller et al.(1975).

<sup>i</sup> $K_m = 1.1$  mM (Hunkapiller et al. 1975).

<sup>j</sup>All constants are reported as the average  $\pm$  standard deviation of at least four determinations.

<sup>k</sup>All amino acid residues have the L-configuration unless otherwise noted.

are presented in Figure 8. The  $k_{\text{cat}}/K_m$  versus pH curve shows the sigmoidal shape typical of hydrolyses catalyzed by the serine proteases (Bender et al., 1964; Bender et al., 1962); the  $\log(k_{\text{cat}}/K_m)$  versus pH profile demonstrates that a basic group of  $\text{pK}_a$   $6.70 \pm 0.05$  in the free enzyme is responsible for catalytic activity.

NMR studies. Table II presents the chemical shift and coupling constant data for the C-2 carbon of  $\alpha$ -lytic protease complexed with both Ac-ala-pro-L-ala-CHO and Ac-ala-pro-gly-CHO. Figures 9 and 10 show representative spectra for the  $\alpha$ -lytic protease/Ac-ala-pro-gly-CHO complex.

The change in chemical shift with pH for both enzyme/aldehyde complexes is shown in Figures 11 and 12. The enzyme/alaninal titration represents at least 95% saturation over the entire pH range of the experiment; due to its larger  $K_I$ , the enzyme/glycinal complex represents greater than 85% saturation. Both curves can be analyzed in terms of a single ionization equilibrium; as described in Chapter II, the data can thus be fit by

$$\frac{\delta_{\text{obs}} - \delta_A}{\delta_B - \delta_A} = \frac{K_a}{K_a + (\text{H}^+)}$$

In the case of the  $\alpha$ -lytic protease/Ac-ala-pro-L-ala-CHO complex, the titration curve can be fit using a  $\text{pK}_a$  of  $6.25 \pm 0.05$  and a  $\delta_B - \delta_A$  of 2.30 ppm. The  $\alpha$ -lytic protease/Ac-ala-pro-gly-CHO complex data coincide well with a  $\text{pK}_a$  of  $6.50 \pm 0.05$  and a  $\delta_B - \delta_A$  of 2.70 ppm.

Figure 8. Plots of  $(k_{\text{cat}}/K_m)$  and  $\log(k_{\text{cat}}/K_m)$  versus pH for the reaction of  $\alpha$ -lytic protease with N-acetyl-L-alanyl-L-prolyl-L-alanine p-nitroanilide in 0.1 M KCl, 0.04 M buffer (acetate or phosphate), at  $25.0 \pm 0.2^\circ\text{C}$ . The  $\log(k_{\text{cat}}/K_m)$  versus pH plot indicates that catalysis is dependent on a group of  $\text{pK}_a = 6.70 \pm 0.05$ . The  $(k_{\text{cat}}/K_m)$  data were then fit to the following equation:

$$(k_{\text{cat}}/K_m) = (k_{\text{cat}}/K_m)^0 \{K_a / (K_a + (\text{H}^+))\}$$

using  $\text{pK}_a = 6.70$  and  $(k_{\text{cat}}/K_m)^0 = 1700 \text{ M}^{-1} \text{ s}^{-1}$ .

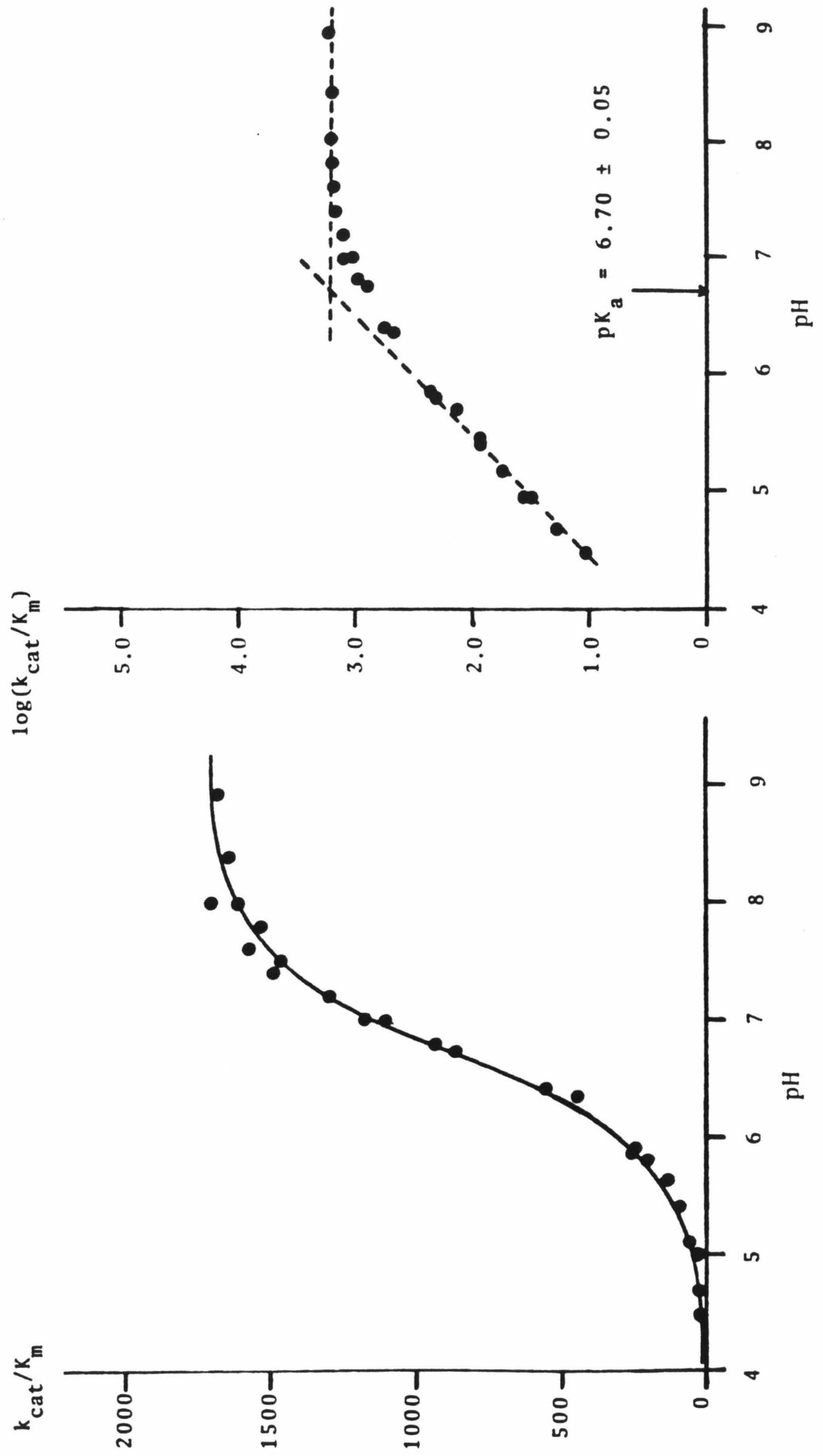


**TABLE II.** NMR parameters for the C-2 carbon of the Histidine 57 residue of  $\alpha$ -lytic protease in the free enzyme and in the enzyme/aldehyde complexes.

pH	$\delta$ (ppm) <sup>a</sup>	$^1J_{CH}$ (Hz) <sup>b</sup>
<u>Free enzyme</u>		
5.2	134.48	222
6.6	135.44	---
8.0	136.80	209
8.1	136.86	204
<u>enzyme + Ac-ala-pro-L-alaCHO<sup>e</sup></u>		
5.2	134.43	222 <sup>c</sup>
6.4	135.48	---
8.4	136.55	206 <sup>d</sup>
<u>enzyme + Ac-ala-pro-glyCHO<sup>f</sup></u>		
5.3	134.19	221 <sup>d</sup>
6.9	136.00	210
8.6	136.80	208 <sup>d</sup>

<sup>a</sup>Chemical shift values are  $\pm 0.10$  ppm, and are reported relative to external tetramethylsilane = 0.00 ppm.

<sup>b</sup> $^1J_{CH}$  values are  $\pm 2$  Hz.

<sup>c</sup>Average of three determinations.

<sup>d</sup>Average of two determinations.

<sup>e</sup>133 mM aldehyde, 1.9 mM enzyme, 0.1 M KCl, 10% (v/v)  $^2H_2O$ .

<sup>f</sup>300 mM aldehyde, 2.1 mM enzyme, 0.1 M KCl, 10% (v/v)  $^2H_2O$ .

Figure 9. 50.3 MHz proton coupled  $^{13}\text{C}$  NMR spectra of the complex of (2- $^{13}\text{C}$ )-histidyl- $\alpha$ -lytic protease with Ac-ala-pro-glyCHO in 0.2 M KCl, 10% (v/v)  $^2\text{H}_2\text{O}$ , at  $25.0 \pm 0.2^\circ\text{C}$ . The sample contained 2.0 mM protein and 300 mM aldehyde. The spectra were taken with a 12500 Hz sweep width, using a 0.15 sec acquisition time and a  $70^\circ$  pulse of 10  $\mu\text{sec}$ . The spectra are NOE-enhanced; the decoupler was turned on during a delay time of 0.10 sec prior to acquisition, and turned off during the acquisition time. In each spectrum, 3750 FID points were zero-filled to a Fourier number of 8192, and were transformed with 12 Hz line broadening.

- A) 22,703 transients, pH 4.0.
- B) 85,706 transients, pH 6.9.
- c) 25,000 transients, pH 8.6.

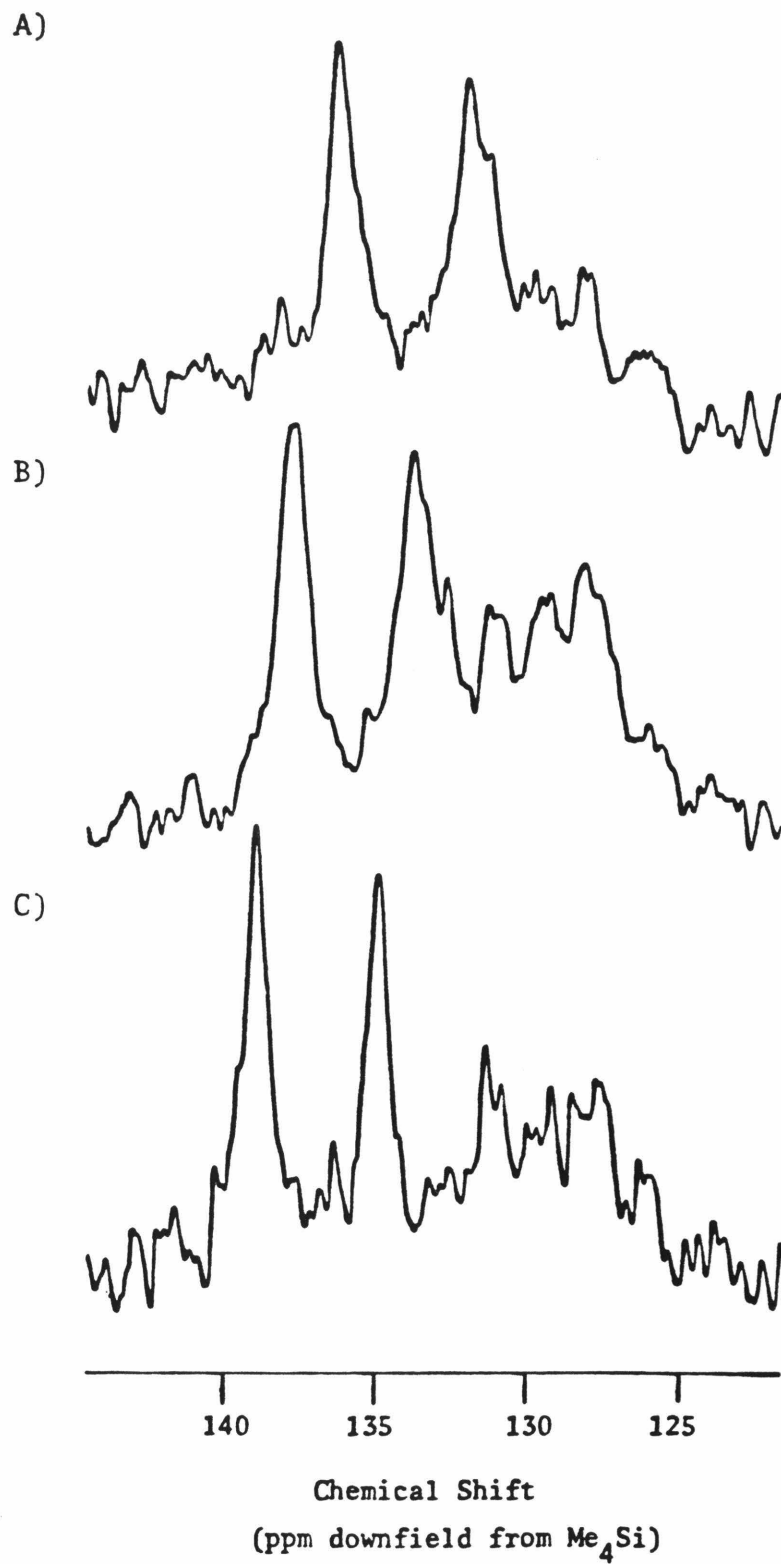


Figure 10. 50.3 MHz broadband proton decoupled  $^{13}\text{C}$  NMR spectra of the complex of (2- $^{13}\text{C}$ )-histidyl- $\alpha$ -lytic protease with Ac-ala-pro-glyCHO in 0.2 M KCl, 10% (v/v)  $^2\text{H}_2\text{O}$ , at  $25.0 \pm 0.2^\circ\text{C}$ . The sample contained 2.0 mM protein and 300 mM aldehyde. The spectra were taken with a 12500 Hz sweep width, using a 0.15 sec acquisition time and a  $70^\circ$  pulse of 10  $\mu\text{sec}$ . Gated decoupling was used to reduce the dielectric heating of the sample. The decoupler was turned off during a 0.10 sec delay prior to acquisition, and turned on during acquisition. In each spectrum, 3750 FID points were zero-filled to a Fourier number of 8192, and were transformed with 10 Hz line broadening.

- A) 10,424 transients, pH 5.2.
- B) 5,120 transients, pH 6.7.
- c) 5,120 transients, pH 8.3.

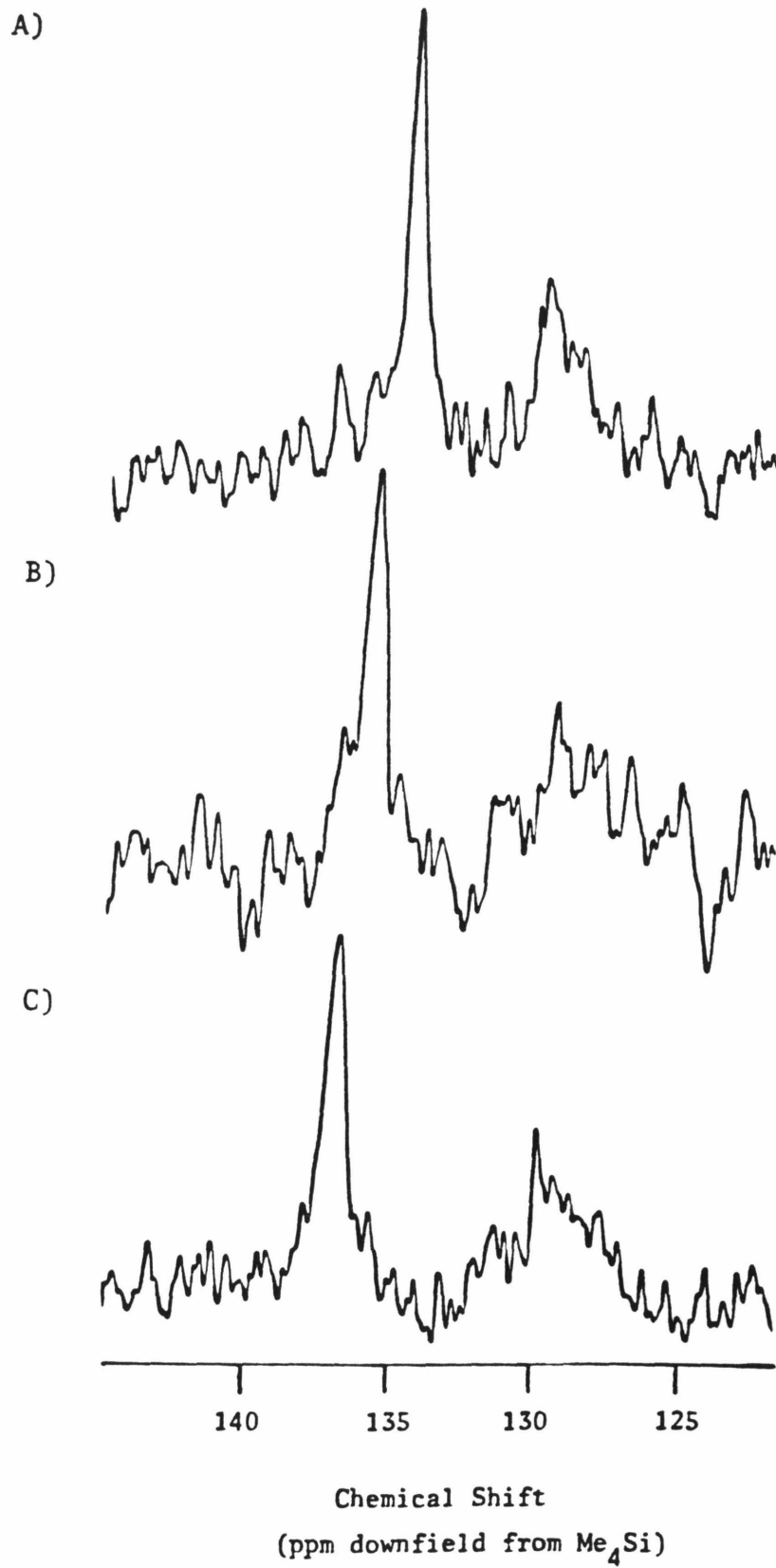


Figure 11. Chemical shift of the Histidine 57 C-2 carbon resonance of the complex of  $\alpha$ -lytic protease and Ac-ala-pro-L-alaCHO as a function of pH. The solid line is the theoretical titration curve calculated using a  $pK_a$  of 6.25 and a value of  $\delta_A - \delta_B$  of 2.30 ppm. The solid circles are for a sample that was 2.2 mM in protein and 110 mM in aldehyde; the solid squares are for a sample that was 1.0 mM in protein and 133 mM in aldehyde.

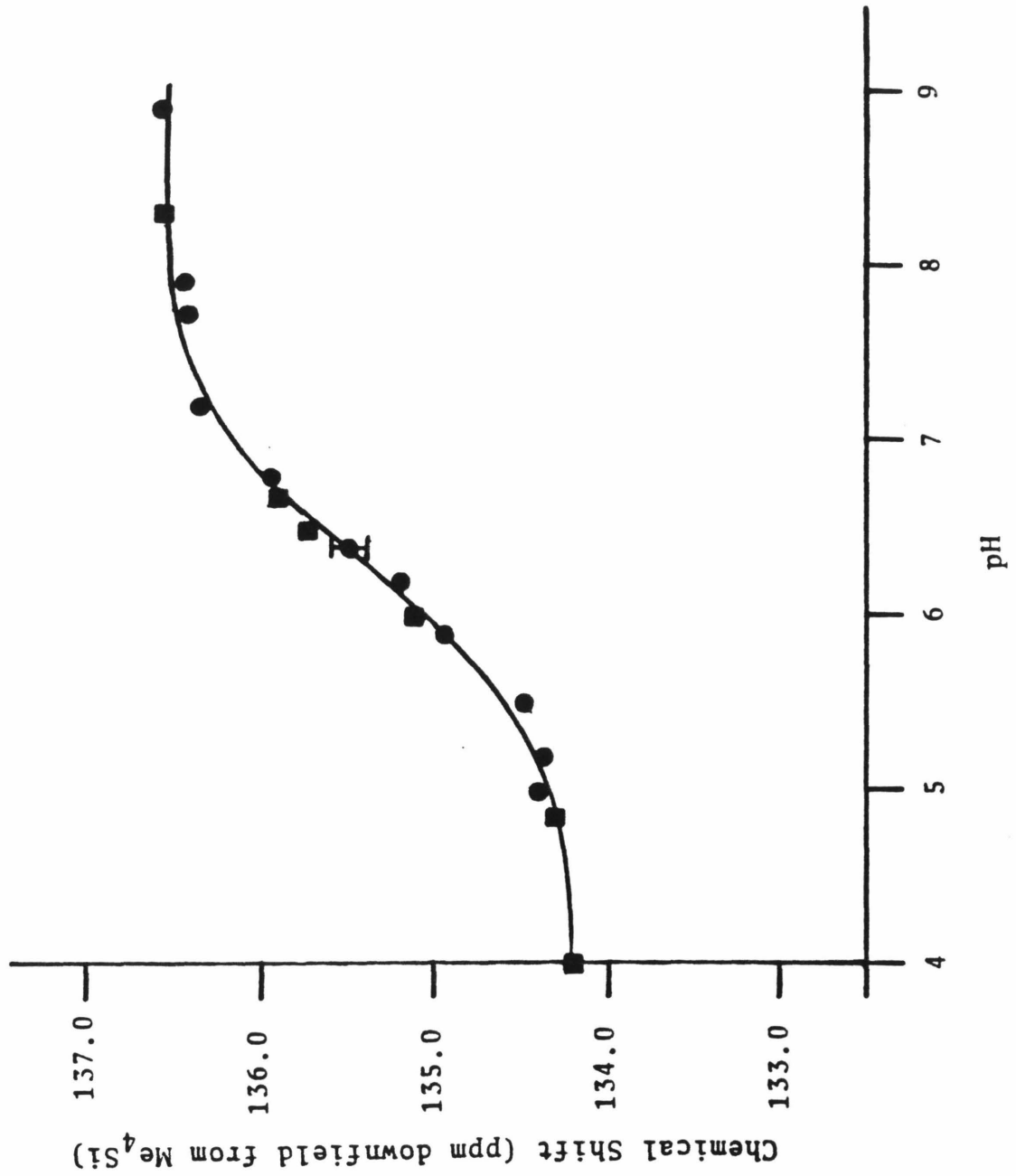
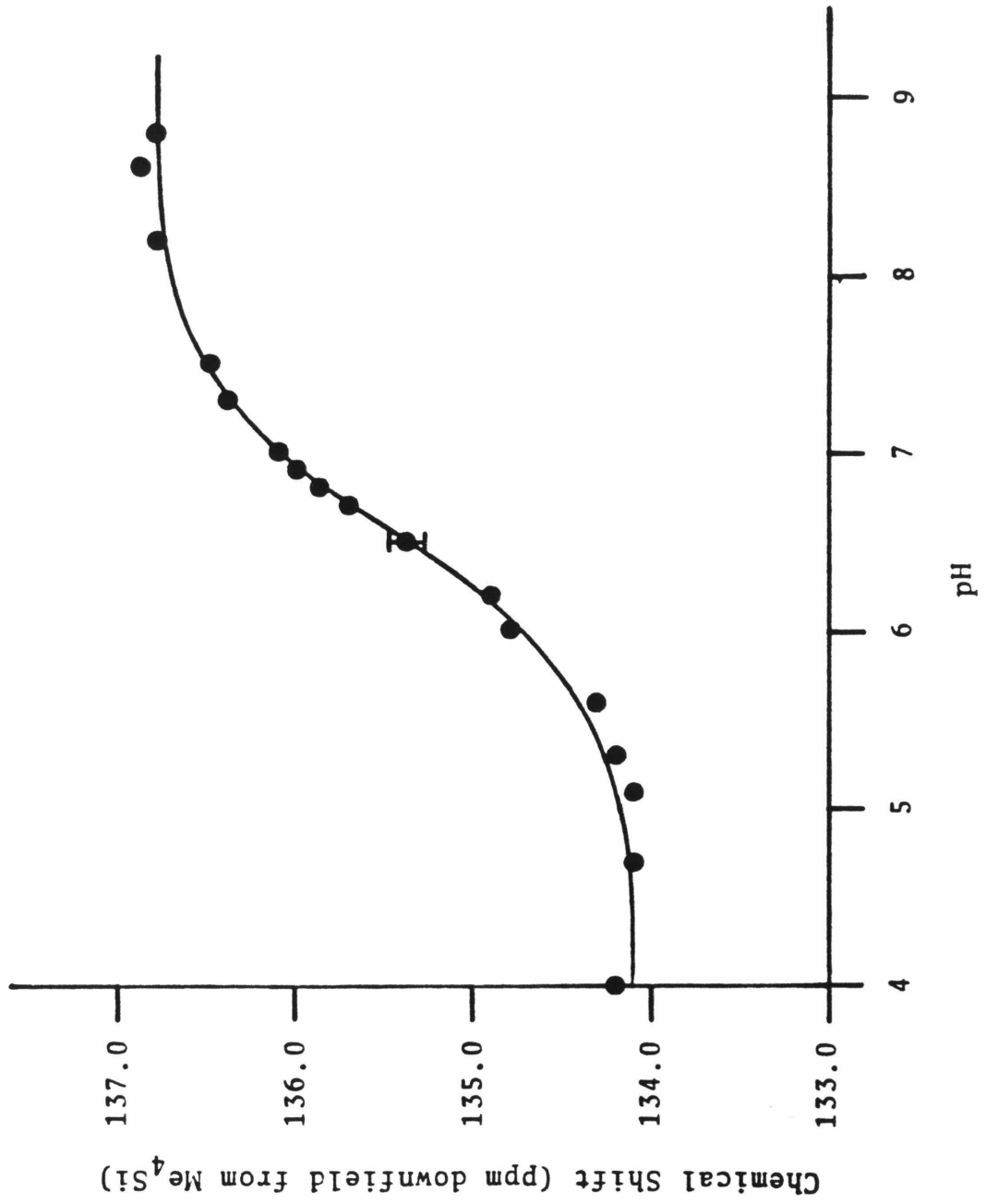


Figure 12. Chemical shift of the Histidine 57 C-2 carbon resonance of the complex of  $\alpha$ -lytic protease and Ac-ala-pro-glyCHO as a function of pH. The solid line is the theoretical titration curve calculated using a  $pK_a$  of 6.50 and a value of  $\delta_A - \delta_B$  of 2.68 ppm.



## DISCUSSION

The binding of aldehyde analogs of good substrates to the serine proteases has been the subject of much recent study and discussion, due to the potential structural similarity between these complexes and the postulated transition states and intermediates of the catalytic process. Two types of interaction have been primarily addressed: i) non-covalent association of the free or hydrated aldehyde with the enzyme; and ii) covalent hemi-acetal formation between aldehyde and enzyme active site.

Kinetic studies on the binding of aldehydes to elastase (Thompson, 1973),  $\alpha$ -lytic protease (Hunkapiller et al., 1975), chymotrypsin (Kennedy and Schultz, 1979), and S. griseus protease A (Brayer et al., 1979b) have all indicated that specific aldehydes bind significantly more tightly to these enzymes than do other substrate derivatives. The small inhibition constants observed for these aldehydes at both basic (catalytic) and acidic (non-catalytic) pH has been interpreted as covalent hemiacetal formation between these molecules and the Ser 195 hydroxyl of the catalytic triad. The  $K_I$  and  $K_m$  values for the various tripeptide derivatives listed in Table I are consistent with these previous studies.

NMR experiments (Schultz and Cheerva, 1975; Lowe and Nurse, 1977; Chen et al., 1979; Gorenstein and Shah, 1982) have indicated that for specific substrate analogs, the free aldehyde is in equilibrium with a covalent enzyme/

inhibitor adduct, while for non-specific aldehydes the complex is probably solely non-covalent (Gorenstein et al., 1976; Lowe and Nurse, 1977). These NMR investigations substantiate the conclusions of the inhibition studies, and further suggest that binding is a two-step process, characterized by initial rapid non-covalent association of the free aldehyde and protein, followed by a slower formation of covalent hemiacetal. This proposal is supported by the stopped-flow binding studies of Kennedy and Schultz (1979). Covalent bond formation is also supported by X-ray crystallographic data for a serine protease/aldehyde complex (Brayer et al., 1979b). The critical role of Ser 195 in the tight binding observed in these complexes is further supported by the observation of severely attenuated association of benzoyl-L-phenylalaninal to anhydrochymotrypsin, in which the hydroxymethyl side-chain of Ser 195 has been converted to a dehydroalanyl side-chain (Chen et al., 1979).

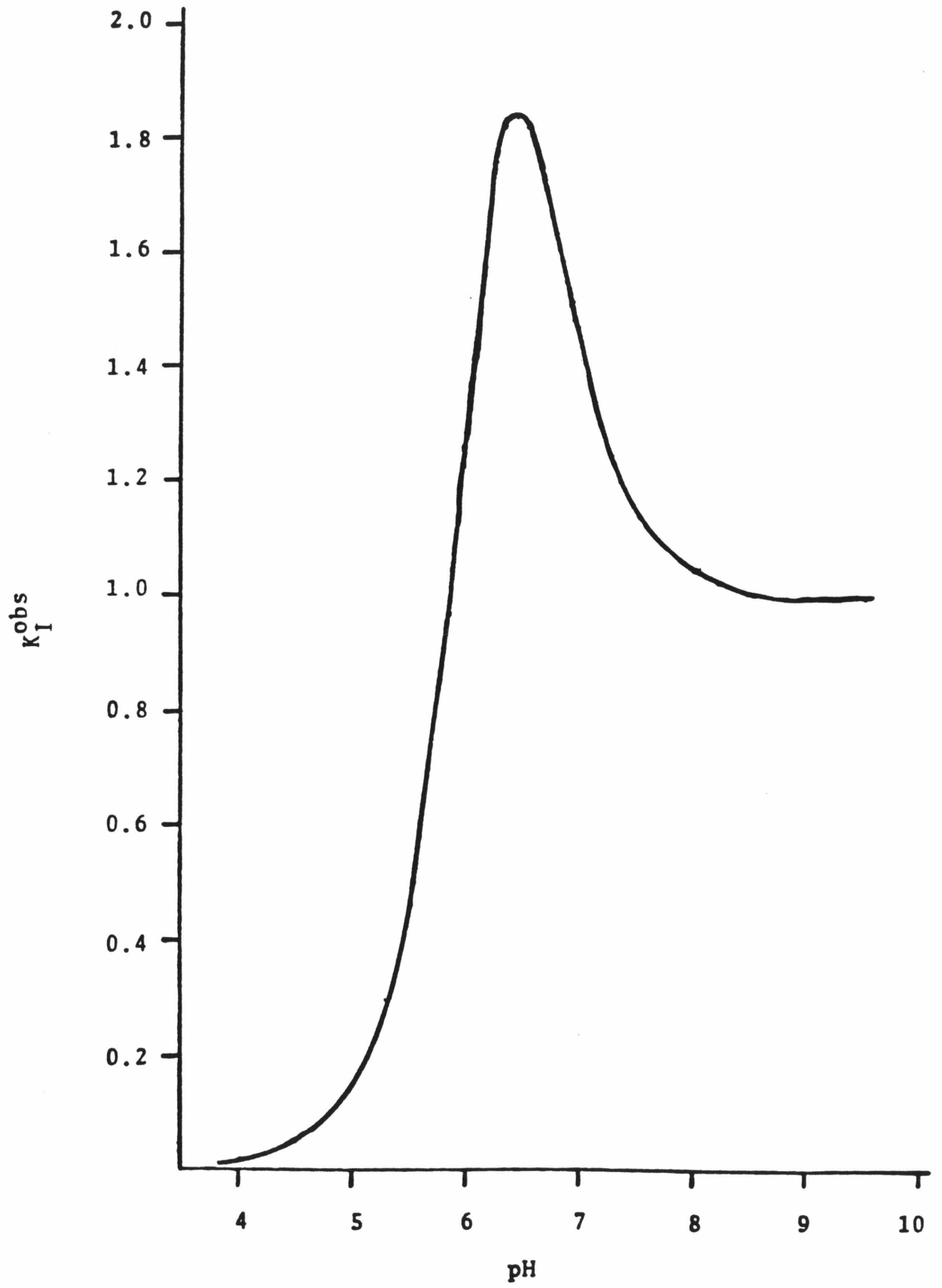
Since the preponderance of evidence suggests that the primary interaction responsible for the tight binding association of specific aldehydes and serine proteases is covalent hemiacetal formation, it is pertinent to inquire as to the degree with which this structure mimics the transient structures of the catalytic pathway.

An attempt to answer this question was provided by Hunkapiller et al. (1975). These researchers studied the  $^{13}\text{C}$  NMR titration behavior of (2- $^{13}\text{C}$ )-histidyl- $\alpha$ -lytic protease in the presence of saturating concentrations of the specific substrate analog N-acetyl-L-alanyl-L-prolyl-L-alaninal (Ac-ala-

pro-L-ala-CHO). They observed an abnormally steep titration curve for the resonance assigned to the C-2 carbon nucleus, indicating to them cooperative addition of two protons to the complex on lowering the pH from 8 to 5. They postulated a tightly hydrogen bonded complex at high pH to explain this cooperativity, a key feature of which was the presence of the hemiacetal adduct in its oxyanion form, stabilized by strong interactions with the "oxyanion hole" of the enzyme active site. Thus it was their interpretation that these enzyme/specific aldehyde complexes were able to mimic the postulated catalytic transition state with a high degree of accuracy. A hemiacetal anion was also postulated for the stable complex of chymotrypsin and hydrocinnamaldehyde (Schultz and Cheerva, 1975).

The pH behavior of  $K_I^{\text{obs}}$  for the enzyme/aldehyde complex as described by Hunkapiller et al. (1975) is highly distinctive and is shown in Figure 13. The plot is based on the mechanism described by equation (1), which assumes i) the existence of two ionizations in both the free enzyme and in the complex that can affect binding, ii) the aldehyde can bind to all three acid-base forms of the protein, unprotonated, mono-protonated, and di-protonated, and iii) equilibrium exists among all forms of enzyme, inhibitor, and complex. These assumptions are predicated on the observation of tight enzyme/aldehyde binding over the entire pH range studied (4-9), and are a logical conclusion of the cooperativity observed by Hunkapiller et al. (1975). Figure 13 has been generated using

Figure 13. Plot of  $K_I^{\text{obs}}$  versus pH for the inhibition of  $\alpha$ -lytic protease by Ac-ala-pro-L-alaCHO assuming normal ionization behavior in the free enzyme and cooperative ionization in the complex (Hunkapiller et al., 1975). The plot is calculated using equation (1) and the following values:  $pK_1 = 6.70$ ,  $pK_2 = 5.00$ ,  $pK_3 = 5.50$ ,  $pK_4 = 7.00$ , and  $pK_I = 1$ . The condition for cooperativity is  $pK_3 < pK_4$ , and  $pK_1 > pK_2$ .



equation (1) and the following pK values:  $pK_1 = 6.7$ ,  $pK_2 = 3.3$ ,  $pK_3 = 5.5$ ,  $pK_4 = 7.0$ , and  $K_I = 1$ . The value of  $pK_1$  is that determined for His 57 of  $\alpha$ -lytic protease in Chapter II of this thesis, and of Asp 102 by Hunkapiller et al. (1973). The value of  $pK_2$  is an estimate of the acid dissociation constant of His 57 determined in this latter report. If this value is not a good estimate, only the magnitude of  $K_I^{obs}$  on the low pH side of the curve will be affected; the general shape of the curve will remain unchanged. The assignment of  $pK_1$  and  $pK_2$  to the actual active site residues is not important to this discussion; it is enough to know that the active site of the free enzyme titrates with approximately these values. The values of  $pK_3$  and  $pK_4$  are taken from Hunkapiller et al. (1975);  $pK_1 > pK_2$  and  $pK_3 < pK_4$  is the condition for the manifestation of cooperativity in the complex. The value of  $pK_1$  is of course unimportant to the shape of the curve and has therefore been chosen arbitrarily.

The experimental  $K_I^{obs}$  versus pH profile (Figure 7) for  $\alpha$ -lytic protease and Ac-ala-pro-L-ala-CHO does not coincide with the predicted curve. Originally we were concerned that this might be due to the mixture of diastereomeric aldehydes in this material; however, Ac-ala-pro-gly-CHO, an isomerically unique aldehyde at the C-terminus, shows substantially the same binding behavior.

A repeat of the  $^{13}C$  NMR study using both of these aldehydes confirms the indications of the inhibition data. Both enzyme/aldehyde complexes show a single, normal ionization

equilibrium occurring between pH 4 and pH 9; this titration is due to the protonation/deprotonation equilibrium of the imidazole side-chain of His 57, as determined from the  $^1J_{\text{CH}}$  at high and low pH in these complexes. An interesting observation is that the  $\text{pK}_a$  values for this ionization are different from that for the free enzyme and from each other, being 6.50 for the complex with Ac-ala-pro-gly-CHO and 6.25 for the complex with Ac-ala-pro-L-ala-CHO. The importance of these values will be touched on later.

The  $K_I^{\text{obs}}$  versus pH profiles for these two aldehydes can still be adequately described by equation (1). The assumptions made in the derivation of equation (1) are still valid, since both aldehydes show only small changes in  $K_I^{\text{obs}}$  over the pH range investigated. The raw data in Figure 7 were fit to equation (1) by hand to generate the curves shown. Certain of the pK values are obtainable from the kinetic and the  $^{13}\text{C}$  NMR data ( $\text{pK}_1$ ,  $\text{pK}_I$ ,  $\text{pK}_3$ ). The value of  $\text{pK}_I'$  can be determined using the "thermodynamic box" approach and the known values of  $K_1$ ,  $K_3$ , and  $K_I$ . We can only make estimates of the other three equilibrium constants, since the kinetic and NMR investigations cannot be accurately carried out to sufficiently low pH. The values of  $\text{pK}_2$  and  $\text{pK}_4$  were chosen iteratively to fit the data; these values may represent the ionization of Asp 102 (since  $\text{pK}_1$  and  $\text{pK}_3$  are known to represent His 57), or, just as conceivably, some other group(s) may be the causative factor(s). We have no experimental evidence bearing on this matter yet. The estimates of  $\text{pK}_4$  agree with the value

of the low pH ionization ( $pK_a$  about 5) affecting both  $K_m$  in the chymotrypsin catalyzed hydrolysis of some N-formyl-L-phenylalanine amides and proflavine binding to this enzyme (Fersht and Requena, 1971).

The  $K_I^{obs}$  versus pH curves obtained in this experiment correlate remarkably well with the pH behavior of  $K_I$  for the association of benzoyl-L-phenylalaninal with chymotrypsin (Kennedy and Schultz, 1979). The  $K_I$  versus pH profile observed in this latter system also exhibits little pH dependency for  $K_I$  at pH values greater than 6, and a small dependency with an apparent  $pK_a$  around 4 at pH values less than 6. The value of  $K_I$  increases only about five-fold between pH 8 and pH 3. These authors interpret this lack of substantial pH dependency for  $K_I$  as demonstrating that the basic form of the catalytic triad, which is absolutely critical for catalysis, is not requisite for the high affinity of this enzyme/aldehyde pair. However, if equation (1) describes their results, as it does the results of the present study, this conclusion does not explicitly follow from the above premise. The pH versus  $K_I$  profile can only indicate changes in the  $pK_a$  values between free and complexed enzyme, since the mechanism from which equation (1) is derived is a purely equilibrium model. Thus, no direct information about the influence of pH on the mechanism of adduct formation is readily available from these profiles. Indeed, if the enzyme/inhibitor complex showed exactly the same  $pK_a$  values as the free enzyme, no pH dependence of  $K_I$  would be observed.

In order to observe a substantial effect of pH on  $K_I$ , as might be expected by analogy with catalysis, the aldehyde would have to bind only to the unprotonated form of the enzyme, and be unable to bind to the protonated forms (see Appendix III). Of course, this argument depends on the appropriateness of our equilibrium model. Since extended incubation of the enzyme and aldehyde prior to kinetic determination of  $K_I^{\text{app}}$  resulted in no significant difference in the measured  $K_I^{\text{app}}$  values from those determined without pre-incubation, the rapid equilibrium assumption is probably appropriate. Furthermore, the model adequately fits the data. The small change in  $K_I^{\text{app}}$  with pH may well indicate a somewhat dormant role for Asp 102 and His 57 in the formation of a covalent enzyme/aldehyde species; however, the best evidence is the observation that benzoyl-L-phenylalaninal binds slightly more strongly to methyl-chymotrypsin, in which the catalytic ability of His 57 has been severely reduced (Henderson, 1971; Byers and Koshland, 1978), than to native enzyme (Kennedy and Schultz, 1979).

Further evidence of covalent attachment of the aldehyde to the enzyme can be found in the kinetic data of Table I. It is well known that  $\alpha$ -lytic protease, like other serine proteases, catalyzes the hydrolysis of L-amino acid derivatives while remaining inert to their D-counterparts (Kaplan, 1970; Whitaker, 1970). An estimate of the inherent binding constants of pure N-acetyl-L-alanyl-L-prolyl-L-alaninal and pure N-acetyl-L-alanyl-L-prolyl-D-alaninal can be made from the data for

Ac-ala-pro-L-ala-CHO, a 70:30 mixture of these two isomers, and Ac-ala-pro-D,L-ala-CHO, a 50:50 mixture. The overall observed binding constant for a mixture of two competitive inhibitors is given by (see Appendix II)

$$\frac{1}{K_I^{\text{app}}} = \frac{f}{K_L} + \frac{1-f}{K_D}$$

where  $K_I^{\text{app}}$  is the observed inhibitor dissociation constant,  $K_L$  and  $K_D$  are the true binding constants for the two pure inhibitors, in this case the (L-L-L) and (L-L-D) aldehydes, and  $f$  and  $1-f$  are the fractional amounts of each inhibitor, (L-L-L) and (L-L-D) respectively. From the data at pH 8.0, we find that  $K_L \approx 1 \times 10^{-5} \text{ M}$ , and the value calculated for  $K_D$  using the above equation is less than zero, due to the error inherent in the measurement of  $K_I^{\text{app}}$ . This implies that  $K_D$  is large relative to  $K_L$ , so that  $K_I^{\text{app}} \approx K_L/f$ . A minimum estimate of  $K_D$  can be made by using the minimum value of  $K_I^{\text{app}}$  for Ac-ala-pro-L-ala-CHO, and the maximum value for Ac-ala-pro-D,L-ala-CHO at this pH; doing this, a value of  $1.2 \times 10^{-5} \text{ M}$  can be calculated for  $K_L$  and  $2.1 \times 10^{-4} \text{ M}$  for  $K_D$ . The actual value of  $K_D$  is probably larger than this value, which is about twenty times that of  $K_L$ . Comparing this to the values for the diastereomeric Ac-ala-pro-ala alcohols ( $K_L = 18 \text{ mM}$ ,  $K_D = 40 \text{ mM}$ ), it may be inferred that simple non-covalent binding, which is the only means of interaction with enzyme for the alcohol inhibitors, cannot account for the over twenty-fold tighter binding of the (L-L-L) aldehyde over

the (L-L-D) form. Since the (L-L-L) aldehyde isomer will be positioned correctly in the active site of the enzyme to allow for covalent bond formation, while the (L-L-D) aldehyde isomer will not (as evidenced by the enzymatic turnover of Ac-ala-pro-L-ala-OMe, but lack of observable turnover of Ac-ala-pro-D-ala-OMe), the observed binding difference should, by analogy, be due to covalent hemiacetal formation with the (L-L-L) isomer and non-covalent binding of the (L-L-D) isomer. The substantially tighter binding of the (L-L-D) aldehyde over the corresponding alcohol probably indicates that it is the trigonal, free aldehyde form, and not the tetrahedral, hydrated form, that is the inhibitory species in this case, since the trigonal form is sterically less demanding. It is interesting to note that  $K_I$  for the (L-L-D) methyl ester and  $K_m$  for the (L-L-L) methyl ester also differ by about twenty-fold.

The large difference in binding constants for the L-alaninal and the glycinal is noteworthy, especially in lieu of the similar affinities of these two substances for water ( $K_H \approx 20$  for both aldehydes). Although this probably represents an orientational effect, the alaninal being more optimally positioned in the active site for covalent bond formation than is the glycinal, it may in fact hint that the enzyme is not merely acting as a passive template, functioning solely to position a highly reactive aldehyde near a reactive hydroxyl, but that the residues of the catalytic triad may actively assist the bond-making process in these complexes, in a manner similar to the catalytic hydrolysis of a substrate.

It is clear, however, that the relationship between the mechanism of hemiacetal formation in these complexes and the mechanism of hydrolysis of amide and ester substrates by these enzymes is not yet well understood.

The interaction of these aldehydes with  $\alpha$ -lytic protease results in a moderate degree of perturbation of the  $pK_a$  of His 57, from 6.70 in the free enzyme to 6.50 in the enzyme/glycinal complex and to 6.25 in the enzyme/alaninal complex. The cause of this shift is not known, nor does the current evidence provide a structural explanation for it. It does, however, suggest an intriguing possibility. If such a  $pK_a$  lowering of the His 57-Asp 102 couple is an intrinsic feature of the catalytic process on conversion of bound substrate to tetrahedral intermediate or transition state, it would enhance the general acid character of the dyad and facilitate the transfer of the proton originally on Ser 195 to the leaving group of the substrate. In other words, by making the Asp-His dyad a stronger acid in the transition state than in the ground state, the enzyme would have the means by which to facilitate both the general base catalyzed formation and the general acid catalyzed decomposition steps of the enzymatic reaction. Such a mechanism would also tend to disfavor the initial formation of the tetrahedral intermediate, however, by facilitating the return of the stored proton to  $\gamma O$  of Ser 195, resulting in the non-productive breakdown of the intermediate to Michaelis complex, unless some measure of kinetic control over the process is available to the enzyme

that favors the productive breakdown of the intermaediate to acyl-enzyme and hinders the non-productive return to ES-complex. Such kinetic control could occur if movement of His 57 from near  $\gamma\text{O}$  of Ser 195, where it must accept a proton during formation of the tetrahedral intermediate, to near the substrate amide nitrogen or ester oxygen, where it must donate a proton during decomposition of the tetrahedral intermediate to acyl-enzyme, is a necessary feature of the catalytic process and is accompanied by the lowering of the  $\text{pK}_a$  of His 57 in some as yet unknown manner. Kinetic control will thus be exerted on the reaction, since by being positioned near the substrate leaving group and far from the Ser 195  $\gamma\text{O}$  in the intermediate, the proton stored on His 57 will be more easily donated to the substrate than back to Ser 195. The productive reaction pathway will then be favored, especially if a strong hydrogen bond between His 57 and the substrate leaving group in the intermediate is formed, as this will tend to restrict the movement of His 57 back to where it can return the stored proton to Ser 195. Such a mechanism has been discussed by Satterthwait and Jencks (1974), and by Matthews et al. (1977).

Also, there is some corroborative kinetic evidence for this hypothesis. Kinetic studies of some chymotrypsin catalyzed hydrolyses of specific substrates (Caplow, 1969; Fersht, 1972; Lucas et al., 1973) have indicated abnormally low  $\text{pK}_a$  values for the pH dependence of  $k_{\text{cat}}$ . Low  $\text{pK}_a$  values for the Asp-His dyad of the sort suggested by the above

hypothesis would be manifested in the pH dependence of  $k_{\text{cat}}$  if proton transfer from the dyad to the incipient product portion of the decomposing tetrahedral intermediate is rate-limiting for certain substrates. It must be recognized however that this hypothesis is at present only speculative, and is based on the existence of a reasonable degree of correlation between the enzyme/aldehyde complexes and the high-energy structures of the catalytic pathway. Nonetheless, it merits further consideration and experimental investigation.

We can offer no obvious explanation for the difference between the results presented here and the Hunkapiller et al. (1975) results. Perhaps the low sensitivity of the NMR instrumentation used in the latter study precluded the accurate determination of the titration curve, or perhaps the aldehyde used in that study contained some impurity capable of interacting with the enzyme to produce the observed abnormal shape of the curve. It is significant that the  $\text{pK}_a$  they obtained for the complex, assuming a single ionization, would be the same as that obtained in this study. The difference in the curves for a normal versus cooperative titration is small, so that only minor experimental perturbations are required to explain the difference between the two studies.

## CONCLUSION

The results presented in this chapter are consistent with the present view (Kennedy and Schultz, 1979; Chen et al., 1979; Gorenstein and Shah, 1982) that specific aldehyde inhibitors form covalent tetrahedral adducts on binding to serine proteases. Furthermore, lack of a pronounced pH dependence for  $K_I^{\text{obs}}$ , demonstrated here for  $\alpha$ -lytic protease and by Kennedy and Schultz (1979) for chymotrypsin, favors the interpretation that these adducts exist as neutral hemiacetals, rather than as the more transition state-like oxyanions.

Are these aldehydes, then, good transition state analogs for these enzymes? To the extent that these complexes mimic the gross tetrahedral configuration of the postulated catalytic transition states, the answer is yes. However, it appears that these aldehydes are unable to reproduce at least one of the key features of the transition state, as the neutral hemiacetals are unable to interact with the "oxyanion hole" in the tight, precise manner of the transition state oxyanion. Recent calculations (Warshel, 1981; Warshel et al., 1982) provide evidence that the development of a negative charge on the substrate carbonyl in the transition state is necessary for the formation of the strong hydrogen bonds between this structure and the backbone amide groups of Ser 195 and Gly 193, and that the special ability of these enzymes to stabilize the transient structures of catalysis depends largely on the strength of this interaction.

The role of the Asp 102 and His 57 in the formation

of the covalent bond between Ser 195 and the aldehydic carbonyl is at present unresolved. Although formation of the hemiacetal is probably more complex than just a favorable equilibrium caused by juxtaposition of a very reactive carbonyl and a hydroxylic nucleophile in which the Asp-His dyad plays little or no active part (as discussed by Jencks (1975)), a more catalytically imitative role for the dyad, in which the Asp-His pair assists the initial formation of a hemiacetal oxyanion by accepting the hydroxyl proton from Ser 195, followed by either stepwise or concerted transfer of the stored proton to the oxyanion to give the neutral hemiacetal, stereochemically requires that the negatively charged oxygen in the oxyanion form of the adduct be close to His 57 N-1 at some point in the reaction to allow for this transfer to occur, and not tightly lodged in the "oxyanion hole", as would be expected for a transition state-like structure (Kennedy and Schultz, 1979).

The enzyme/aldehyde complexes are useful, however, in that they provide support for the theory that the serine proteases have evolved to preferentially stabilize the tetrahedral transition states occurring during the catalytic process. Furthermore, they can provide suggestions as to what considerations are important in assigning the ultimate catalytic roles of the residues of the active site of these enzymes. Since an "ideal" transition state analog can never be designed because a stable molecule can never accurately reproduce the unstable structure of a transition state species, the epithet "good transition state analog" should probably be linked to the

amount of information pertinent to the description of the catalytic process that can be obtained from the study of such molecules, and as such these aldehydes deserve this designation.

## APPENDIX I

The following is the derivation of the equation used to calculate the values of the inhibition constants.

In the absence of inhibitor, assuming  $S_o \gg E_o$  and that the system obeys Michaelis-Menten kinetics,

$$v_o = \frac{k_{cat} E_o S_o}{K_m + S_o} .$$

In the presence of a purely competitive inhibitor of total concentration  $I_o \gg E_o$ ,

$$v_i = \frac{k_{cat} E_o S_o}{K_m \{1 + (I_o/K_I)\} + S_o} .$$

Under conditions where  $S_o \gg K_m$ ,  $v_o$  and  $v_i$  reduce to

$$v_o = (k_{cat}/K_m) E_o S_o$$

and

$$v_i = \frac{k_{cat}}{K_m \{1 + (I_o/K_I)\}} E_o S_o ,$$

or, for a given  $E_o$ ,

$$v_o = k_o S_o$$

and

$$v_i = k_i S_o ,$$

where  $k_o$  and  $k_i$  are both pseudo-first-order rate constants.

For a given  $S_o$ ,

$$(v_o/v_i) = (k_o/k_i) = 1 + (I_o/K_I) .$$

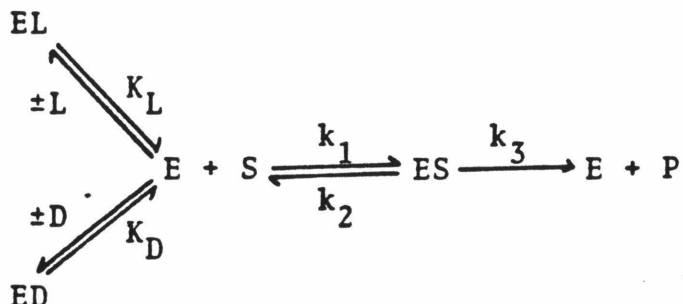
Therefore,

$$K_I = \frac{I_o}{(k_o/k_i) - 1} .$$

## APPENDIX II

The following is the derivation of the observed inhibition constant for the case of a mixture of two purely competitive inhibitors.

The kinetic scheme diagrammed below describes this case:



where E represents free enzyme; S, substrate; ES, non-covalent Michaelis complex; P, product(s); L and D, two different competitive inhibitors.  $K_L$  and  $K_D$  are the dissociation constants of the EL and ED complexes, respectively.

We assume that  $S_0 \gg E_0$ , so that the steady-state assumption can be made:

$$d(\text{ES})/dt = 0 = (k_2 + k_3)(\text{ES}) - k_1(\text{E})(\text{S})$$

and

$$(\text{ES}) = (\text{E})(\text{S})/K_m,$$

where  $K_m = k_1/(k_2 + k_3)$ .

Now,

$$E_0 = (\text{E}) + (\text{EL}) + (\text{ED}) + (\text{ES})$$

and

$$I_0 = L_0 + D_0$$

so that

$$E_0 - (\text{ES}) = (\text{E})\{1 + (L_0/K_L) + (D_0/K_D)\},$$

assuming  $I_0 \gg E_0$ .

or

$$(E) = \{E_0 - (ES)\} \{1 + (L_0/K_L) + (D_0/K_D)\}^{-1}.$$

Thus,

$$K_m(ES)/(S) = \{E_0 - (ES)\}A,$$

where

$$A^{-1} = 1 + (L_0/K_L) + (D_0/K_D).$$

Solving for (ES),

$$(ES) = E_0(S) / \{(K_m/A) + (S)\}.$$

Now, since  $v = d(P)/dt = k_3(ES)$ , and assuming  $(S) = S_0$  in the initial stages of the reaction,

$$v = k_3 E_0 S_0 / \{(K_m/A) + S_0\}$$

or

$$v = \frac{k_3 E_0 S_0}{K_m \{1 + (L_0/K_L) + (D_0/K_D)\} + S_0}.$$

Now, we shall define  $(L_0/I_0) = \alpha$  and  $(D_0/I_0) = (1 - \alpha)$  so that

$$1 + (L_0/K_L) + (D_0/K_D) = 1 + (I_0/K_I^{app}),$$

where

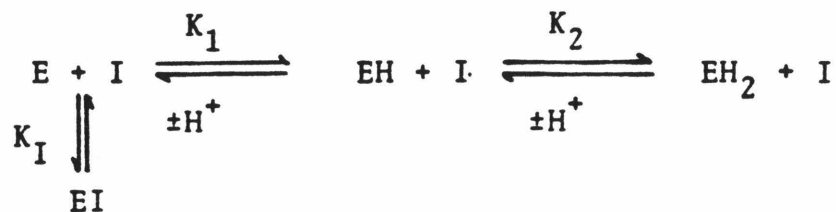
$$(1/K_I^{app}) = (\alpha/K_L) + \{(1-\alpha)/K_D\},$$

and standard competitive inhibition is observed:

$$v = V_{max} S_0 / \{K_m (1 + (I_0/K_I^{app})) + S_0\}.$$

## APPENDIX III

If the aldehydes are assumed to bind only to the unprotonated (catalytically active) form of the enzyme, and not to the mono- or diprotonated forms, the following equilibria apply:



Once again,

$$\begin{aligned}
 K_I^{\text{obs}} &= \frac{(\text{all forms of E})(\text{all forms of I})}{(\text{all forms of EI})} \\
 &= \frac{\{(E) + (EH) + (EH_2)\}(I)}{(EI)} \\
 &= \frac{(E)(I)}{(EI)} \{1 + ((H^+)/K_1) + ((H^+)^2/K_1K_2)\} \\
 &= K_I \{1 + ((H^+)/K_1) + ((H^+)^2/K_1K_2)\} .
 \end{aligned}$$

Thus,  $K_I^{\text{obs}}$  will exhibit a sigmoidal pH dependence characteristic of the titration of a diprotic acid.

## REFERENCES

- Andersson, L., Isley, T.C., and Wolfenden, R. (1982), Biochemistry 21, 4177-4180.
- Aoyagi, T., Miyata, S., Nanbo, M., Kojima, F., Matsuzaki, M., Ishizuka, M., Takeuchi, T., and Umezawa, H. (1969), J. Antibiotics 27, 558-568.
- Bailey, J.L. (1955), Biochem. J. 60, 170-172.
- Bauer, C.-A., Brayer, G.D., Sielecki, A.R., and James, M.N.G. (1981), Eur. J. Biochem. 120, 289-294.
- Bender, M.L., Schonbaum, G.R., and Zerner, B. (1962), J. Am. Chem. Soc. 84, 2562-2570.
- Bender, M.L., and Kezdy, F.J. (1964), J. Am. Chem. Soc. 86, 3704-3714.
- Bender, M.L., Kezdy, F.J., and Gunter, C.R. (1964), J. Am. Chem. Soc. 86, 3714-3721.
- Birktoft, J.J., and Blow, D.M. (1972), J. Mol. Biol. 68, 652-656.
- Blow, D.M. (1976), Acc. Chem. Res. 9, 145-152.
- Bode, W., and Schwager, P. (1975), J. Mol. Biol. 98, 693-717.
- Brayer, G.D., Delbaere, L.T.J., and James, M.N.G. (1978), J. Mol. Biol. 124, 261-283.
- Brayer, G.D., Delbaere, L.T.J., and James, M.N.G. (1979a), J. Mol. Biol. 131, 743-775.
- Brayer, G.D., Delbaere, L.T.J., James, M.N.G., Bauer, C.-A., and Thompson, R.C. (1979b), Proc. Natl. Acad. Sci. USA 76, 96-100.
- Byers, L.D., and Koshland, D.E. Jr. (1978), Bioorg. Chem. 7, 15-33.

- Caplow, M. (1969), J. Am. Chem. Soc. 91, 3639-3645.
- Chen, C., Gorenstein, D.G., Kennedy, W.P., Lowe, G., Nurse, D.,  
and Schultz, R.M. (1979), Biochemistry 18, 921-926.
- Collins, J.C., Hess, W.W., and Frank, F.J. (1968), Tetra. Letters  
30, 3363-3366.
- Delbaere, L.T.J., Brayer, G.D., and James, M.N.G. (1979), Can.  
J. Biochem. 57, 135-144.
- Dixon, M. (1953), Biochem. J. 55, 170-171.
- Fastrez, F., and Fersht, A.R. (1973), Biochemistry 12, 2025-  
2034.
- Fersht, A.R., and Requena, Y. (1971), J. Am. Chem. Soc. 93,  
7079-7087.
- Fersht, A.R. (1972), J Am. Chem. Soc. 94, 293-295.
- Fersht, A.R. (1974), Proc R. Soc. Lond. B. 187, 397-407.
- Fink, A.L. (1979), Trends Biochem. Sci. 4, 8-10.
- Firouzabadi, H., and Ghaderi, E. (1978), Tetra. Letters 9,  
839-840.
- Gorenstein, D.G., Kar, D., and Momii, R.K. (1976), Biochem.  
Biophys. Res. Commun. 73, 105-111.
- Gorenstein, D.G., and Shaw, D.O. (1982), Biochemistry 21, 4679-  
4686.
- Henderson, R. (1970), J. Mol. Biol. 54, 341-354.
- Henderson, R. (1971), Biochem. J. 124, 13-18.
- Hunkapiller, M.W., Smallcombe, S.H., and Richards, J.H. (1975),  
Org. Magn. Res. 7, 262-265.
- Hunkapiller, M.W., Forgac, M.D., and Richards, J.H. (1976),  
Biochemistry 15, 5581-5588.

- Jencks, W.P. (1975), Adv. Enzymol. 43, 219-410.
- Kaplan, H., Symonds, V.B., Dugas, H., and Whitaker, D.R. (1970), Can. J. Biochem. 48, 649-658.
- Kawamura, K., Kondo, S., Maeda, K., and Umezawa, H. (1969), Chem. Pharm. Bull. 17, 1902-1909.
- Kennedy, W.P., and Schultz, R.M. (1979), Biochemistry 18, 349-356.
- Kondo, S., Kawamura, K., Iwanaga, J., Hamada, M., Aoyagi, T., Maeda, K., Takeuchi, T., and Umezawa, H. (1969), Chem. Pharm. Bull. 17, 1896-1901.
- Kraut, J. (1977), Ann. Rev. Biochem. 46, 331-358.
- Lewis, C.A., and Wolfenden, R. (1977a), Biochemistry 16, 4886-4890.
- Lewis, C.A., and Wolfenden, R. (1977b), Biochemistry 16, 4890-4895.
- Lienhard, G.E., Secemski, I.I., Koehler, K.A., and Lindquist, R.N. (1972), Cold Spring Harbor Symp. Quant. Biol. 36, 45-51.
- Lienhard, G.E. (1973), Science 180, 149-154.
- Lineweaver, H., and Burk, D. (1934), J. Am. Chem. Soc. 56, 658-666.
- Lowe, G., and Nurse, D. (1977), J. Chem. Soc. Chem. Commun., 815-817.
- Lucas, E.C., Caplow, M., and Bush, K.J. (1973), J. Am. Chem. Soc. 95, 2670-2673.
- Mancuso, A.J., Huang, S.-L., and Swern, D. (1978), J. Org. Chem. 43, 2480-2482.

- Matthews, D.A., Alden, R.A., Birktoft, J.J., Freer, S.T., and Kraut, J. (1977), J. Biol. Chem. 252, 8875-8883.
- Mattis, J.A., Heneş, J.B., and Fruton, J.S. (1977), J. Biol. Chem. 252, 6776-6782.
- Mozingo, R. (1955), in "Organic Syntheses--Collected Volume 3", E.C. Horning, ed., John Wiley and Sons, New York, 685-690.
- O'Leary, M.H., and Kluetz, M.D. (1972), J. Am. Chem. Soc. 94, 3585-3589.
- Pauling, L. (1948), Amer. Sci. 36, 51-58.
- Pfritzner, K.E., and Moffatt, J.G. (1963), J. Am. Chem. Soc. 85, 3027-3028.
- Pfritzner, K.E., and Moffatt, J.G. (1965), J. Am. Chem. Soc. 87, 5661-5670.
- Ratcliffe, R., and Rodehorst, R. (1970), J. Org. Chem. 35, 4000-4001.
- Robertus, J.D., Kraut, J., Alden, R.A., and Birktoft, J.J. (1972), Biochemistry 11, 4293-4303.
- Rosenmund, K.W. (1918), Ber. 51, 585-593.
- Rosenmund, K.W., and Zetzsche, F. (1921), Ber. 54, 425-440.
- Satterthwait, A.C., and Jencks, W.P. (1974), J. Am. Chem. Soc. 96, 7018-7031.
- Sawyer, L., Shotton, D.M., Campbell, J.W., Wendell, P.L., Muirhead, H., Watson, H.C., Diamond, R., and Ladner, R.C. (1978), J. Mol. Biol. 118, 137-208.
- Schultz, R.M., and Cheerva, A.C. (1975), FEBS Letters 50, 47-49.
- Shaw, M.C., and Whitaker, D.R. (1973), Can. J. Biochem. 51, 112-114.

- Stroud, R.M. (1974), Sci. Amer. 231, 74-88.
- Stroud, R.M., Krieger, M., Koeppe, R.E. II, Kossiakoff, A.A., and Chambers, J.L. (1975), in "Proteases and Biological Control", E. Reich, D.M. Rifkin, and E. Shaw, eds., Cold Spring Harbor Laboratory, Cold Spring Harbor, New York, 13-32.
- Suda, H., Aoyagi, T., Hamada, M., Takeuchi, T., and Umezawa, H. (1972), J. Antibiotics 25, 263-265.
- Thompson, R.C. (1973), Biochemistry 12, 47-51.
- Thompson, R.C. (1977), in "Methods in Enzymology", vol. XLVI, W.B. Jakoby and M. Wilchek, eds., Academic Press, New York, 220-225.
- Umezawa, H., Aoyagi, T. Morishima, H., Kunimoto, S., Matsuzaki, M., Hamada, M., and Takeuchi, T. (1970), J. Antibiotics 23, 425-427.
- Umezawa, H., Aoyagi, T., Okura, A., Morishima, H., Takeuchi, T., and Okami, Y. (1973), J. Antibiotics 26, 787-789.
- Warshel, A. (1981), Biochemistry 20, 3167-3177.
- Warshel, A., Russell, S., and Weiss, R.M. (1982), in "Chemical Approaches to Understanding Enzyme Catalysis", B.S. Green, Y. Ashani, and D. Chipman, eds., Elsevier Scientific Publishing Company, New York, 267-274.
- Westerik, J.O., and Wolfenden, R. (1972), J. Biol. Chem. 247, 8195-8197.
- Whitaker, D.R. (1970), in "Methods in Enzymology", vol. XIX, G.E. Perlmann and L. Lorand, eds., Academic Press, New York, 599-612.

Wolfenden, R. (1972), Acc. Chem. Res. 5, 10-18.

Wolfenden, R. (1976), Ann. Rev. Biophys. Bioeng. 5, 271-306.

## CHAPTER V

KINETIC AND NUCLEAR MAGNETIC RESONANCE STUDIES  
OF  $\alpha$ -LYTIC PROTEASE AND TRANSITION STATE ANALOGS

## II. BENZENE BORONIC ACID

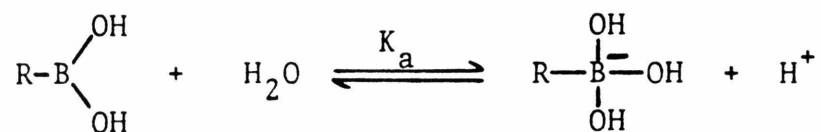
## ABBREVIATIONS

Asp	L-Aspartic acid
Ser	L-Serine
His	L-Histidine
PEBA	2-Phenylethane boronic acid
BBA	Benzeneboronic acid
NMR	Nuclear magnetic resonance
FID	Free induction decay
ppm	Parts per million
CD <sub>3</sub> OD	Perdeuterated methanol

## CHAPTER V--INTRODUCTION

The transition state of the acylation or deacylation process in the serine protease catalyzed hydrolysis of esters and amides is proposed to be a covalent tetrahedral adduct of the substrate and Ser 195 of the active site of these enzymes (Blow, 1976; Kraut, 1977; and references cited therein). The usefulness of transition state analogs (Wolfenden, 1972; Lienhard et al., 1972; Lienhard, 1973; Wolfenden, 1976) in studying the transient structures of catalysis has been described in the preceding chapter of this thesis. These reagents are stable molecules capable of binding to the active site of the enzyme and, in the case of the serine proteases, assuming a tetrahedral configuration similar to that of the substrate portion of the transition state. Transition state theory (Fersht, 1974; Wolfenden, 1976) predicts that these molecules will be potent reversible inhibitors of these enzymes.

The boronic acids have been studied as potential transition state analogs of the serine proteases. Boronic acids ionize in water by the mechanism depicted in Scheme I below.



Scheme I

Since these molecules can exist as negatively charged tetrahedral adducts, it is possible that they may combine with the active site serine residue of these enzymes to yield structures similar to the proposed transition state.

The interaction of boronic acids with serine proteases has been discussed in terms of three possible structures, as depicted in Figure 1, although other structures are possible. Figure 1A represents an esterification of the boronic acid by the hydroxyl side-chain of Ser 195; in this case, the boron atom remains trigonal. Figure 1B represents the addition of the imidazole side-chain of His 57 to the boronic acid to form a tetrahedral adduct; such an adduct has been observed for the interaction of N-methylimidazole and imidazole with boronic acids (Rawn and Lienhard, 1974; Philipp and Bender, 1971). Figure 1C represents the addition of the hydroxyl side-chain of Ser 195 to the boronic acid to form a tetrahedral adduct, akin to the transition state of enzymatic hydrolysis.

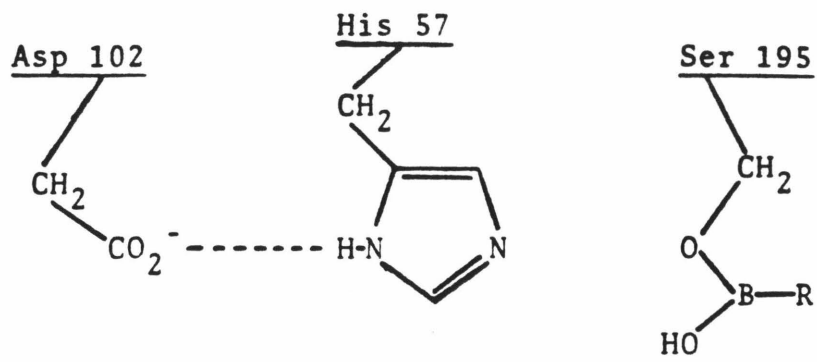
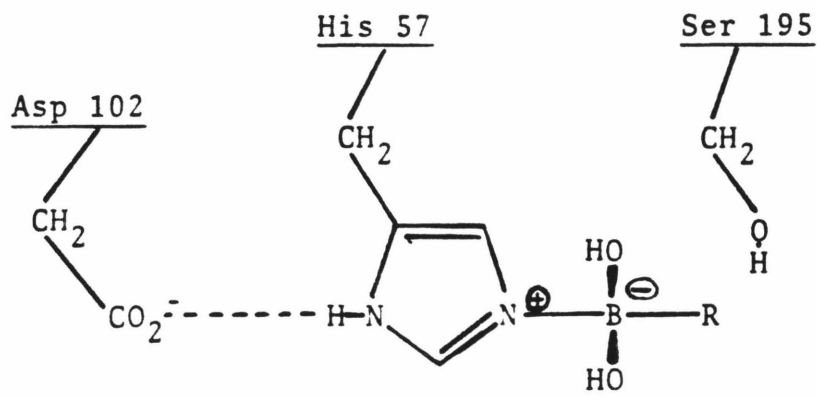
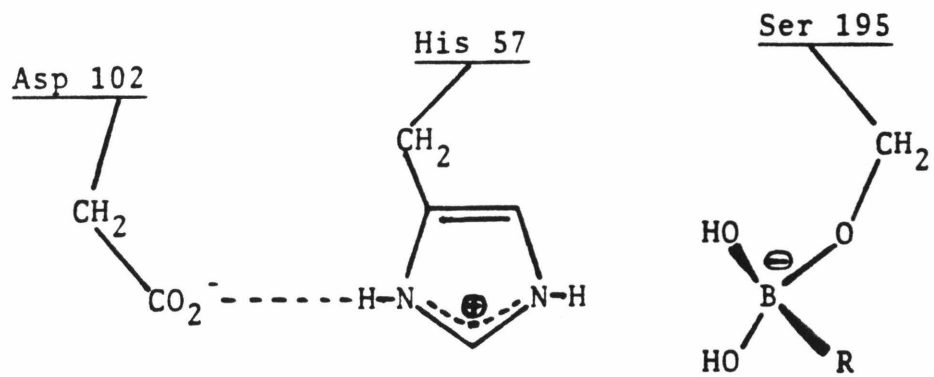
Early studies (Antonov et al., 1970; Philipp and Bender, 1971; Antonov et al., 1972) interpreted the competitive inhibition of the homologous serine proteases chymotrypsin and subtilisin by alkyl and aryl boronic acids in terms of structure 1B. However, more recent studies (Lindquist and Terry, 1974; Koehler and Lienhard, 1971; Rawn and Lienhard, 1974; Nakatani et al., 1975 a,b; Hanai, 1976; Hanai, 1977; Hess et al., 1975; Matteson et al., 1981; Philipp and Maripuri, 1981) have suggested that the interaction between these enzymes and specific and non-specific boronic acids corresponds to the structure of Figure 1C; this has also been suggested by a study of acetylcholine esterase inhibition by a specific boronic acid acetylcholine analog (Koehler and Hess, 1974). Byers and Koshland (1978) have shown that 2-phenylethane boronic

Figure 1. Proposed structures of the interaction between boronic acids and the catalytic triad of serine proteases.

A) Esterification of the boronic acid by the hydroxyl side-chain of Ser 195.

B) Addition of N-1 of His 57 to the boron atom of the boronic acid.

C) Addition of  $\gamma$ O of Ser 195 to the boron atom of the boronic acid.

ABC

acid binds moderately well ( $K_I = 18 \text{ mM}$ ) to methylchymotrypsin, a synthetic derivative of chymotrypsin in which N-1 of the imidazole ring of His 57 has been methylated, further suggesting an adduct of Ser 195 and the boronic acid.

X-ray crystallographic determinations (Matthews et al., 1975) of the structure of the complexes of subtilisin and 2-phenylethane boronic acid (PEBA) and of subtilisin and benzenboronic acid (BBA) have supported the interpretation that these complexes exist as tetrahedral adducts of Ser 195 and the boronic acid. This conclusion was based on the observation that the boron atom of the inhibitor is within covalent bond distance of the Ser 195  $\gamma$ O in the complexes; furthermore, the boron atom is too distant from N-1 of the imidazole ring of His 57 for a covalent bond to exist between these two atoms, thus contraindicating the structure in Figure 1B. A  $^1\text{H}$  NMR investigation of the proton located between Asp 102 and His 57 in these complexes and in the chymotrypsin complexes with these boronic acids is also consistent with this structural assignment (Robillard and Shulman, 1974b).

We discovered that BBA is a moderately effective inhibitor of  $\alpha$ -lytic protease, albeit that it is a non-specific substrate analog of this enzyme. This fortuitous observation allowed us to study both the enzyme and inhibitor portions of the complex by  $^{13}\text{C}$  and  $^{11}\text{B}$  NMR, respectively, in order to gain some insight into the nature of the complex and its relationship to the catalytic process of the serine proteases.

## EXPERIMENTAL

Materials.

Benzeneboronic acid (BBA) was purchased from Aldrich, and was recrystallized twice from hot water after treatment with decolorising charcoal (Norit). The long white needles were dried overnight in air and were stored at  $-20^{\circ}\text{C}$ .

$\alpha$ -Lytic protease was isolated and purified as described in Chapters II and III of this thesis. All enzyme solutions for kinetics were made up in double-distilled water as needed.

All buffer materials were reagent grade; buffers were made up in double-distilled water. All pH measurements were made using a Radiometer model PHM26 pH meter equipped with a combination electrode (Radiometer model GK2322C), and are uncorrected for the small amounts of organic solvents used in the experiments.

Methods.

Kinetics. Inhibition kinetics were performed either in a Radiometer pH-Stat using N-benzoyl-L-alanine methyl ester as the substrate, or in a Beckman Acta CIII UV-visible spectrophotometer using N-acetyl-L-alanyl-L-prolyl-L-alanine p-nitro-anilide as the substrate. In general, the procedures used were the same as those described in Chapter IV of this thesis. All kinetic runs were done in  $0.1 \text{ M}$  KCl, at  $25.0 \pm 0.2^{\circ}\text{C}$ . In the spectrophotometric method,  $S_0$  was always less than  $0.05 K_m$ , so that good pseudo-first-order kinetics were observed. The substrate solution was buffered to the desired pH by

addition of an aliquot of 1 M buffer component (sodium acetate or sodium dihydrogen phosphate, final concentration in the cuvette 0.04 M, see Chapter IV). In order to prevent a substantial change in the pH on addition of the (acidic) inhibitor, especially around pH 8-9 where ionization of BBA occurs, stock BBA solutions in 50% (v/v) aqueous methanol were titrated to near the desired pH with concentrated KOH solution. In all cases, the difference in pH between solutions with and without added inhibitor was less than 0.05 pH unit. Preliminary experiments performed in the pH-Stat using the method of Dixon (1953) indicated that the inhibition was purely competitive within experimental error. Therefore, inhibition constants ( $K_I^{\text{app}}$ ) were calculated from the equation

$$K_I^{\text{app}} = \frac{I_0}{(v_0/v_i) - 1}$$

where  $I_0$  is the total concentration of BBA (>> total enzyme concentration), and  $v_0$  and  $v_i$  are the initial zero-order velocities in the absence of and in the presence of inhibitor, respectively (see Appendix II, Chapter IV). Values of  $I_0$  ranged from 0.2 to 5 times  $K_I^{\text{app}}$  except at low pH where solubility considerations prevented  $I_0$  from being larger than  $K_I$ .

NMR samples. Samples were made up by dissolving the desired amount of protein in 0.1 M KCl, 80% double-distilled water/20%  $^2\text{H}_2\text{O}$  (v/v). A small aliquot of concentrated BBA solution (in either methanol or dimethylformamide) was then added, and the pH of the resulting solution was adjusted to the

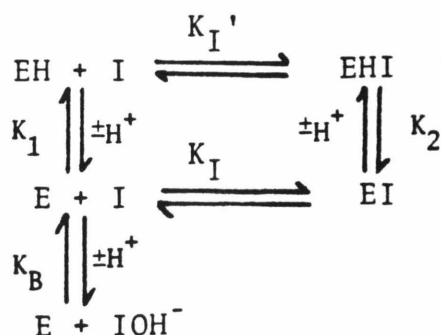
desired value by the procedure outlined in Chapter II. Any insoluble material was removed by centrifugation at 10,000 rpm for 15 minutes at room temperature, since BBA is only sparingly soluble in cold water. The pH of each sample was checked prior to and following each spectrum; in all cases, the initial and final pH readings agreed to within 0.04 pH unit. As in Chapter IV, it was assumed that the concentration of active protein throughout the NMR experiment was constant, since activity assays were not reliable in the presence of large concentrations of inhibitor.

NMR spectra.  $^{13}\text{C}$  and  $^{11}\text{B}$  NMR spectra were taken on a Varian XL-200 spectrometer operating at 50.3 MHz for  $^{13}\text{C}$  and 64.17 MHz for  $^{11}\text{B}$  using standard pulsed Fourier transform technology. All spectra were taken with the constant temperature device of the spectrometer operating at  $25.0 \pm 0.2^\circ\text{C}$ . All samples were 2.5-3.0 ml in 10 mm diameter tubes, containing 20% (v/v)  $^2\text{H}_2\text{O}$  to provide an internal field-frequency lock. Chemical shifts for carbon are reported relative to the arginine guanidinium carbons of the protein which resonate at 157.25 ppm down-field from the methyl carbons of external tetramethylsilane and whose position did not change ( $\pm 0.05$  ppm) over the pH range investigated. Chemical shifts for boron are reported relative to external boric acid (a saturated  $\text{H}_3\text{BO}_3$  in 20%  $^2\text{H}_2\text{O}/80\% \text{H}_2\text{O}$  (v/v)).

RESULTS

Inhibition kinetics. Table I presents binding constants for the inhibition of  $\alpha$ -lytic protease activity by BBA and other structurally related ring compounds at pH 8. Clearly, BBA interacts with the enzyme in some special way, as  $\alpha$ -lytic protease normally shows little affinity for compounds possessing a phenyl ring. Interestingly, the enzyme appears to exhibit a slightly greater affinity for benzaldehyde than for p-toluene-sulfonic acid, aniline, or benzyl alcohol, in accord with the ability of aldehydes to form covalent adducts with serine proteases as described in Chapter IV.

The values of  $K_I^{\text{app}}$  as a function of pH are presented in Figure 2. The general shape of the curve described by these data is similar to that seen for the inhibition of chymotrypsin by PEBA (Koehler and Lienhard, 1971) and BBA (Hanai, 1976), of subtilisin by PEBA (Lindquist and Terry, 1974) and BBA (Philipp and Bender, 1971), and of acetylcholine esterase by N,N-trimethylpropylammonium bromide methanaborinic acid (Koehler and Hess, 1974). Such data have generally been interpreted according to the following mechanism (Koehler and Hess, 1974; Lindquist and Terry, 1974):

Scheme II

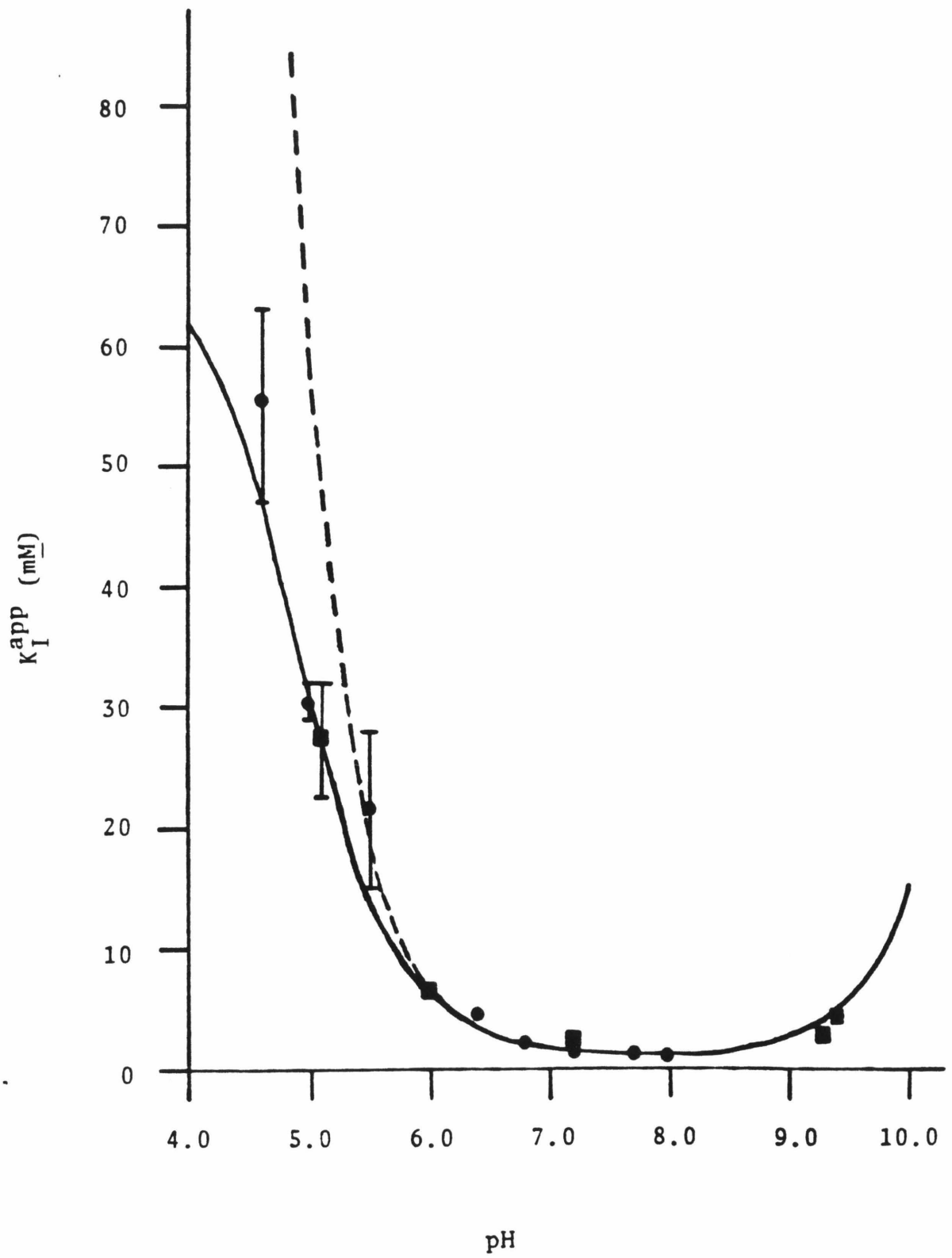
**TABLE I.** Kinetic constants for the inhibition of  $\alpha$ -lytic protease by various aromatic compounds.<sup>a</sup>

Inhibitor	$K_I^{\text{app}}$ (M)
p-Toluenesulfonic acid $p\text{-CH}_3\text{C}_6\text{H}_4\text{SO}_3\text{H}$	$0.11 \pm 0.01^b$
Aniline $\text{C}_6\text{H}_5\text{NH}_2$	$0.18 \pm 0.03^b$
Benzyl alcohol $\text{C}_6\text{H}_5\text{CH}_2\text{OH}$	$0.20 \pm 0.05^b$
Benzaldehyde $\text{C}_6\text{H}_5\text{CHO}$	$0.06 \pm 0.02^b$
Benzeneboronic acid $\text{C}_6\text{H}_5\text{B(OH)}_2$	$0.0013 \pm 0.0002^b$

<sup>a</sup>All constants are reported as the average  $\pm$  one standard deviation of at least four determinations.

<sup>b</sup>Determined using the pH-Stat. Solution conditions: 0.25 M KCl, 5 mM sodium phosphate, 4% (v/v) methanol, pH 8.1, 25.0  $\pm$  0.2°C.

Figure 2.  $K_I^{\text{app}}$  as a function of pH for the benzenboronic acid inhibition of  $\alpha$ -lytic protease. Solution conditions: 0.1 M KCl, 0.04 M buffer (acetate or phosphate),  $25.0 \pm 0.2^\circ\text{C}$ . The closed circles represent kinetic runs performed spectroscopically using N-acetyl-L-alanyl-L-prolyl-L-alanine p-nitro-anilide as the substrate ( $E_0 = 1.0 - 2.5 \mu\text{M}$ ,  $S_0 = 0.2 - 0.5 \text{mM}$ ; see Methods). The closed squares represent kinetic runs performed in the pH-Stat using N-benzoyl-L-alanine methyl ester as the substrate ( $E_0 = 2 - 5 \mu\text{M}$ ,  $S_0 = 5 - 10 \text{mM}$ ; see Methods). The solid curve was fit to equation (1) using  $\text{p}K_1 = 6.7$ ,  $\text{p}K_2 = 4.9$ ,  $\text{p}K_B = 8.9$ , and  $K_I = 1.1 \times 10^{-3} \text{M}$ . The dashed curve was fit to equation (2) using  $\text{p}K_A = 6.7$ ,  $\text{p}K_B = 8.9$ , and  $K_I = 1.3 \times 10^{-3} \text{M}$ . Both curves overlap for  $\text{pH} > 6$ . The error bars in all cases represent  $\pm$  (one standard deviation of the average of at least six determinations of  $K_I^{\text{app}}$ ).



The mechanism indicates that the free boronic acid can interact with both the basic (E) and acidic (EH) forms of the active site of the enzyme only when the boronic acid is present in solution in its neutral, trigonal configuration (I). The basic, tetrahedral form of the free inhibitor in solution ( $\text{IOH}^-$ ) is assumed not to bind appreciably to the enzyme. This assumption accords with the observation of the poor binding affinity of  $\alpha$ -lytic protease for peptide alcohols and acetals discussed in Chapter IV. The expression relating  $K_I^{\text{app}}$  to the constants of Scheme II and the pH is given by equation (1):

$$K_I^{\text{app}} = \frac{(1 + \{(H^+)/K_1\})(1 + \{K_B/(H^+)\})}{(1 + \{(H^+)/K_2\})} K_I. \quad (1)$$

However, the previously published studies were carried out using inhibitors resembling specific substrates of the enzymes investigated (chymotrypsin and subtilisin). In the present experiment, BBA does not resemble the good substrates of  $\alpha$ -lytic protease (alanine derivatives), and thus is a non-specific analog for this enzyme. As such, BBA might be expected to bind with high affinity only to catalytically active enzyme (the basic form E in Scheme II), and poorly to catalytically disabled enzyme (the acidic form EH). Thus  $K_I^{\text{app}}$  may be so large in this case as to be unimportant, so that the expression in equation (1) is modified to that of equation (2):

$$K_I^{\text{app}} = K_I (1 + \{(H^+)/K_1\})(1 + \{K_B/(H^+)\}) . \quad (2)$$

The raw data in Figure 2 have been compared to the expectations of both equation (1) and equation (2). The solid line in the figure has been fit to equation (1) using  $pK_1 = 6.7$ ,  $pK_2 = 4.9$ ,  $pK_B = 8.9$ , and  $K_I = 1.1 \text{ mM}$ . The dashed line in the figure has been fit to equation (2) using  $pK_1 = 6.7$ ,  $pK_B = 8.9$ , and  $K_I = 1.3 \text{ mM}$ . The relative merit of each fit will be mentioned later.  $^{13}\text{C}$  NMR results. It is not possible to carry out a full titration of the  $\alpha$ -lytic protease/BBA complex under conditions where the enzyme is saturated with inhibitor due to the limited solubility of BBA in aqueous solution, especially at low pH, and the unfavorable dissociation constant for the complex at  $\text{pH} > 6$  or  $\text{pH} < 9.5$ . However, we were able to determine the chemical shift and coupling constant of the  $^{13}\text{C}$  resonance assigned to C-2 of His 57 of  $\alpha$ -lytic protease in the complex over the pH range 6 to 9, under conditions where the enzyme is at least 96% saturated with BBA. These data are reported in Table II, and representative spectra are shown in Figures 3 and 4. Over this range, the chemical shift of the resonance does not change appreciably, within experimental error. Furthermore, the coupling constant remains constant at  $211 \pm 2 \text{ Hz}$  for pH 6 to 9, contrary to its behavior in the free enzyme.

We also investigated the NMR parameters of C-2 of imidazole in the complex of imidazole and BBA in both aqueous and perdeuterated methanolic ( $\text{CD}_3\text{OD}$ ) solution. This complex is reported to be a tetrahedral adduct of the imidazole and the

TABLE II.  $^{13}\text{C}$  NMR parameters for the C-2 carbon of the Histidine 57 residue of  $\alpha$ -lytic protease in the free enzyme and in the enzyme/benzeneboronic acid (BBA) complex.

pH	$\delta$ (ppm) <sup>a</sup>	$^1J_{\text{CH}}$ (Hz) <sup>b</sup>
<u>Free enzyme</u> <sup>c</sup>		
5.2	134.48	222
6.0	134.68	---
7.0	135.90	216
8.0	136.80	---
8.6	136.78	206
9.0	136.86	---
<u>Enzyme + BBA</u> <sup>g</sup>		
6.0	135.53	---
6.5	135.81	---
7.0	135.79	213 <sup>d</sup>
7.5	135.80	---
8.0	135.81	211 <sup>e</sup>
8.5	135.87	---
9.0	135.83	---
9.5	135.90	210 <sup>f</sup>

<sup>a</sup>Chemical shift values are  $\pm 0.10$  ppm, and are reported relative to external tetramethylsilane = 0.00 ppm.

<sup>b</sup> $^1J_{\text{CH}}$  values are  $\pm 2$  Hz.

<sup>c</sup>Data from Chapter II.

<sup>d</sup>Average of two determinations : 213, 212.

<sup>e</sup>Average of three determinations: 212, 212, 209.

<sup>f</sup>Single determination.

<sup>g</sup>3.5 mM enzyme, 0.175 M BBA, 0.1 M KCl, 20% (v/v)  $^2\text{H}_2\text{O}$ .

Figure 3. 50.3 MHz broadband proton decoupled  $^{13}\text{C}$  NMR spectra of the complex of (2- $^{13}\text{C}$ )-histidyl- $\alpha$ -lytic protease and benzenboronic acid in 0.1 M KCl, 20% (v/v)  $^2\text{H}_2\text{O}$ , 8% (v/v) dimethylformamide, at  $25.0 \pm 0.2^\circ\text{C}$ . The sample contained 3.5 mM protein and 175 mM inhibitor. The spectra were taken with a 12000 Hz sweep width, using a 0.20 sec acquisition time and a  $90^\circ$  pulse of 14  $\mu\text{sec}$ . In each spectrum, 4800 FID points were zero-filled to a Fourier number of 8192, and were transformed with 10 Hz line broadening.

A) 23,215 transients, pH 8.0.

B) 18,000 transients, pH 6.0.

The starred resonance in each spectrum is that assigned to C-2.

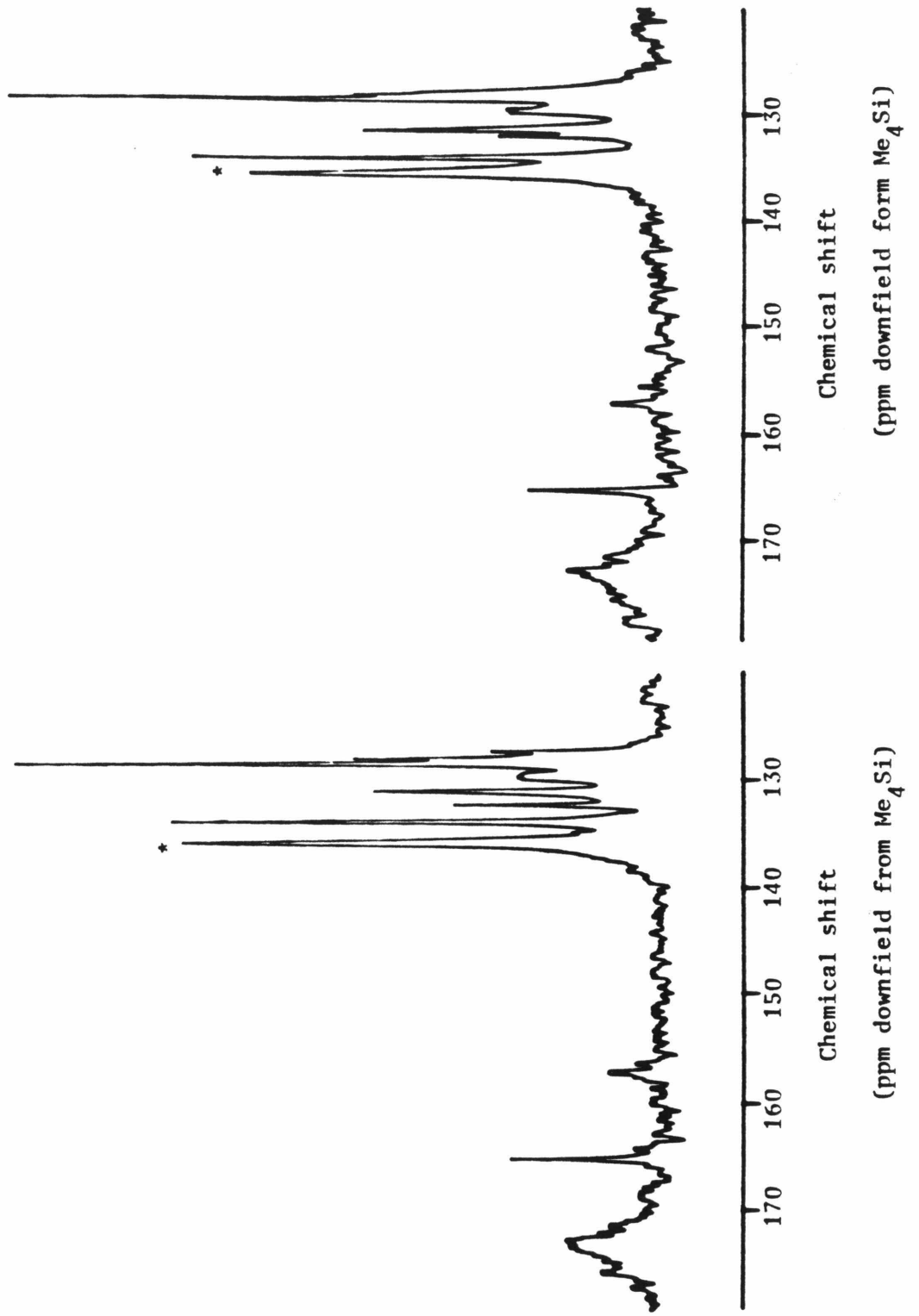
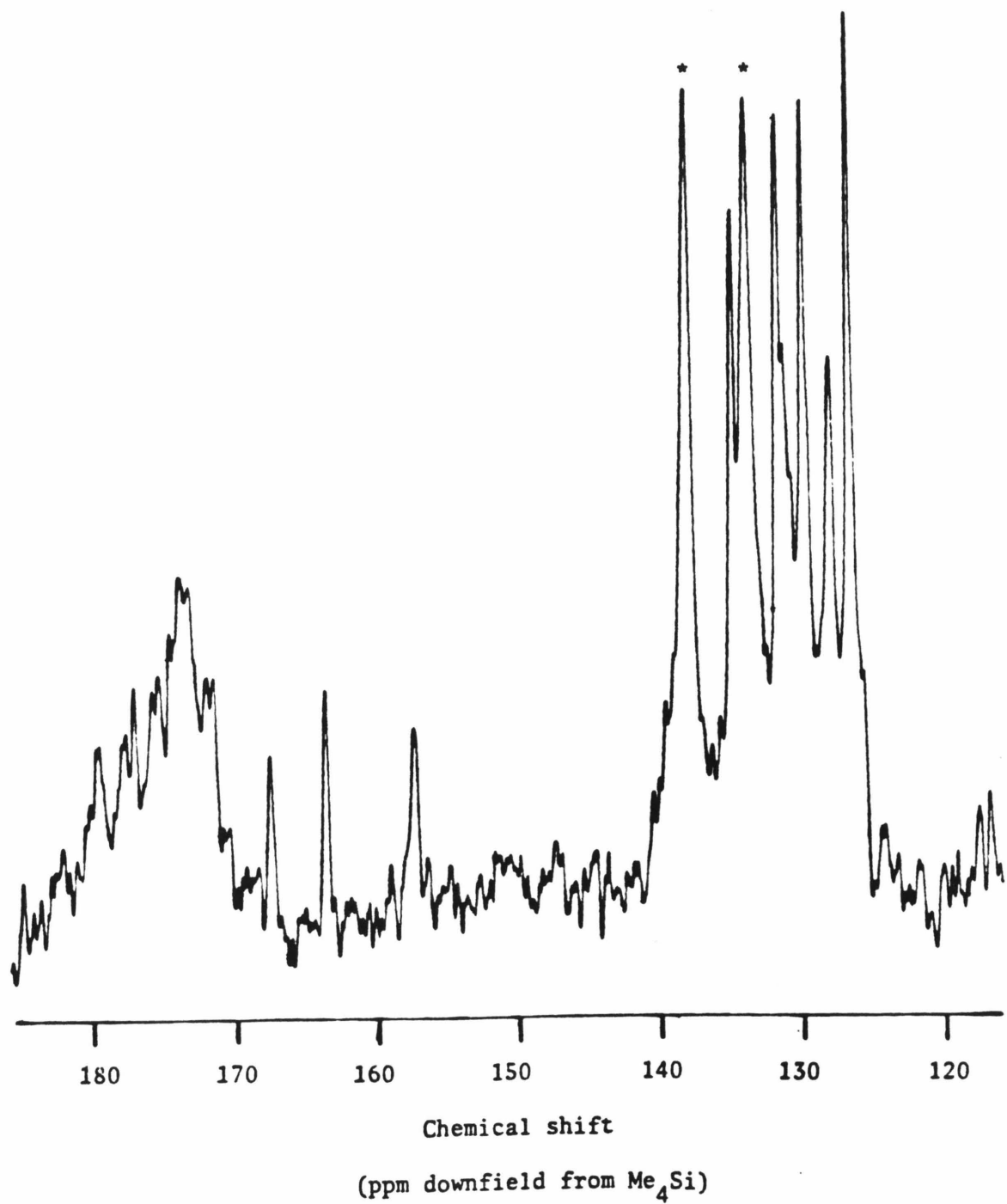
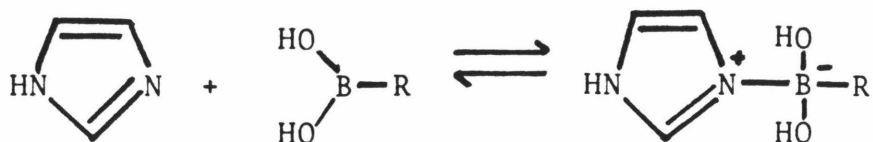


Figure 4. 50.3 MHz proton coupled  $^{13}\text{C}$  NMR spectra of the complex of (2- $^{13}\text{C}$ )-histidyl- $\alpha$ -lytic protease and benzenboronic acid in 0.1 M KCl, 20% (v/v)  $^2\text{H}_2\text{O}$ , 8% (v/v) dimethylformamide, at  $25.0 \pm 0.2^\circ\text{C}$ . The sample contained 3.5 mM protein and 175 mM inhibitor. The spectrum was taken with a 12000 Hz sweep width, using a 0.2 sec acquisition time and a  $90^\circ$  pulse of 14  $\mu\text{sec}$ . 4800 FID points were zero-filled to a Fourier number of 8192, and were transformed with 10 Hz line broadening. The starred resonances in the spectrum are those assigned to C-2. The pH of the sample was 8.1.



boronic acid (Philipp and Bender, 1971; Noth and Wrackmeyer, 1978), as depicted in Scheme III.



Scheme III

These results are summarized in Table III. The most interesting observation is the value of the coupling constant of C-2 of imidazole in this complex. The result of five determinations gives  $^1J_{\text{CH}} = 211 \pm 2$  Hz, either in  $\text{CD}_3\text{OD}$  or at pH 8.1 in aqueous solution. This value is about 10 Hz smaller than that usually observed for protonated imidazoles (Wasylishen and Tomlinson, 1975; Hunkapiller et al., 1973).

$^{11}\text{B}$  NMR results. Philipp and Bender (1971) have reported large (17-18 ppm) chemical shift changes for  $^{11}\text{B}$  nuclei between trigonal and tetrahedral configurations. Table IV summarizes the relevant NMR parameters for the transition between neutral, trigonal symmetry and anionic, tetrahedral symmetry for boric acid and BBA on the addition of hydroxide ion. The  $^{11}\text{B}$  chemical shift values show an 18-26 ppm upfield shift for this transition; moreover, there is a significant line narrowing for this transition as well. This is to be expected, since the primary relaxation mechanism for  $^{11}\text{B}$  nuclei ( $I = 3/2$ ) is due to the quadrupole moment of the  $^{11}\text{B}$  nucleus; thus, relaxation should be more efficient in the less symmetric trigonal configuration than in the more symmetric tetrahedral configuration. This is

TABLE III.  $^{13}\text{C}$  NMR parameters for the C-2 carbon of imidazole in the absence and in the presence of benzenboronic acid (BBA).

Sample	pH	$\delta$ (ppm) <sup>a</sup>	$^1J_{\text{CH}}$ (Hz) <sup>b</sup>
0.5 M imidazole in 0.1 M KCl, 20% (v/v) $^2\text{H}_2\text{O}$	8.4	136.10	208
	5.1	134.08	221
0.5 M imidazole in $\text{CD}_3\text{OD}$	---	136.69	207
0.1 M imidazole and 0.1 M BBA in 0.1 M KCl, 20% (v/v) $^2\text{H}_2\text{O}$	6.1	134.33	217
	8.1	136.46	211 <sup>c</sup>
	9.9	136.74	210
0.5 M imidazole and 0.5 M BBA in $\text{CD}_3\text{OD}$	---	136.50	211 <sup>d</sup>

<sup>a</sup>Chemical shift values are  $\pm$  0.1 ppm and are reported relative to external tetramethylsilane = 0.00 ppm.

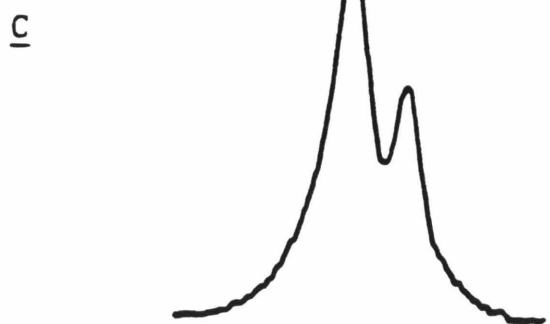
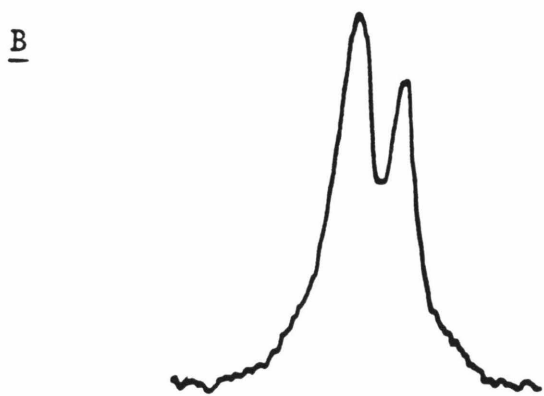
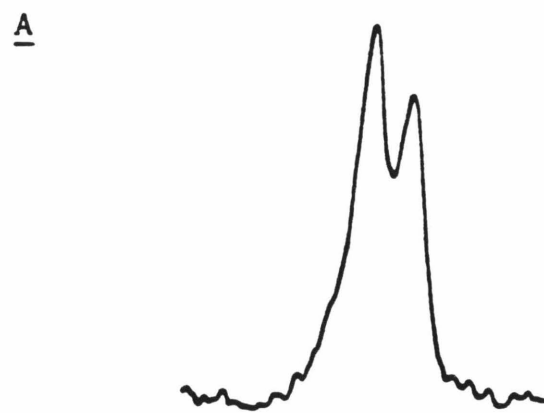
<sup>b</sup> $^1J_{\text{CH}}$  values are  $\pm$  2 Hz.

<sup>c</sup>Average of five determinations: 212, 211, 213, 210, 211.

<sup>d</sup>Average of three determinations: 210, 211, 211.

Figure 5. 64.17 MHz  $^{11}\text{B}$  NMR spectra of the complex of  $\alpha$ -lytic protease with benzenboronic acid in 0.1 M KCl, 20% (v/v)  $^2\text{H}_2\text{O}$ , 0.04 M sodium phosphate, 4% (v/v) methanol, pH 8.1, at  $25.0 \pm 0.2^\circ\text{C}$ . The sample contained 5.0 mM enzyme. The spectra were taken with a 20,000 Hz sweep width, using a 0.05 sec acquisition time and a  $90^\circ$  pulse of 12.0  $\mu\text{sec}$ . In each spectrum, 2000 FID points were zero-filled to a Fourier number of 4096, and were transformed using a line broadening of 50 Hz.

- A) 5.0 mM benzenboronic acid, 38,931 transients.
- B) 10.0 mM benzenboronic acid, 50,646 transients.
- C) 20.0 mM benzenboronic acid, 26,978 transients.



40 20 0 -20 -40

Chemical Shift  
(ppm from sat'd  $\text{H}_3\text{BO}_3$ )

TABLE IV.  $^{11}\text{B}$  NMR parameters for some boron-containing acids.

Sample	pH	$\delta$ (ppm) <sup>a</sup>	$\nu_{1/2}$ (Hz) <sup>b</sup>
$\text{H}_3\text{BO}_3$ (saturated aqueous solution, 20% (v/v) $^2\text{H}_2\text{O}$ )	---	0.0	80
$\text{Na}_2\text{B}_4\text{O}_7 \cdot 10\text{H}_2\text{O}$ (0.09 M aqueous solution, 20% (v/v) $^2\text{H}_2\text{O}$ )	12.5	-17.0	35
Benzenboronic acid (BBA) (0.17 M aqueous solution, 4% (v/v) methanol, 20% (v/v) $^2\text{H}_2\text{O}$ )	5.6	9.7	240
	6.2	9.4	260
	8.0	5.3	260
	8.3	5.0	250
	9.9	-13.7	120
	12.2	-16.7	120
BBA (0.5 M in $\text{CD}_3\text{OD}$ )	---	10.9	240
BBA + Imidazole (0.17 M aqueous solution, 4% (v/v) methanol, 20% (v/v) $^2\text{H}_2\text{O}$ )	6.1	7.8	240
	8.1	-4.1	230
	9.9	-13.7	120
BBA + Imidazole (0.5 M in $\text{CD}_3\text{OD}$ )	---	0.0	300

<sup>a</sup>Chemical shift values are  $\pm 0.2$  ppm, and are reported relative to external saturated aqueous Boric acid = 0.00 ppm. Positive values are downfield of 0.00; negative values are upfield of 0.00.

<sup>b</sup> $\nu_{1/2}$  values are  $\pm 10\%$ .

reflected in the broader lines for  $^{11}\text{B}$  nuclei in the neutral, trigonal species as opposed to the anionic, tetrahedral species.

Table IV also gives the NMR parameters for  $^{11}\text{B}$  in equimolar mixtures of imidazole and BBA in water and in  $\text{CD}_3\text{OD}$ . From the chemical shift and linewidth data we determine that little complex formation occurs at pH 6.1, where the imidazole is extensively protonated, and at pH 9.9, where the boronic acid exists primarily in its ionized form, but that at pH 8.1 the mixture is predominantly a tetrahedral addition complex of the boronic acid and imidazole. This adduct is also the major species existing in  $\text{CD}_3\text{OD}$ . It should be noticed that the chemical shift difference between free BBA in solution and BBA in the complex with imidazole is smaller (9-11 ppm) than that observed for free BBA and BBA in a complex with hydroxide ion (18-26 ppm).

The  $^{11}\text{B}$  NMR data for the  $\alpha$ -lytic protease/BBA complex at pH 8.1 is given in Table V; representative spectra are shown in Figure 5. The acquisition of these spectra are complicated by the low concentrations of BBA used in order to assure that a suitably large fraction of the total  $^{11}\text{B}$  NMR signal is due to BBA in the enzyme/inhibitor complex, the broadness of the lines due to chemical exchange, and a moderate degree of interference from  $^{11}\text{B}$  nuclei in the borosilicate glass of the NMR tube. However, two overlapping resonances in slow to intermediate exchange are observed for a mixture of  $\alpha$ -lytic protease and BBA. Both signals are extensively line broadened due to chemical exchange ( $\nu_{1/2} = 600-$

**TABLE V.**  $^{11}\text{B}$  NMR parameters for benzenboronic acid in the presence of and in the absence of  $\alpha$ -lytic protease at pH 8.1 in 0.1 M KCl, 0.04 M sodium phosphate, 20% (v/v)  $^2\text{H}_2\text{O}$ ,  $25.0 \pm 0.2^\circ\text{C}$ .

$(I_0)$ (mM) <sup>a</sup>	$\delta_{\text{F}}$ (ppm) <sup>b</sup>	$\delta_{\text{B}}$ (ppm) <sup>c</sup>	$\delta_{\text{N}}$ (ppm) <sup>d</sup>	% Bound <sup>e</sup>
3.0	-1.2	-12.2	5.1	69
5.0	-1.0	-12.2	5.1	60
10.0	1.0	-12.3	5.1	41
20.0	3.3	-12.5	5.1	23

<sup>a</sup> $(I_0)$  = concentration of added benzenboronic acid.

<sup>b</sup> $\delta_{\text{F}}$  = chemical shift of the more downfield BBA peak observed in the presence of protein. All chemical shift values are  $\pm 0.2$  ppm and are reported relative to saturated aqueous boric acid = 0.00 ppm. Positive values are downfield of 0.00; negative values are upfield.

<sup>c</sup> $\delta_{\text{B}}$  = chemical shift of the more upfield BBA peak observed in the presence of protein.

$\delta_{\text{N}}$  = chemical shift of BBA in the absence of protein.

<sup>e</sup>% Bound = % of total BBA as enzyme-bound species in the presence of protein, as calculated from  $(I_0)$ ,  $K_{\text{I}}^{\text{app}} = 1.3 \times 10^{-3} \text{ M}$  at pH 8.1, and  $E_0 = 5.0 \text{ mM}$ .

750 Hz). The downfield peak is near the position expected for free BBA in solution at pH 8.1, and is therefore assigned to uncomplexed BBA in the enzyme/inhibitor mixture. The moderate upfield shift for this resonance in the presence of protein may be due to the exchange process, or to some non-specific interaction of BBA with the protein which could be substantial under the conditions of concentration used in the experiment, or to a combination of these effects. The observation that this peak shifts downfield toward the position of the  $^{11}\text{B}$  resonance of BBA in the absence of protein on increasing the BBA concentration from 3 mM to 20 mM in the presence of enzyme is consistent with the latter explanation.

The upfield peak observed in the  $^{11}\text{B}$  NMR spectrum of the  $\alpha$ -lytic protease/BBA complex can be assigned to BBA bound to the protein active site. This resonance is shifted upfield of the peak representing uncomplexed BBA in the presence of protein by 11-16 ppm, and of the peak representing BBA in the absence of protein at this pH by 17-18 ppm. For reasons to be discussed subsequently, we feel that this upfield peak represents a tetrahedral adduct of BBA and  $\alpha$ -lytic protease.

## DISCUSSION

Aryl boronic acids are moderate to potent reversible inhibitors of the serine proteases chymotrypsin and subtilisin. Since these compounds are capable of forming stable tetrahedral adducts with hydroxide ion in aqueous solution, and since both enzymes are specific for substrates possessing large hydrophobic moieties, it has been proposed that these aryl boronic acids are good transition state analogs of these enzymes, and as such the complex of boronic acid and serine protease exists as a negatively charged tetrahedral adduct of Ser 195 of the enzyme and the boron atom of the inhibitor.

The pH dependence of  $K_I^{\text{app}}$  for the inhibition of  $\alpha$ -lytic protease by BBA, an inhibitor related to structurally non-specific substrates of the enzyme, closely resembles the pH dependence of chymotrypsin inhibition by PEBA (Koehler and Lienhard, 1971) and BBA (Hanai, 1976), and of subtilisin inhibition by PEBA (Lindquist and Terry, 1874). This is somewhat surprising when one considers that substrates containing aromatic side-chains are normally poor substrates of  $\alpha$ -lytic protease but good substrates of the other two enzymes. This indicates that the favorable interactions of boronic acids with the serine proteases are largely due to the nature of the active site of these enzymes, and not their binding sites, and thus it implies that the affinity of  $\alpha$ -lytic protease for BBA is due to covalent bond formation between BBA and the active site of the enzyme, contraindicating the structure in Figure 1A.

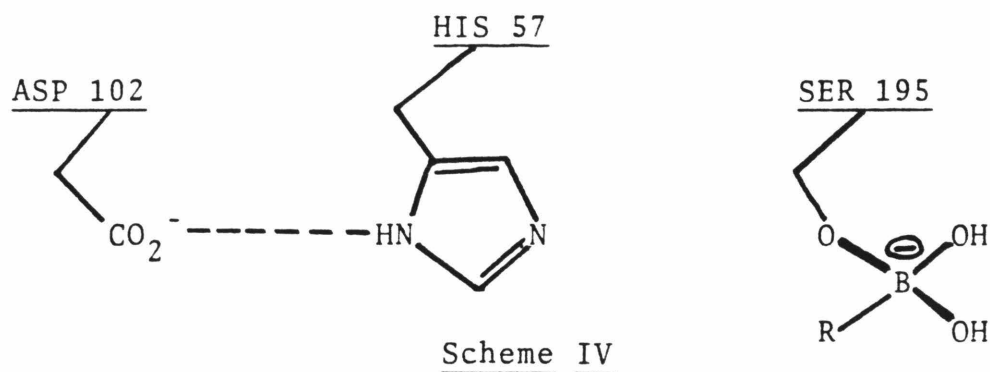
The  $K_I^{\text{app}}$  versus pH data of Figure 2 is fit more closely by equation (1) than equation (2). The value of  $pK_1$ , the ionization of the free enzyme, is the value determined in Chapters II and IV of this thesis, and represents the ionization of the His 57 residue of the protein. The value of  $pK_B$  approximates the acid dissociation constant of BBA (8.86, Branch et al., 1934); furthermore, since no catalytic dependence on a high pH ionization of the enzyme has been observed in kinetic studies of  $\alpha$ -lytic protease to date,  $pK_B$  can be assigned to the ionization of the inhibitor. The value of  $K_I$  was chosen to give the best fit to the data between pH 7.5 and 8.5, where  $K_I^{\text{app}} \approx K_I$ . The value of  $pK_2$  was chosen to give the best fit to the low pH arm of the data. The value of 4.9 used here accords well with the previously published reports for the subtilisin and chymotrypsin (4.8-5.0, Hanai;  $\leq 4.8$ , Lindquist and Terry, 1974;  $\leq 4.8$ , Koehler and Lienhard, 1971). The similarity of these  $pK_2$  values for the three different enzymes indicates that this  $pK_a$  represents a group in common to all three proteins. From  $pK_1$ ,  $pK_2$ , and  $K_I$  we can calculate a value for  $K_I'$  using the "thermodynamic box" approach; this value is 0.07 M, a value similar to that observed for binding of other aromatic compounds to  $\alpha$ -lytic protease. This may indicate that the low pH structure of the complex is a non-covalent one.

The  $^{11}\text{B}$  NMR spectra show two resonances for mixtures of BBA and  $\alpha$ -lytic protease at pH 8.1, ascribable to free and enzyme-bound forms of the inhibitor. The magnitude and

direction of the chemical shift difference between the downfield resonance and the upfield resonance confirms the implication of the data on the relation between  $K_I^{\text{app}}$  and pH. The complex is a covalent adduct at this pH, and it contains a tetrahedral  $^{11}\text{B}$  nucleus. The magnitude of this shift (-16 to -18 ppm) suggests that the adduct is formed between BBA and Ser 195, and not His 57, since the corresponding difference for the adducts of imidazole and BBA is only -9 to -11 ppm, while that for the addition of hydroxide ion to BBA is -18 to -26 ppm.

The  $^{13}\text{C}$  NMR data in Table II indicate that His 57 is the residue ionizing with a  $\text{pK}_a$  of 4.9 in the complex. The chemical shift of the C-2 nucleus of the imidazole ring of this residue in the complex remains nearly constant over the pH range 6.0 to 9.5, indicating that the  $\text{pK}_a$  of His 57 in the complex has been perturbed from its value in the free enzyme. The value of this chemical shift (135.8 ppm) is nearly midway between that observed for a neutral His 57 (136.8 ppm) and that for a protonated His 57 (134.5 ppm) in the free enzyme, and is of little help in determining the charge state of the ring. The value of the coupling constant ( $211 \pm 2$  Hz) is within experimental error of the value expected for a neutral imidazole ( $208 \pm 2$  Hz), but substantially smaller than that expected for a protonated imidazole ( $221 \pm 2$  Hz). It may be argued that this value is also that observed for C-2 in the model imidazole/BBA complexes (an interesting observation in itself), but the kinetic and  $^{11}\text{B}$  NMR results do not support this premise.

The results of this experiment therefore indicate that a modification of the structure depicted in Figure 1C (rather than those in Figure 1A and 1B) in which the boronic acid is covalently bound to the hydroxyl of Ser 195 in a tetrahedral fashion at catalytic pH. A modification of Figure 1C is required since it appears that His 57 is neutral in the complex between pH 6 and 9. Thus, the appropriate structure is diagrammed in Scheme IV.



If this is the case, then the proton originally of Ser 195 must be released into solution during complex formation. Preliminary experiments were attempted using the pH-Stat to measure this release of protons at catalytic pH in the  $\alpha$ -lytic protease/BBA system. Unfortunately, this apparatus proved not to be sensitive enough to provide reliable data, probably due to the buffering effect of both BBA and protein at the concentrations necessary to make the measurements. However, Hanai (1976) has reported the release of protons for the chymotrypsin/BBA system at catalytic pH.

The  $^{13}\text{C}$  NMR results on the  $\alpha$ -lytic protease/BBA complex

presented here accord nicely with the  $^1\text{H}$  NMR results of Robillard and Shulman (1974b) for the complexes of PEBA and BBA with chymotrypsin and subtilisin. These researchers observed no change in the chemical shift of the  $^1\text{H}$  resonance assigned to the proton located between Asp 102 and His 57 over the pH range 6 to 9; the chemical shift value for this proton was intermediate between that reported for a proton between Asp 102-neutral His 57 and for a proton between Asp 102-protonated His 57 in the free enzymes (Robillard and Shulman, 1972, 1974a). These researchers also interpreted their results according to the structure of Scheme IV, and explained the abnormal chemical shift value observed for the shared proton in the complex as a result of enhanced hydrogen bonding between the Asp and His residues on formation of the complex. Possibly this is also the source of the abnormal  $^{13}\text{C}$  chemical shift of C-2 in the  $\alpha$ -lytic protease/BBA complex.

## CONCLUSION

The current evidence strongly suggests that the serine protease/boronic acid complexes exist as tetrahedral adducts of Ser 195 and boronic acid at catalytic pH. Furthermore, the  $pK_a$  of His 57 in these complexes is substantially lowered relative to its value in the free enzymes. This phenomenon was also observed for the complexes of  $\alpha$ -lytic protease and specific aldehyde inhibitors, but to a much lesser extent (see Chapter IV of this thesis). The most striking difference between the enzyme/aldehyde and the enzyme/boronic acid complexes is that the boronic acid adducts possess a negative charge, while the aldehyde adducts do not. The putative transition states and intermediates of serine protease catalysis also possess a negative charge, which is stabilized by hydrogen bonding to the "oxyanion hole" of the protein (Henderson, 1970; Robertus et al., 1972; Kraut, 1977). Thus, the boronic acids may interact more favorably with the "oxyanion hole" than do the aldehydes, resulting in a greater similarity between the boronic acid/enzyme adducts and the transition states of catalysis. Thus boronic acids may indeed serve as good transition state analogs of the serine proteases.

The origin of the  $pK_a$  lowering of the His 57 residue in the enzyme/transition state analog complexes is unknown at present. The results of this chapter and the previous chapter indicate that the strength of the interaction between the bound analog and the "oxyanion hole" is important in

determining the magnitude of the  $pK_a$  shift. This has definite implications for catalysis. It strongly suggests that these enzymes may manifest behaviors in the presence of substrate that are not observed in the free enzyme, and that their ability to do so may be a function of the strength and number of the interactions developed between substrate and enzyme in the transition state of catalysis.

## REFERENCES

- Antonov, V.K., Ivanina, T.V., Berezin, I.V., and Martinek, K. (1970), FEBS Letters 7, 23-25.
- Antonov, V.K., Ivanina, T.V., Ivanova, A.G., Berezin, I.V., Levashov, A.V., and Martinek, K. (1972), FEBS Letters 20, 37-40.
- Bachovchin, W.W., and Roberts, J.D. (1978), J. Am. Chem. Soc. 100, 8041-8047.
- Blow, D.M., Birktoft, J.J., and Hartley, B.S. (1969), Nature (London) 221, 337-339.
- Blow, D.M. (1976), Acc. Chem. Res. 9, 145-152.
- Branch, G.E.K., Yabroff, D.L., and Bettman, B. (1934), J. Am. Chem Soc. 56, 937-941.
- Byers, L.D., and Koshland, D.E. Jr. (1978), Bioorg. Chem. 7, 15-33.
- Dixon, M. (1953), Biochem. J. 55, 170-171.
- Fersht, A.R. (1974), Proc. R. Soc. Lond. B. 187, 397-407.
- Hanai, K. (1976), J. Biochem. 79, 107-116.
- Hanai, K. (1977), J. Biochem. 81, 1273-1283.
- Henderson, R. (1970), J. Mol. Biol. 54, 341-354.
- Hess, G.P., Seybert, D. Lewis, A., Spoonhower, J., and Cookingham, R. (1975), Science 189, 384-386.
- Hunkapiller, M.W., Smallcombe, S.H., Whitaker, D.R., and Richards, J.H. (1973), Biochemistry 12, 4732-4743.
- Koehler, K.A., and Lienhard, G.E. (1971), Biochemistry 10, 2477-2483.

- Koehler, K.A., and Hess, G.P. (1974), Biochemistry 13, 5345-5350.
- Kraut, J. (1977), Ann. Rev. Biochem. 46, 331-358.
- Lienhard, G.E., Secemski, I.I., Koehler, K.A., and Lindquist, R.N. (1972), Cold Spring Harbor Symp. Quant. Biol. 36, 45-51.
- Lienhard, G.E. (1973), Science 180, 149-154.
- Lindquist, R.N., and Terry, C. (1974), Arch. Biochem. Biophys. 160, 135-144.
- Matteson, D.S., Sadhu, K.M., and Lienhard, G.E. (1981), J. Am. Chem. Soc. 103, 5241-5242.
- Matthews, D.A., Alden, R.A., Birktoft, J.J., Freer, S.T., and Kraut, J. (1975), J. Biol. Chem. 250, 7120-7126.
- Nakatani, H., Uehara, Y., and Hiromi, K. (1975a), J. Biochem. 78, 611-616.
- Nakatani, H., Hanai, K., Uehara, Y., and Hiromi, K. (1975b), J. Biochem. 77, 905-908.
- Noth, Heinrich, and Wrackmeyer, B. (1978), in "NMR: Basic Principles and Progress", vol. 14, P. Diehl, E. Fluck, and R. Kosfeld, Springer-Verlag, Berlin, Germany, 90-91.
- Philipp, M., and Bender, M.L. (1971), Proc. Natl. Acad. Sci. USA 68, 478-480.
- Philipp, M., and Maripuri, S. (1981), FEBS Letters 133, 36-38.
- Rawn, J.D., and Lienhard, G.E. (1974), Biochemistry 13, 3124-3130.
- Robertus, J.D., Kraut, J., Alden, R.A., and Birktoft, J.J. (1972), Biochemistry 11, 4293-4303.

- Robillard, G., and Shulman, R.G. (1972), J. Mol. Biol. 71,  
507-511.
- Robillard, G., and Shulman, R.G. (1974a), J. Mol. Biol. 86,  
519-540.
- Robillard, G., and Shulman, R.G. (1974b), J. Mol. Biol. 86,  
541-558.
- Wayslishen, R.E., and Tomlinson, G. (1975), Biochem. J. 147,  
605-607.
- Wolfenden, R. (1972), Acc. Chem. Res. 5, 10-18.
- Wolfenden, R. (1976), Ann. Rev. Biophys. Bioeng. 5, 271-306.

## CHAPTER VI

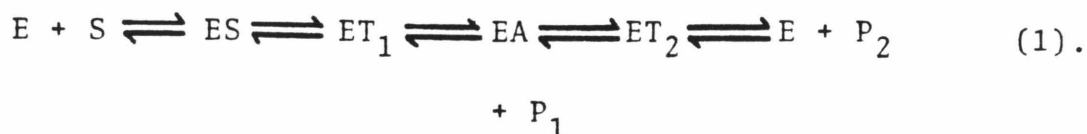
INVESTIGATIONS OF THE TETRAHEDRAL INTERMEDIATE  
FORMED IN THE ELASTASE CATALYZED HYDROLYSIS OF  
SPECIFIC TRIPEPTIDE *p*-NITROANILIDES  
BY STOPPED-FLOW SPECTROPHOTOMETRY

## ABBREVIATIONS

Ser	L-Serine
Asp	L-Aspartic acid
His	L-Histidine
APAPNA	N-acetyl-L-alanyl-L-prolyl-L-alanine p-nitroanilide
STAPNA	N-succinyl-L-alanyl-L-alanyl-L-alanine p-nitroanilide
TRIS	Tris(hydroxymethyl)aminomethane
A	Absorbance



an amide substrate. The proton originally on the serine hydroxyl is stored on the Asp102-His57 dyad during formation of the tetrahedral adduct; it is donated to the leaving group in the decomposition of this adduct to acyl-enzyme. The minimal mechanism for hydrolysis by the serine proteases is then



ES represents the non-covalent Michaelis complex;  $ET_1$  represents the tetrahedral adduct of Ser195 and the substrate; EA represents the acyl-enzyme;  $ET_2$  represents a tetrahedral adduct of solvent water and the acyl-enzyme (analogous to  $ET_1$ ); and  $P_1$  and  $P_2$  are the amine (or alcohol) and carboxylic acid portions of the amide (or ester) substrate respectively.

Support for the above mechanism has been, for the most part, based on indirect kinetic and crystallographic evidence. Caplow and co-workers (Caplow, 1969; Lucas and Caplow, 1972; Lucas et al., 1973) determined that in the hydrolysis of acetyl-L-tyrosinyl and acetyl-L-tryptophanyl anilides by chymotrypsin, breakdown of a postulated tetrahedral intermediate, formed in a pre-equilibrium reaction between enzyme and bound substrate to acyl enzyme, was the rate-limiting step in the reaction. Furthermore, they proposed that electron-withdrawing substituents on the aniline ring should allow this intermediate to accumulate. Nitrogen isotope effects (O'Leary and Kluetz, 1970, 1972; O'Leary, 1978) supported the existence of this intermediate; the magnitude of the isotope effects indicated that a carbon-nitrogen bond-breaking step prior to the acyl-enzyme was at least partially rate-determining. Substituent effects on the chymotrypsin-catalyzed hydrolysis of specific ester substrates also

indicated the existence of some, presumably tetrahedral, intermediate during the course of the reaction (Williams and Bender, 1971). The kinetic studies of Fersht and co-workers supported the existence of an intermediate, but, in the case of both amides and anilides, they postulated that this intermediate did not accumulate but existed in a low, steady-state concentration (Fersht, 1972; Fersht and Requena, 1971; Fastrez and Fersht, 1973). Further kinetic work has served to support these interpretations (Fersht et al., 1973; Hirohara et al., 1974; Philipp et al., 1973).

Crystallographic support for the existence of a tetrahedral adduct comes primarily from the determination of the structures of trypsin/natural protein trypsin inhibitor complexes (Blow et al., 1974; Sweet et al., 1974; Ruhlmann et al., 1973). These researchers determined that the observed crystallographic bond lengths and bond angles were consistent with the formation of a tetrahedral adduct between enzyme and inhibitor, although subsequent refinement of these structures suggested that the observed atomic coordinates might actually reflect a pyramidal distortion of the carbonyl of the scissile bond of the inhibitor on binding to trypsin, resulting in a pro-tetrahedral structure without actual covalent bond formation (Huber et al., 1974; Huber et al., 1975; Bode et al., 1976). Nuclear magnetic resonance studies of these complexes (Hunkapiller et al., 1979; Baillargeon et al., 1980; Richarz et al., 1980) have been unable to detect any tetrahedral structure.

More recently, direct observation of pre-acyl-enzyme intermediates in the hydrolytic process has been accomplished using stopped-flow (Hunkapiller et al., 1976; Balny and Bieth, 1977; Petkov, 1978) and cryoenzymologic techniques (for reviews of this latter technique see Fink, 1979; Fink and Geeves, 1979; Fink, 1977; Fink, 1976a). Using a

specific substrate of the homologous enzymes elastase and  $\alpha$ -lytic protease (N-acetyl-L-alanyl-L-prolyl-L-alanine p-nitroanilide) specifically engineered to stabilize the putative tetrahedral intermediate, Hunkapiller et al., (1976) observed, by stopped-flow visible spectrophotometry, a biphasic production of a p-nitroaniline-like species. Using a cogent and thorough series of arguments, they assigned the initial phase of the reaction to buildup of a tetrahedral adduct (to about 80% of enzyme-bound substrate), and the final phase to a slower turnover reaction.

Further support for the presence of a discrete tetrahedral intermediate in the reaction of elastase with several peptide p-nitroanilide substrates at low temperature in fluid aqueous-organic solvent mixtures (Fink and Meehan, 1979; Fink, 1979). These experimenters were able to trap a species at appropriately low temperature having the characteristic spectrophotometric and kinetic properties ascribed to a tetrahedral intermediate. Subsequently they also observed such a species in the reaction of trypsin with N <sup>$\alpha$</sup> -carbobenzoxy-L-lysine p-nitroanilide (Compton and Fink, 1980). Unfortunately, they were unable to observe this intermediate in the case of chymotrypsin with N-acetyl-L-phenylalanine p-nitroanilide (Fink, 1976b). Furthermore, they were unsuccessful at trapping this intermediate in a crystal of elastase suffused with succinyl-trialanine p-nitroanilide at low temperature (Fink and Petsko, 1981).

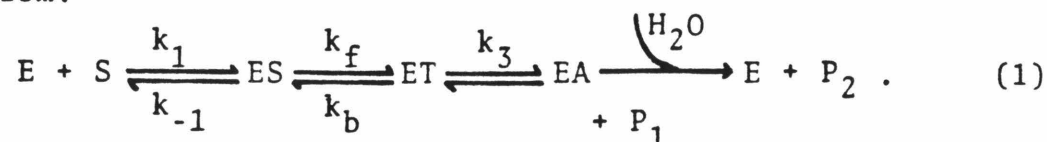
Recently, the results of the stopped-flow and cryoenzymological studies have been called into question. Markley et al. (1981) conducted stopped-flow experiments similar to the Hunkapiller et al. (1976) experiments at a variety of temperatures. They did not observe the "burst" kinetics typical of intermediate buildup and accumulation; furthermore, they stated that the previous studies were fraught with theoretical

inconsistencies and experimental inadequacies.

In lieu of these conflicting reports, we have re-examined the reaction between elastase and two specific substrates, N-acetyl-L-alanyl-L-prolyl-L-alanine p-nitroanilide (APAPNA) and succinyl-L-alanyl-L-alanyl-L-alanine p-nitroanilide (STAPNA), by stopped-flow spectrophotometry in an attempt to observe the tetrahedral intermediate, to characterize the kinetics of its formation and breakdown, and to correlate these results with the proposed mechanism of hydrolysis by the serine proteases (equation 1).

## THEORY

The hydrolysis of peptide p-nitroanilide substrates of porcine elastase can be described by the following proposed mechanism:



In this formulation, E represents free enzyme; S, substrate (peptide p-nitroanilide); ES, non-covalent Michaelis complex; ET, tetrahedral intermediate (covalent adduct of enzyme and substrate); EA, covalent acyl-enzyme intermediate;  $P_1$ , p-nitroaniline;  $P_2$ , acid component of peptide substrate.

In order to make the kinetic analysis tractable, three reasonable assumptions must be made. First, we assume that  $S_0 \gg E_0$  so that the steady-state assumption can be made for appropriate species. Second, we assume  $k_3$  is the rate determining step for this sequence (in accord with the results of Hunkapiller et al., 1976 and Petkov, 1978) so that during the initial portion of the reaction, (EA) is negligible. Third, we assume that the reverse of  $k_3$ , the reversion of EA to ET, does not occur to any appreciable extent, since initially  $P_1$  and  $P_2$  are small.

Steady-state phase. We shall assume that ET reaches a steady-state concentration during the initial portion of the reaction, so that

$$d(ET)/dt = k_f(ES) - (k_b + k_3)(ET) = 0. \quad (2)$$

Since (ET) is assumed to be in steady-state, then ES must also

be in steady-state, as it occurs prior to ET in the kinetic sequence. Therefore,

$$d(ES)/dt = k_1(E)(S) + k_b(ET) - (k_{-1} + k_f)(ES) = 0. \quad (3)$$

Also, since  $(EA) = 0$ ,

$$E_o = (E) + (ES) + (ET) \quad (4)$$

and, from (1),

$$(ES) = (ET)(k_b + k_3)/k_f \quad (5)$$

so that

$$E_o = (E) + (ET)\{1 + ((k_b + k_3)/k_f)\} \quad (6)$$

or

$$(E) = E_o - C(ET) \quad \text{where } C = (k_b + k_3 + k_f)/k_f. \quad (7)$$

Rearranging and inserting (7) into (3),

$$k_1 E_o (S) - k_1 C (ET) (S) + k_b (ET) - (k_{-1} + k_f) \{(k_b + k_3)/k_f\} (ET) = 0$$

or

$$(ET) = \frac{k_1 E_o (S)}{\left[ \frac{k_1 (S) (k_f + k_b + k_3)}{k_f} \right] - k_b + (k_{-1} + k_f) (k_b + k_3) / k_f} \quad (8)$$

If we assume that initially  $(S) = S_o$ , then

$$(ET) = \frac{k_1 E_o S_o}{\left[ \frac{k_1 S_o (k_f + k_b + k_3)}{k_f} \right] - k_b + (k_{-1} + k_f) (k_b + k_3) / k_f} \quad (9)$$

The rate of the steady-state (turnover) reaction is given by

$$d(P_1)/dt = k_3(ET). \quad (10)$$

Therefore,

$$\frac{d(P_1)}{dt} = \frac{k_1 k_3 E_0 S_0}{\left[ \frac{k_1 S_0 (k_f + k_b + k_3)}{k_f} \right] - k_b + (k_{-1} + k_f)(k_b + k_3)/k_f} \quad (11)$$

$$\text{or } \frac{d(P_1)}{dt} = \frac{k_3 E_0 S_0}{\left[ \frac{k_f + k_b + k_3}{k_f} \right] S_0 + \left[ \frac{-k_{-1} k_f + k_{-1} k_b + k_f k_b + k_{-1} k_3 + k_f k_3}{k_1 k_f} \right]} \quad (12)$$

$$= \frac{k_3 E_0 S_0}{\left[ \frac{k_f + k_b + k_3}{k_f} \right] S_0 + \left[ \frac{k_{-1} k_b + k_{-1} k_3 + k_f k_3}{k_1 k_f} \right]} \quad (13)$$

This is standard Michaelis-Menten kinetics of the form

$$v = \frac{k_{\text{cat}} E_0 S_0}{K_m + S_0}$$

with, in this case,

$$k_{\text{cat}} = k_3 k_f / (k_f + k_b + k_3) \quad (14)$$

and

$$K_m = \frac{k_{-1} k_b + k_{-1} k_3 + k_f k_3}{k_1 k_f + k_1 k_b + k_1 k_3} \quad (15)$$

If  $k_f k_3 \ll k_{-1} k_b + k_{-1} k_3$  and  $k_1 k_f \ll k_1 k_b + k_1 k_3$ , then  $K_m$  reduces to  $(k_{-1}/k_1) = K_s$ .

Pre-steady-state phase. From the kinetic derivation,

$$d(ET)/dt = k_f(ES) - (k_b + k_3)(ET). \quad (2)$$

Once again, we must assume that ES is in steady-state, so that  $d(ES)/dt = 0$ . Then,

$$k_1(E)S_0 + k_b(ET) - (k_{-1} + k_f)(ES) = 0. \quad (3)$$

From (4),

$$d(ES)/dt = k_1 E_0 S_0 - k_1 S_0 (ES) - k_1 S_0 (ET) + k_b (ET) - (k_{-1} + k_f)(ES) = 0 \quad (16)$$

$$\text{and } k_1 E_0 S_0 - k_1 S_0 (ET) + k_b (ET) = \{k_1 S_0 + (k_{-1} + k_f)\}(ES) \quad (17)$$

or

$$(ES) = \frac{k_1 E_0 S_0}{k_1 S_0 + (k_{-1} + k_f)} + \frac{(k_b - k_1 S_0)}{k_1 S_0 + (k_{-1} + k_f)} (ET) \quad (18)$$

Therefore, using (17) and (2),

$$\frac{d(ET)}{dt} = \frac{k_1 k_f E_0 S_0}{k_1 S_0 + (k_{-1} + k_f)} - \left[ (k_b + k_3) - \frac{k_f (k_b - k_1 S_0)}{k_1 S_0 + (k_{-1} + k_f)} \right] (ET) \quad (19)$$

Equation (19) is of the form  $d(ET)/dt = A - B(ET)$ , with

$$A = \frac{k_1 k_f E_0 S_0}{k_1 S_0 + (k_{-1} + k_f)}$$

and

$$B = \frac{k_b k_1 S_0 + k_3 k_1 S_0 + k_b k_{-1} + k_b k_f + k_3 k_{-1} + k_3 k_f}{k_1 S_0 + (k_{-1} + k_f)} - \frac{k_f k_b - k_f k_1 S_0}{k_1 S_0 + (k_{-1} + k_f)}$$

$$= \frac{k_1 S_0 (k_f + k_b + k_3) + (k_{-1} k_b + k_{-1} k_3 + k_f k_3)}{k_1 S_0 + (k_{-1} + k_f)}$$

Hence,

$$(ET) = (A/B)(1 - \exp(-Bt)) \quad (20)$$

with A and B as given above.

Burst analysis. Unlike the kinetic scheme presented in Chapter III of this thesis, where the absorbance versus time traces were for the production of only one species ( $P_1$ ) at two different rates, in this case the absorbance versus time trace contains information about two co-existing species, ET and  $P_1$ . Therefore, the burst analysis is slightly different in this case.

Since we are assuming that the only two species to absorb at 410 nm are ET and  $P_1$  (see Discussion for substantiation of this assumption),

$$A_{410} = \epsilon'_{410} (\text{ET}) + \epsilon''_{410} (P_1), \quad (21)$$

where  $\epsilon'_{410}$  is the extinction coefficient for ET and  $\epsilon''_{410}$  is the extinction coefficient for  $P_1$ . Therefore,

$$dA_{410}/dt = \epsilon'_{410} d(\text{ET})/dt + \epsilon''_{410} d(P_1)/dt. \quad (22)$$

If  $\epsilon'_{410} = \epsilon''_{410} = \epsilon$  (Hunkapiller et al., 1976; Fink and Meehan, 1979), then from (19) and (10)

$$\begin{aligned} (1/\epsilon)(dA_{410}/dt) &= d(\text{ET})/dt + d(P_1)/dt \\ &= (A - B(\text{ET})) + k_3(\text{ET}) \\ &= A + (k_3 - B)(\text{ET}) \\ &= A + (k_3 - B)(A/B)(1 - \exp(-Bt)). \end{aligned} \quad (23)$$

Integrating from  $t=0$  to  $t=t$ ,

$$\begin{aligned} (1/\epsilon)A_{410} &= \left\{ A + (k_3 A/B) - A \right\}_{t=0}^{t=t} - \left\{ (k_3 - B)(A/B)e^{-Bt} \right\}_{t=0}^{t=t} \\ &= (k_3 A/B)t + (k_3 - B)(A/B^2)(e^{-Bt} - 1). \end{aligned} \quad (24)$$

If  $t$  is large (that is, steady-state is obtained),  $e^{-Bt} \ll 1$ , so that

$$\begin{aligned}
 (1/\varepsilon)A_{410} &= (k_3 A/B)t + (B-k_3)(A/B^2) \\
 &= Ct + \pi,
 \end{aligned}
 \tag{25}$$

where  $C = k_3 A/B$  and  $\pi = (B-k_3)(A/B^2)$ .

Now,

$$\begin{aligned}
 A/B &= \frac{k_1 k_f E_0 S_0}{k_1 S_0 (k_f + k_b + k_3) + (k_{-1} k_b + k_{-1} k_3 + k_f k_3)} \\
 &= (k_{\text{cat}}/k_3) E_0 S_0 / (K_m + S_0)
 \end{aligned}$$

so that  $C = v_{ss}$ , as expected.

$$\begin{aligned}
 \pi &= (B - k_3)(A/B^2) \\
 &= (B - k_3)(1/B) \{k_f / (k_f + k_b + k_3)\} \{S_0 / (K_m + S_0)\} E_0 \\
 &= \{1 - (k_3/B)\} \{k_f / (k_f + k_b + k_3)\} \{S_0 / (K_m + S_0)\} E_0.
 \end{aligned}
 \tag{26}$$

If  $k_3 \ll B$  and  $k_f \gg (k_b + k_3)$  and  $S_0 \gg K_m$ , then

$$\pi = E_0.$$

Otherwise,  $\pi < E_0$ .

Biphasic kinetics will be observed if  $B$ , the rate constant for buildup of a steady-state concentration of ET, is larger than  $k_3$ , the rate constant for breakdown of ET to products.

## EXPERIMENTAL

### Materials.

p-Nitroaniline was purchased from Sigma. It was recrystallized several times from hot water (using decolorizing charcoal), and dried in vacuo. It melted at 144-146°C (uncorrected (lit. 146°C)).

N-acetyl-L-alanyl-L-prolyl-L-alanine p-nitroanilide was synthesized as described in Chapter IV. For this experiment, it was further recrystallized from a concentrated solution of methanol in the cold. This produced a beautifully crystalline, very pale yellow material. It was stored desiccated at 4°C.

N-succinyl-L-alanyl-L-alanyl-L-alanine p-nitroanilide was purchased from Sigma, and was used as received. It was stored desiccated at 4°C.

Acetonitrile was a product of Eastman. It was distilled twice from phosphorous pentoxide, and then fractionated.

Potassium chloride was a product of Mallinkrodt. Phosphoric acid (86%) and potassium hydroxide were purchased from Baker. Tris(hydroxymethyl)aminomethane (TRIS) was purchased from Sigma.

The water used was deionized and glass distilled.

Porcine elastase (lyophilized powder) was purchased from Calbiochem-Behring (lot 203006); its specific activity was 108 units/mg.

Tri-alanine-CH-Sepharose 4B was a product of Pierce.

### Methods.

Elastase purification. The commercial elastase was purified on Tri-alanine-CH-Sepharose 4B as described by Katagiri et al. (1978). The lyophilized enzyme (about 100 mg) is dissolved in 10 ml of 0.01 M TRIS/HCl buffer and is loaded onto the column (2.5 cm x 25 cm, equilibrated

in the same buffer at 4°C). The column is washed with 250 ml of this buffer, and then the buffer is changed to 0.02 M sodium acetate, 0.2 M sodium chloride, pH 4.5. About 200 ml of this buffer are passed through the column; 7 ml fractions are collected. A small amount of protein (non-elastolytic) is eluted early in the fractionation; near the end of the elution, elastase begins to bleed off the column. This is contrary to the published procedure, indicating that the column is probably overloaded under these conditions. The rest of the elastase is eluted with 0.5 M D, L-alanine/HCl, pH 4.0. The combined elastase fractions (~200 ml) are dialyzed thrice versus 8 l of distilled water and lyophilized. This purified enzyme is at least 95% pure (active) by weight as determined by active site titration with diethyl p-nitrophenyl phosphate (Bender et al., 1966), indicating that the original enzyme preparation was about 75% active elastase. The lyophilized enzyme is stored at -20° until needed.

Samples for Kinetics. The buffer for this study was made up by dissolving 0.1 mole of phosphoric acid in water (800 ml), and the solution was titrated to about pH 8.5 with 40% KOH. Acetonitrile (100 ml) is then added, and the solution is mixed thoroughly. When equilibrium is reached, the solution is made up to 1 liter with water. The pH of the resulting solution was  $8.25 \pm 0.02$  (as measured using a pH meter standardized against buffers). The buffer solution was then filtered through a Millipore 0.22 $\mu$  filter to remove any suspended solids that might interfere in the spectroscopic observations. The solution was degassed overnight on a water aspirator.

Both enzyme and substrate solutions were made up in the above buffer in order to minimize mixing artifacts in the initial portion of the stopped-flow observations. Substrate solutions were made up the day

prior to the kinetic study due to the long period of time needed to dissolve the substrates. The solutions were once again filtered through 0.22 $\mu$  Millipore filters, and stored at 2°C overnight until ready for use. Enzyme solutions were made up immediately prior to use in ice-cold buffer. These solutions were centrifuged at 10,000 rpm (4°C) for fifteen minutes to remove insoluble material, if any, and were stored on ice whenever not in use in the spectrophotometer to reduce autolytic inactivation.

Stopped-Flow Kinetics. Stopped-flow experiments were performed on a Durrum Model D-110 spectrophotometer equipped with a 75-W xenon lamp. The amplified photomultiplier output was collected by using a Biomation Model 805 transient recorder connected to a Digital Equipment Corporation MINC computer and a Tektronix 5103N storage oscilloscope. The syringes and cuvette were thermostatted at 25°C for at least 5 minutes prior to mixing of the reagents. One syringe was reserved for the enzyme solution; the other contained the substrate. Extra care was taken to exclude air bubbles from the syringe solutions. All measurements were made at 410 nm in transmittance mode and converted to absorbance by hand. The oscilloscope traces were saved in the computer and plotted using a Hewlett-Packard 7004-B XY-recorder interfaced with the computer. The light path of the cuvette was 2.0 cm.

A critical difficulty had to be overcome prior to successful completion of the experiment. Initially, we attempted to inject 150  $\mu$ l from each syringe into the sample cuvette. However, consecutive injections showed little reproducibility using this volume. It appeared that inadequate flushing of the sample cuvette from tenacious p-nitroaniline product was occurring. Increasing the injection volume to 500  $\mu$ l from each syringe resulted in reproducibility to within 5% for each of five

consecutive injections; although not all absorbing material could be washed from the cuvette the starting transmittance of each trace could be reproduced to within a few percent of the others in the series. One hundred percent transmittance was set using buffer in both syringes.

Each trace was taken on the 0-10V (0-1A) scale of the instrument. The sequence of experiments was such that, for a given substrate concentration, the entire range of enzyme concentrations (low to high) was tested. Both syringes of the instrument were then flushed well with buffer, and the sequence was repeated with another substrate solution. The first injection for each enzyme/substrate combination was discarded in each case to assure reproducibility.

Spectroscopic Measurements. The value of the molar absorptivity of the product chromophore, p-nitroaniline, was determined in the reaction buffer on a Beckman Acta III UV-Visible Spectrophotometer thermostatted at 25°C and using a 1.0 cm cell path-length. A value of  $8,820 \pm 90 \text{ M}^{-1}$  was determined for  $\epsilon_{410}^{1\text{cm}}$ , and  $830 \pm 100 \text{ M}^{-1}$  for  $\epsilon_{450}^{1\text{cm}}$ . The value for  $\epsilon_{410}^{1\text{cm}}$  agrees well with the reported values of  $\epsilon_{410}^{1\text{cm}} = 8,860 \text{ M}^{-1}$  (Hunkapiller et al., 1976) and  $\epsilon_{410}^{1\text{cm}} = 8,800 \text{ M}^{-1}$  (Erlanger et al., 1961). Absorbance measurements of p-nitroaniline solutions on the stopped-flow spectrophotometer were consistent with the above value.

## RESULTS

Figure 1 presents a typical example of the raw data obtained from the stopped-flow spectrophotometer. A smooth curve was drawn through each trace (see Figure 2) in order to facilitate the calculation of absorbance values from the transmittance data. The "subjective error" in this transformation from transmittance to absorbance was determined to be  $< \pm 0.003$  absorbance units per point from a thrice-repeated calculation on the same trace. Twenty-five equally-spaced time/transmittance points were transformed per trace. The instrument shows an operational dead-time of  $< 10$  msec for this set of experiments.

Figure 3 shows two typical absorbance at 410 nm versus time plots (calculated as described in the preceding paragraph) for the reaction of N-acetyl-L-alanyl-L-prolyl-L-alanine p-nitroanilide (APAPNA) with porcine elastase at pH 8.25. The biphasic nature of the curves is apparent. As suggested by the proposed mechanism (equation 1), and the attendant kinetic derivation, we can define a "burst"  $\pi$  as the difference between the absorbance value of the steady-state (linear) portion of the curve extrapolated back to  $t = 0$  and the observed absorbance.

Two easily testable predictions are made by the kinetic derivation for the proposed mechanism. First,  $\pi$  should be a linear function of  $E_0$ ; second,  $B$  should be independent of  $E_0$ .

Figures 4 and 5 present representative  $A_{410}$  versus  $t$  plots of the early portion of the reaction between porcine elastase and APAPNA (Figure 4) and succinyl-L-alanyl-L-alanyl-L-alanine p-nitroanilide (STAPNA) (Figure 5). Tables I and II give the kinetic parameters determined from such plots. The steady-state (linear) portion of the curve was determined by fitting the last twelve time points ( $t = 574$  ms to  $t = 1025$  ms for STAPNA,

Figure 1. Typical raw transmittance at 410 nm versus time data for the reaction of porcine elastase with N-succinyl-L-alanyl-L-alanyl-L-alanine p-nitroanilide in 0.1 M  $\text{H}_3\text{PO}_4/\text{KOH}$ , pH 8.25, 10% (v/v) acetonitrile/water,  $25.0 \pm 0.2^\circ\text{C}$ . The upper trace (100% T) is an injection in which both syringes contained only buffer. The lower trace is an injection in which  $E_0 = 3.95 \times 10^{-5}$  M and  $S_0 = 1.09$  mM.

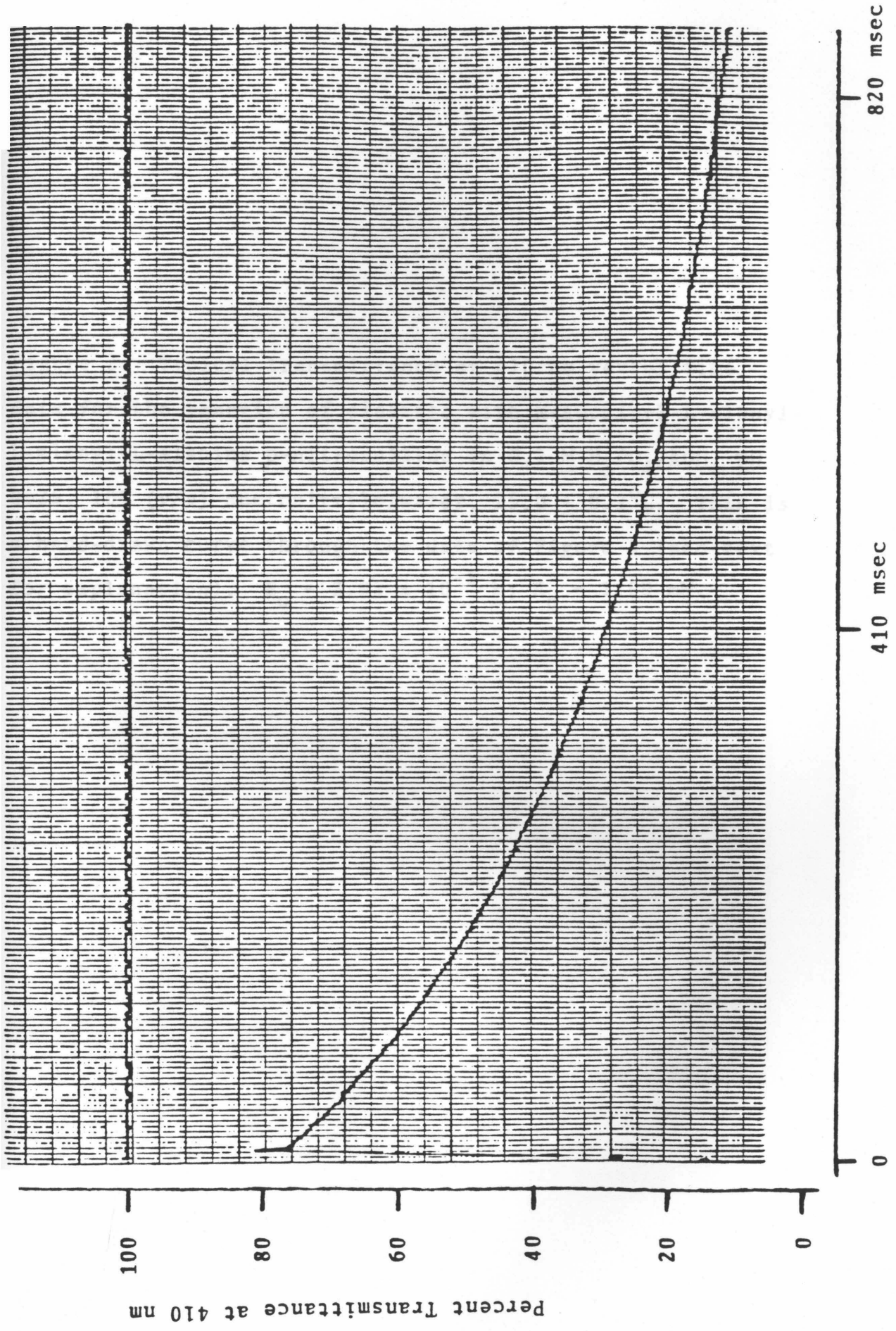


Figure 2. Typical transmittance at 410 nm versus time data for the reaction of elastase with N-succinyl-L-alanyl-L-alanyl-L-alanine p-nitroanilide in 0.1 M  $\text{H}_3\text{PO}_4/\text{KOH}$ , pH 8.25, 10% (v/v) acetonitrile/water,  $25.0 \pm 0.2^\circ\text{C}$ . This is a hand-drawn curve through the data of Figure 1 (see text for explanation).  $E_0 = 3.95 \times 10^{-5}$  M;  $S_0 = 1.09$  mM.

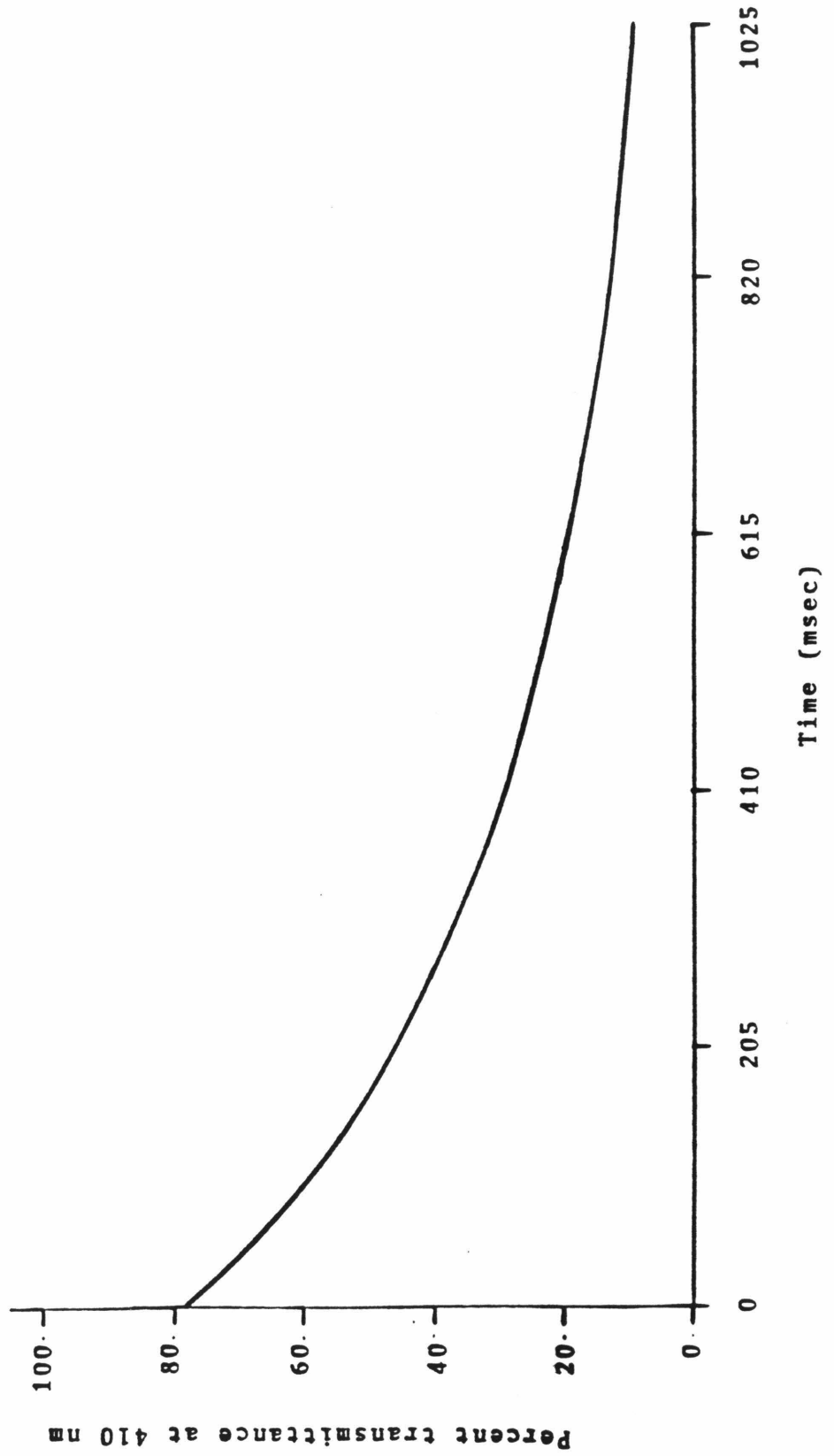


Figure 3. Typical  $A_{410}$  versus time plots for the reaction of porcine elastase with N-acetyl-L-alanyl-L-prolyl-L-alanine p-nitroanilide in 0.1 M  $H_3PO_4/KOH$ , pH 8.25, 10% (v/v) acetonitrile/water,  $25.0 \pm 0.2^\circ C$ . The lower curve (solid circles) is for  $E_0 = 2.20 \times 10^{-5}$  M and  $S_0 = 1.09$  mM. The upper curve (open circles) is for  $E_0 = 4.40 \times 10^{-5}$  M and  $S_0 = 1.09$  mM. The lines in the figure are obtained by applying a linear least-squares regression to the last twelve data points of each plot (see text for explanation).

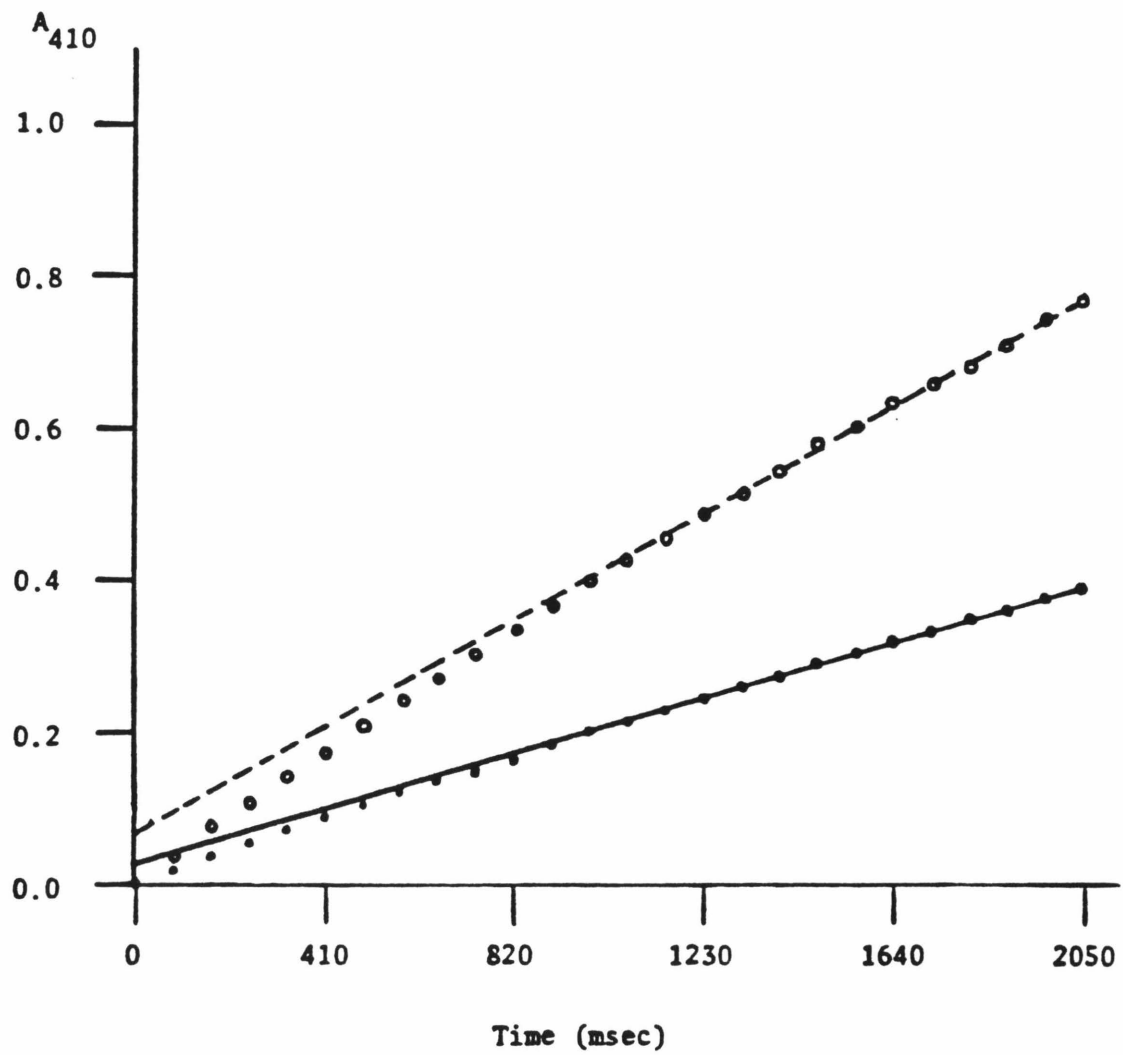


Figure 4. Typical  $A_{410}$  versus time plots for the reaction of porcine elastase with N-acetyl-L-alanyl-L-prolyl-L-alanine p-nitroanilide in 0.1  $\underline{M}$   $\text{H}_3\text{PO}_4/\text{KOH}$ , pH 8.25, 10% (v/v) acetonitrile/water,  $25.0 \pm 0.2^\circ\text{C}$ . These plots are calculated for the transmittance versus time data such as that of

Figure 1.  $S_o = 2.02 \text{ mM}$ .

- A)  $E_o = 2.20 \times 10^{-5} \underline{M}$ ;  $\pi_m = 0.055 \text{ A}$ .
- B)  $E_o = 2.95 \times 10^{-5} \underline{M}$ ;  $\pi_m = 0.084 \text{ A}$ .
- C)  $E_o = 3.65 \times 10^{-5} \underline{M}$ ;  $\pi_m = 0.103 \text{ A}$ .
- D)  $E_o = 4.40 \times 10^{-5} \underline{M}$ ;  $\pi_m = 0.125 \text{ A}$ .

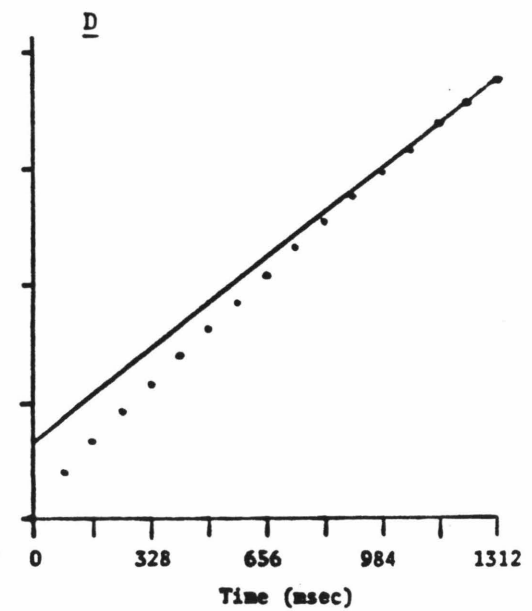
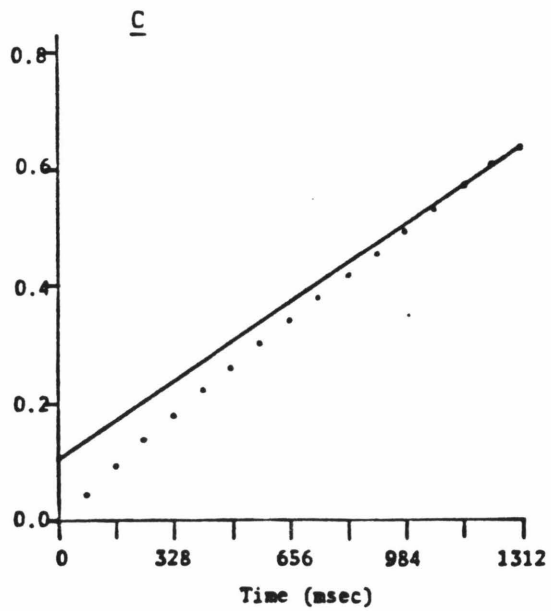
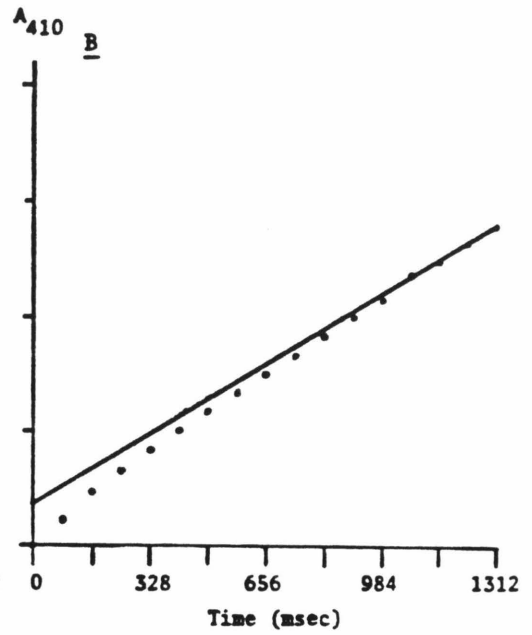
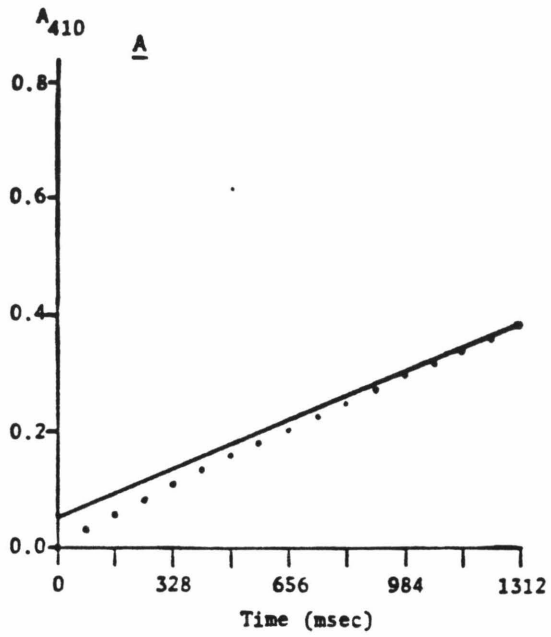
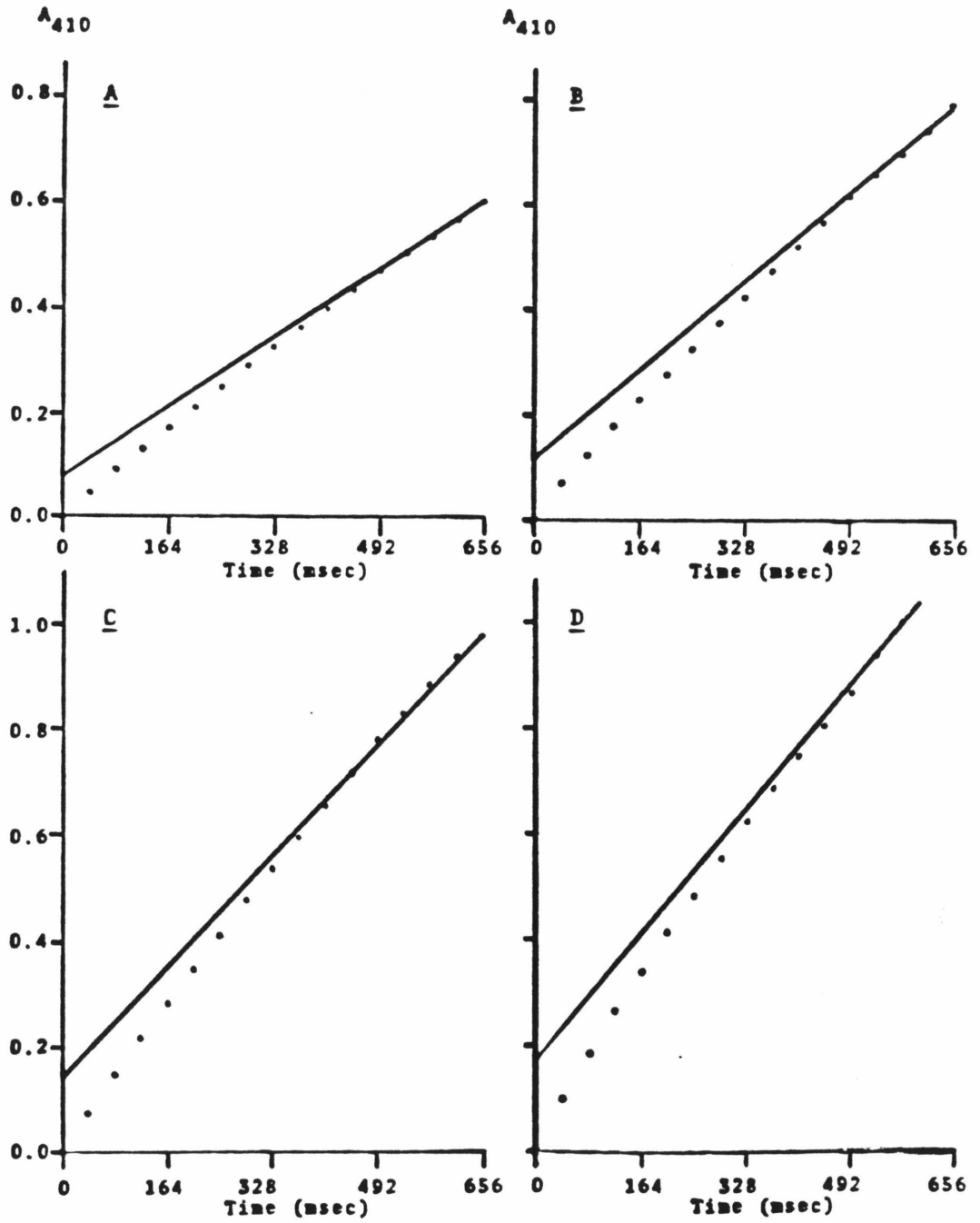


Figure 5. Typical  $A_{410}$  versus time plots for the reaction of porcine elastase with N-succinyl-L-alanyl-L-alanyl-L-alanine p-nitroanilide in 0.1 M  $H_3PO_4/KOH$ , pH 8.25, 10% (v/v) acetonitrile/water,  $25.0 \pm 0.2^\circ C$ . These plots are calculated for the transmittance versus time data such as that of Figure 1.  $S_o = 2.05 \text{ mM}$ .

- A)  $E_o = 2.20 \times 10^{-5} \text{ M}$ ;  $\pi_m = 0.078 \text{ A}$ .
- B)  $E_o = 2.95 \times 10^{-5} \text{ M}$ ;  $\pi_m = 0.117 \text{ A}$ .
- C)  $E_o = 3.65 \times 10^{-5} \text{ M}$ ;  $\pi_m = 0.144 \text{ A}$ .
- D)  $E_o = 4.40 \times 10^{-5} \text{ M}$ ;  $\pi_m = 0.174 \text{ A}$ .



$t = 1148$  ms to  $t = 2050$  ms for APAPNA) with a linear least-squares regression. The regression coefficient  $r$ , in all cases but one, was  $> 0.9990$  (the exception was  $r = 0.997$ ). The slope of the linear regression analysis gives  $v_{ss}$ , the steady-state velocity.

Figure 6 shows representative calculations for  $B$ , the first-order rate constant for the buildup of a steady-state concentration of intermediate. The first ten time points ( $t = 0$  to  $t = 369$  ms for STAPNA,  $t = 0$  to  $t = 738$  for APAPNA) were used.  $B$  is the slope of the  $\ln(A_{ss} - A_{obs})$  versus time plot, where  $A_{ss}$  = extrapolated steady-state value and  $A_{obs}$  = observed value at time  $t$ . A calculated value of the burst,  $\pi_c$ , can be determined from the  $y$  intercept of these plots.

The values of  $B$  obtained justify the choice of time points for the calculation of  $v_{ss}$ . For STAPNA,  $B \approx 4s^{-1}$ , so that for  $t \geq 574$  ms,  $e^{-Bt} = 0.1$ , so that 90% of steady-state has been obtained. Similarly, for APAPNA,  $B \approx 2s^{-1}$ , so that for  $t \geq 1148$ ,  $e^{-Bt} = 0.1$ .

The results presented in Tables I and II are consistent with the predictions of the proposed mechanism. For both substrates,  $B$  is clearly independent of  $E_o$  over a six-fold range. Furthermore, it is interesting that  $B$  is a fairly insensitive function of  $S_o$  at the concentrations employed in this study (2.02 mM APAPNA,  $B = 1.87 \pm 0.57s^{-1}$ ; 1.9 mM STAPNA,  $B = 4.49 \pm 1.14s^{-1}$ ). Unfortunately,  $B$  is such a complicated function of rate constants and  $S_o$  that little useful information can be gained from this observation.

Figure 7 demonstrates the dependence of  $\pi$  on  $E_o$ . The linear increase in  $\pi$  with increasing  $E_o$  is apparent. The lines drawn in the figure assume intersection of the axes at zero and are a linear regression fit using the measured values,  $\pi_m$ . The fact that all four lines

Figure 6. Typical analysis of the first-order pre-steady-state reaction of N-acetyl-L-alanyl-L-prolyl-L-alanine p-nitro-anilide with elastase.  $S_0 = 2.02 \text{ mM}$ ;  $0.1 \text{ M H}_3\text{PO}_4/\text{KOH}$ , pH 8.25, 10% (v/v) acetonitrile/water,  $25.0 \pm 0.2^\circ\text{C}$ . The lines in the figure were obtained by applying a linear least-squares regression to the data.  $r$  is the correlation coefficient of the regression.

	$E_0 = 44.0 \text{ M}, r = -0.9986.$
	$E_0 = 36.5 \text{ M}, r = -0.9980.$
	$E_0 = 29.5 \text{ M}, r = -0.9908.$
	$E_0 = 22.0 \text{ M}, r = -0.9984.$
	$E_0 = 13.0 \text{ M}, r = -0.9900.$

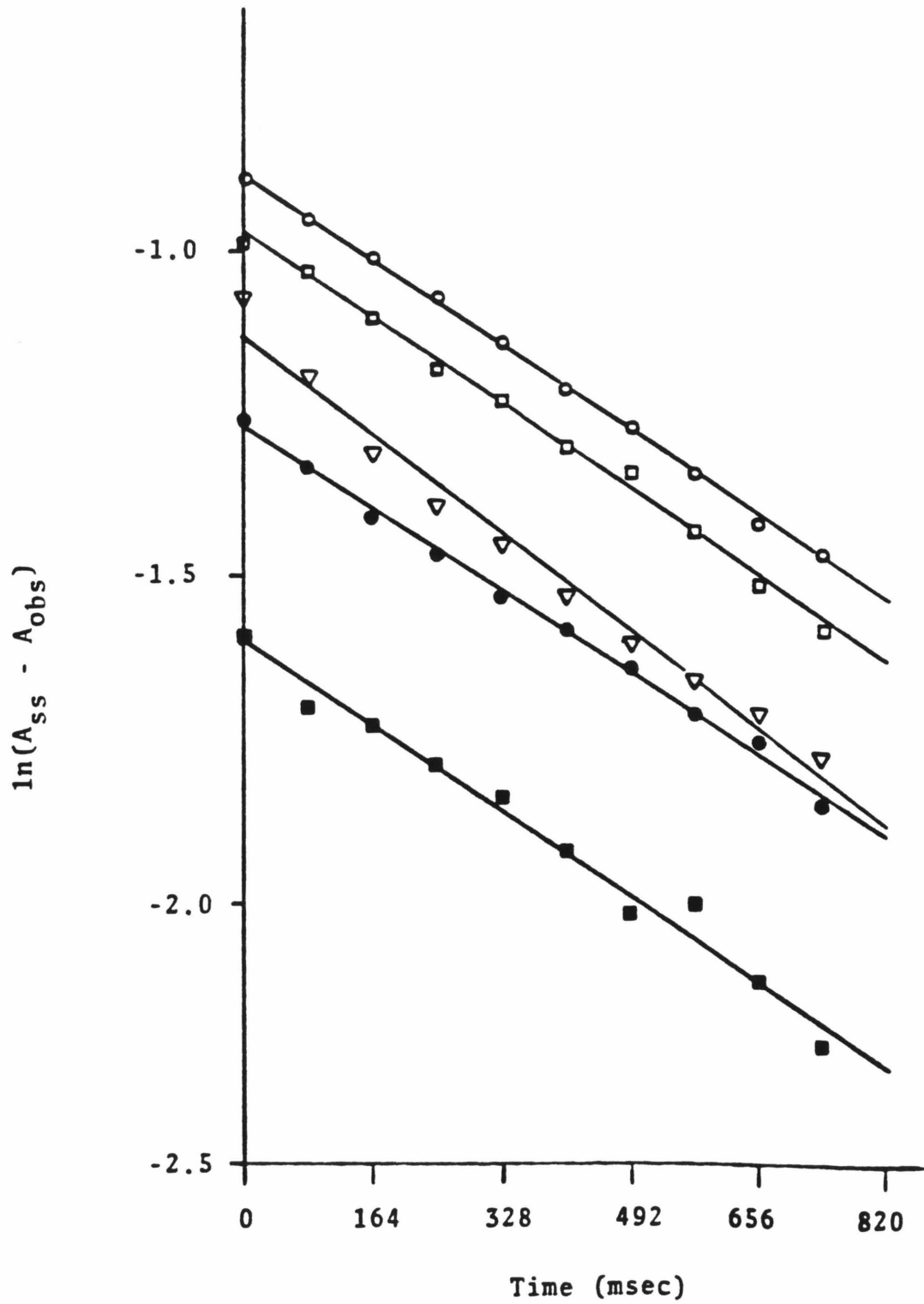


**TABLE I.** Kinetic parameters for the reaction of elastase with N-acetyl-L-alanyl-L-prolyl-L-alanine p-nitroanilide.<sup>a</sup>

$S_o$ (mM)	$E_o$ ( $\mu$ M)	$\pi_m^b$ ( $A_{410}$ )	$\pi_c^c$ ( $A_{410}$ )	B ( $s^{-1}$ ) <sup>d</sup>	$v_{ss}$ ( $\times 10^5 \text{ Ms}^{-1}$ ) <sup>e</sup>	$k_{cat}$ ( $s^{-1}$ ) <sup>f</sup>
2.02	13.0	0.026	0.025	1.82	0.87	1.20
	22.0	0.055	0.053	1.75	1.45	1.18
	29.5	0.084	0.074	2.11	2.05	1.24
	36.5	0.103	0.107	1.86	2.33	1.15
	44.0	0.125	0.130	1.83	2.58	1.05
1.09	7.5	0.011	0.008	2.13	0.35	1.15
	22.0	0.028	0.026	1.50	1.05	1.18
	29.5	0.042	0.039	1.58	1.32	1.14
	44.0	0.062	0.063	1.89	1.95	1.09
	13.0	0.016	0.017	1.73	0.64	1.21
	13.0	0.019	-----	-----	0.65	1.24
	22.0	0.030	-----	-----	1.02	1.14
average						1.16

<sup>a</sup> 0.1 M  $H_3PO_4/KOH$ , pH 8.25, 10% (v/v) acetonitrile/water, 25.0  $\pm$  0.2°C.

<sup>b</sup>  $\pi_m \equiv$  value of burst as measured from  $A_{410}$  versus time plot (see Figure 4).

<sup>c</sup>  $\pi_c \equiv$  value of burst as calculated for the first-order plot (see Figure 6 and text).

<sup>d</sup> B  $\equiv$  first-order rate constant for buildup of intermediate.

<sup>e</sup>  $v_{ss} \equiv$  steady-state (linear) velocity.

<sup>f</sup>  $k_{cat} = (v_{ss}/E_o)((S_o + K_m)/S_o)$ , using  $K_m = 1.6$  mM.

**TABLE II.** Kinetic parameters for the reaction of elastase with N-succinyl-L-alanyl-L-alanyl-L-alanine p-nitroanilide.<sup>a</sup>

$S_o$ (mM)	$E_o$ ( $\mu$ M)	$\pi_m$ ( $A_{410}$ )	$\pi_c$ ( $A_{410}$ )	B ( $s^{-1}$ )	$v_{ss}$ ( $\times 10^5$ $M_s^{-1}$ )	$k_{cat}$ ( $s^{-1}$ ) <sup>b</sup>
2.05	7.5	0.025	0.018	4.06	1.61	3.31
	13.0	0.040	0.038	3.65	2.57	3.04
	22.0	0.078	0.080	4.55	4.56	3.19
	29.5	0.117	0.111	3.70	5.85	3.05
	36.5	0.144	0.147	5.15	7.21	3.04
	44.0	0.174	0.169	4.13	8.31	2.91
1.09	7.5	0.012	0.009	2.78	1.29	3.44
	13.0	0.021	0.018	5.05	2.01	3.09
	22.0	0.044	0.040	4.24	3.26	2.96
	29.5	0.059	0.072	4.04	4.19	2.84
	36.5	0.071	0.076	6.20	5.54	3.04
	44.0	0.081	0.082	4.61	5.78	2.63
average						3.05

<sup>a</sup>See Table I for the reaction conditions and the definitions of the symbols.

<sup>b</sup>Calculated using  $K_m = 1.1$  mM.

Figure 7. The dependence of the burst,  $\pi$ , on the total concentration of enzyme,  $E_0$ , for the elastase-catalyzed hydrolysis of tripeptide p-nitroanilides. The lines in the figure were obtained by applying a linear least-squares regression to the observed values of the burst,  $\pi_m$  (closed circles). The origin was also included in the least-squares analysis. Calculated values of the burst,  $\pi_c$  (open circles), are included for comparison.

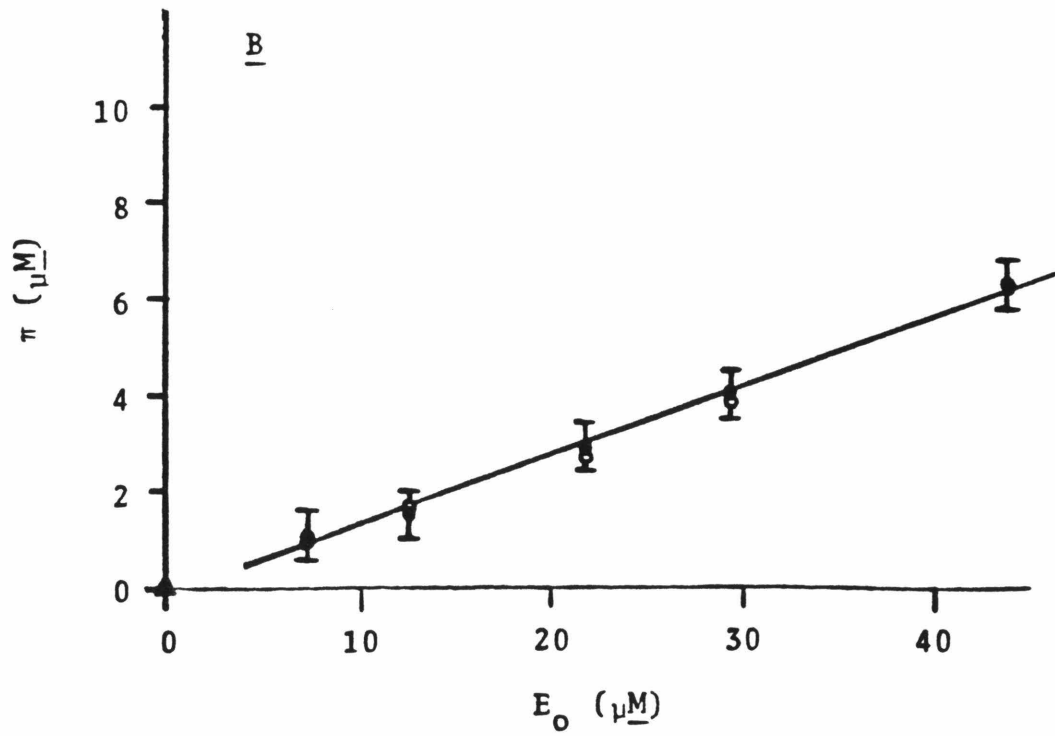
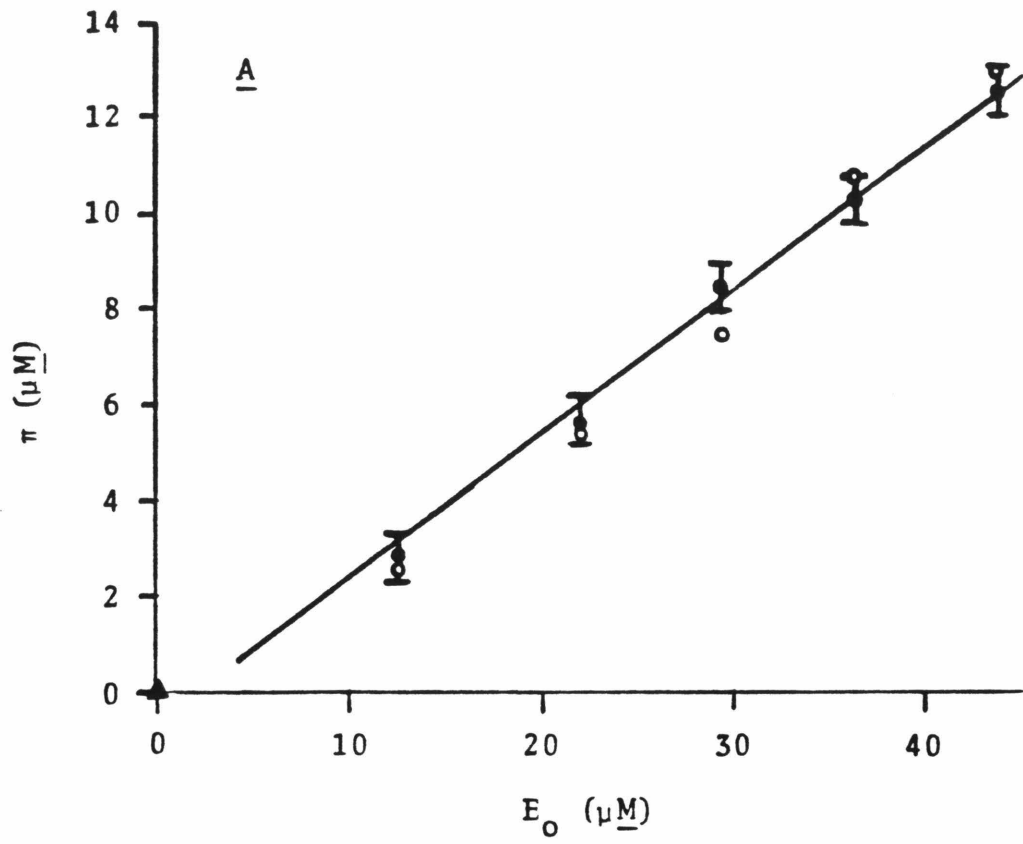
A)  $S_0 = 2.02 \text{ mM APAPNA}$ .  $r$ , the correlation coefficient of the regression, is 0.995.

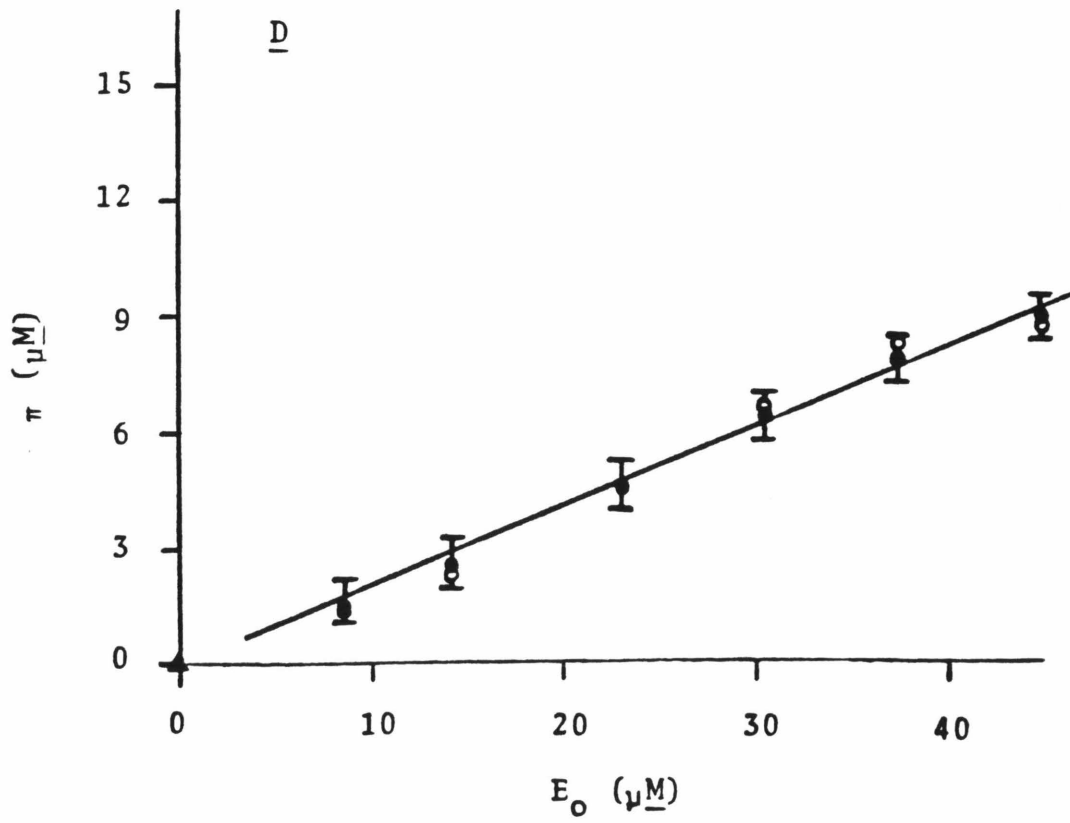
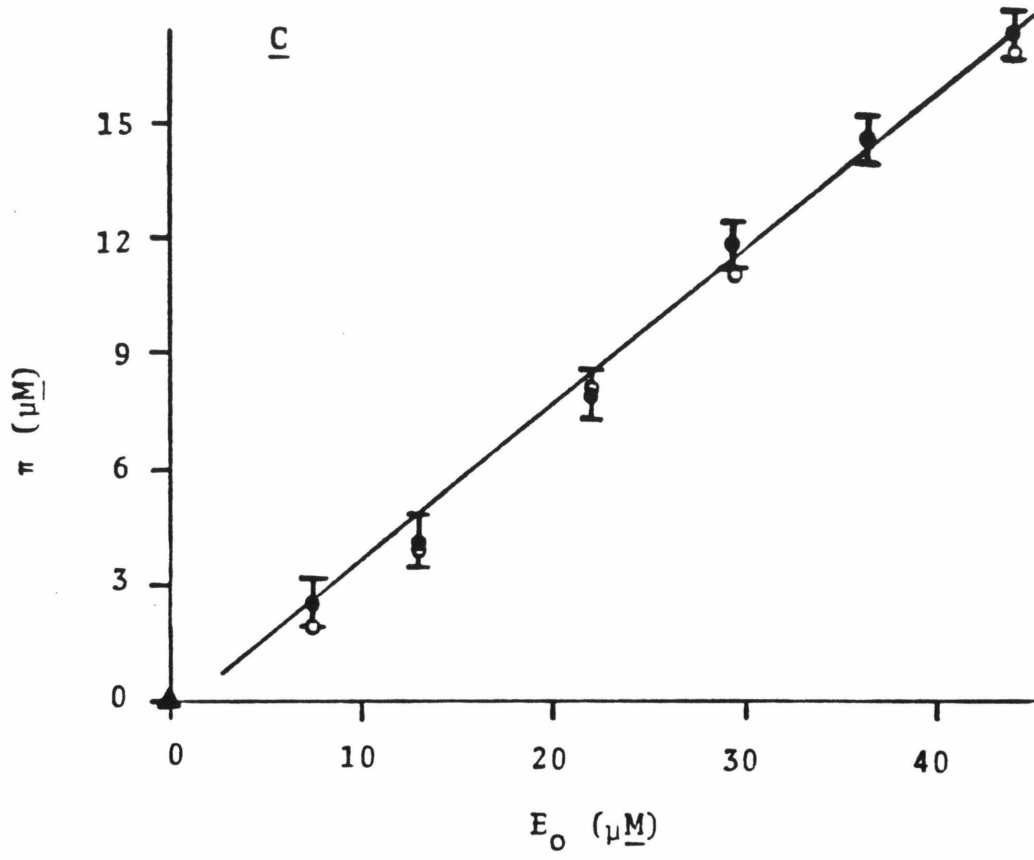
B)  $S_0 = 1.09 \text{ mM APAPNA}$ .  $r = 0.998$ .

C)  $S_0 = 2.05 \text{ mM STAPNA}$ .  $r = 0.997$ .

D)  $S_0 = 1.09 \text{ mM STAPNA}$ .  $r = 0.997$ .

The error bars in the figures represent  $\pm 0.005$  absorbance unit.





intersect the  $\pi$ -axis at negative values of  $\pi$  implies i) the values of  $\pi$  used are too small; ii) the values of  $E_0$  used are too large; or iii) a combination of (i) and (ii). Although it is difficult to determine  $\pi_m$  accurately (due to the dead-time of 10 ms) especially at small  $E_0$ , the fact that  $\pi_c$  and  $\pi_m$  are within  $\pm 0.010$  A for all but one measurement mitigates against the possibility of severe errors in  $\pi$ . An error in  $E_0$  is a much more likely possibility, either due to unequal mixing in the cuvette or, more likely, moderate autolysis of the enzyme during the time required to perform the experiment. Even though the enzyme samples were kept on ice whenever not in the spectrophotometer, at the concentration used in this study significant autolysis might be occurring. In any case, this error is only of the order of 1 or 2  $\mu$ M.

Several internal checks are available in the experiment. Since for any given kinetic run, the decrease in  $S_0$  over the time period of observation is less than 5%,  $v_{ss}$  should be directly proportional to  $E_0$  for a particular value of  $S_0$ . Assuming a value of 1.6 mM for  $K_m$  for APAPNA (Hunkapiller et al., 1976) and 1.1 mM for  $K_m$  for STAPNA (Bieth et al., 1974)<sup>1</sup>, values of  $k_{cat} = 1.16 \pm 0.06$  (average  $\pm$  standard deviation) can be calculated (from Table I); for STAPNA,  $k_{cat} = 3.05 \pm 0.21$  (from Table II). The precision of these values implies a linear correlation between  $v_{ss}$  and  $E_0$ , as predicted from Michaelis-Menten kinetics. Furthermore, these observations substantiate the steady-state assumption necessary for the theoretical treatment, even though the minimum  $S_0$  to  $E_0$  ratio of 25 is probably near the lower limit for the validity of this assumption.

---

<sup>1</sup>Although these experiments were carried out at different pH values,  $K_m$  is constant over the pH range 8-10 (Shotton, 1970). Hence we can use these values here.

Another internal check is  $K_m$ . The value of this parameter can be calculated from  $V_{SS}$  as a function of  $S_0$  for the same  $E_0$ . Although there are only two  $S_0$  points for any given  $E_0$ , values of  $K_m = 1.5 \pm 0.3$  for APAPNA and  $K_m = 1.8 \pm 0.7$  for STAPNA are obtained, in reasonable agreement with the previously published values considering the crudeness of the calculation. The larger error in  $K_m$  for STAPNA is due to the more rapid rate of hydrolysis of this substrate, and reflects the difficulty in measuring  $v_{SS}$  accurately at large  $E_0$  and  $S_0$  by this method.

DISCUSSION

The use of the two substrates of porcine pancreatic elastase examined in this study is predicated upon three factors: i) hydrolysis can be monitored conveniently by spectrophotometric observation of the p-nitroaniline chromophore; ii) the strongly electron-withdrawing nature of the p-nitro group should stabilize the negative charge of the putative tetrahedral intermediate; and iii) both substrates exhibit strong, specific interactions with the protein and bind in predominantly productive modes. Elastase is well known to have an extended substrate-binding region (Thompson and Blout, 1970; Thompson and Blout, 1973a; Thompson and Blout, 1973b; Atlas and Berger, 1973; Thompson and Blout, 1973c); increased occupation of these subsites by substrate amino-acid residues allows the enzyme to manifest catalytic abilities not seen with smaller, less-specific substrates (Thompson, 1974; Hunkapiller et al., 1976; Elrod et al., 1980; Quinn et al., 1980).

Both substrates show clear biphasic kinetics with the enzyme. The kinetic results are in good agreement with the proposed mechanism, and indicate the presence of a discrete tetrahedral adduct of enzyme and substrate. The assignment of the pre-steady state absorbance increase to a tetrahedral intermediate has been cogently and completely argued (Hunkapiller et al., 1976) previously; we are in complete agreement with their arguments.

One unfortunate difficulty with this experiment is the small values of  $\pi$  obtained, especially for low enzyme concentrations. However, we can get an estimate for the steady-state concentration of intermediate from these data. Table III presents calculations that show about 20% of enzyme-bound substrate is initially in the form of tetrahedral addition

TABLE III. Calculation of the amount of accumulated intermediate in the elastase-catalyzed hydrolysis of tripeptide p-nitro-anilide substrates.<sup>a</sup>

<u>N-acetyl-L-alanyl-L-prolyl-L-alanine p-nitroanilide</u>					
$S_0$ (mM)	$E_0$ ( $\mu$ M)	$\pi$ ( $\mu$ M) <sup>b</sup>	(ES) ( $\mu$ M) <sup>c</sup>	$(\pi/E_0)$ (%)	$(\pi/ES_T)$ (%) <sup>d</sup>
2.02	13.0	1.4	6.5	11	18
	22.0	3.0	10.6	14	22
	29.5	4.2	14.1	14	23
	36.5	6.1	16.9	17	25
	44.0	7.4	20.2	17	25
1.09	7.5	0.5	2.8	7	15
	22.0	1.5	8.3	7	15
	29.5	2.2	11.0	7	17
	44.0	3.6	16.2	8	18
<u>N-succinyl-L-alanyl-L-alanyl-L-alanine p-nitroanilide</u>					
2.05	7.5	1.1	4.2	15	22
	13.0	2.1	7.1	16	23
	22.0	4.5	11.4	20	28
	29.5	6.3	15.0	21	30
	36.5	8.3	18.3	23	31
	44.0	9.6	22.3	22	30
1.09	7.5	0.5	3.5	7	15
	13.0	1.0	6.0	8	16
	22.0	2.3	9.8	10	19
	29.5	3.5	12.8	12	21
	36.5	4.3	15.9	12	21
	44.0	4.7	19.3	11	20

<sup>a</sup>0.1 M  $H_3PO_4/KOH$ , pH 8.25, 10% (v/v) acetonitrile/water, 25.0  $\pm$  0.2°C.

<sup>b</sup>Assuming  $\epsilon_{410} = 8,800 M^{-1}cm^{-1}$  and a 2.0 cm light path.

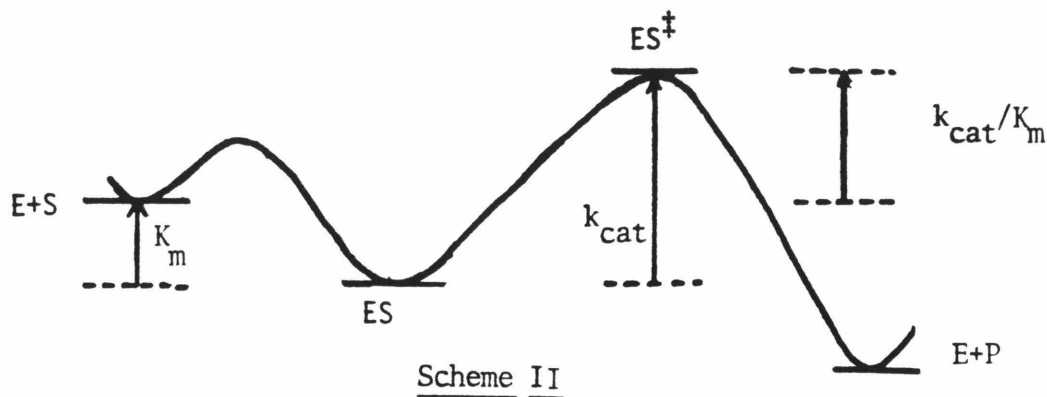
<sup>c</sup>Concentration of Michaelis complex, assuming  $K_m = K_s = (E)(S)/(ES)$ .

<sup>d</sup> $ES_T = \pi + (ES) \equiv$  concentration of total enzyme-bound substrate species. This value depends heavily on the accuracy of  $K_m = K_s$ .

complex at steady-state for APAPNA and about 25% for STAPNA. Of course, the accuracy of these values depends on the closeness of the approximation that  $K_m = K_s$ . The similarity of the two values is interesting and not entirely unexpected, since the stabilizing forces for this intermediate should come primarily from interactions between the active site residues and the carboxyl-terminal residue of the peptides. Since both substrates have an L-alanine p-nitroanilide residue as the c-terminus, similar stabilizing forces should be involved.

The large difference in  $k_{cat}$  values for the two substrates ( $1.16s^{-1}$  for APAPNA,  $3.05s^{-1}$  for STAPNA) appears to be in conflict with the above observation, as it is difficult to equate a 5% increase in intermediate concentration with a three-fold increase in  $k_{cat}$ . Therefore, it is apparent that the rate increase must be due to some consideration other than intermediate stabilization.

Fersht (1974, 1977, 1980) has presented arguments to show that an enzyme will exhibit its maximum catalytic efficiency when the structure of the enzyme is complementary to the structure of the substrate in the transition state, rather than in the Michaelis complex. In this case, the intrinsic binding energy of the enzyme and substrate is used for catalysis rather than tight enzyme-substrate binding. Catalytic efficiency is reflected in a large value of  $k_{cat}/K_m$ , which is related to the energy difference between  $E + S$  in their respective ground states and  $ES^\ddagger$ , the transition state, rather than in  $k_{cat}$  alone, which is related to the difference in energy between  $ES$ , the Michaelis complex, and  $ES^\ddagger$ . These ideas are diagrammed in Scheme II;  $K_m$  in this instance is assumed to represent the dissociation constant of  $ES$ . Tight binding of the substrate



by the enzyme (as indicated by a small value of  $K_m$ ) will result in a larger barrier for the transformation of ES to  $ES^\ddagger$ , as the energy difference between E + S and ES increases, and thus in a smaller value for  $k_{cat}/K_m$ .

A corollary of this hypothesis of maximization of rate by maximization of  $k_{cat}/K_m$  is that no intermediate should accumulate after the initial Michaelis complex (Fersht, 1974). If any intermediate accumulates, the apparent  $K_m$  of the reaction will decrease; furthermore, the rate of decomposition of the intermediate will be slower than its rate of formation, so that  $k_{cat}$  will decrease. Thus, the overall rate of the reaction, as reflected in  $k_{cat}/K_m$ , may be lowered.

Thompson has discussed the importance of extensive, specific enzyme-substrate interactions on the rate of hydrolysis of peptide substrates of elastase (Thompson, 1974; Thompson and Blout, 1973). His conclusion is that elastase displays its maximal catalytic potential when certain exact contacts are made between the substrate and an extended portion of the enzyme binding surface in the Michaelis complex; when these contacts cannot be made properly, the substrate cannot be oriented optimally with respect to the catalytic active site residues, and the efficiency of hydrolysis decreases as a result.

The application of these ideas to the results of this study yields

some intriguing suggestions. Both  $k_{\text{cat}}$  and  $B$ , the rate constants readily accessible from the data, are complicated functions of many rate constants. Specifically,  $k_{\text{cat}} = k_3 k_f / (k_f + k_B + k_3)$  (equation 14). If the rate of formation of ET ( $k_f$ ) is larger than the rate of its breakdown ( $k_B + k_3$ ), then  $k_{\text{cat}} = k_3$ . In other words, the turnover rate will be solely dependent on the rate of breakdown of ET to EA. Furthermore,  $\pi = \{1 - (k_3/B)\} \{S_0 / (S_0 + K_m)\} E_0$ . Since  $S_0$  and  $K_m$  are both known, we can estimate the proportionality factor between  $\pi$  and  $E_0$  and compare it to  $\{1 - (k_3/B)\} \{S_0 / (S_0 + K_m)\}$ .

The calculations for this comparison are presented in Table IV. Although the precision of the relevant data is low, the calculations are probably indicative. The assumption that  $k_{\text{cat}} = k_3$  appears to be a better approximation for STAPNA than for APAPNA. If  $k_{\text{cat}} < k_3$ , the observed rate of hydrolysis is dependent both on the rate of formation and breakdown of ET. Since the maximal turnover rate will be obtained when  $k_{\text{cat}} = k_3$ , and since this rate will be observed only when all of the correct interactions between the enzyme and the substrate are realized, it follows that STAPNA makes more of the necessary contacts with the elastase binding site than APAPNA. Furthermore, if  $k_f > (k_b + k_3)$ , then  $K_s > K_m$ , since only if  $k_f < (k_b + k_3)$  can  $K_s$  be equal to  $K_m$  (see Theory). Thus, STAPNA may be less tightly bound to elastase than is APAPNA (that is,  $K_s$  for STAPNA  $>$   $K_s$  for APAPNA), so that ET may be a significantly larger fraction of enzyme-bound substrate for STAPNA than for APAPNA. These two considerations imply that the increased catalytic efficiency of elastase with STAPNA as opposed to APAPNA is due to greater destabilization of the relevant ES-complex relative to the transition state of the reaction with the former substrate. The

TABLE IV. Comparison of the results of Table III with the hypothesis  $k_{\text{cat}} = k_3$ .

---

<u>N-acetyl-L-alanyl-L-prolyl-L-alanine p-nitroanilide</u>		
$k_{\text{cat}} = 1.16 \text{ s}^{-1}$ $K_m = 1.6 \text{ mM}$ $B = 1.82 \text{ s}^{-1}$ $1 - (k_{\text{cat}}/B) = 0.36$	For $S_o = 2.02 \text{ mM}$ , $S_o/(K_m + S_o) = 0.56$ . From Table III, $\pi = 0.15E_o$ . Calculated <sup>a</sup> , $\pi = 0.20E_o$ .	For $S_o = 1.09 \text{ mM}$ , $S_o/(K_m + S_o) = 0.41$ . From Table III, $\pi = 0.07E_o$ . Calculated <sup>a</sup> , $\pi = 0.15E_o$ .
<u>N-succinyl-L-alanyl-L-alanyl-L-alanine p-nitroanilide</u>		
$k_{\text{cat}} = 3.05 \text{ s}^{-1}$ $K_m = 1.1 \text{ mM}$ $B = 4.35 \text{ s}^{-1}$ $1 - (k_{\text{cat}}/B) = 0.30$	For $S_o = 2.05 \text{ mM}$ , $S_o/(K_m + S_o) = 0.65$ . From Table III, $\pi = 0.20E_o$ . Calculated <sup>a</sup> , $\pi = 0.20E_o$ .	For $S_o = 1.09 \text{ mM}$ , $S_o/(K_m + S_o) = 0.50$ . From Table III, $\pi = 0.10E_o$ . Calculated <sup>a</sup> , $\pi = 0.15E_o$ .

---

<sup>a</sup>Calculated from  $(1 - (k_{\text{cat}}/B))(S_o/(K_m + S_o))$ .

tetrahedral intermediate formed between elastase and STAPNA more readily decomposes to products rather than returning to ES-complex, than does the intermediate formed between elastase and APAPNA. It therefore appears that the increased rate of the hydrolysis of STAPNA stems both from a change in rate-determining-step (primarily decomposition of ET in the case of STAPNA as opposed to a combination of formation and decomposition in the case of APAPNA) and an increased destabilization of the ES-complex.

This argument is reinforced by the low temperature results of Fink and Meehan (1979). These researchers were able to detect virtually 100% tetrahedral intermediate, under appropriate conditions, during the reaction of STAPNA with elastase, while only observing 30-40% intermediate in the APAPNA-elastase system under the same conditions. Since this cryoenzymological approach depends on the kinetic trapping of intermediates, it is clear that the ES → ET conversion favors ET over ES for STAPNA, while ES and ET are rapidly interconverting in the APAPNA system, even at low temperature.

It should be mentioned that Fink and co-workers have also detected a non-covalent intermediate between the Michaelis-complex and the tetrahedral adduct of elastase and p-nitroanilide substrates (Fink and Meehan, 1979), trypsin and a p-nitroanilide substrate (Compton and Fink, 1980), chymotrypsin and a p-nitroanilide substrate (Fink, 1976), and papain, a thiol-protease, and a p-nitroanilide substrate (Angelides and Fink, 1978, 1979). The mechanism proposed in this study has assumed that this intermediate and the Michaelis-complex are in equilibrium, and are both included in the ES structure, mainly for simplicity. They assign this intermediate to a conformational realignment of the active site residues relative to the non-covalently bound substrate; inherent

in the structure of such an intermediate may be the understanding of the forces engaged in the destabilization the scissile substrate bond. Previous studies. The results of this experiment are quantitatively at odds with those presented by Hunkapiller, et al., (1976). They reported biphasic kinetics with  $B \approx 17 \text{ sec}^{-1}$  and  $k_{\text{cat}} = 3 \text{ sec}^{-1}$  for the reaction of APAPNA and elastase. The difference in the steady-state rate constant  $k_{\text{cat}}$  is probably due to the difference in organic solvent and salt content of the buffers employed in the two studies. In our case, 10% acetonitrile was employed to aid in the dissolution of the p-nitroaniline product and in the cleansing of the old reaction mixture from the cuvette by the following injection.

The difference between the values of B obtained in the two studies can be explained by observing the raw data of the Hunkapiller et al. (1976) experiment. Figure 8 presents representative oscilloscope traces. In the early portion of the trace a rapid increase in absorbance is seen, even in the absence of enzyme. This is the result of a mixing artifact, probably brought on by the mixing of a solution containing 8% methanol (the substrate) with one containing 0.2 M TRIS/HCl (the enzyme). In the study reported here we dissolved the enzyme and substrate in the same buffer and were able to reduce this artifact considerably. Apparently this artifact was not taken into account in their observations, resulting in the over-estimation of B and  $\pi$ .

These results are also in direct contradiction with the results presented by Markley, et. al. (1981). These researchers reported linear kinetics for the elastase-STAPNA and elastase-APAPNA systems; they observed no biphasic kinetics occurring in these systems. Their published results are replete with experimental inadequacies, however. In Figure

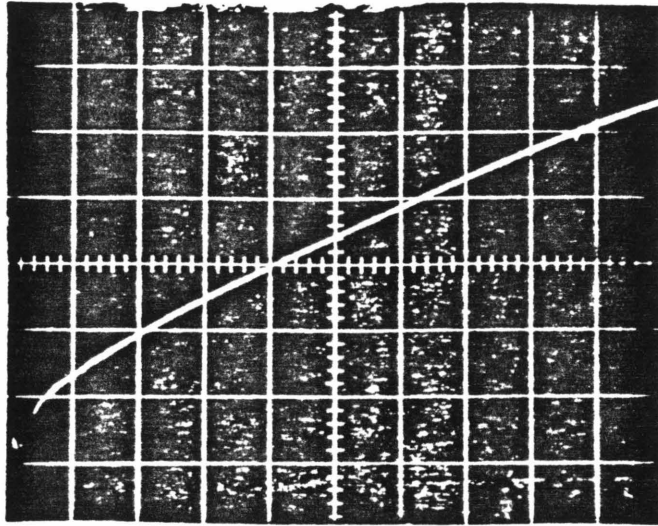
Figure 8. Raw data for the Hunkapiller, Forgacs, and Richards (1976) paper. These are photographs of the oscilloscope traces for the reaction of elastase with APAPNA.

A)  $E_o = 3.49 \times 10^{-5} \underline{M}$ ,  $S_o = 1.50 \underline{mM}$ ;  $\Delta A_{410}/\text{cm} = 0.2$ ;  
 $\Delta t/\text{cm} = 100$ .

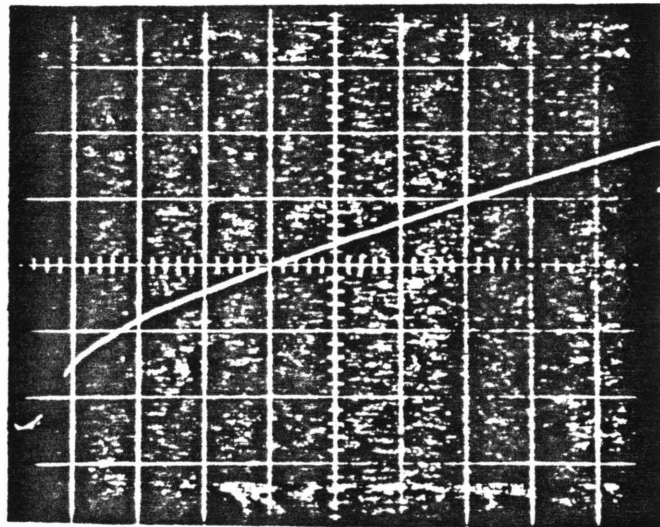
B)  $E_o = 2.13 \times 10^{-5} \underline{M}$ ,  $S_o = 1.50 \underline{mM}$ ;  $\Delta A_{410}/\text{cm} = 0.1$ ;  
 $\Delta t/\text{cm} = 50$ .

C)  $E_o = 0$ ,  $S_o = 1.50 \underline{mM}$ ;  $\Delta A_{410}/\text{cm} = 0.02$ ;  $\Delta t/\text{cm} = 100$ .

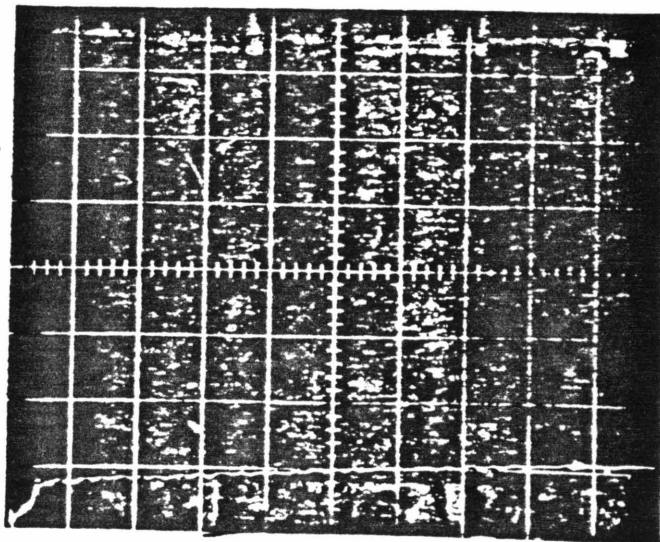
A



B



C



2 of their paper, they present a trace of the reaction of 15  $\mu\text{M}$  elastase with 1.4 mM STAPNA at 2°C, on a 0-2 sec time scale. The trace appears linear. However, from the results of the present experiment, at 25°C the burst in only 0.040 absorbance units from 2.05 mM STAPNA, 13  $\mu\text{M}$  elastase. At 2°C, both  $B$  and  $k_{\text{cat}}$  should be smaller than at 25°C, and if the magnitudes of  $B$  and  $k_{\text{cat}}$  approach each other, the already small burst will be severely attenuated and the reaction will appear to be linear.

The reaction of 7.5mM APAPNA with varying elastase concentrations is shown in Figure 3 of their paper. The time scale of the traces is 0-250 sec, clearly too large to observe the biphasic kinetics of this study which occur over a one to two-second time scale. Furthermore, the authors appear confused over the definition of the steady-state reaction.

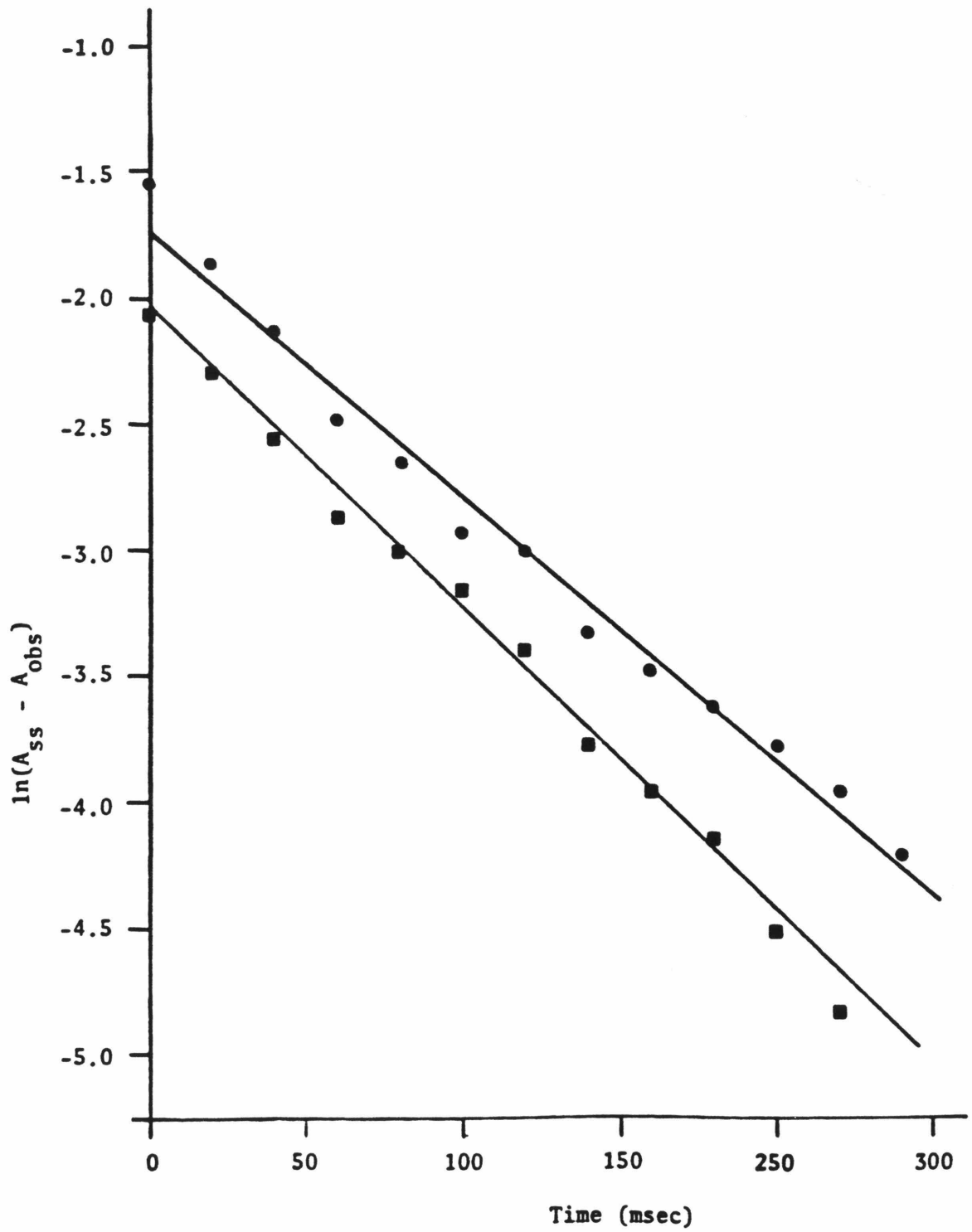
The steady state reaction is actually a pseudo-first order reaction which, in our formulation, occurs after the tetrahedral intermediate reaches a steady-state concentration, and represents turnover of the substrate. Linearity (that is, zero order hydrolysis) is an approximation made by assuming a change in the substrate concentration of only a few percent. While the steady-state reaction will appear to be linear over any portion of the reaction that conforms to this approximation, the initial steady-state rate, from which  $k_{\text{cat}}$  can be extracted, must be calculated assuming that the initial substrate concentration has been reduced by less than five percent. However, Markley et al. (1981) have chosen to define the initial portion of the steady-state reaction as occurring only after at least eight percent of the initial substrate has been hydrolyzed.

A more important inadequacy of the experiment presented in Figure 3 of their paper is the use of 450 nm as the wavelength for their absorbance measurements. This wavelength was used due to the large substrate concentration employed in order to remain within the linear range of the spectrophotometer. However, our calculations show that at 450 nm the molar absorptivity of p-nitroaniline is only one-tenth that at 410 nm. Although increasing  $S_0$  from 2.05 mM to 7.5 mM results in a 50% increase in  $S_0/(S_0 + K_m)$  (0.56 to 0.82), the decrease in  $\epsilon$  will overwhelm this slight increase and render the burst kinetics unobservable in most cases.

The results of the present study also render the objections raised by Markley et al. (1981) to the previous study (Hunkapiller et al., 1976) untenable. A primary objection was the apparent non-linear relationship between  $\pi$  and  $E_0$  as calculated from the Figure 1 data of the Hunkapiller et al. paper. This conclusion is documented in Figure 7 of the Markley et al. paper. However, it is clear that these authors have weighted the least accurate portion of the data (that part where  $A_{ss} - A_{obs}$  is small) the heaviest in determining the lines drawn in the figure. A similar plot of the data done by us (see Figure 9) using points for  $t \leq 200$  msec and weighting all points equally in the linear least squares regression gives, for  $E_0 = 35 \mu\text{M}$ ,  $b = 9.45\text{s}^{-1}$  and  $\pi = 0.178A$ , and for  $E_0 = 21 \mu\text{M}$ ,  $b = 11.3\text{s}^{-1}$  and  $\pi = 0.129A$ . The ratio of the two values of  $\pi$  is 1.38, whereas the ratio of the values of  $E_0$  is 1.67. Within experimental error, therefore, these data conform to the predictions of the proposed mechanism.

Markley et al. (1981) attempted to explain the non-linear kinetics observed by Hunkapiller et al. (1976) as due to the presence of two forms of the APAPNA substrate, which exist as two conformational isomers

Figure 9. Calculation of  $\pi$  and B for the data from Figure 1 of Hunkapiller, Forgac , and Richards (1976). The upper line (circles) is a linear least squares fit of the reaction of  $35 \times 10^{-6}$  M elastase with 1.50 mM APAPNA; the bottom line (squares) is for  $21 \times 10^{-6}$  M elastase with 1.50 mM APAPNA.



(cis and trans) about the Ala-Pro peptide bond. It was postulated that these two forms were hydrolyzed at different rates, resulting in the biphasic absorbance versus time traces. This cannot be the case, however, since STAPNA also shows biphasic kinetics with elastase, and this substrate is isomerically homogenous.

One last consideration. The similarity in magnitude between B and  $k_{cat}$  raises the question: Is the observed rate decrease simply due to the decrease in  $S_0$  according to the Michaelis-Menten equation? As an example, we shall consider the reaction of 44 M elastase with 2.02 mM APAPNA (see Figure 4D). The initial rate of this reaction (as approximated by a straight line through the first two data points) is  $5.40 \times 10^{-5} \text{ Ms}^{-1}$ . The rate which we have described at  $v_{ss}$  is  $2.58 \times 10^{-5} \text{ Ms}^{-1}$ ; this rate occurs for  $\Delta S_0 \leq 5\%$ . For Michaelis-Menten kinetics,  $v_1/v_2 = [S_1/(K_m + S_1)] / [(K_m + S_2)/S_2]$ . For  $K_m = 1.6 \text{ mM}$ ,  $v_1/v_2 = 1.02$ , clearly less than the factor of 0.5 calculated for the ratio for the steady-state rate and initial rate. Therefore, this biphasic kinetics cannot be due to a simple rate decrease corresponding to substrate hydrolysis according to a Michaelis-Menten mechanism.

CONCLUSION

The stopped-flow kinetic studies reported in this chapter are shown to fully support a mechanism of peptide p-nitroanilide hydrolysis in which a tetrahedral addition complex of enzyme and substrate is intermediate in the conversion of the Michaelis-complex to the acyl-enzyme, in accord with previous studies (Hunkapiller et al., 1976; Fink and Meehan, 1979; Compton and Fink, 1980; Balny and Bieth, 1977; Petkov, 1978). Objections to these previous studies (Markley et al., 1981) have been shown to be untenable. This intermediate exists in a moderate steady-state concentration (~20% of total enzyme-bound substrate) during the initial portion of the reaction. Breakdown of this intermediate to acyl-enzyme is partially to fully rate-determining, in agreement with O'Leary and Kluetz (1972, 1974). The results also suggest that the catalytic efficiency of the enzyme is highly dependent on the proper orientation of the catalytic groups in the enzyme active site with respect to the scissile bond of the substrate; extended contacts along the binding sites of the protein are crucial in realizing full catalytic potency (Thompson, 1974; Hunkapiller et al., 1976). In this regard, further studies of this sort with longer peptides (tetra- and pentapeptide p-nitroanilides) should prove instructive.

It is our contention that the tetrahedral intermediate is a common feature of the serine protease-catalyzed hydrolysis of amide bonds. The ability to observe this intermediate in cases where the substrate has not been so carefully engineered to provide special stabilization of a negatively charged tetrahedral adduct may not be kinetically realizable (Fersht, 1972) since it is quite possible that intermediates of this sort occurring during the catalytic sequence for normal substrates

(peptides, proteins) of these enzymes will closely resemble the transition states of formation and breakdown of these structures. Observation of accumulated intermediate will depend on the fulfillment of two conditions: i) the rate of breakdown of ET must be no greater than the rate of its formation, so that the intermediate will have a significant lifetime; and ii) the difference in energy between ES and ET must not be so large as to render ET only a small fraction of the total amount of enzyme-bound substrate. These conditions may not be met for certain substrates: this will be especially true in the case of substrates that are unable to interact with a substantial portion of the enzyme binding surface in a productive manner. However, it does not generally benefit any enzyme designed to hydrolyze proteins to their component amino acids to stabilize any intermediate structure too strongly, since it would be catalytically inefficient to incapacitate a sizeable quantity of enzyme as any intermediate complex.

## REFERENCES

- Angelides, K.J., and Fink, A.L. (1978), Biochemistry 17, 2659-2668.
- Angelides, K.J., and Fink, A.L. (1979), Biochemistry 18, 2363-2369.
- Atlas, D., and Berger, A. (1973), Biochemistry 12, 2573-2577.
- Baillargeon, M.W., Laskowski, M Jr., Neves, D.E., Porubcan, M.A., Santini, R.E., and Markley, J.L. (1980), Biochemistry 19, 5703-5710.
- Balny, C., and Bieth, J.G. (1977), FEBS Letters 80, 182-186.
- Bender, M.L., and Kaiser, E.T. (1962), J. Am. Chem. Soc. 84, 2556-2561.
- Bender, M.L., Schonbaum, G.R., and Zerner, B. (1962), J. Am. Chem. Soc. 84, 2562-2570.
- Bender, M.L., Kezdy, F.J., and Gunter, C.R. (1964), J. Am. Chem. Soc. 86, 3714-3721.
- Bender, M.L., Begue-Canton, M.L., Blakeley, R.L., Brubacher, L.J., Feder, J., Gunter, C.R., Kezdy, F.J., Killheffer, J.V. Jr., Marshall, T.H., Miller, C.G., Roeske, E.W., and Stoops, J.K. (1966), J. Am. Chem. Soc. 88, 5890-5913.
- Bernhard, S.A., Lau, S.T., and Noller, H. (1965), Biochemistry 4, 1108-1118.
- Bieth, J., Speiss, B., and Wermuth, C.G. (1974), Biochem. Med. 11, 350-357.
- Blow, D.M., Janin, J., and Sweet, R.M. (1974), Nature (London) 249, 54-57.

- Breaux, E.J., and Bender, M.L. (1976), Biochem. Biophys. Res. Commun. 70, 235-240.
- Caplow, M. (1969), J. Am. Chem. Soc. 91, 3639-3645.
- Compton, P., and Fink, A.L. (1980), Biochem. Biophys. Res. Commun. 93, 427-431.
- Elrod, J.P., Hogg, J.L., Quinn, D.M., Venkatasubban, K.S., and Schowen, R.L. (1980), J. Am. Chem. Soc. 102, 3917-3922.
- Erlanger, B.F., Kokowsky, N., and Cohen, W. (1961), Arch. Biochem. Biophys. 95, 271-278.
- Fastrez, J., and Fersht, A.R. (1973), Biochemistry 12, 2025-2034.
- Fersht, A.R., and Requena, Y. (1971), J. Am. Chem. Soc. 93, 7079-7087.
- Fersht, A.R. (1972), J. Am. Chem. Soc. 94, 293-295.
- Fersht, A.R., Blow, D.M., and Fastrez, J. (1973), Biochemistry 12, 2035-2041.
- Fersht, A.R. (1974), Proc. R. Soc. Lond. B. 187, 397-407.
- Fersht, A.R. (1977), "Enzymes Structu  
Freeman and Company,
- Fersht, A.R. (1980), in "Enzymic and Non-Enzymic Catalysis",  
P. Dunnill, ed., Ellis Horwood, Ltd., Chichester, England,  
13-27.
- Fink, A.L. (1976a), J. Theor. Biol. 61, 419-445.
- Fink, A.L. (1976b), Biochemistry 15, 1580-1586.
- Fink, A.L. (1977), Acc. Chem. Res. 10, 232-239.
- Fink, A.L., and Meehan, P. (1979), Proc. Natl. Acad. Sci. USA 76, 1566-1569.

- Fink, A.L. (1979), Trends Biochem. Sci. 4, 8-10.
- Fink, A.L., and Geeves, M.A. (1979), in "Methods in Enzymology", vol. 63, D. L. Purich, ed., Academic Press, New York, 336-370.
- Fink, A.L., and Petsko, G.A. (1981), Adv. Enzymol. 52, 177-246.
- Gutfreund, H., and Sturtevant, J.M. (1956), Biochem. J. 63, 656-661.
- Hirohara, H., Bender, M.L., and Stark, R.S. (1974), Proc. Natl. Acad. Sci. USA 71, 1643-1647.
- Huber, R., Kukla, D., Bode, W., Schwager, P., Bartels, K., Deisenhofer, J., and Steigemann, W. (1974), J. Mol. Biol. 89, 73-101.
- Huber, R., Bode, W., Kukla, D., Kohl, U., and Ryan, C.A. (1975), Biophys. Struct. Mechanism 1, 189-201.
- Hunkapiller, M.W., Forgac, M.D., and Richards, J.H. (1976), Biochemistry 15, 5581-5588.
- Hunkapiller, M.W., Forgac, M.D., Yu, E.H., and Richards, J.H. (1979), Biochem. Biophys. Res. Commun. 87, 25-31.
- Kasserra, H.P., and Laidler, K.J. (1970), Can. J. Chem. 48, 1793-1802.
- Katagiri, K., Takeuchi, T., Taniguchi, K., and Sasaki, M. (1978), Anal. Biochem. 86, 159-165.
- Klinman, J.P. (1978), Adv. Enzymol. 46, 415-595.
- Kogan, R.L., Fee, J.A., and Fife, T.H. (1982), J. Am. Chem. Soc. 104, 3569-3576.

- Lucas, E.C., and Caplow, M. (1972), J. Am. Chem. Soc. 94, 960-963.
- Lucas, E.C., Caplow, M., and Bush, K.J. (1973), J. Am. Chem. Soc. 95, 2670-2673.
- Markley, J.L., Travers, F., and Balny, C. (1981), Eur. J. Biochem. 120, 477-485.
- Miller, C.G., and Bender, M.L. (1968), J. Am. Chem. Soc. 90, 6850-6852.
- O'Leary, M.H., and Kluetz, M.D. (1970), J. Am. Chem. Soc. 92, 6089-6090.
- O'Leary, M.H., and Kluetz, M.D. (1972), J. Am. Chem. Soc. 94, 3585-3589.
- Petkov, D.D. (1978), Biochim. Biophys. Acta 523, 538-541.
- Philipp, M., Pollack, R.M., and Bender, M.L. (1973), Proc. Natl. Acad. Sci. USA 70, 517-520.
- Quinn, D.M., Elrod, J.P., Ardis, R., Friesen, P., and Schowen, R.L. (1980), J. Am. Chem. Soc. 102, 5358-5365.
- Richarz, R., Tschesche, H., and Wuthrich, K. (1980), Biochemistry 19, 5711-5715.
- Ruhlmann, A., Kukla, D., Schwager, P., Bartels, K., and Huber, R. (1973), J. Mol. Biol. 77, 417-436.
- Satterthwait, A.C., and Jencks, W.P. (1974), J. Am. Chem. Soc. 96, 7018-7031.
- Shotton, D.M. (1970), in "Methods in Enzymology", vol. XIX, G.E. Perlmann and L. Lorand, eds., Academic Press, New York, 113-139.
- Sweet, R.M., Wright, H.T., Janin, J., Chothia, C.H., and Blow, D.M. (1974), Biochemistry 13, 4212-4228.

- Thompson, R.C., and Blout, E.R. (1970), Proc. Natl. Acad. Sci. USA 67, 1734-1740.
- Thompson, R.C., and Blout, E.R. (1973a), Biochemistry 12, 57-65.
- Thompson, R.C., and Blout, E.R. (1973b), Biochemistry 12, 66-71.
- Thompson, R.C., and Blout, E.R. (1973c), Biochemistry 12, 51-57.
- Thompson, R.C. (1974), Biochemistry 13, 5495-5501.
- Williams, R.E., and Bender, M.L. (1971), Can. J. Biochem. 49, 210-217.

## CHAPTER VII

$^{13}\text{C}$  NUCLEAR MAGNETIC RESONANCE STUDY OF  
THE EFFECT OF ENVIRONMENTAL CONDITIONS ON  
THE IONIZATION BEHAVIOR OF IMIDAZOLE-4-ACETIC  
ACID AND trans-UROCANIC ACID

## ABBREVIATIONS

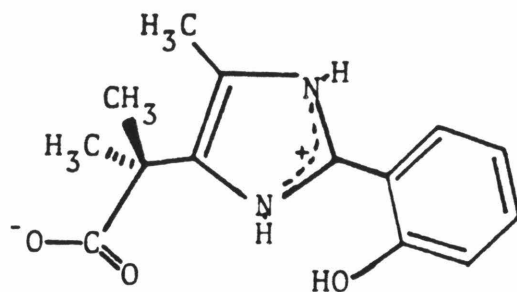
NMR	Nuclear Magnetic Resonance
Asp	L-Aspartic acid
Ser	L-Serine
His	L-Histidine
DMSO	Dimethyl sulfoxide
d <sub>6</sub> -DMSO	Perdeuterated dimethyl sulfoxide
ppm	Parts per million
FID	Free induction decay
Me <sub>4</sub> Si	Tetramethylsilane

## INTRODUCTION

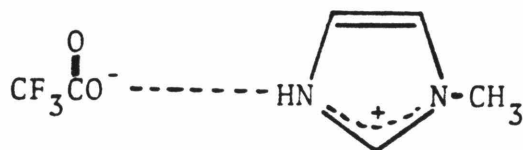
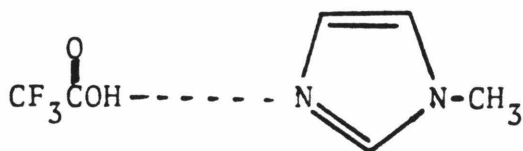
The serine proteases are a family of enzymes evolved to catalyze the hydrolysis of peptide bonds at near neutral pH. A key feature of the proposed mechanism of hydrolysis of these enzymes is the formation of a tetrahedral adduct of Ser 195 of the active site and the carbonyl carbon of the scissile bond of the substrate, assisted by the transfer of a proton from  $\gamma\text{O}$  of Ser 195 to the Asp 102-His 57 couple of the catalytic triad. A "charge relay" hypothesis has been proposed (Blow et al., 1969; Hunkapiller et al., 1973) to explain the enhanced nucleophilicity of this serine residue. This hypothesis postulates that the concerted transfer of the proton on  $\gamma\text{O}$  of Ser 195 to N-1 of His 57 coupled with transfer of the proton on N-3 of His 57 to the carboxylate of Asp 102 allows for both polarization of Ser 195 through partial transfer of the negative charge originally residing on Asp 102 at catalytic pH to Ser 195, thus enhancing the nucleophilic character of this residue, and for the alleviation of unfavorable charge separation in a predominantly hydrophobic active site environment (Hunkapiller et al., 1973). Both of these effects could help account for the special potency of these enzymes as catalysts. However, crucial to the "charge relay" hypothesis is the requirement that the imidazole side-chain of His 57 be a weaker base than the carboxylate side-chain of Asp 102, so that proton transfer from His 57 to Asp 102 is energetically favorable. This is contrary to the normal behavior of these two basic groups in aqueous solution.

An early  $^{13}\text{C}$  study (Hunkapiller et al., 1973) of the ionization behavior of His 57 in the bacterial serine protease,  $\alpha$ -lytic protease, provided support for the "charge relay" hypothesis. However, subsequent  $^{15}\text{N}$  (Bachovchin and Roberts, 1978),  $^1\text{H}$  (Westler and Markley, 1979; Westler et al., 1982), and  $^{13}\text{C}$  (Bachovchin et al., 1981; Chapter II of this thesis) nmr studies have convincingly demonstrated that the  $\text{pK}_a$  of Asp 102 in the free enzyme is less than that of His 57, although the relationship of this evidence concerning the free enzyme to the behavior of the enzyme during the catalytic process when substrate is bound is as yet unclear (see Chapter II).

Attempts to probe both the question of the effectiveness of "charge relay" for catalysis and the question of the environmental qualities necessary to effect  $\text{pK}_a$  reversal through the use of model systems have resulted in conflicting evidence. Hunkapiller et al. (1973) have reported that  $^{13}\text{C}$  measurements of the chemical shift and coupling constant for the C-2 carbon of imidazole in concentrated solutions of imidazole and acetic acid in pure dioxane show no protonation of the imidazole by the acetic acid, unless water (as little as 1-2 molar equivalents) is added to the solution. However, kinetic studies on the hydrolysis of acetate esters of model compounds for the catalytic triad (4(5)-methyl-5(4)-dimethylacetic acid derivatives of 2(2'-hydroxyphenyl)imidazole) (1) indicate that even in 96% dioxane/4% water the  $\text{pK}_a$  of the imidazolium cation is substantially greater than that of the carboxylic acid (Rogers and Bruice, 1974).

1

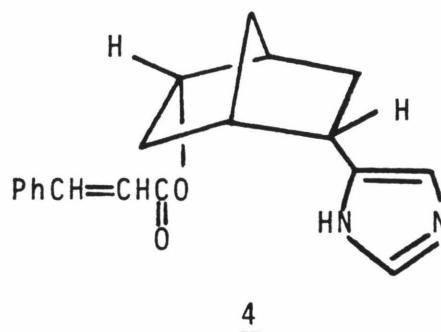
Furthermore, Schuster and Roberts (1979) have reported that equimolar amounts of 1-methylimidazole and trifluoroacetic acid in chloroform exhibit  $^{15}\text{N}$  chemical shifts for the imidazole that are consistent with structure 2, rather than 3, below.

23

However, this is not entirely unexpected, owing to the acid strength of trifluoroacetic acid.

Bender and coworkers (Komiya et al., 1977a,b) have observed that the intramolecular general base catalysis by the imidazole group of endo-5-(4'(5')imidazolyl)bicyclo(2.2.1)hept-endo-2-yl-trans-cinnamate (4) is markedly enhanced by the presence of benzoate in dioxane/water mixtures, but not in

purely aqueous solution. They have interpreted these findings in terms of a mechanism similar to the "charge relay" hypothesis, whereby increasing the dioxane content of the solution causes an increase in the basicity of the benzoate anion, and as such an increase in its catalytic effectiveness as the ultimate proton acceptor during the hydrolysis. However,  $^{13}\text{C}$  nmr



studies of solutions of benzoic acid and 4-methylimidazole in 42 mole percent dioxane in water at pH\* 9 indicate that the imidazole is a stronger base than the benzoate under these conditions (Roberts and Kanamori, 1980). As such, it was postulated that the increased catalytic effectiveness of the imidazole moiety of 4 in the presence of benzoate in dioxane/water mixtures was due to, first, increased nucleophilicity of the imidazole ring on hydrogen bonding to benzoate prior to the transition state of hydrolysis, and second, additional stabilization of this transition state by improved solvation of the positive charge developed on the imidazole ring due to proton transfer during hydrolysis in the presence of negatively charged benzoate, and not to a "charge relay" mechanism.

We have investigated imidazole-4-acetic acid (5) and, to a lesser extent, trans-urocanic acid (6), as models of the

Asp 102-His 57 dyad in pure water, pure anhydrous dimethylsulfoxide, and in mixtures of these two solvents by  $^{13}\text{C}$  NMR spectroscopy in an effort to determine the effect of the dielectric of the environment on the ionization behavior of these two acid-base groups, and thus by analogy to gain some insight into the role of "charge relay" in catalysis by the serine proteases.

## EXPERIMENTAL

Materials. Imidazole-4-acetic acid hydrochloride and trans-urocanic acid were both purchased from Sigma. The former compound was used as received, while the latter was recrystallized from boiling water using decolorising charcoal, and dried in air to give the crystalline monohydrate, mp. 218-220°C. Both compounds were stored dessicated at -20°C.

Imidazole-4-acetic acid and its corresponding sodium salt were prepared by treating one equivalent of the hydrochloride in water with one equivalent of sodium bicarbonate and sodium carbonate, respectively. The aqueous solutions were lyophilized to give white powders in both cases, consisting of the imidazole-4-acetic acid derivative and sodium chloride. These powders were not further purified, but were stored dessicated at -20°C.

Dimethylsulfoxide (DMSO) was purchased from Baker. It was dried by stirring the liquid with excess calcium hydride, followed by distillation from calcium hydride and storage over oven-dried 4A molecular sieves under dry nitrogen.

Perdeuterated DMSO ( $d_6$ -DMSO) was purchased from KOR Isotopes; it contained 99.5 atom percent deuterium. Deuterium oxide (99.8 atom percent deuterium) was purchased from Aldrich. All water used in the experiment was doubly distilled in an all glass apparatus.

Methods. NMR Samples. Aqueous samples were prepared by suspending 100 mg of the desired solid in 3.0 ml of 80% H<sub>2</sub>O/20% <sup>2</sup>H<sub>2</sub>O (v/v), shaking the suspension well to promote dissolution, and centrifuging at room temperature at 10,000 rpm

to remove insoluble material.

Samples in DMSO or in DMSO/water mixtures were prepared by first suspending 100 mg of the desired solid in 0.6 ml of  $d_6$ -DMSO, then adding the appropriate volumes of DMSO and water, shaking to promote dissolution, and centrifuging at room temperature at 10,000 rpm to remove insoluble material.

Aqueous samples were titrated to the desired pH with either 6N HCL or 6N NaOH solution directly in the NMR tube. The pH of each sample was checked prior to and following each spectral acquisition using a Radiometer model PHM26 pH meter equipped with a Radiometer GK2322C combination electrode that could be inserted into the NMR tube. The agreement between readings was  $\pm 0.03$  pH units. The electrode was standardized versus standard pH 4 and pH 7 buffers, and the reported pH values are uncorrected for the  $^2H_2O$  present in the samples.

NMR Spectra.  $^{13}C$  NMR spectra were taken in 10 mm diameter sample tubes on a Varian XL-200 spectrometer operating at 50.3 MHz for carbon-13 in the pulsed Fourier transform mode. Chemical shifts have been reported relative to an external solution of tetramethylsilane in chloroform which resonates at 0.00 ppm. Either 20% (v/v)  $^2H_2O$  or 20% (v/v)  $d_6$ -DMSO were used to provide an internal field-frequency lock. The constant temperature device of the spectrometer was operated at  $25.0 \pm 0.2^\circ C$  for all spectral acquisitions.

## RESULTS AND DISCUSSION

In order to determine the  $^{13}\text{C}$  NMR parameters for C-2 in imidazole-4-acetic acid (5), as well as the pH domains of each of the three acid-base forms of the molecule, a titration of the compound in aqueous solution was performed.

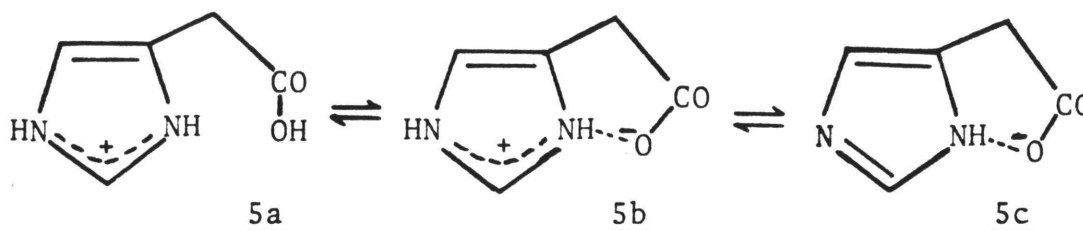


Figure 1 presents these data. The curve has been fit to the data using the following equation (i):

$$\delta - \delta_N = \frac{(\text{H}^+)}{(\text{H}^+) + K_1} \Delta_1 + \frac{K_2}{(\text{H}^+) + K_2} \Delta_2 \quad (\text{i})$$

where  $\delta$  = the observed chemical shift of C-2,  $\delta_N$  = the chemical shift for the neutral species 5b ( $\delta_N = 133.06$  ppm),  $\Delta_1$  is the chemical shift difference between the neutral species 5b and the cationic species 5a ( $\Delta_1 = -0.24$  ppm),  $\Delta_2$  is the chemical shift difference between the anionic species 5c and the neutral species 5b ( $\Delta_2 = 2.84$  ppm), and  $K_1$  and  $K_2$  are the acid dissociation constants for the two processes  $\text{5a} \rightleftharpoons \text{5b}$  and  $\text{5b} \rightleftharpoons \text{5c}$  respectively. The curve has been obtained for  $\text{p}K_1 = 2.9 \pm 0.1$  and  $\text{p}K_2 = 7.4 \pm 0.1$ , in good agreement with the results of a  $^{15}\text{N}$  NMR determination ( $\text{p}K_1 = 2.9$ ,  $\text{p}K_2 = 7.5$ , Roberts et al., 1982).

Table I presents the  $^{13}\text{C}$  NMR parameters for 5a, 5b, and 5c; in this case, species 5b and 5c were obtained by addition of one equivalent of sodium bicarbonate or sodium carbonate

Figure 1. Chemical shift of the C-2 carbon of imidazole-4-acetic acid as a function of pH. The solid line is a theoretical titration curve calculated according to equation (i) (see text) with  $pK_1 = 2.9$  and  $pK_2 = 7.4$ .

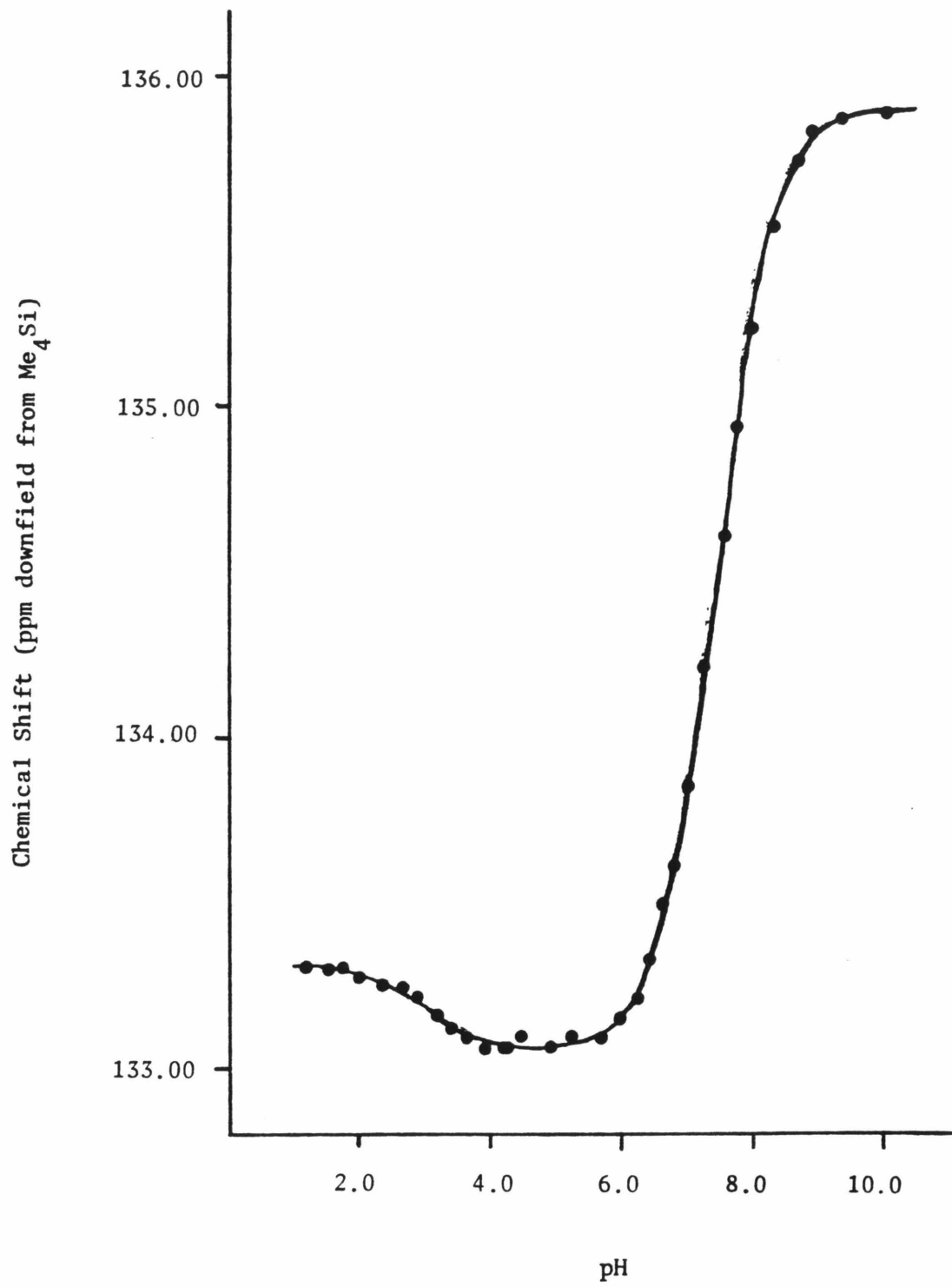


TABLE I.  $^{13}\text{C}$  NMR parameters for the C-2 carbon of imidazole-4-acetic acid (I) and trans-urocanic acid (II) derivatives under various conditions.

Sample	Solvent <sup>a</sup>	$\delta$ (ppm) <sup>b</sup>	$^1J_{\text{CH}}$ (Hz) <sup>c</sup>
I, hydrochloride	A	133.22	222
I	A	133.14	220
I, sodium salt	A	135.90	208
I, hydrochloride	B	136.16	219
I	B	137.20	206
I, sodium salt	B	136.95	208
II + 2 eq. triethylamine	A	136.33	210
II	A	134.29	223
II + 1.2 eq. p-toluene-sulfonic acid	A	134.32	222
II + 2 eq. triethylamine	B	137.12	207
II	B	137.35	208
II + 1.2 eq. p-toluene-sulfonic acid	B	136.16	222
II, benzyl ester	B	137.55	208

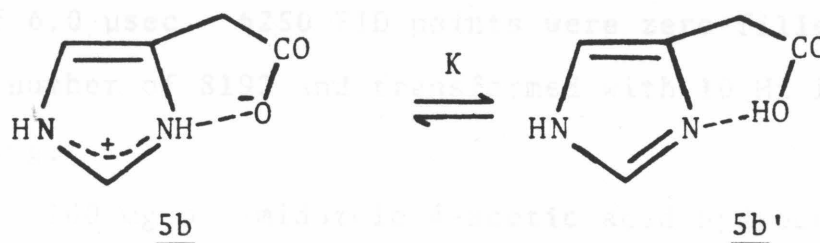
<sup>a</sup>Solvent system A is 80%  $\text{H}_2\text{O}$ /20%  $^2\text{H}_2\text{O}$  (v/v). Solvent system B is 80% DMSO/20%  $d_6$ -DMSO (v/v). See Experimental for description of sample preparation.

<sup>b</sup>Chemical shift values are reported relative to the methyl carbons of external tetramethylsilane = 0.00 ppm and are  $\pm$  0.1 ppm.

TABLE I. (continued)

<sup>c</sup>Coupling constant values are  $\pm 2$  Hz.

to a solution of 5a in water (see Experimental). The pH of each NMR sample so prepared was: 5a, 1.53; 5b, 5.70; 5c, 9.34. This indicates that each sample was at least 96% of the desired species. The  $^{13}\text{C}$  NMR spectra corresponding to each of these samples are shown in Figure 2. It is clear from both the chemical shift ( $\delta = 133.14$  ppm) and the coupling constant ( $^1J_{\text{CH}} = 220$  Hz) that the neutral species 5b is predominantly in the zwitterionic form in aqueous solution, so that  $K$  in Scheme I below is very small ( $K = (\text{5b}')/(\text{5b})$ ). Therefore, as expected, the imidazole ring is a stronger base than the carboxylate anion in aqueous solution.



Scheme I

Table I also presents data for a similar compound, trans-urocanic acid (6). This compound is not as good a model as 5 for the Asp-His dyad of the serine proteases, as the trans-double bond precludes efficient intramolecular hydrogen bond formation between the ring and the carboxylic acid, an important feature of the enzymic couple and one that can be mimicked by 5. However, it is once again clear from the  $^{13}\text{C}$  parameters ( $\delta = 134.29$  ppm,  $^1J_{\text{CH}} = 223$  Hz) that the neutral species is predominantly in the zwitterionic form, as expected.

When DMSO is used as the solvent instead of water, the situation is quite different. Table I presents the relevant

Figure 2. 50.3 MHz proton coupled  $^{13}\text{C}$  NMR spectra of imidazole-4-acetic acid in 20%  $^2\text{H}_2\text{O}$ /80%  $\text{H}_2\text{O}$  (v/v) at  $25.0 \pm 0.2^\circ\text{C}$ . Each spectrum represents 6000 transients taken with an acquisition time of 0.25 sec, a spectral width of 12,500 Hz, and a  $40^\circ$  pulse of 6.0  $\mu\text{sec}$ . 6250 FID points were zero-filled to a Fourier number of 8192 and transformed with 10 Hz line broadening.

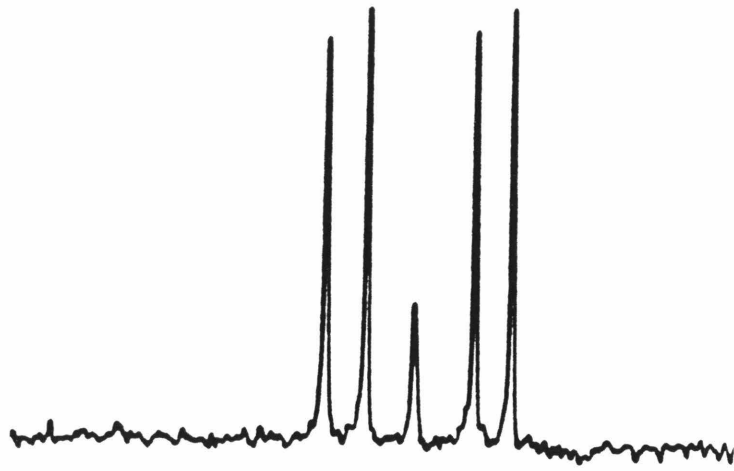
A) 100 mg of imidazole-4-acetic acid hydrochloride in 3.0 ml, pH 1.53.

B) 100 mg of imidazole-4-acetic acid (see Experimental for sample preparation) in 3.0 ml, pH 5.70.

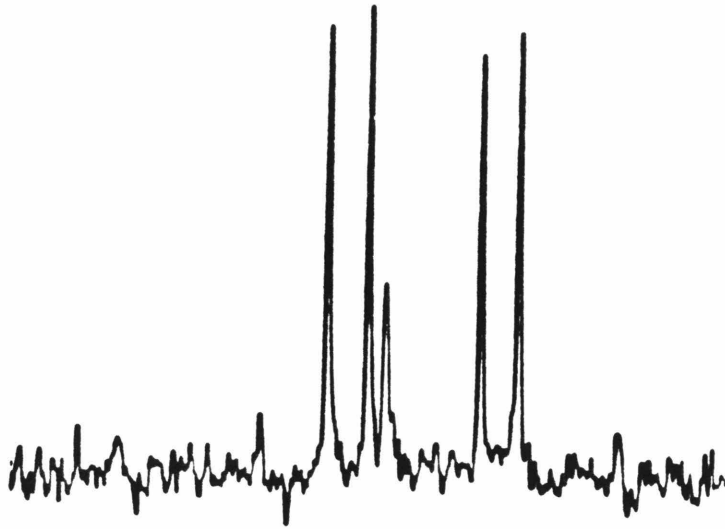
C) 100 mg of sodium imidazole-4-acetate (see Experimental for sample preparation) in 3.0 ml, pH 9.34.

341

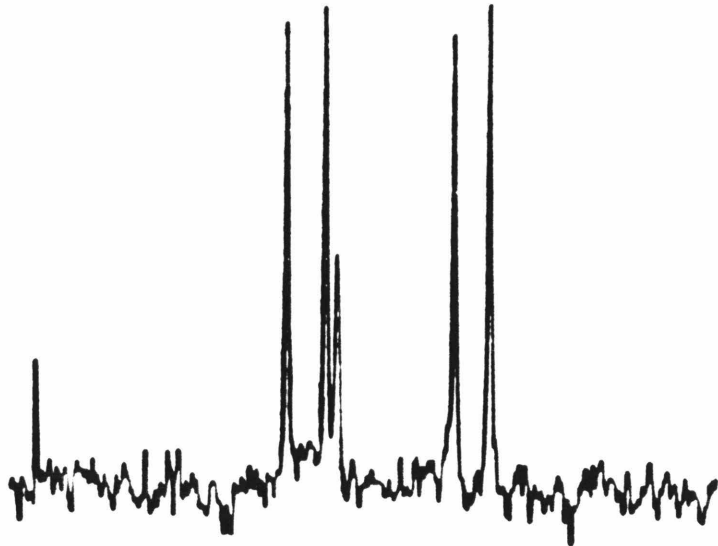
A



B



C



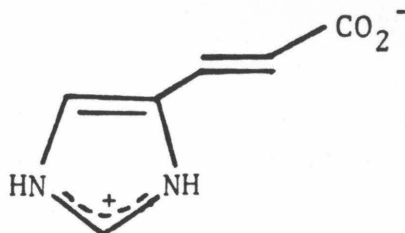
160

140

120

100

Chemical Shift  
(ppm downfield from Me<sub>4</sub>Si)

6

$^{13}\text{C}$  NMR data for the three acid-base forms of both 5 and 6 in pure DMSO; Figure 3 gives the appropriate spectra for 5 in DMSO. The data clearly indicate that, in this solvent, the neutral species for both compounds is predominantly in the neutral imidazole--neutral carboxylic acid form, in contrast to the situation in aqueous solution, and hence that  $K$  in Scheme I is now very large. This comparison is illustrated in Figure 4. Thus, in DMSO, the carboxylic acid moiety of these compounds is a stronger base than the imidazole.

Since DMSO is miscible with water, we can observe the change in  $K$  with increasing water content of water/DMSO mixtures. These data are given in Table II for imidazole-4-acetic acid; representative spectra are shown in Figure 5. It is interesting to note that at least 10 volume percent (or about 30 mole percent) of water can be added to a DMSO solution of 5b with little or no apparent change in the value of  $K$ ; furthermore, even with 20 volume percent (or 50 mole percent) water, the value of  $K$  is on the order of 1, judging by the observed value of  $^1J_{\text{CH}}$  (213 Hz). Because the solvent system is changing, the chemical shift values

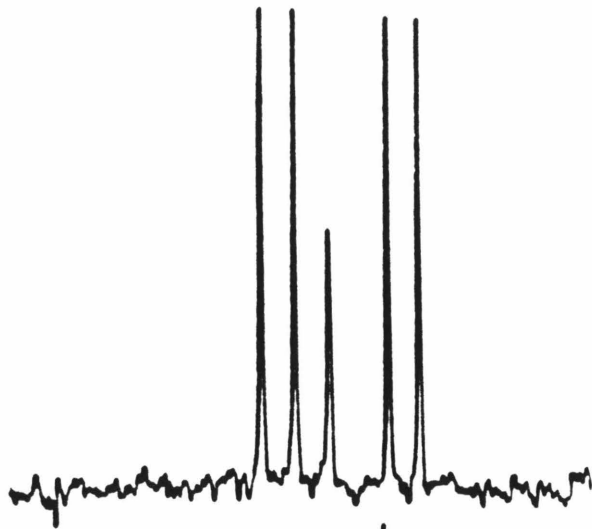
Figure 3. 50.3 MHz proton coupled  $^{13}\text{C}$  NMR spectra of imidazole-4-acetic acid in 20%  $\text{d}_6$ -DMSO/80% DMSO (v/v) at  $25.0 \pm 0.2^\circ\text{C}$ . Each spectrum represents 6000 transients taken with an acquisition time of 0.25 sec, a spectral width of 12,500 Hz, and a  $40^\circ$  pulse of 6.0  $\mu\text{sec}$ . 6250 FID points were zero-filled to a Fourier number of 8192 and transformed with 10 Hz line broadening.

A) 100 mg of imidazole-4-acetic acid hydrochloride in 3.0 ml.

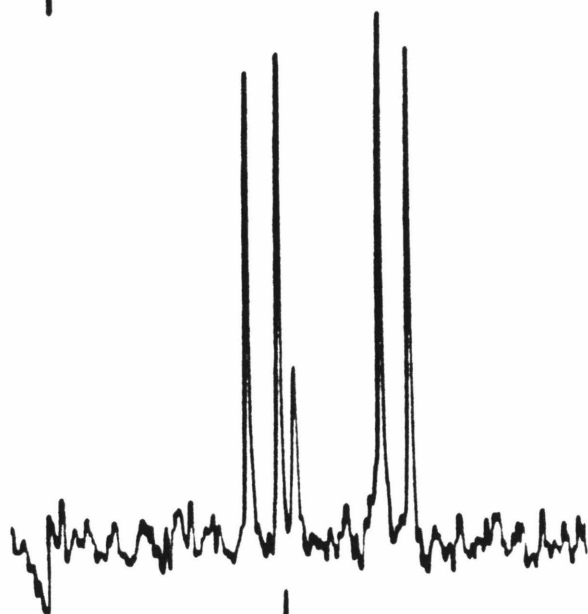
B) 100 mg of imidazole-4-acetic acid (see Experimental for sample preparation) in 3.0 ml.

C) 100 mg of sodium imidazole-4-acetate (see Experimental for sample preparation) in 3.0 ml.

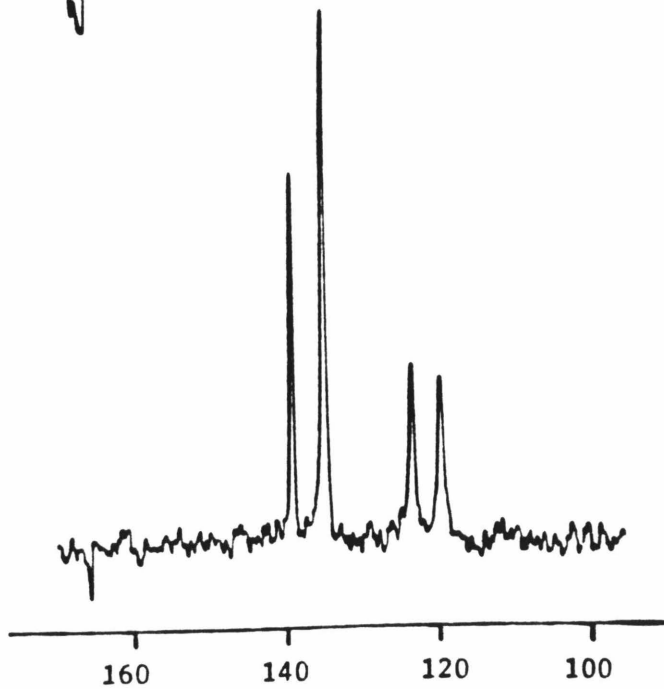
A



B



C



Chemical Shift  
(ppm downfield from Me<sub>4</sub>Si)

Figure 4. 50.3 MHz proton coupled  $^{13}\text{C}$  NMR spectra of imidazole-4-acetic acid.

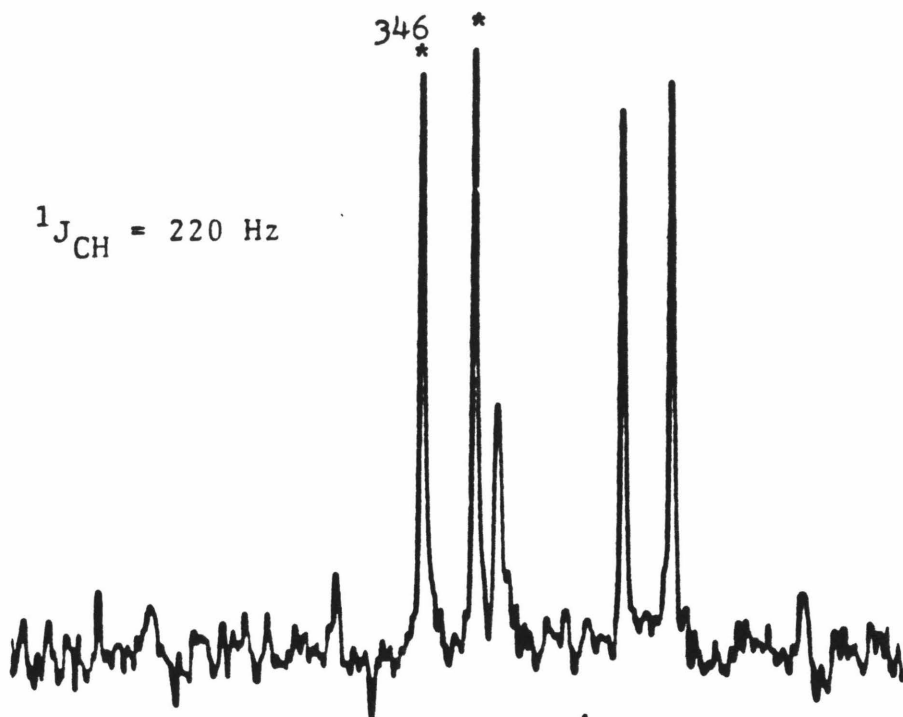
A) The sample was 100 mg of imidazole-4-acetic acid·HCL that had been neutralized with one equivalent of  $\text{NaHCO}_3$  in 3.0 ml of 20%  $^2\text{H}_2\text{O}$ /80%  $\text{H}_2\text{O}$  (v/v) at  $25.0 \pm 0.2^\circ\text{C}$ . The pH of the resulting solution was 5.70. The spectrum represents 5000 transients taken with an acquisition time of 0.25 sec and a  $40^\circ$  pulse of 6.0  $\mu\text{sec}$ . The spectral width was 12,500 Hz. 6250 FID points were zero-filled to a Fourier number of 8192 and transformed with 10 Hz line broadening.

B) The sample was prepared in the same manner as in (A) above, lyophilized, and redissolved in anhydrous dimethylsulfoxide. Accumulation and processing of the spectral data was carried out in the same manner as in (A) above.

In both spectra, the starred resonances are those assigned to C-2.

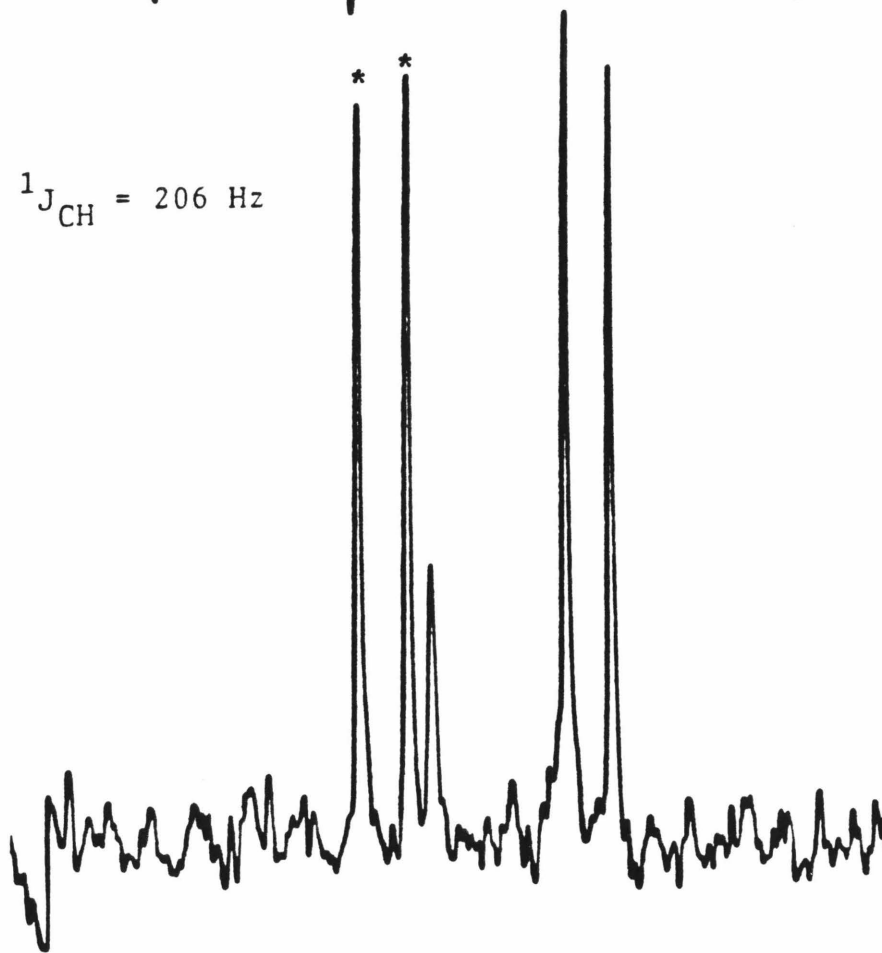
A

$^1J_{CH} = 220 \text{ Hz}$



B

$^1J_{CH} = 206 \text{ Hz}$



160

140

120

100

Chemical shift  
(ppm downfield from  $\text{Me}_4\text{Si}$ )

TABLE II.  $^{13}\text{C}$  NMR parameters for the C-2 carbon of Imidazole-4-acetic acid in DMSO/H<sub>2</sub>O mixtures.

Volume % H <sub>2</sub> O	Mole % H <sub>2</sub> O <sup>a</sup>	$\delta$ (ppm) <sup>b</sup>	$^1J_{\text{CH}}$ (Hz) <sup>c</sup>
0	0	137.23	206
10	31	137.02	207
20	50	136.87	213
30	63	136.40	216
40	72	135.65	220
50	80	135.38	222
60	86	135.28	222
70	90	135.25	223
100	100	133.14	220

<sup>a</sup>Calculated from the volume percent of water by assuming that the density of water is 1.0 g/ml, and the density of DMSO is 1.1 g/ml under the conditions of the experiment. The values given are  $\pm$  3%.

<sup>b</sup>Chemical shift values are reported relative to the methyl carbons of external tetramethylsilane = 0.00 ppm, and are  $\pm$  0.10 ppm.

<sup>c</sup>Coupling constant values are  $\pm$  2 Hz.

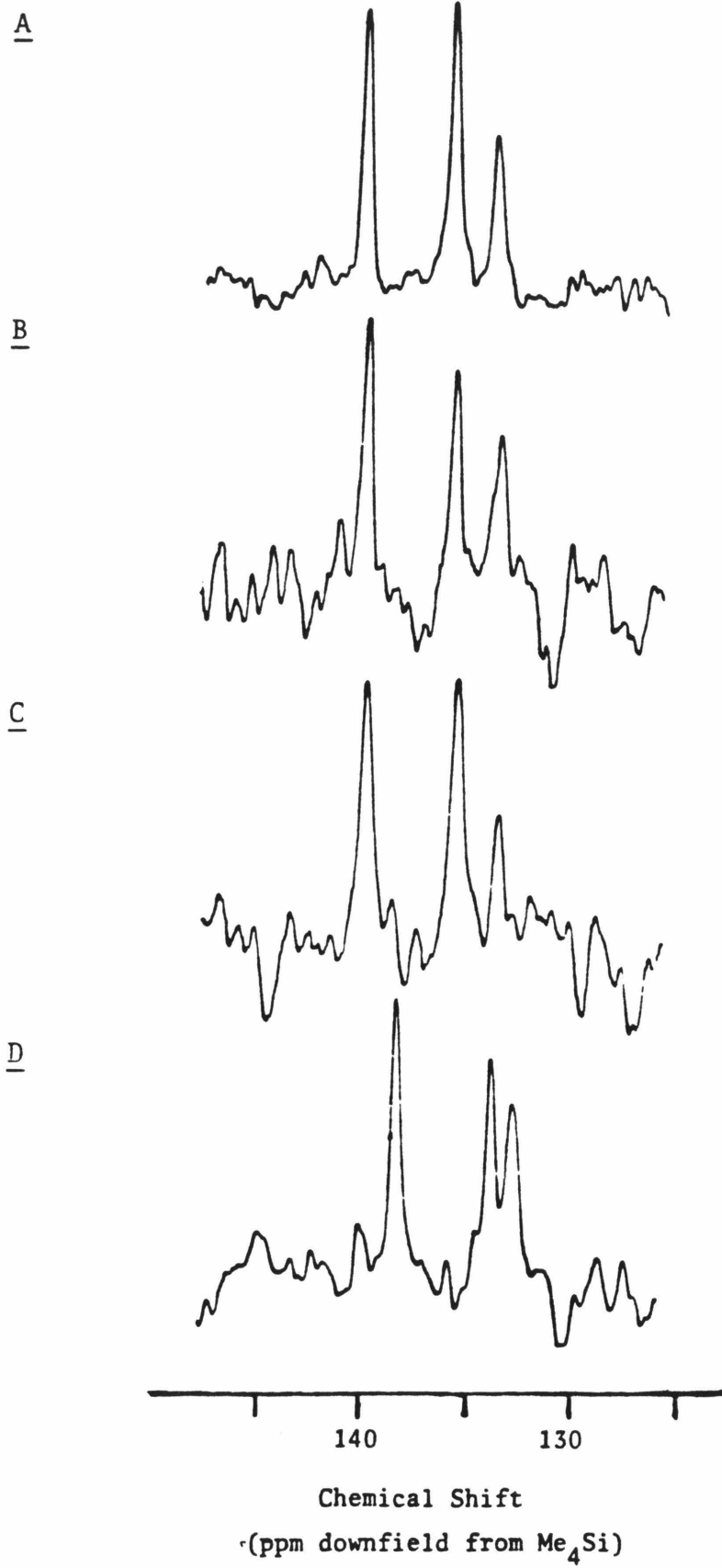
Figure 5. 50.3 MHz proton coupled  $^{13}\text{C}$  NMR spectra of imidazole-4-acetic acid in DMSO/water solution. Samples contained either 20% (v/v)  $\text{d}_6$ -DMSO or  $^2\text{H}_2\text{O}$  to provide an internal field-frequency lock. Spectra were taken at  $25.0 \pm 0.2^\circ\text{C}$ . Each spectrum represents 2500 transients taken with an acquisition time of 0.25 sec, a spectral width of 12,500 Hz, and a  $40^\circ$  pulse of 6.0  $\mu\text{sec}$ . 6250 FID points were zero-filled to a Fourier number of 8192 and transformed with 15 - 20 Hz line broadening.

A) 100 mg of imidazole-4-acetic acid in 3.0 ml of anhydrous DMSO.

B) 100 mg of imidazole-4-acetic acid in 3.0 ml of 10 volume percent water in DMSO.

C) 100 mg of imidazole-4-acetic acid in 3.0 ml of 20 volume percent water in DMSO.

D) 100 mg of imidazole-4-acetic acid in 3.0 ml of 50 volume percent water in DMSO.



are of less assistance than usual in assigning a charge state to the imidazole ring; however, the coupling constant data are still indicative.

What bearing does this information have on the role of the Asp 102-His 57 dyad of the serine proteases during catalysis? The "charge relay" hypothesis requires that, during catalysis, the Asp 102 carboxylate be a stronger base than the His 57 imidazole, contrary to their normal behavior in the free enzyme. Pure DMSO has a dielectric constant of 45, while pure water has a dielectric constant of 81 (Stecker, 1968). Thus, if the enzyme, on binding substrate, can sufficiently lower the dielectric of the local environment of the Asp-His dyad, the  $pK_a$  values of the two residues might be reversed. This might require subtle shifts in the positions of critical active site residues on substrate binding or intermediate formation, or may simply require correct positioning of the substrate with respect to the active site to prevent the access of solvent water to this region. The data in Tables I and II suggest that the change in dielectric may not need to be very large for  $pK_a$  reversal to occur, and therefore may not require any large conformational changes, since it is known that Asp 102 is shielded from solvent by His 57 and is located in a hydrophobic environment in the free enzyme already (Blow et al., 1969). Furthermore, such a  $pK_a$  reversal can occur even under highly polar conditions (30 - 50 mole percent water in DMSO). Brayer et al. (1979) have argued that although

Asp 102 in  $\alpha$ -lytic protease is in a pocket of the enzyme that is lined with hydrophobic residues and is shielded from water, it is the recipient of at least four hydrogen bonds from the backbone amide NH groups of His 57 and Gly 56, from N-3 of His 57, and from the hydroxyl of Ser 214. Thus, it is in an extremely polar environment, so that a "charge relay" mechanism is precluded. The results of this experiment render this conclusion invalid, however. It therefore appears that the "charge relay" system may yet be a viable mechanistic explanation of the catalytic process of the serine proteases.

## CONCLUSION

The "charge relay" mechanism of serine protease hydrolysis has been recently rejected by several authors (Bachovchin and Roberts, 1978; Delbaere et al., 1979; Markley, 1979) since the discovery of a normal pattern of ionization for the Asp 102-His 57 dyad in the free enzymes. However, two model compounds for this dyad, imidazole-4-acetic acid and trans-urocanic acid, exhibit normal ionization behaviors in aqueous solution (dielectric constant = 81,  $pK_a(\text{carboxylate}) < pK_a(\text{imidazole})$ ) but reversed ionization behaviors in pure DMSO solution (dielectric constant = 45,  $pK_a(\text{carboxylate}) > pK_a(\text{imidazole})$ ), and in a solution of at least 30 mole percent water in DMSO. Thus,  $pK_a$  reversal can be achieved under conditions of suitable dielectric, even in a highly polar medium.

If the serine proteases have evolved such that at some point during the catalytic process (either during initial substrate binding or during intermediate formation) the local dielectric of the Asp-His dyad is reduced (probably by blocking the access of solvent water with groups on the enzyme or substrate or both), such a  $pK_a$  reversal might be possible for this couple, resulting in an operative "charge relay" system. Furthermore, the results of the present study indicate that this reversal will not require massive changes in the positions of residues in the active site; small changes will probably suffice, since  $pK_a$  reversal can occur even under

fairly polar conditions. The possibility of such a  $pK_a$  reversal has further been suggested by studies of serine proteases in the presence of transition state analogs (see Chapters IV and V of this thesis).

Therefore, it is still possible that the "charge relay" mechanism is an acceptable explanation of the catalytic process of the serine proteases. It is likely that "charge relay" occurs only with natural substrates, that is, those for which the enzyme and substrate are able to make strongly interactive contacts over an extended region of the protein, so that the enzyme can manifest all of its catalytic abilities (see Chapters II and VI). For less natural substrates, it may well be that the imidazole of His 57 is the ultimate catalytic base. Furthermore, the ability of a substrate to employ the Asp-His dyad effectively may be a manifestation of evolutionary control, so that the most efficient catalysis occurs only with the substrates for which the enzyme has been primarily designed.

## REFERENCES

- Bachovchin, W.W, and Roberts, J.D. (1978), J. Am. Chem. Soc. 100, 8041-8047.
- Bachovchin, W.W, Kaiser, R., Richards, J.H., and Roberts, J.D. (1981), Proc. Natl. Acad. Sci. USA 78, 7323-7326.
- Blow, D.M., Birktoft, J.J., and Hartley, B.S. (1969), Nature (London) 221, 337-339.
- Brayer, G.D., Delbaere, L.T.J., and James, M.N.G. (1979), J. Mol. Biol. 131, 743-775.
- Hunkapiller, M.W., Smallcombe, S.H., Whitaker, D.R., and Richards, J.H. (1973), Biochemistry 12, 4732-4743.
- Komiyama, M., Roesel, T.R., and Bender, M.L. (1977a), Proc. Natl. Acad. Sci. USA 74, 23-25.
- Komiyama, M., Bender, M.L., Utaka, M., and Takeda, A. (1977b), Proc. Natl. Acad. Sci. USA 74, 2634-2638.
- Markley, J.L. (1979), in "Biological Applications of Magnetic Resonance", R. Shulman, ed., Academic Press, New York, 397-461.
- Roberts, J.D., and Kanamori, K. (1980), Proc. Natl. Acad. Sci. USA 77, 3095-3097.
- Roberts, J.D., Yu, C., Flanagan, C., and Birdseye, T.R. (1982), J. Am. Chem. Soc. 104, 3945-3949.
- Rogers, G.A., and Bruice, T.C. (1974), J. Am. Chem. Soc. 96, 2473-2481.
- Schuster, I.I., and Roberts, J.D. (1979), J. Org. Chem. 44, 3864-3867.

Stecher, P.D., ed. (1968), "The Merck Index", Merck and Company, Inc., Rahway, New Jersey.

Westler, W.M., and Markley, J.L. (1979), Fed. Proc. FASEB 3, 1795.

Westler, W.M., Markley, J.L., and Bachovchin, W.W. (1982), FEBS Letters 138, 233-235.